

**SYNERGISTIC EFFECTS BETWEEN THIOL
COLLECTORS USED IN THE FLOTATION
OF PYRITE**

By:

Deirdre Jane Bradshaw

B.Sc. Eng. (Chemical), University of Cape Town

A thesis submitted to the University of Cape Town in fulfilment of the requirements for the degree of Doctor of Philosophy

Department of Chemical Engineering
University of Cape Town
July 1997



The copyright of this thesis vests in the author. No quotation from it or information derived from it is to be published without full acknowledgement of the source. The thesis is to be used for private study or non-commercial research purposes only.

Published by the University of Cape Town (UCT) in terms of the non-exclusive license granted to UCT by the author.

UT 660 BRAD

98/1780

*"... 'tis **grace** that brought me safe thus far,
and **grace** will take me home ..."*

From 'Amazing Grace' by John Newton

ACKNOWLEDGEMENTS

It is impossible for me to even begin to quantify the help and support which has come to me in so many ways and from so many people. However, I owe the following people my special thanks and appreciation:

Firstly, Prof Cyril O' Connor for his outstanding supervision and guidance as well as for his continued patience and encouragement without which this thesis would not have got to this point. Secondly, Dr Peter Harris for his invaluable insight and advice at crucial times.

Jules Aupias, Dr Amor Jordaan and Dr Philip Viviers from SENMIN and Karbochem for their financial, as well as technical and moral support. Thanks also to the FRD for financial support.

All the members of the UCT Flotation Group, past, particularly Prof JP Franzidis, Dr Jan Cilliers and Dr Peter Mills, and present, especially Martin Harris and Dave Deglon, for their support and encouragement. Antionette Upton, "my former flotation partner", Helen Divey and Lorna Wall for their assistance in the batch flotation testwork and assaying. Jeremy Tucker, for his practical help, particularly in the building of the bubble loading apparatus. Bill Randall, Granville de la Cruz and Craig Balfour for the help and patience in electronic and computer matters. Tony Barker for his practical help and assistance, particularly for building and maintaining the modified Leeds cell. Not forgetting, all the student members of the group for their inputs at various times, including Imraan Bacus for the proof reading. Also thanks to the visiting academics, Prof Janusz Laskowski, Dr Noel Finkelstein, Prof John Davidz and Prof Tim Napier Munn for their many helpful discussions, as well as Prof John Ralston and his colleagues for discussions in Adelaide. Thanks also to Rob Dunne for his encouragement and advice.

Prof Joe Cruywagen and Dr Derrick Moolman from the University of Stellenbosch, for their assistance in the thermochemical testwork and surface froth image analysis, respectively.

The Chemical Engineering staff, in general, for all the miscellaneous, but vital help, Pauline, Meg, Nellie and Jackie in the office and at the photocopy machine; Gill for the 'Word' advice; Linda; Suzanna and Maria in the lab; Coral in the library; and all the 'girls' for their encouragement .

My parents, extended family, and friends, including those at Harfield Road Assembly of God and the running group, for their prayers, encouragement and support. Also to those who provided the back up for me on the domestic front, particularly Ascind Kayi and the Miller and Sweeny families.

Finally, special thanks to my husband, Mike, and sons, John, Steven and Charles for living with me through the heights and depths of this period.

CERTIFICATION BY SUPERVISOR

In terms of paragraph GP 8 of "General rules for the degree of PhD ", I Prof. C.T. O' Connor, as supervisor of the candidate, D.J. Bradshaw, certify that I approve of the incorporation in this thesis of material that has been published.

Professor C. T. O'Connor
Department of Chemical Engineering
University of Cape Town
Private Bag
Rondebosch
7700

LIST OF PUBLICATIONS

O' Connor, C.T., Bradshaw, D.J. and Upton. A.E., 1990. The use of dithiophosphates and dithiocarbamates for the flotation of arsenopyrite. *Miner. Engng.*, vol. 3, nos 5., pp 447-459.

Bradshaw, D.J., Upton. A.E. and O' Connor, C.T., 1991. A study or the pyrite flotation efficiency of dithiocarbamates using factorial design techniques. *Miner. Engng.*, vol. 5, nos 3-5, pp 317-329.

Bradshaw, D.J. and O' Connor, C.T., 1993. The flotation of pyrite using mixtures of dithiocarbamates and other thiol collectors. *Miner. Engng.*, vol. 7, nos 5-6, pp 681-690.

Bradshaw, D.J., Cruywagen, J.J. and O' Connor, C.T., 1995. Measurement of the heat of adsorption and surface reactions of cyclohexyl dithiocarbamate, potassium n-butyl xanthate and a thiol mixture on pyrite. *Miner. Engng.*, vol. 8, no 10, pp 1175 - 1184.

Moolman, D.W., Aldrich, C., van Deventer, J.S.J. and Bradshaw, D.J., 1995. The interpretation of flotation froth surfaces using digital analysis and neural networks. *Chem. Eng. Sci.*, vol. 50, no 22, pp 3501 - 3513.

Cilliers, J.J. and Bradshaw, D.J., 1996. The flotation of fine pyrite using colloidal gas aphrons. *Miner. Engng.*, vol. 9, no 2, pp 235 - 241.

Bradshaw, D.J. and O' Connor, C.T., 1996. Measurement of the sub-process of bubble loading in flotation. *Miner. Engng.*, vol. 9, no 4, pp 443 - 448.

Bradshaw, D.J. and O' Connor, C.T. 1996. The flotation of low grade pyrite ores using mixtures of collectors. in proceedings *Hidden Wealth: Unlocking values from low grade and refractory ores and wastes*. S. Afr. Inst. Min. Metall., Johannesburg. pp 89-95.

Bradshaw, D.J. and O' Connor, C.T. The synergism of mixtures of thiol collectors in the flotation of low grade pyrite ores, XX International Minerals Processing Congress, (accepted for publication).

TABLE OF CONTENTS

	PAGE
Acknowledgements	v
Certification by supervisor	vi
List of Publications	vii
Table of Contents	ix
List of Appendices	xv
List of Figures	xv
List of Tables	xxi
Nomenclature	xxii
Greek Letters	xxiii
List of Abbreviations	xxiv
Synopsis	xxv

CHAPTER 1: INTRODUCTION

1.1 SCOPE OF THESIS	1
1.2 PRINCIPLES OF FLOTATION	3
1.2.1 The sub - processes of flotation	5
1.2.2 Mathematical description of flotation	6
1.2.2.1 Klimpel model	7
1.2.3 Influential parameters in flotation	8
1.2.3.1 Equipment components	9
1.2.3.2 Operational components	9
1.2.3.2.1 Mineral type	9
1.2.3.2.2 Particle size effects	10
1.2.3.3 Chemical components	12
1.2.3.3.1 Collectors	13
1.2.3.3.2 Frothers	13
1.2.3.3.3 Depressants and dispersants	14
1.2.3.3.4 Activators	14
1.2.3.3.5 pH and Eh modifiers	15
1.2.3.3.6. Water	15
1.2.3.3.7 Interactions between chemical parameters	17
1.3 MEASUREMENT OF HYDROPHOBICITY AND FLOTABILITY	17
1.3.1 Surface hydrophobicity	18
1.3.1.1 Contact angle (θ)	19
1.3.1.2 Limitations of hydrophobicity measurements	20
1.3.2 Particle flotability	20
1.3.2.1 Bubble loading	21
1.4 MINERAL - COLLECTOR INTERACTIONS	23

1.4.1 Methods of Identification	23
1.4.1.1 Spectrophotometric measurements	23
1.4.1.2 Thermochemical measurements	24
1.4.1.3 Electrochemical measurements	25
1.4.1.4 Solubility measurements	26
1.4.2 Role of mineral	26
1.4.2.1 Sulphide minerals.....	26
1.4.2.1.1 Pyrite.....	29
1.4.3 Role of collectors	32
1.4.3.1 Thiol collectors	33
1.4.3.1.1. Xanthates.....	37
1.4.3.1.2. Dithiocarbamates	39
1.4.4 Role of copper sulphate in the activation of pyrite	40
1.4.5 Collector adsorption onto mineral surfaces	44
1.4.5.1 Possible thiol - sulphide adsorption mechanisms.....	44
1.4.5.1.1 Chemisorption	47
1.4.5.1.2 Catalytic oxidation	47
1.4.5.1.3 Metal - thiol formation (EC - mechanism).....	48
1.4.5.1.4 Metathetical substitution.....	48
1.4.5.2. Comparison of xanthates and dithiocarbamates	49
1.4.5.2.1 Galena	49
1.4.5.2.2 Copper sulphides	50
1.4.5.2.3 Pyrite.....	51
1.4.5.3 Mixtures of collectors and sulphide minerals.....	55
1.5. PROPOSED MECHANISMS OF SYNERGISM	59
1.6. RESEARCH OBJECTIVES	61

CHAPTER 2: BATCH FLOTATION TESTS

2.1 INTRODUCTION	63
2.2 EXPERIMENTAL PROCEDURES	64
2.2.1 Flotation tests	64
2.2.1.1 Flotation cell	64
2.2.1.2. Ore samples	65
2.2.1.3. Reagents.....	67
2.2.1.3.1 Collectors	67
2.2.1.3.2 Frothers.....	68
2.2.1.3.3 pH control.....	69
2.2.2 Flotation procedures	69
2.2.2.1 Batch flotation of Buffelsfontein ore (B-)	69
2.2.2.2 Batch flotation of St Helena ore (SH-).....	70

2.2.3 Analytical procedures	71
2.2.3.1 Sulphur assays	71
2.2.3.2 Digital image analysis of froth surface	72
2.2.4 Experimental design and statistical analysis	73
2.2.4.1 Factorial design of experiments	73
2.3 RESULTS	74
2.3.1 Investigation with Buffelsfontein ore	74
2.3.1.1 Reproducibility (Tests: B-R 1-8).....	74
2.3.1.1.1. Analysis by size of reproducibility results.....	75
2.3.1.2 Flotation with PNBX and cyclohexyl DTC (Tests: B-R 9-12).....	79
2.3.1.2.1 Sulphur grade vs sulphur recovery	81
2.3.1.2.2 Rate of sulphur recovery.....	82
2.3.1.2.3 Sulphur recovery by size	82
2.3.1.2.4 Water recovery	84
2.3.1.2.5 Image analysis of froth surface.....	87
2.3.1.3 Effect of ratio of PNBX to cyclohexyl DTC in collector mixture	91
2.3.1.3.1 Sulphur grade vs sulphur recovery	92
2.3.1.3.2 Rate of sulphur recovery.....	94
2.3.1.3.3 Sulphur recovery by size	95
2.3.1.3.4 Water recovery	99
2.3.1.4. Effect of dosage with PNBX and the 90:10 mixture of PNBX and cyclohexyl DTC.....	102
2.3.1.4.1 Sulphur grade vs sulphur recovery	103
2.3.1.4.2 Rate of sulphur recovery.....	104
2.3.1.4.3 Sulphur recovery by size	104
2.3.1.4.4 Water recovery	107
2.3.1.4.5 Image analysis of froth surface.....	109
2.3.1.4.6 Statistical analysis	111
2.3.2 Investigation with St Helena ore	114
2.3.2.1 Reproducibility (Tests: SH-R 1-4)	115
2.3.2.2 Comparison of PNBX to the 90:10 mixture PNBX and cyclohexyl DTC.....	117
2.3.2.3 The effect of sequence of reagent addition	119
2.4 DISCUSSION	121
2.5 CONCLUSIONS	129

CHAPTER 3: BUBBLE LOADING TESTS

3.1 INTRODUCTION	131
3.2 EXPERIMENTAL DETAILS	132
3.2.1. Apparatus and samples	132

3.2.1.1 Flow - through microflotation cell.....	132
3.2.1.2 Bubble sizer	133
3.2.1.3 Mineral sample.....	134
3.2.1.4 Reagents / collectors.....	135
3.2.2 Procedures	135
3.2.2.1 Measurement of bubble loading.....	135
3.2.2.2 Measurement of bubble size	136
3.3 RESULTS	137
3.3.1 Reproducibility	137
3.3.1.1 Bubble size measurement.....	137
3.3.1.2 Bubble loading measurement	138
3.3.2 The effect of mineral particle size.....	141
3.3.3 The effect of collector type on bubble loading	142
3.4 DISCUSSION.....	143
3.5 CONCLUSIONS.....	146

CHAPTER 4: INVESTIGATION OF THE ADSORPTION OF COLLECTORS ONTO PYRITE

4.1 INTRODUCTION.....	147
4.2 EXPERIMENTAL DETAILS.....	148
4.2.1 Mineral sample	148
4.2.2 Reagents	148
4.2.3 Apparatus and procedures.....	150
4.2.3.1 Thermochemical measurements.....	150
4.2.3.1.1 Apparatus.....	150
4.2.3.1.2 Procedure.....	151
4.2.3.2 Kinetic measurements.....	151
4.2.3.2.1 Apparatus.....	151
4.2.3.2.2 Procedure.....	152
4.2.3.3 Solubility measurements of ferrous salts.....	152
4.2.3.3.1 Apparatus.....	152
4.2.3.3.2 Procedure.....	153
4.3 RESULTS	153
4.3.1 Thermochemical tests	153
4.3.1.1 Reproducibility tests with cyclohexyl DTC.....	155
4.3.1.2 Comparison between cyclohexyl DTC and PNBX with pyrite.....	156
4.3.1.3 Comparison between cyclohexyl DTC and PNBX with ferrous ions	158
4.3.1.4 The effect of pH on cyclohexyl DTC with pyrite.....	160

4.3.1.5 The effect of the 90:10 mixture of PNBX:cyclohexyl DTC with pyrite	161
4.3.1.6 Summary of thermochemical results	162
4.3.2 Kinetic adsorption measurements	163
4.3.3 Solubility product measurements	165
4.4 DISCUSSION	167
4.5 CONCLUSIONS	172

CHAPTER 5: THE ROLE OF COPPER SULPHATE

5.1 INTRODUCTION	173
5.2 BATCH FLOTATION TESTS	174
5.2.1 Investigation with Buffelsfontein ore	174
5.2.1.1 Sulphur grade vs sulphur recovery	174
5.2.1.2 Rate of sulphur recovery	174
5.2.1.3 Sulphur recovery by size	177
5.2.1.4 Water recovery	180
5.2.1.5 Image analysis of froth surface	182
5.2.1.6 Statistical analysis	185
5.2.2 Investigation with St Helena ore	188
5.3. THE EFFECT OF COPPER SULPHATE ADDITION ON BUBBLE	
LOADING	193
5.4 DISCUSSION	195
5.5 CONCLUSIONS	198

CHAPTER 6: CONCLUDING REMARKS 201

LIST OF REFERENCES	207
---------------------------------	------------

LIST OF APPENDICES

APPENDIX 2A*: Milling curve: Buffelsfontein ore

APPENDIX 2B: Sulphur Analysis by LECO SC32

APPENDIX 2C: Statistical Analysis of Results

APPENDIX 2D: Flotation Reproducibility Results

(i): Reproducibility of sulphur assays

(ii): Reproducibility tests obtained with Buffelsfontein ore

(iii): Summary of Buffelsfontein results and standard deviations

(iv): Reproducibility tests obtained with St Helena ore

(v): Summary of St Helena results and standard deviations

APPENDIX 2E: Flotation Results

(i): Results obtained with Buffelsfontein ore

(ii): Results obtained with St Helena ore

APPENDIX 3A: Reproducibility data for bubble sizes

APPENDIX 5A:

(i): Results with copper sulphate obtained with Buffelsfontein ore

(ii) Results with copper sulphate obtained with St Helena ore

* refers to relevant Chapters

LIST OF FIGURES

	PAGE
Figure 1.1: The scope of the thesis	2
Figure 1.2: Schematic of the flotation process.....	4
Figure 1.3: Triangular representation of flotation [Klimpel, 1984].....	8
Figure 1.4: Flotation threshold values as a function of particle size showing the existence of a flotation domain [Crawford and Raiston, 1988].....	11
Figure 1.5: Size by size recovery of selected sulphide minerals after 60 secs flotation [Jowett, 1979]	11
Figure 1.6: The tetrahedral structure of water molecules [Israelachvili, 1992]	16
Figure 1.7: The relationship between flotation recovery and conditioning potential for chalcocite, bornite, chalcopyrite and pyrite with ethyl xanthate at pH = 9 [Richardson and Walker 1985]	29
Figure 1.8: The crystal structure of pyrite [Persson, 1994]	30
Figure 1.9: The Eh - pH diagram of pyrite in water [Kocabag, 1990]	31
Figure 1.10: The flotation recovery of pyrite in a Hallimond Tube as a function of pH with various dosages of potassium ethyl xanthate (KEX) [Fuerstenau and Mishra, 1980]	32
Figure 1.11 Examples of typical thiol collectors [Adkins and Pearse, 1992].....	34
Figure 1.12: A summary of the hydrolysis and oxidation reactions of ethyl xanthate in aqueous solutions [Cases et al, 1993]	38
Figure 1.13: A summary of the rates and reaction paths of ethyl xanthate with pyrite [Montaldi et al, 1993]	53
Figure 1.14 Stability diagram of Fe species for the Fe- X-H ₂ O system at a concentration of [Fe] = [EX] = 1.0x10 ⁻³ moles/l [Wang and Forsberg 1991]	53
Figure 1.15: Relationship of species distribution for the Fe- X-H ₂ O system at a concentration of [Fe] = 1.0 x 10 ⁻³ moles/l and [EX] = 2.5 x 10 ⁻⁵ moles/l compared to pyrite flotation recovery from Trahar,[1983], [Wang and Forsberg 1991].....	54
Figure 2.1: The modified Leeds flotation cell	65
Figure 2.2: Sulphur recovery by size for reproducibility tests (B-R 1-3) using SMBT as collector and 200 mmoles/t Copper sulphate (Buffelsfontein Ore)	77
Figure 2.3: Mean Sulphur grade vs Sulphur recovery by size after 1 and 13 mins for the reproducibility tests (B-R 1-8) using SMBT as collector and 200 mmoles/t copper sulphate (Buffelsfontein Ore).....	78
Figure 2.4: The calculated sulphur grade by size for the reconstituted feed samples compared to the measured feed grades (Buffelsfontein ore).....	78
Figure 2.5: Sulphur grade vs sulphur recovery obtained using 310 mmoles/t PNBX and cyclohexyl DTC (Buffelsfontein ore).....	81
Figure 2.6: Sulphur recovery by size obtained using 310 mmoles/t PNBX and cyclohexyl DTC (Buffelsfontein ore)	83
Figure 2.7: Sulphur grade vs sulphur recovery by size obtained using 310 mmoles/t PNBX and cyclohexyl DTC (Buffelsfontein ore)	83

Figure 2.8: Water recovery vs time obtained using 310 mmoles/t PNBX and cyclohexyl DTC and with no collector addition (Buffelsfontein ore).....	85
Figure 2.9: Sulphur recovery vs water recovery obtained using 310 mmoles/t PNBX, cyclohexyl DTC and with no collector addition (Buffelsfontein ore)	86
Figure 2.10: Gangue recovery vs water recovery obtained using PNBX ,cyclohexyl DTC and with no collector addition (Buffelsfontein ore).....	86
Figure 2.11 : The change in average bubble size of surface froth with time for tests using 310 mmoles/t PNBX and cyclohexyl DTC (Buffelsfontein ore).....	88
Figure 2.12: Instability feature measure for tests using 310 mmoles/t PNBX and cyclohexyl DTC (Buffelsfontein ore)	89
Figure 2.13: The froth speed of flotation tests using 310 mmoles/t PNBX and cyclohexyl DTC mixture (Buffelsfontein ore).....	89
Figure 2.14: Sulphur grade vs sulphur recovery obtained using 310 mmoles/t of collector containing varying ratios of PNBX and cyclohexyl DTC (Buffelsfontein ore)	92
Figure 2.15: Comparison of measured vs predicted sulphur grades at 80% sulphur recovery obtained using 310 mmoles/t of collector containing varying ratios of PNBX and cyclohexyl DTC (Buffelsfontein ore)	93
Figure 2.16: Comparison of measured vs predicted sulphur recoveries at 25% sulphur grade obtained using 310 mmoles/t of collector containing varying ratios of PNBX and cyclohexyl DTC (Buffelsfontein ore).....	94
Figure 2.17: Comparison of measured vs predicted constants, k and R, from Klimpel obtained using 310 mmoles/t of collector containing varying ratios of PNBX and cyclohexyl DTC (Buffelsfontein ore).....	95
Figure 2.18: Sulphur recovery by size obtained using 310 mmoles/t of collector containing varying ratios of PNBX and cyclohexyl DTC (Buffelsfontein ore).....	96
Figure 2.19: Sulphur grade vs sulphur recovery for < 25 μm size fraction obtained using 310 mmoles/t of collector containing varying ratios of PNBX and cyclohexyl DTC (Buffelsfontein ore)	97
Figure 2.20: Sulphur grade vs sulphur recovery for 25 x 75 μm size fraction obtained using 310 mmoles/t of collector containing varying ratios of PNBX and cyclohexyl DTC (Buffelsfontein ore)	98
Figure 2.21: Sulphur grade vs sulphur recovery for > 75 μm size fraction obtained using 310 mmoles/t of collector containing varying ratios of PNBX and cyclohexyl DTC (Buffelsfontein ore)	98
Figure 2.22: Water recovery vs time obtained using 310 mmoles/t of collector containing varying ratios of PNBX and cyclohexyl DTC (Buffelsfontein ore).....	99
Figure 2.23: Comparison of measured vs predicted water recovery after 7 mins obtained using 310 mmoles/t of collector containing varying ratios of PNBX and cyclohexyl DTC (Buffelsfontein ore)	100
Figure 2.24: Sulphur recovery vs water recovery obtained using 310 mmoles/t of collector containing varying ratios of PNBX and cyclohexyl DTC (Buffelsfontein ore)	100
Figure 2.25: Gangue recovery vs water recovery obtained using 310 mmoles/t of collector containing varying ratios of PNBX and cyclohexyl DTC (Buffelsfontein ore)	101

Figure 2.26: Gangue recovery vs sulphur recovery obtained using 310 mmoles/t of collector containing varying ratios of PNBX and cyclohexyl DTC (Buffelsfontein ore)	101
Figure 2.27: Sulphur grade vs sulphur recovery obtained using 310 mmoles/t and 465 mmoles/t of PNBX and the 90:10 mixture of PNBX and cyclohexyl DTC (Buffelsfontein ore).....	103
Figure 2.28: Constants, k and R from Klimpel obtained using pure PNBX, pure cyclohexyl DTC and the 90:10 PNBX:cyclohexyl DTC mixture with a dosage of 310 mmoles/t and 465 mmoles/t (Buffelsfontein ore)	104
Figure 2.29: Sulphur recovery by size obtained using dosages of 310 mmoles/t and 465 mmoles/t of PNBX and the 90:10 PNBX:cyclohexyl DTC mixture (Buffelsfontein ore).....	105
Figure 2.30: Sulphur grade vs sulphur recovery by size obtained using 310 mmoles/t and 465 mmoles/t of pure PNBX (Buffelsfontein ore).....	106
Figure 2.31: Sulphur Grade vs sulphur recovery by size obtained using 310 mmoles/t and 465 mmoles/t of 90:10 mixture of PNBX and cyclohexyl DTC (Buffelsfontein ore).....	106
Figure 2.32: Water recovery vs time obtained using 310 mmoles/t and 465 mmoles/t of PNBX and the 90:10 mixture of PNBX and cyclohexyl DTC at (Buffelsfontein ore).....	107
Figure 2.33: Sulphur recovery vs water recovery obtained using 310 mmoles/t and 465 mmoles/t of PNBX and the 90:10 mixture of PNBX and cyclohexyl DTC at (Buffelsfontein ore).....	108
Figure 2.34: Gangue recovery vs water recovery obtained using 310 mmoles/t and 465 mmoles/t of PNBX and the 90:10 mixture of PNBX and cyclohexyl DTC at (Buffelsfontein ore).....	108
Figure 2.35: The change in the bubble size of surface froth with time for tests using PNBX and the 90:10 mixture of PNBX and cyclohexyl DTC at a dosage of 310 mmoles/t (Buffelsfontein ore).....	109
Figure 2.36: Instability feature measure for tests using PNBX and the 90:10 mixture of PNBX and cyclohexyl DTC at a dosage of 310 mmoles/t(Buffelsfontein ore)	110
Figure 2.37: The froth speed of flotation tests using PNBX and the 90:10 mixture of PNBX and cyclohexyl DTC at a dosage of 310 mmoles/t (Buffelsfontein ore).....	111
Figure 2.38: Sulphur grade vs sulphur recovery obtained using 400 moles/t PNBX and a 90:10 mole ratio mixture of PNBX and cyclohexyl DTC (St Helena ore)	116
Figure 2.39: Water recovery vs time obtained using 400 moles/t PNBX and a 90:10 mole ratio mixture of PNBX and cyclohexyl DTC (St Helena ore).....	117
Figure 2.40: Sulphur grade vs sulphur recovery obtained using differing methods of addition of the 90:10 mole ratio mixture of PNBX and cyclohexyl DTC (St Helena ore)	119
Figure 2.41: Water recovery vs time obtained using differing methods of addition of the 90:10 mole ratio mixture of PNBX and cyclohexyl DTC (St Helena ore).....	120

Figure 3.1: The flow - through microflotation cell.....	132
Figure 3.2: A schematic of the flow - through microflotation cell.....	133
Figure 3.3: The UCT Bubble Sizer.....	134
Figure 3.4: The effect of particle size on the mass and number of particles collected per bubble with a dosage of 1.4×10^{-2} mmoles PNBX / 2 g pyrite	141
Figure 4.1: The Microcalorimeter used in the testwork [Haung and Miller, 1978].....	150
Figure 4.2: Reproducibility of the heat flux recorded when 1.4×10^{-2} mmoles of cyclohexyl DTC was added to 4 g pyrite at pH = 4	156
Figure 4.3: A comparison of the heat flux recorded when 1.4×10^{-2} mmoles of cyclohexyl DTC and PNBX was added to 4g pyrite	157
Figure 4.4: The change in pH and Eh recorded when 1.4×10^{-2} mmoles of PNBX was added to 4 g pyrite in 0.2 ml aliquots.....	158
Figure 4.5: Comparison of the heat flux recorded when 1.75×10^{-2} mmoles of cyclohexyl DTC and PNBX was added to $(\text{NH}_4)_2\text{Fe}(\text{SO}_4)_2 \cdot 6\text{H}_2\text{O}$	159
Figure 4.6: The effect of pH on the heat flux recorded when 1.4×10^{-2} mmoles of cyclohexyl DTC was added to 4 g pyrite.....	160
Figure 4.7: The heat flux recorded when 1.4×10^{-2} mmoles of a 90:10 mixture of PNBX and cyclohexyl DTC was added to 4g pyrite	161
Figure 4.8: The rate of adsorption of PNBX, cyclohexyl DTC and the 90:10 mole ratio mixture of PNBX and cyclohexyl DTC onto pyrite.....	164
Figure 5.1: Sulphur grade vs sulphur recovery obtained using PNBX, cyclohexyl DTC and the 90:10 PNBX:cyclohexyl DTC mixture at 310 mmoles/t with nil and 200 mmoles/t copper sulphate addition (Buffelsfontein Ore)	175
Figure 5.2: Constants k and R from Klimpel obtained using PNBX and cyclohexyl DTC and the 90:10 PNBX:cyclohexyl DTC mixture at 310 mmoles/t with nil and 200 mmoles/t copper sulphate addition (Buffelsfontein Ore)	175
Figure 5.3: Sulphur recovery by size obtained using PNBX, cyclohexyl DTC and the 90:10 PNBX:cyclohexyl DTC mixture at 310 mmoles/t with nil and 200 mmoles/t copper sulphate addition (Buffelsfontein Ore)	177
Figure 5.4: Sulphur grade vs sulphur recovery for $< 25 \mu\text{m}$ size fraction obtained using PNBX, cyclohexyl DTC and the 90:10 PNBX:cyclohexyl DTC mixture at 310 mmoles/t with nil and 200 mmoles/t copper sulphate addition (Buffelsfontein Ore).....	178
Figure 5.5: Sulphur grade vs sulphur recovery for $25 \times 75 \mu\text{m}$ size fraction obtained using PNBX, cyclohexyl DTC and the 90:10 PNBX:cyclohexyl DTC mixture at 310 mmoles/t with nil and 200 mmoles/t copper sulphate addition (Buffelsfontein Ore).....	178
Figure 5.6: Sulphur grade vs sulphur recovery for $> 75 \mu\text{m}$ size fraction obtained using PNBX, cyclohexyl DTC and the 90:10 PNBX:cyclohexyl DTC mixture at 310 mmoles/t with nil and 200 mmoles/t copper sulphate addition (Buffelsfontein Ore).....	179
Figure 5.7: Water recovery vs time obtained using PNBX, cyclohexyl DTC and the 90:10 PNBX:cyclohexyl DTC mixture at 310 mmoles/t and nil and 200 mmoles/t copper sulphate addition (Buffelsfontein Ore)	180

Figure 5.8: Sulphur recovery vs water recovery obtained using PNBX, cyclohexyl DTC and the 90:10 PNBX:cyclohexyl DTC mixture at 310 mmoles/t and nil and 200 mmoles/t copper sulphate addition (Buffelsfontein Ore).....	181
Figure 5.9: Gangue recovery vs water recovery obtained using PNBX, cyclohexyl DTC and the 90:10 PNBX:cyclohexyl DTC mixture at 310 mmoles/t and nil and 200 mmoles/t copper sulphate addition (Buffelsfontein Ore).....	181
Figure 5.10: The change in average bubble size of surface froth with time for tests using PNBX and the 90:10 PNBX:cyclohexyl DTC mixture at 310 mmoles/t and nil and 200 mmoles/t copper sulphate addition (Buffelsfontein Ore)	183
Figure 5.11: Instability feature measure for tests using PNBX and the 90:10 PNBX:cyclohexyl DTC mixture at 310 mmoles/t and nil and 200 mmoles/t copper sulphate addition (Buffelsfontein Ore)	183
Figure 5.12: The froth speed of flotation tests using PNBX, cyclohexyl DTC and the 90:10 PNBX:cyclohexyl DTC mixture at 310 mmoles/t and nil and 200 mmoles/t copper sulphate addition (Buffelsfontein Ore)	184
Figure 5.13: Sulphur grade vs sulphur recovery obtained using 400 moles/t PNBX and a 90:10 mole ratio mixture of PNBX and cyclohexyl DTC with copper sulphate addition of nil and 200 mmoles/t (St Helena Ore)	189
Figure 5.14: Sulphur recovery vs time obtained using 400 moles/t PNBX and a 90:10 mole ratio mixture of PNBX and cyclohexyl DTC with copper sulphate addition of nil and 200 mmoles/t (St Helena Ore).....	189
Figure 5.15: Sulphur grade vs sulphur recovery for different points of 200 mmoles/t copper sulphate addition on the performance of the 90:10 mole ratio mixture of PNBX and cyclohexyl DTC (St Helena Ore)	191
Figure 5.16: Water recovery vs time for different points of 200 mmoles/t copper sulphate addition on the performance of the 90:10 mole ratio mixture of PNBX and cyclohexyl DTC (St Helena Ore).....	191
Figure 5.17: The effect of collector type on bubble loading by pyrite with a dosage of 1.4×10^{-2} mmoles collector / 2 g pyrite.....	194

LIST OF TABLES

	PAGE
Table 1.1: The rest potentials of various sulphide minerals in water at pH = 4 [Majima and Peters, 1969]	28
Table 2.1: The sulphur distribution of the Buffelsfontein and St Helena ore samples.....	66
Table 2.2: Chemical structures and molecular weights of the collectors used in this investigation.....	67
Table 2.3: The stability of the collectors used in this investigation at pH = 4.....	68
Table 2.4: Design Matrix for a full factorial design, 2 ³ (three parameters, each at two levels in eight runs).....	73
Table 2.5: Analysis by size of reproducibility tests B-R 1-3 (Buffelsfontein Ore).....	77
Table 2.6: Summary of results obtained with PNBX, cyclohexyl DTC and mixtures of PNBX and cyclohexyl DTC (Buffelsfontein Ore).....	80
Table 2.7: Statistical evaluation of differences obtained with PNBX and the 90:10 mixture of PNBX and cyclohexyl DTC (Buffelsfontein Ore).....	113
Table 2.8: Summary of flotation results with PNBX and the 90:10 mixture of PNBX and cyclohexyl DTC (St Helena Ore).....	116
Table 2.9: Statistical evaluation of differences obtained with PNBX and the 90:10 mixture of PNBX and cyclohexyl DTC (St Helena Ore)	118
Table 2.10: Summary of flotation responses affected and the possible industrial implications of the use of the mixture of collectors in place of the pure collectors at a dosage of 310 mmoles/t.....	129
Table 3.1: Reproducibility of bubble size data.....	137
Table 3.2: Reproducibility results with 2 g pyrite of 75 x 106 μm size fraction and a dosage of 1.4x10 ⁻² mmoles of PNBX / 2 g pyrite	138
Table 3.3: A sample calculation of bubble loading data (cf. Test Number 1, Table 3.2).....	139
Table 3.4: The effect of particle size on bubble loading of pyrite with a dosage of 1.4x10 ⁻² mmoles PNBX / 2 g pyrite	140
Table 3.5: The effect of collector type on bubble loading by pyrite with a dosage of 1.4x10 ⁻² mmoles collector / 2 g pyrite	143
Table 3.6: A comparison of the conditions for bubble loading and batch flotation tests	144
Table 4.1: The molar extinction coefficients of the collectors	148
Table 4.2: Summary of thermochemical measurements of the reactions between thiol collectors and pyrite or ferrous sulphate	154
Table 4.3: The first order rate constants for PNBX, cyclohexyl DTC and the 90:10 mixture of PNBX and cyclohexyl DTC	155
Table 4.4: The solubility products (pK _{sp}) of ferrous - thiol salts	166

Table 5.1: Summary of results to show the effect of copper sulphate addition with a collector dosage of 310 mmoles/t (Buffelsfontein ore).....	174
Table 5.2: Statistical evaluation of the effects of copper sulphate addition and collector type on flotation performance (Buffelsfontein ore).....	187
Table 5.3: Summary of results with varying the dosage and point of 200 mmoles/t copper sulphate addition to the reagent suite (St Helena Ore).....	188
Table 5.2: Statistical evaluation of the effects of copper sulphate addition and collector type on flotation performance (St Helena Ore).....	192
Table 5.5: The effect of collector type on bubble loading by pyrite with a dosage of 1.4×10^{-2} mmoles / 2 g pyrite of collector	194

NOMENCLATURE

A	Adsorbance of clear solution at set wavelength
A_b	Surface area per bubble (mm^2)
A_p	Contact area of particle (mm^2)
A_{sp}	Surface area of particle (mm^2)
A_t	Total surface area in time interval (mm^2)
b	Path length of radiation (cm)
C	Molar concentration (moles l^{-1})
C_m	Measured concentrate mass (g)
c_m	Measured overall concentrate grade (%)
d_b	Mean diameter of bubble (mm)
d_b^{cr}	Critical diameter of bubble (mm)
Df	Degrees of freedom
d_p	Mean diameter of particle (mm)
$D_{R,t}$	Particle diameter for a given recovery R and flotation time t
E_a	Attachment efficiency
E_c	Collision efficiency, the fraction of all particles swept out by the projected area of the bubble that actually collide with the bubble
E_d	Fraction of particles remaining attached (detachment efficiency)
E_k	Collection efficiency of flotation
F	Factor for F test
f_{calc}	Calculated feed assay (%)
f_m	Measured feed assay (%)
F_m	Measured feed mass (g)
ΔG^{xs}	Change in Gibbs free energy
ΔH	Enthalpy change / Heat flux (kJ/min)
ΔH_{ads}	Heat of adsorption (kJ)
k	Rate constant (min^{-1})
$L_{R,t}$	Quantitative measure of flotability at R and t
M	Mineral recovery from first order kinetics (%)

M_0	Initial mass of mineral in cell (g)
M_b	Average mass per bubble R/N_b (g)
M_{fl}	Actual loading as a fraction of total possible load M_b/M_{max}
M_{max}	Maximum loading for bubble to still rise ($V_b/\rho - \rho_{air}$)
M_p	Mass of particle (g)
MS	Mean square
M_{sa}	Mass per bubble surface area R/A_t (g/mm ²)
n	Number of tests
N_b	Number of bubbles in time interval t
N_{pb}	Number of particles per bubble M_b/M_p
Q	Total heat (J)
r	Recovery at time t (%)
R_b	Overall mass recovery from bubble loading tests (g)
t	Time (mins)
T	T factor for T test
T_m	Measured tails mass (g)
t_m	Measured tails assay (%)
t_s	Contact time between bubble and particle after collision (msecs)
V_b	Volume of bubble (mm ³)
x_i	Result of test i
x_m	Mean result (n tests)

GREEK LETTERS

θ	Aqueous contact angle between bubble and mineral surface (°)
σ	Standard deviation
γ_c	Critical surface tension of wetting of the solid (N/m)
ΔH	Enthalpy change / Heat flux (kJ/min)
ΔH_{ads}	Heat of adsorption (kJ)
ϵ	Molar extinction coefficient (l moles ⁻¹ cm ⁻¹)
γ_{Lg}	Surface tension between liquid and gas (N/m)

μ	Induction time for bubble - particle attachment to occur (msecs)
ρ_{air}	Density of air (g/cm^3)
ρ	Particle density (g/cm^3)
ρ_w	Density of water (g/cm^3)

LIST OF ABBREVIATIONS

B	Buffelsfontein Ore
CuSO_4	Copper sulphate
DTP	Dithiophosphate class of collectors
DTC	Dithiocarbamate class of collectors
FeS_2	Pyrite
FTIR	Fourier transform infra red spectroscopy
NNU	The Non Number Uniformity (coarseness of surface froth image)
MFI	Microflot Flotability Index [Chudacek and Fichera, 1991]
Mixture	90:10 mole ratio mixture of PNBX and cyclohexyl DTC
oC6 DTC	Sodium cyclohexyl dithiocarbamate
PI	Bubble pick up index
PNBX	Potassium n-butyl xanthate
SH	St Helena ore
SMBT	Sodium mercaptobenzothiazole
TEB	1,1,3, triethoxybutane
TOF LIMS	Time of flight laser ionisation mass spectroscopy
TOF SIMS	Time of flight secondary ion mass spectroscopy
UV	Ultra violet spectroscopy
X	Xanthate class of collectors
X^-	Xanthate ion
X_2	Dixanthogen
XPS	X-ray photoelectron spectroscopy
XRD	X ray diffraction (analysis technique)

SYNOPSIS

This thesis investigates, firstly, whether synergism occurs between the thiol collectors, potassium n-butyl xanthate (PNBX) and cyclohexyl dithiocarbamate (cyclohexyl DTC) when a mixture of these collectors is used in the flotation of pyrite at pH =4 and, secondly, why synergistic effects are observed, if any. The focus of the investigation was a 90:10 mole ratio mixture of PNBX and cyclohexyl DTC, although other collector ratios were compared in the batch flotation tests. This ratio was chosen to test the effect of a small amount of the one component in a manner synonymous with studying thermodynamic excess properties. The high cost of dithiocarbamate collectors also argued in favour of the ratio. The effect of copper sulphate on the flotation performance obtained with pure cyclohexyl DTC and PNBX as well as with the collector mixture was also investigated.

Synergism is defined as 'an effect that exceeds the sum of the parts', and the effects on the various flotation responses obtained using the mixtures were compared with the linearly additive contributions of the component collectors. The batch flotation tests with ore from Buffelsfontein and St Helena gold mines showed that sulphur grades, sulphur recoveries and rates of recovery, for all ratios of PNBX and cyclohexyl DTC tested, were enhanced above those predicted from the linear contribution of the component collectors. The water recovery was approximately proportional to the ratio of the component collectors in the mixture and thus showed no synergistic enhancement. The increase in sulphur recovery indicated that the particle collection in the pulp improved. The increase in the sulphur grades as well as the changes in water recovery and surface froth behaviour indicated that the froth zone was also affected by using a mixture of collectors.

In order to gain further understanding of the mechanisms causing the synergism observed in the batch flotation tests, the sub - processes of bubble loading and of the collector - mineral adsorption interactions were investigated

using gravity concentrated pyrite from Durban Roodepoort Deep gold mine. The results from the bubble loading tests were consistent with the batch flotation tests and showed that increased bubble loading was obtained with the mixture of collectors. In order to investigate the cause of the increased bubble loading, thermochemical, kinetic and solubility measurements were also made with the pure collectors and with the 90:10 mole ratio mixture of collectors and pyrite. The thermochemical tests showed a marked difference in the adsorption reactions between PNBX and cyclohexyl DTC and the pyrite surface. The enthalpy changes observed when PNBX was added to pyrite corresponded to the established mechanisms showing the initial formation of the ferrous - thiolate followed by the formation of dixanthogen. In the case of the dithiocarbamate, only the formation of ferrous - thiolate was indicated. The results from the kinetic adsorption tests were consistent with the results of the thermochemical tests, with the adsorption of PNBX continuing until total reagent depletion and the adsorption of cyclohexyl DTC reaching equilibrium. The measurements of the solubility products showed that the metal thiolate salt formed in the case of cyclohexyl DTC was considerably less soluble than that formed with PNBX which was added evidence supporting the formation of the different surface products with the two collectors. The use of techniques such as TOF SIMS, FTIR or XPS would be required to determine the nature of these products.

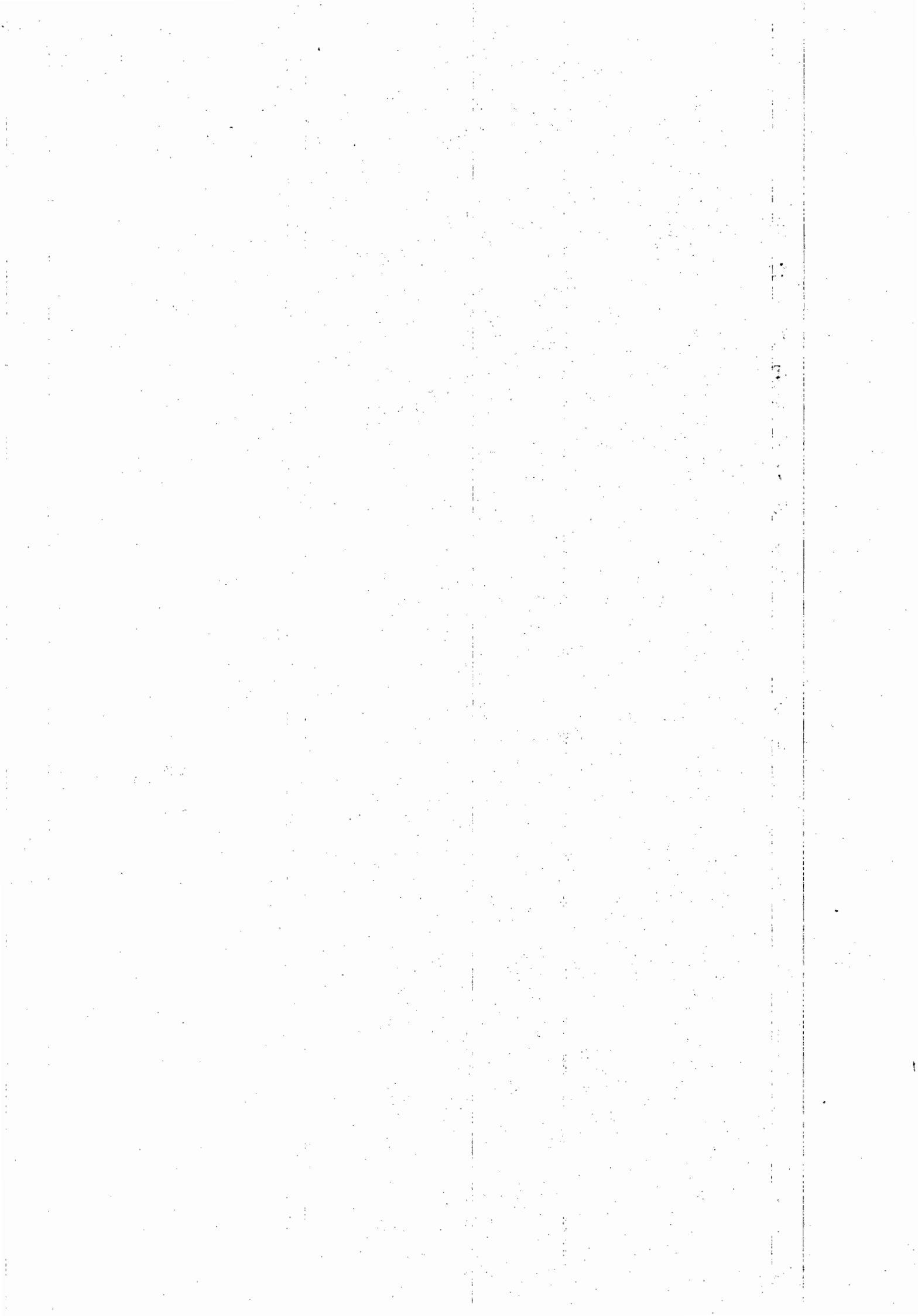
The thermochemical measurements of the adsorption reaction between the 90:10 mole ratio mixture of PNBX and cyclohexyl DTC gave a greater enthalpy change than that observed with either of the pure collectors. The increased hydrophobicity of this product could be used to explain the synergistic behaviour observed in the bubble loading and batch flotation tests.

On the basis of these findings it is proposed that the enhancement of flotation performance observed, when a mixture of PNBX and cyclohexyl DTC is used, is due to the fact that the cyclohexyl DTC adsorbs more rapidly than PNBX and forms the metal thiolate on the surface of the pyrite. The presence of the

cyclohexyl DTC on the surface appears to facilitate the formation of dixanthogen by the PNBX, as is indicated by the increased enthalpy change observed when mixture was used. Dixanthogen is a neutral molecule which would be physisorbed. It is proposed that the ferrous cyclohexyl DTC is chemisorbed to the pyrite surface and the dixanthogen adsorbs around the complex, thus increasing the strength of collector attachment to the mineral surface, increasing the hydrophobicity of the pyrite surface. Alternatively, the increased enthalpy change may result from the formation of a thiol complex involving both the cyclohexyl DTC and the PNBX also leading to same increased hydrophobicity and strength of collector attachment to the pyrite surface. A more precise determination of the actual mechanism is not possible at this stage. The net effect of increased hydrophobicity is to decrease induction time, increasing the rate of flotation or to increase the tenacity of bubble - particle attachment, preventing elutriation and increasing the grade in the froth.

The addition of copper sulphate was shown to predominantly affect the froth phase in the batch flotation tests. In the case of PNBX and the 90:10 mole ratio mixture of PNBX and cyclohexyl DTC, copper sulphate addition resulted in the increased rate of flotation and sulphur recovery but with a decrease in sulphur grade, showing that the overall grade - recovery relationship was unchanged. In the case of cyclohexyl DTC, the addition of copper sulphate substantially reduced recoveries in both batch flotation and bubble loading experiments, probably due to the formation of a hydrophilic copper - dithiocarbamate complex, thus preventing the cyclohexyl DTC from playing its collecting role.

This thesis has shown that synergistic effects between different thiol collectors can result in enhanced flotation performance due to a combination of adsorption, bubble loading and froth phase effects thus opening up exciting possibilities for further research.



CHAPTER 1: INTRODUCTION

1.1 SCOPE OF THESIS

Froth flotation is a complex mineral beneficiation process, first patented in 1877 [Schulze, 1984] that utilises the difference in surface properties to effect the separation between the desired mineral and the unwanted gangue in the ore. Collision and subsequent attachment of mineral particles to bubbles is promoted in the pulp. The hydrophobic mineral is then carried up from the pulp into a stabilised froth zone from where the concentrated mineral is removed. Mineral surface hydrophobicity is, in most cases, created through the use of a class of chemicals known as “collectors”. The success of the process is governed by physical, chemical and operational parameters and much attention has been focused on optimising these parameters.

One means of attaining better flotation performance is with the use of mixtures of collectors. Although long been used in practice [Taggart, 1945], the mechanisms of performance enhancement with collector mixtures have not been clearly established. On the one hand, better performance is attributed to the differing contributions of the respective collectors, and, on the other, synergism between the collectors is hypothesised to occur. The Oxford dictionary defines synergism as “that combined effect that exceeds the sum of the parts” and this thesis investigates whether, in the case of the use of mixtures of collectors in the flotation of pyrite at pH = 4, the change in flotation performance results from the combined contributions of the individual collectors or whether a synergistic interaction occurs.

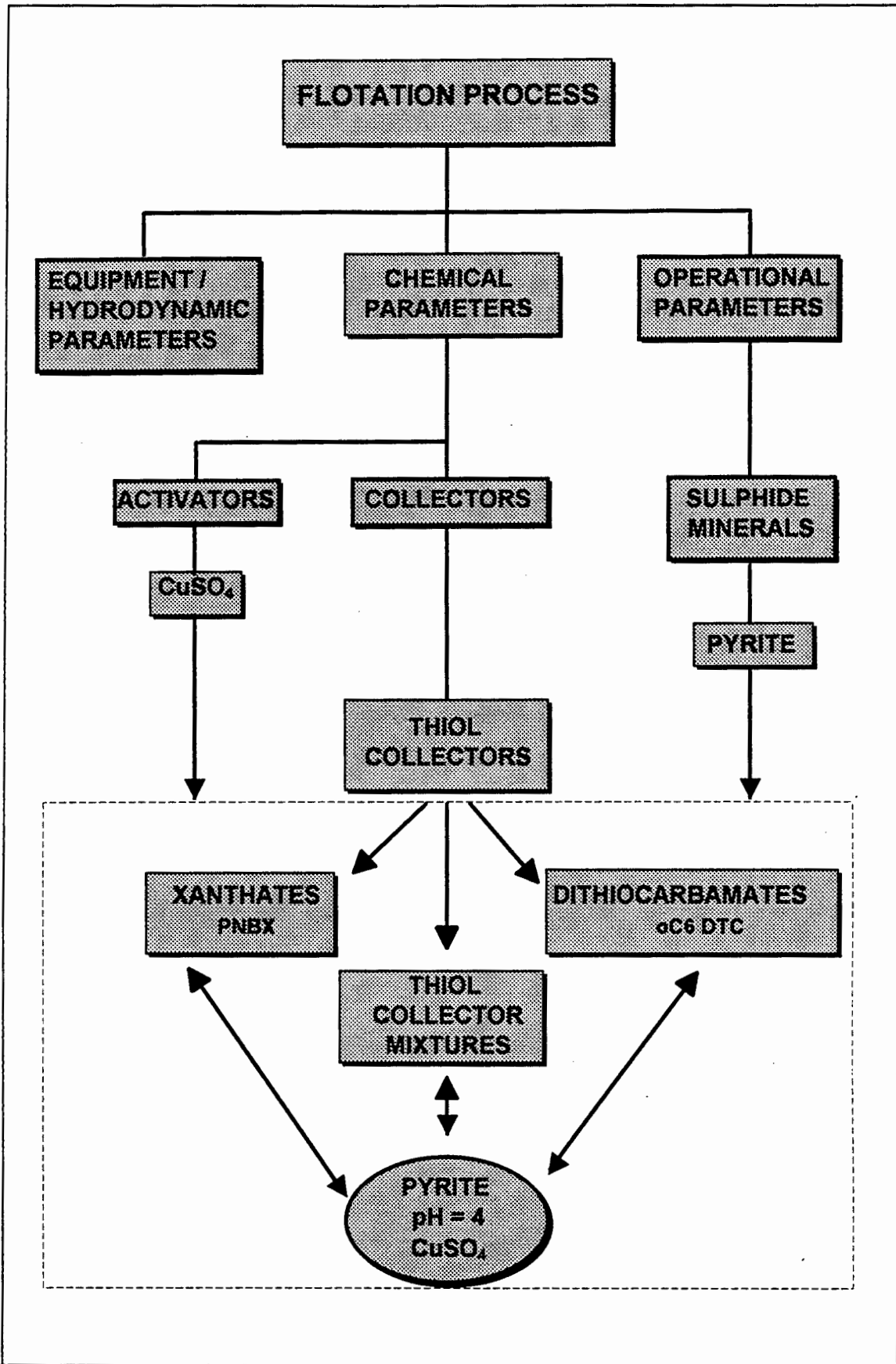


Figure 1.1: The scope of the thesis

Pyrite flotation in South Africa is historically an important process due to the strong association of gold and uranium with pyrite deposits [Bushell, 1970; Lloyd, 1981; Allison et al, 1982, O' Connor and Dunne, 1991]. The pyrite is also used for sulphuric acid production once the valuable metals have been removed.

This chapter provides the background and establishes the motivation for the thesis. Firstly, the principles of flotation are discussed, breaking the overall process into sub - processes and discussing the most influential parameters on the process. The role of the collector is to change the nature of the mineral surface and various methods to characterise the mineral hydrophobicity and flotability of a mineral and their limitations are discussed. The controversial role of copper sulphate as an activator in the flotation of pyrite is discussed in the context of this investigation. The reactions of thiol collectors are dependent on the chemical environment of the flotation pulp and the possible reaction pathways are compared with particular reference to the possible surface reactions occurring with pyrite at $\text{pH} = 4$. The evidence of the benefits of the use of mixtures as well as the proposed mechanisms of enhancement are presented. Finally the research objectives of the thesis are outlined. Figure 1.1 shows a schematic of the scope of the thesis.

1.2 PRINCIPLES OF FLOTATION

Figure 1.2 shows a simplified schematic of the flotation process. There are two distinct zones: The pulp zone, in which the mineral recovery occurs and the froth zone, in which the concentrated mineral is separated from the bulk. Particles can either reach the froth attached to the bubbles or by entrainment in the water passing from the pulp zone to the froth zone. While the former process is selective and is responsible for the collection of the hydrophobic valuables, the latter is unselective and results in the unwanted gangue reporting to the concentrate. It is thus desirable to maximise the recovery by

true flotation and minimise the entrainment contribution. The contribution to overall flotation of the entrained material increases linearly with increase in water recovery [Engelbrecht and Woodburn, 1975; Warren, 1985].

The froth zone provides the environment for the separation of the valuable mineral from the gangue, allowing drainage of the entrained material back into the pulp. There is an optimum froth stability. When the froth is not stable enough the mineralised bubbles rupture before collection, when the froth is too stable, not enough drainage occurs and the water and gangue recoveries are too high. The nature and dosage of the frother as well as the nature of the particles in the froth affect its stability [Livshits and Dudenkov, 1965; Harris, 1982].

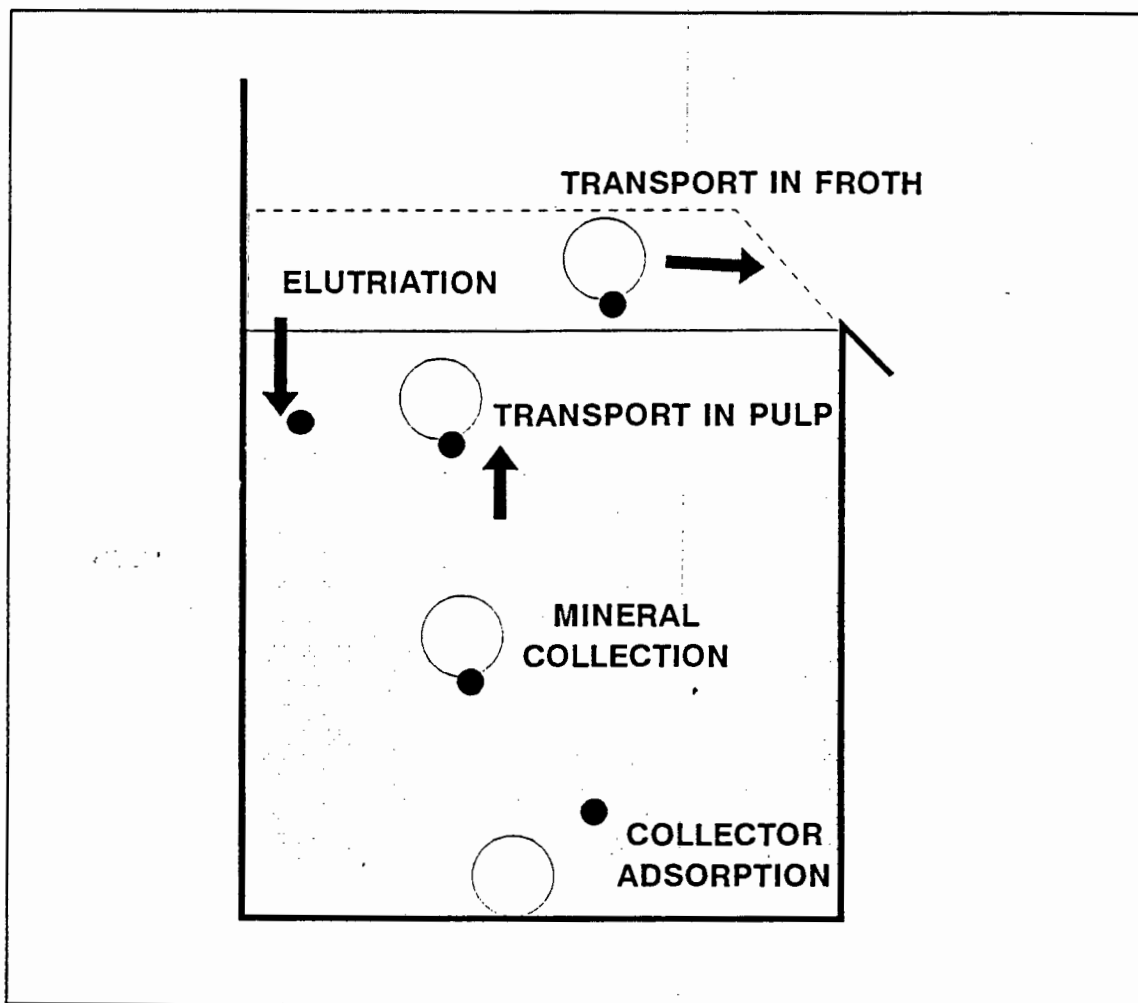


Figure 1.2: Schematic of the flotation process

1.2.1 THE SUB - PROCESSES OF FLOTATION

The overall flotation process can be divided into various consecutive sub - processes which all contribute to the success of the separation of the valuable mineral from the gangue. They can be summarised by the following:

- 1) The creation of the hydrophobic mineral particle surface, which may consist of the collector adsorption onto the surface of the mineral particles and the manipulation of the pulp environment viz. pH, agitation pulp density etc.
- 2) Formation of stable bubbles of a set size and distribution.
- 3) Mineral particle - bubble collision, resulting in possible attachment. This requires the thinning and rupture of the film between the bubble and particle and subsequent stable attachment. Detachment of the mineral from the bubble is also possible. This sub - process is also known as the particle collection.
- 4) The transport of the loaded bubble through the pulp phase.
- 5) Transfer from the pulp phase to the froth phase. There is possible elutriation of particles falling back from the froth into the pulp and entrainment of particles, not collected by bubbles, passing from the pulp into the froth.
- 6) The transport and collection of the loaded bubble in the froth phase.

1.2.2 MATHEMATICAL DESCRIPTION OF FLOTATION

A model for the collection process first proposed by Derjaguin and Dukhin [1960] has been described by Finch and Dobby [1990]. The collection efficiency (E_k) of flotation can be expressed as a function of three components, viz.

$$E_k = E_c E_a E_d$$

where

- E_c = collision efficiency, the fraction of all particles swept out by the projected area of the bubble that actually collide with the bubble,
- E_a = attachment efficiency, the fraction of the particles colliding with the bubble that become attached to it,
- E_d = detachment efficiency, the fraction of attached particles detaching.

The collision efficiency is determined by the hydrodynamics of the system. The attachment efficiency and detachment probability are strongly affected by the hydrophobicity of the mineral particle. Upon collision between the bubble and particle, the particle can either "bounce" off the bubble surface causing it to be strongly deformed, or the particle can slide around the bubble. Finch and Dobby [1990] and Schulze [1989] have shown that the particle is more likely to slide around the bubble. The particle remains in contact with the bubble for a time referred to as the sliding time, t_s . If the sliding time is sufficiently long, the film will thin to a point where rupture will occur spontaneously to form a stable three phase aggregate. The total time required for this process is known as the induction time, t_i . If the induction time, t_i is less than the sliding time, t_s , particle attachment will proceed [Jowett, 1979].

Attempts to mathematically describe the rate of flotation have been made with varying degrees of success for different systems. Zuniga [1935] was the first to

show that the recovery - time data from the flotation process could be fitted, within limitations, to first order kinetics, viz.

$$M = M_0 (1 - \exp^{-kt})$$

where M = mineral recovery at time t (%),
 M_0 = Initial amount of mineral in the cell (%),
 k = rate constant (min^{-1}).

The fit is considerably improved if the heterogeneous behaviour of the mineral particles is accounted for and distributed rate constants are used. Kelsall [1961] separated the floatable particles into fast floating and slow floating classes, each class with a differing rate constant. More phenomenologically correct, but complex, models have also been proposed but due to the difficulties in the measurements of some of the parameters, they are not suitable for predictive use [Fichera and Chudacek, 1992].

1.2.2.1 KLIMPEL MODEL

Klimpel [1984] developed the model first proposed by Huber Panu et al [1976] where the flotation process was divided into two regimes, viz. a rate controlled and an equilibrium, or ultimate recovery controlled regime. Two constants, R and k , are used to describe these characteristics and can be obtained from the following modified first order model of the recovery - time data, viz.

$$r = R \{1 - (1/kt)[1 - \exp^{-kt}]\}$$

where r = recovery at time t (%),
 R = infinite time recovery (%),
 k = rate constant (min^{-1}).

The rate constant k' represents the maximum rate constant of a distributed function $f(k)$, where $f(k)$ is a probability density function between 0 and k' .

1.2.3 INFLUENTIAL PARAMETERS IN FLOTATION

There are many factors that affect the flotation processes, both directly and indirectly. Crozier [1992] has listed over 25 clearly identifiable parameters which can be more fully described by over 100 variables which affect the flotation performance.

Klimpel [1984] has divided the major variables into 3 interactive groups, viz. the equipment components, the operation components and the chemical components. The interactive nature of these components makes it very difficult to analyse the effect of any particular component and careful planning and analysis of experiments is necessary to interpret the effects on performance of a particular parameter.

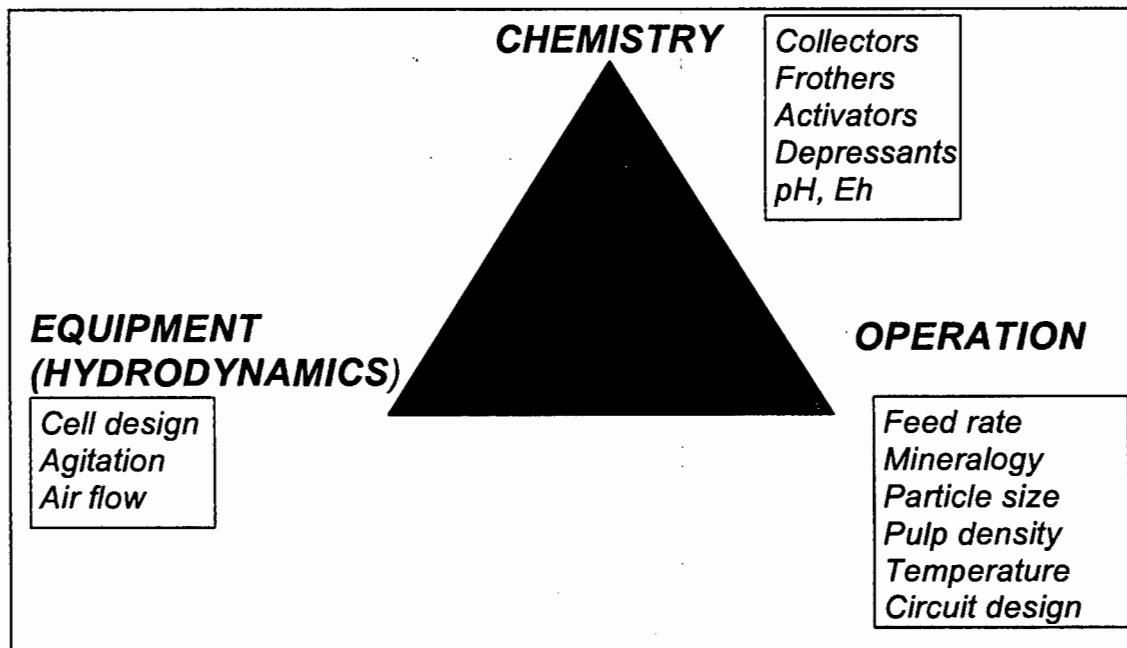


Figure 1.3: Triangular representation of flotation [Klimpel, 1984]

1.2.3.1 EQUIPMENT COMPONENTS

These factors include the cell design and size, the impeller type and speed, the method of bubble generation, bubble size and air flow rate. Decreasing the bubble size for the same gas flow rate increases both the collision and attachment efficiencies [Anfruns and Kitchener, 1976]. Gorain et al [1995] have demonstrated the linear relationship between the flotation rate constant and the bubble surface area flux passing through the flotation cell.

Although these factors strongly influence the successful operation of a flotation plant the investigation of the equipment parameters is not the focus of this thesis and therefore no further details are included.

1.2.3.2 OPERATIONAL COMPONENTS

These factors include the mineral and gangue types, circuit design, pulp feed rate, particle size distribution and pulp density. The two operational components that require further discussion due to the focus of this thesis are the mineral type and particle size effects.

1.2.3.2.1. MINERAL TYPE

Minerals are defined as the naturally occurring inorganic compounds of defined structure containing some element of economic value to be extracted. The nature of the mineral to be beneficiated and the nature of the undesired gangue in the mined ore determines the necessary flotation conditions and more specifically the nature of the collector to be used. This thesis investigates the flotation of pyrite, which is a sulphide mineral that requires an anionic collector (cf. Sec. 1.4.2).

Sulphide minerals oxidise in the presence of air and the extent of oxidation of the mineral surface is determined by the chemical environment, resulting in the dissolution of ions which also affects the chemical environment and the overall flotation performance.

The role of the mineral in the collector - mineral adsorption reactions is discussed in Sections 1.4.2 and 1.4.5.

1.2.3.2.2 PARTICLE SIZE EFFECTS

The particle size of the mineral affects the particle collision and collection sub-processes and has been investigated in numerous studies, viz. Trahar and Warren [1976], Crawford and Ralston [1988] and Finch and Dobby [1990]. The collection efficiency has been defined as the product of the collision efficiency (E_C), the attachment efficiency (E_A) and the detachment efficiency (E_D) (cf. Sec. 1.2.2).

The particle size affects all these efficiencies in different ways. The collision efficiency is a combination of the interception effect of the particle by the bubble, the gravitational effect and the inertial effect. The collision efficiency increases with increase in particle size and is particularly low for particles below 20 μm [Ralston, 1994, Schulze, 1989].

The attachment efficiency increases with decreasing particle size and increasing contact angle or hydrophobicity [Ralston, 1994]. The particle size limits of the flotation domain are governed by the hydrophobicity of material to be floated. Crawford and Ralston [1988] showed that the size limits of flotability can be extended by improving the hydrophobicity of the material as measured by the contact angle.

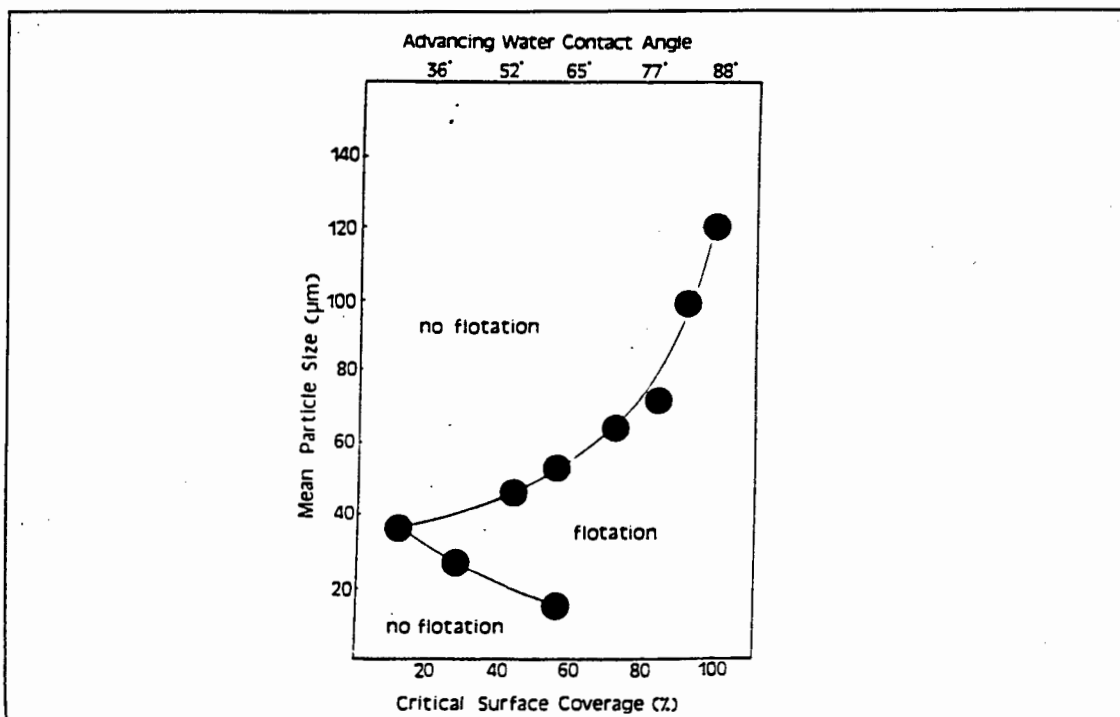


Figure 1.4: Flotation threshold values as a function of particle size showing the existence of a flotation domain [Crawford and Ralston, 1988]

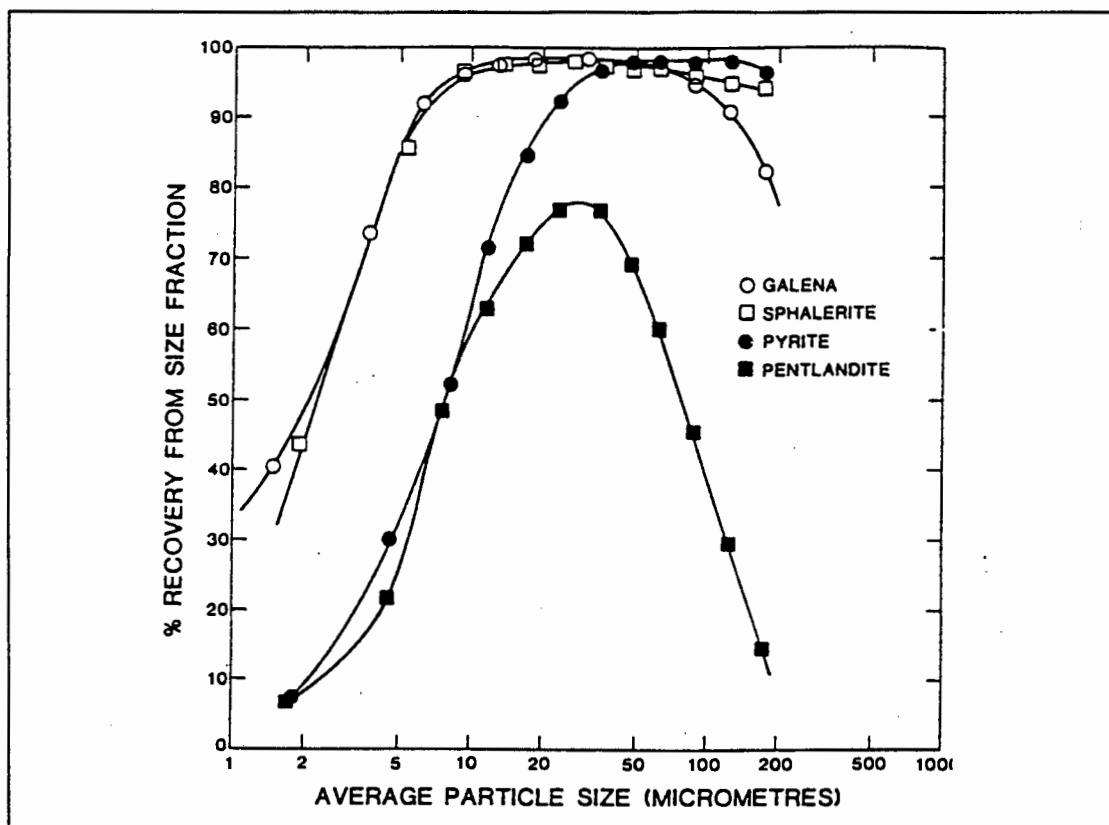


Figure 1.5: Size by size recovery of selected sulphide minerals after 60 secs flotation [Jowett, 1979]

However, increasing the hydrophobicity of the fine particle sizes, below 10 μm , as measured by reduced induction time, has less effect on the attachment efficiency than similar increases of hydrophobicity on coarse particles [Finch and Dobby, 1990].

The detachment efficiency of the mineral particles increases with increase in particle size and turbulence or hydrodynamics of the system [Woodburn et al, 1971; Jowett, 1979 and Finch and Dobby, 1990]. These factors contribute to the existence of a flotation domain with upper and lower limits of particle size in any particular system. Imaizumi and Inoue [1965] reported that the optimum particle size range for pyrite was between 50 and 150 μm . Jowett [1979] showed that the upper limit for pyrite in another system was over 200 μm (Figure 1.5).

Trahar [1981] showed that the entrainment of gangue material into the froth increases with decrease in particle size. This provides the lower size limit of effective mineral separations and a means to diminish the entrainment contribution is required.

1.2.3.3 CHEMICAL COMPONENTS

As shown in Figure 1.3 there are many factors that make up the chemical environment. These factors are interactive, viz. the pH affects the oxidation potential of the pulp (Eh) which in turn affects the state of the mineral surface, and this determines which collector - mineral reactions are possible or dominant. Some of the factors are more easily controllable or manipulated than others. Reagents are added to manipulate the environment to improve the mineral separation possible, but these too, interact.

The reagents are categorised according to the role they fulfil in the flotation process. The categories of reagents are not mutually exclusive however and

reagents can have different roles according to the particular flotation system. Some frothers have collecting properties and some collectors have frothing properties. Depressants and dispersants also often have interchangeable functions.

1.2.3.3.1 COLLECTORS

The predominant function of collectors is to selectively induce hydrophobicity onto the desired mineral. Collectors are therefore concentrated at the mineral - water interface. Collectors are heteropolar molecules containing a non-polar hydrocarbon chain (hydrophobic contribution) and a polar group that interacts with the mineral surface. The non - polar group creates the hydrophobic surface in contact with the water.

The mechanism of mineral - collector bonding depends on the collector type and mineral surface nature and charge and can result in the collector being physisorbed or chemisorbed (cf. Sec. 1.4.5).

1.2.3.3.2 FROTHERS

Frothers are added to stabilise bubble formation, to create a reasonably stable froth, to allow selective drainage from the froth of entrained gangue and to increase the flotation kinetics. Frothers are non-ionic heteropolar molecules. The polar end of the frother molecule forms hydrogen bonds with the water and no mineral - frother bonds are formed. The non-polar end is hydrophobic so that the frother concentrates at the air - water interface. The frother is thus described as being surface active. This affects the surface tension and comparisons of surface tension measurements have been used to indicate differences of different frothers in surface activity [Klimpel and Hansen, 1988].

In general, increased surface activity results in increased persistence and froth stability.

1.2.3.3.3 DEPRESSANTS AND DISPERSANTS

It is often difficult to distinguish between these classes of reagents and the terms are used interchangeably. The role of both of these reagents is to reduce the collection of unwanted gangue material, typically talc or other oxide minerals. This is done by either enhancing the hydrophilic nature of the gangue surface or by preventing the formation of hydrophilic species on the mineral surface. Dispersants achieve this by preventing the coating of unwanted slimes on the mineral surface. Mechanisms of depression also include the formation of large aggregates and the complexation of the collector in solution [King, 1972].

1.2.3.3.4. ACTIVATORS

These are reagents which are used to enhance flotation performance. Commonly used activators are copper sulphate, (CuSO_4) and sodium sulphide or bisulphide, which is used as a sulphidising reagent for tarnished or oxidised ores.

Copper sulphate was first patented as an activator by Bradford in 1913 [Sutherland and Wark, 1955] and is widely used for sulphide minerals. The predominant use is the copper activation of sphalerite which has been extensively investigated [Finkelstein and Allison, 1976; Ralston and Healy, 1980; Yoon, et al, 1995 and Laskowski et al, 1996]. Zeta potential and microflotation studies of the activation of sphalerite by copper ions by Yoon et al [1995] and Laskowski et al [1996] have highlighted the differing mechanisms occurring at acidic and alkaline conditions.

The copper activation of pyrite is part of the focus of this thesis and this topic is more fully discussed in Section 1.4.4.

1.2.3.3.5 pH AND Eh MODIFIERS

Flotation is generally sensitive to pH, which is the measure of H⁺ ion concentration and strongly influences the chemistry of the system. This is also described by the Eh of the system which is a measure of the oxidation - reduction potential of the system, also known as ORP. Eh refers to the pulp potential measured relative to the standard hydrogen electrode. These parameters are generally modified by the same reagents although they can be varied or controlled independently of each other.

1.2.3.3.6 WATER

The mineral separation takes place in the medium of water and both the characteristics and nature of the water molecules as well as the presence of other dissolved salts and ions affect the flotation process. Water is in contact with both the valuable mineral and unwanted gangue and the different interactions determine the outcome of the separation.

The distinctive behaviour of water is attributed to its molecular structure which results in the key interactions of hydrogen bonding and the hydrophobic forces [Israelachvili, 1992]. Hydrogen bonds, which are directional electrostatic bonds, stronger than Van der Waals forces and weaker than covalent bonds, cause the water molecules to become associated with each other. Each water molecule forms four linkages with other molecules resulting in a tetrahedral co-ordination of water molecules. This tetrahedral character allows the formation of three dimensional networks and gives water structure a versatility comparable to carbon or silicon.

When water molecules come into contact with non - polar molecules, such as the hydrocarbon chain of the collector on the mineral surface, they re-orientate so as to preserve the existing hydrogen bonds. Thus a "cage," known as a clathrate, is formed around the non - polar molecule. These water molecules are more structured than those in the bulk, although the bonds are no stronger. This ordering of the molecules is driven by entropy and the force causing it is known as the hydrophobic force.

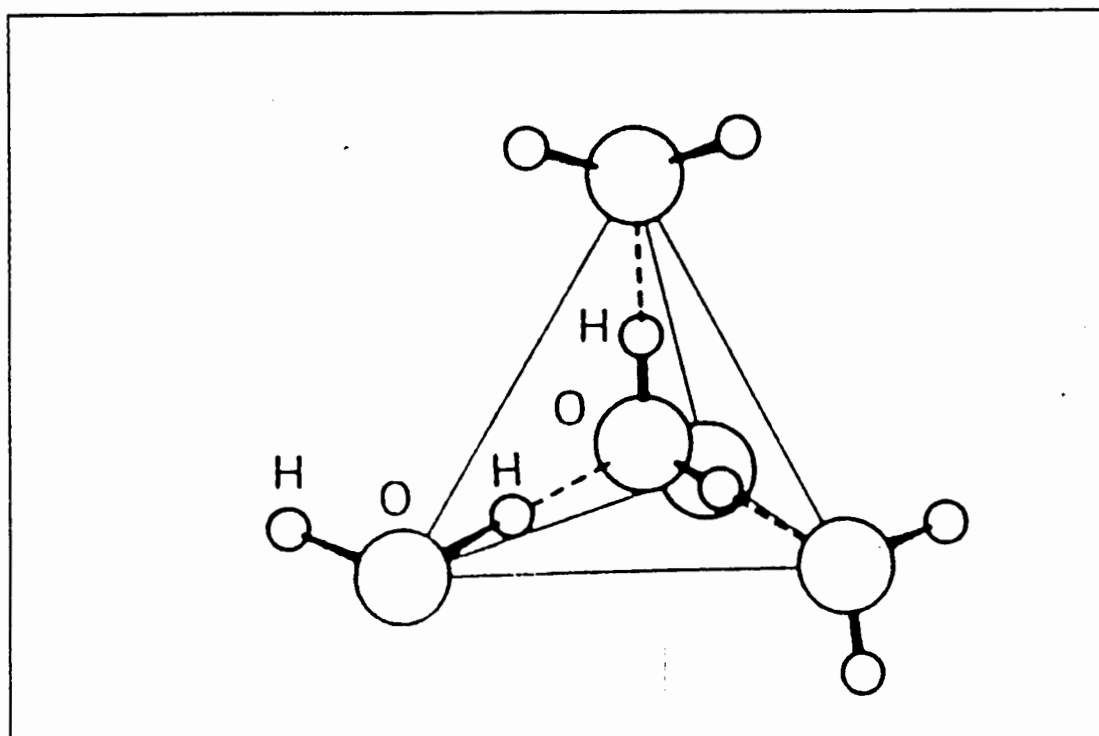


Figure 1.6: The tetrahedral structure of water molecules [Israelachvili, 1992]

In the case of a hydrophilic gangue particle there is no repulsive force, or pressure on the hydrogen bonding so that the gangue remains associated with the water and can only be 'collected' by entrainment.

Dissolved salts, resulting from either contaminated ground water, upstream process such as milling or from the recycle have also been shown to affect the performance of the collectors and frothers [Hodgson and Agar, 1989; Barker, 1984; Levay, 1996].

1.2.3.3.8 INTERACTIONS BETWEEN CHEMICAL PARAMETERS

As noted at the outset of Section 1.2.3, all the factors influencing flotation interact to a greater or lesser extent, viz. the pH and Eh of the pulp, influence the oxidation of the mineral surface which affects the mineral - collector reactions. One of the important chemical interactions is the collector - frother interactions [Lekki and Laskowski, 1971; Lekki and Laskowski, 1975; Crozier, 1992]. The collector is predominantly present on the surface of the mineral and the frother is predominantly present at the surface of the bubble and in the bulk solution. At the moment of mineral - bubble collision there will be interactions between the frother and the collector molecules which influence the attachment of the particle to the bubble.

Lekki and Laskowski [1975] proposed a method to identify the optimum dosage of frother and collector by testing a grid of dosages of both reagents and then calculating contours of equal recoveries and of equal grades. This method could be extended to test the effect on flotation performance of dosage and proportional addition of different collectors. This method of experimental design is also known as surface response methodology.

1.3. MEASUREMENT OF HYDROPHOBICITY AND FLOTABILITY

The terms hydrophobicity and flotability are both used to characterise the mineral surface's susceptibility to flotation and are often, incorrectly, used interchangeably. In the past, measurements of hydrophobicity have been used to predict flotation with varying success. The definitions, measurements and limitations of these two different characteristics are discussed in the following sections.

1.3.1 SURFACE HYDROPHOBICITY

Hydrophobicity refers to the ability of the mineral surface to repel water and so favour attachment to a colliding air bubble. Upon contact with a non-polar surface, the water molecules reorientate to form clathrates in order to minimise the hydrogen bond disruption [Israelachvili, 1992] (cf. Sec. 2.2.3.6). This is a thermodynamic equilibrium property and is represented by the following formula known as Young's equation, viz.

$$\Delta G^{xs} = \gamma_{Lg}(1 - \cos \theta)$$

where ΔG^{xs} = Change in Gibbs free energy,
 γ_{LV} = Surface tension between liquid and gas,
 $\cos \theta$ = Aqueous contact angle between the mineral surface and bubble.

This equation is the thermodynamic criterion of flotation, the larger the contact angle, θ , the more negative ΔG^{xs} and the higher the probability of flotation.

Measurement of these parameters can be used to indicate surface hydrophobicity, which is also known as the thermodynamic probability of flotation. The most well known method to measure hydrophobicity is that of contact angle and this is discussed further in Section 1.3.1.1. Other measurements that have been used to describe surface hydrophobicity are: The critical surface tension of solid wetting (γ) [Hornsby and Leja, 1983; Finch and Smith, 1979]; Gibbs free energy (G^{xs}) [Davidtz, 1994]; and Bubble pick up index (PI) [Sun, 1957; Lee, 1969].

1.3.1.1 CONTACT ANGLE (θ)

Generally the contact angle is measured between the bubble generated on the end of a glass capillary and a polished section of mineral with a goniometer. The more hydrophobic the mineral, the larger the angle between the air bubble and mineral surface. In subsequent studies Crawford and Ralston [1988] have showed the relationship between particle size and contact angle in flotation. They identified a flotation domain determined by particle size and contact angle within which flotation is possible, showing that contact angles are a factor but are not the sole criterion for flotation (cf. Sec. 1.2.3.2.2). Jowett [1979] also showed the dependence of critical particle size for aggregate disruption on mineral density and contact angle in flotation.

The contact angle was shown to be dependent on the nature of the adsorbate. Collectors with different functional groups but the same alkyl group have been shown to give the same contact angle [Sutherland and Wark, 1955]. The contact angle is unaffected by the nature of the mineral [Ravindrath and Patel, 1969]. Ravindrath and Patel [1969] showed that the characteristic contact angles for di-ethyl, di-iso-propyl, di-n-butyl and di-iso-butyl were the same for both xanthates and dithiocarbamates, viz 60°, 72°, 74° and 81° respectively. These were also characteristic of the best results for any of the sulphide minerals tested. These results show that although differences in alkyl chain length could be measured, differences in functional group could not be tested using contact angle measurements.

Contrary to these indications, different collectors show different flotation responses [Leja, 1982, Crozier, 1991]. Flotation has also been achieved at conditions where zero contact angles have been recorded [Finch and Smith, 1979; Crozier, 1991]. The recently developed method of Prestidge and Ralston [1996] using mineral particles and not mineral "slabs" shows the potential for more reliable measurements, however the measurement of contact angle remains a thermodynamic measurement, and flotation is a kinetic process.

Leja [1982] reports that "...contact angle measurements are an indicator and not a measure of flotation performance..." Laskowski [1986] also notes that although the formation of a contact angle is a prerequisite to flotation it may be of no practical significance and it is now widely recognised that a more meaningful characterisation of the surface is necessary [Woods, 1994].

1.3.1.2 LIMITATIONS OF HYDROPHOBICITY MEASUREMENTS

All the measurements of hydrophobicity are thermodynamic equilibrium values and are not necessarily related to rate of flotation, nor are they necessarily controlled by the same variables [Laskowski, 1986]. Although the thermodynamics of the system, *per se*, will determine whether or not flotation will take place, other criteria, such as the kinetics, hydrodynamics or mineral size may overshadow the thermodynamic criteria in determining the success of the flotation process.

This means that the thermodynamic measurements do not fully describe the effectiveness of the collector in creating a hydrophobic mineral surface. Other measurements are proposed as better indicators of the success of the collector in creating a hydrophobic surface.

1.3.2 PARTICLE FLOTABILITY

Flotability refers to the ability of the mineral particle in a flotation pulp to be removed by attachment to an air bubble and reflects the surface properties of the mineral, the hydrodynamic conditions and the pulp environment and is a function of mineral size. In contrast to hydrophobicity measurements, flotability measurements include both the thermodynamic and kinetic aspects of the process and thus are considered more representative or reliable indicators of the collector effectiveness and overall flotation process. Flotability

measurements include; The induction time (μ) [Jowett, 1979; Ye et al, 1988; Finch and Dobby, 1990 and Schulze, 1989]; The Microflot Flotability Index (MFI) [Chudacek and Fichera, 1991]; Flotability Measure (L) [Drysmala et al, 1992]. The technique of bubble loading is used in this thesis and is thus discussed in more detail (Section 1.3.2.1).

1.3.2.1 BUBBLE LOADING

Bubble loading can be defined as the mass of mineral collected by the air bubbles and can be reported as

mass mineral / individual bubble;

mass mineral / m^2 of bubble surface area;

mass mineral / max possible for bubble of that size which can be calculated as a function of the mineral density [Szatkowski and Freyberger, 1985].

Bubble loading gives a dynamic measure of flotability taking into account the hydrodynamics of the system under investigation. It can be used to investigate the effect on flotation of parameters such as particle size, frother and collector type or dosage.

The focus of previous studies was to include a bubble loading term in the modelling of the overall process. King et al [1974] developed an apparatus to hold a bubble stationary in a moving pulp so that the loading could be measured. They correlated the available surface area on the bubble to the collection efficiency and thus to the rate of flotation.

Szatkowski and Freyberger [1985] calculated the amount of air required to carry a given mineral load (Flotation Air Factor). Their model was constructed on the assumption that the three most important phenomena governing flotation are the collection efficiency, rate of bubble coalescence in the pulp and the

buoyancy of the mineral laden particles. They identified the critical bubble diameter as a function of the density and size fraction of the mineral to be floated, below which a fully loaded bubble would not rise, viz.

$$d_b^{cr} = N_p d_p^3 (\rho - \rho_w) / \rho_w$$

where N_p = Number of particles per bubble,
 d_p = Diameter of particle (cm),
 ρ = Particle density (g/cm³),
 ρ_w = Density of water (g/cm³).

The maximum load that each bubble can carry and still rise is;

$$M_{max} = V_b (\rho - \rho_{air})$$

where V_b = Volume of bubble (cm³),
 ρ = Particle density (g/cm³),
 ρ_{air} = Density of air (g/cm³).

Hewitt et al [1994] measured the bubble loading of quartz for different particle and bubble sizes in order to quantify the collection efficiency.

Bubble loading as a technique takes into account the thermodynamic as well as the kinetic properties of the flotability of the mineral particle and was evaluated as the best potential measure of collector effectiveness for use in this thesis. A method was developed to compare the difference in bubble loading behaviour obtained with different collector types. (cf. Ch. 4).

1.4. MINERAL - COLLECTOR INTERACTIONS

1.4.1 METHODS OF IDENTIFICATION

A wide range of techniques, both direct and indirect, have been used to identify and analyse the surface reactions. There are confusions and discrepancies between much of reported data for the same mineral - collector interactions. This is largely attributed to the complexity of the interactions and the sensitivity of the measurements [Chander, 1991]. Some of the spectrophotometric measurements are *ex situ* and require the sample to be under vacuum, whereas others are *in situ* and can be analysed in the aqueous solution. Some compounds have also been mistakenly identified due to poor assignments and the presence of overlapping peaks, viz. Winter [1975] reported the similarity of the IR spectra of dixanthogen and sulphur dixanthate; Finkelstein and Poling [1977] report the mistakes arising from solvent extraction techniques and Wang [1995] reports that the similarity of the IR spectra of dixanthogen and ferric xanthate can lead to misinterpretation. Methods of analysis can be divided into four main categories: Spectrophotometric, Thermochemical, Electrochemical and Solubility measurements.

1.4.1.1 SPECTROPHOTOMETRIC MEASUREMENTS

Ultra violet spectroscopy, which is an indirect method of analysis and can be used to confirm the kinetics of the reaction mechanisms. The rate of disappearance of the collector from solution is monitored using the absorbance of the collector at a specified wavelength as a measure of concentration using the Beer Lambert law, viz.

$$A = \epsilon b C$$

where

- A = Absorbance of clear solution at set wavelength,
- ϵ = Molar extinction coefficient, ($l \text{ moles}^{-1} \text{ cm}^{-1}$),
- b = Path length of radiation (cm),
- C = Molar concentration (moles l^{-1}).

The collector leaving the bulk solution is assumed to report to the mineral surface. In cases where chemisorption is the collector adsorption mechanism and monolayer coverage of the mineral occurs, adsorption isotherms can be plotted for different temperatures and the activation energy of the reaction calculated [Haung and Miller, 1978].

Other spectrophotometric methods include: Infrared spectroscopy, [Leja et al, 1963; Leppinen, 1990; Leppinen et al, 1989]; X-Ray photoelectron spectroscopy [Smart, 1991]; Time of flight laser ionisation mass spectroscopy (TOF LIMS) and time of flight secondary ion mass spectroscopy (TOF SIMS) [Stowe et al, 1994; Kim et al, 1995; Nagaraj and Brinen, 1995 Nagaraj, 1995].

1.4.1.2 THERMOCHEMICAL MEASUREMENTS

Chemical reactions are accompanied by enthalpy changes and by measuring these enthalpy changes and correlating these to known possible reactions the reaction mechanisms can be elucidated. Thermochemical measurements with thiol collectors and various sulphide minerals have been reported by Mellgren [1966], Mellgren and Rao [1968], Rao [1972], Mellgren et al [1973] and Haung and Miller [1978].

Measurements can be isothermal, in which the reactor temperature is kept constant and the heat flux required to keep the temperature constant is measured, or isoperibolic in which the temperature change inside the reactor is measured.

Isothermal measurements may be made by titrating the collector with a motor driven burette into the reactor containing the mineral pulp. A disadvantage of this method is that the water is in contact with the mineral slurry until constant temperature is established and mineral surface oxidation may take place.

In the isoperibolic measurement a sealed ampoule is positioned in the reactor containing the reagent. The ampoule is broken with the breaking rod to start the test. This method also has its disadvantages as the mineral surface may not be "clean" and the heat of wetting must be taken into consideration.

The interpretation of the thermochemical measurements must be made with a knowledge of the chemical reactions involved. Mellgren [1966] interpreted the reactions occurring between ethyl xanthate and galena in the light of those occurring between ethyl xanthate and various lead salts. He reported that the heat of reaction obtained with ethyl xanthate and galena was the same as that obtained for the corresponding bulk lead salt and could be interpreted as the formation of the metal thiolate. Mellgren and Rao [1968] showed that the correlation of reactions was also the case for diethyl dithiocarbamate.

The enthalpy change (ΔH) due to chemisorption is considerably larger than the heat of physisorption. Adsorption processes with ΔH values less negative than -25 KJ/mole are regarded as involving physisorption and values more negative than -40 KJ/mole are regarded as chemisorption [Persson, 1993].

1.4.1.3 ELECTROCHEMICAL MEASUREMENTS

Electrochemical methods are used to control the state of oxidation of the mineral and collector, determine the type and amount of electroactive species at the surface and study the kinetics of the electrode processes. These measurements include: Cyclic Voltametry [Chander, 1988]; Potentiometry [Finkelstein and Goold, 1972; Persson, 1993]; Zeta Potential Measurements [Hanson and Fuerstenau, 1993].

1.4.1.4 SOLUBILITY MEASUREMENTS

Taggart and Hassialis [1946] first proposed the theory that the hydrophobicity of the mineral surface formed between the collector and the mineral surface depended on the solubility of the collector mineral salt formed. This was in accordance with the Paneth - Horovitz principle which relates the adsorption of an element onto a solid to the insolubility of the salt formed on the surface of the solid [Sutherland and Wark, 1955]. It follows that the collectors that formed the more insoluble metal salts on the mineral surfaces were credited with creating the surfaces more susceptible to flotation. This theory was used by Glembotsky et al [1988] and Glembotsky et al [1995] to select dithiocarbamates as a class of reagents with better potential than xanthates as collectors.

Yoon and Basilio [1993] developed the Paneth - Horovitz principle in conjunction with the organic electrochemistry mechanism known as the coupled electrochemical and chemical reactions of the EC type [Nicholson and Shain, 1964]. They correlated the solubility products of the adsorbed species of different collectors to the reaction product formed on the surfaces of different minerals (cf. Sec. 1.4.5). They reported that the pK_{sp} values for the thionocarbamates were approximately ten orders of magnitude larger than those of xanthates. Consequently, with certain minerals, thionocarbamates formed the metal thiolates and with xanthates the dithiolates (dixanthogen) were formed.

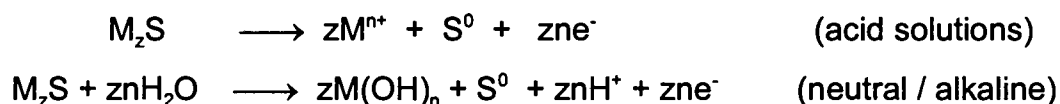
1.4.2 THE ROLE OF THE MINERAL

1.4.2.1 SULPHIDE MINERALS

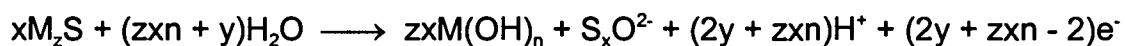
Deposits of sulphide minerals are found throughout the world and are important as the primary source of the majority of base metals beneficiated using flotation. The structure and characteristics of sulphide mineral samples from

different locations vary [Wards, 1996] and this results in differences in the flotation behaviour of samples [Bothelho de Sousa, 1984]. The reactions of these minerals, such as the oxidation characteristics and interactions with water or other reagents used in flotation are known to strongly influence the conditions necessary for successful flotation.

The surface of sulphide minerals oxidise in the presence of water and oxygen, with the reduction of oxygen being facilitated by the semiconducting properties of the mineral. This oxidation hinders flotation performance, however in some circumstances reduced performance can be overcome by increased collector addition [Leja, 1982]. Different sulphide minerals oxidise at different rates and the extent of oxidation and the product of oxidation depends on the mineral under investigation, pH, time of contact [Subrahmanyam and Forssberg, 1993]. The general sulphide oxidation proceeds as follows;



Further oxidation may form the oxy - sulphur species



In general the minerals which oxidise to form sulphur exhibit the highest flotation rates [Woods, 1984] and while the sulphur rich surface can promote flotability the presence of oxy - sulphur species depresses flotation. Hydroxide species also suppress flotation by forming on the metal deficient sulphur surfaces.

Majima and Peters [1969] measured the rest potentials of ten sulphide minerals in water at pH = 4. Table 1.1 shows that pyrite had the highest rest potential and was the most readily oxidised mineral.

Table 1.1: The rest potentials of various sulphide minerals in water at pH = 4 [Majima and Peters, 1969]

<u>Mineral</u>		<u>Rest Potential</u> (V vs. SHE)
Molybdenite	MoS ₂	0.11
Stibnite	Sb ₂ S ₃	0.12
Argentite	AgS	0.28
Galena	PbS	0.40
Bornite	Cu ₅ FeS ₄	0.42
Covellite	CuS	0.45
Sphalerite	ZnS	0.46
(Chalcopyrite	CuFeS ₂	0.56)*
Marcasite	(Zn, Fe)S	0.63
Pyrite	FeS	0.66 : most readily oxidized

* (anomalous)

Allison et al [1972] measured the rest potentials of sulphide minerals at pH = 7 in solutions of 6.25×10^{-4} moles of different thiol collectors. Although the trend was not exactly the same as that found by Majima and Peters [1969] in all cases pyrite had the highest rest potentials, viz. 0.21 V with potassium ethyl xanthate and 0.475 V with diethyl dithiocarbamate.

It has been shown that the ease of collectorless flotation of sulphide minerals follows approximately the opposite ranking as the ease of oxidation [Guy and Trahar, 1984]. The order of descending collectorless flotation is as follows; Chalcopyrite > galena > pyrrhotite > pentlandite > covellite > bornite > chalcocite > sphalerite > pyrite > arsenopyrite.

Chalcopyrite is the anomalous mineral, with the highest natural flotability but was not the least susceptible to oxidation as seen in Table 1.1. Chalcopyrite is the anomalous mineral in the sulphide mineral series, as it has the highest natural flotability but not the lowest susceptibility to oxidation in the series.

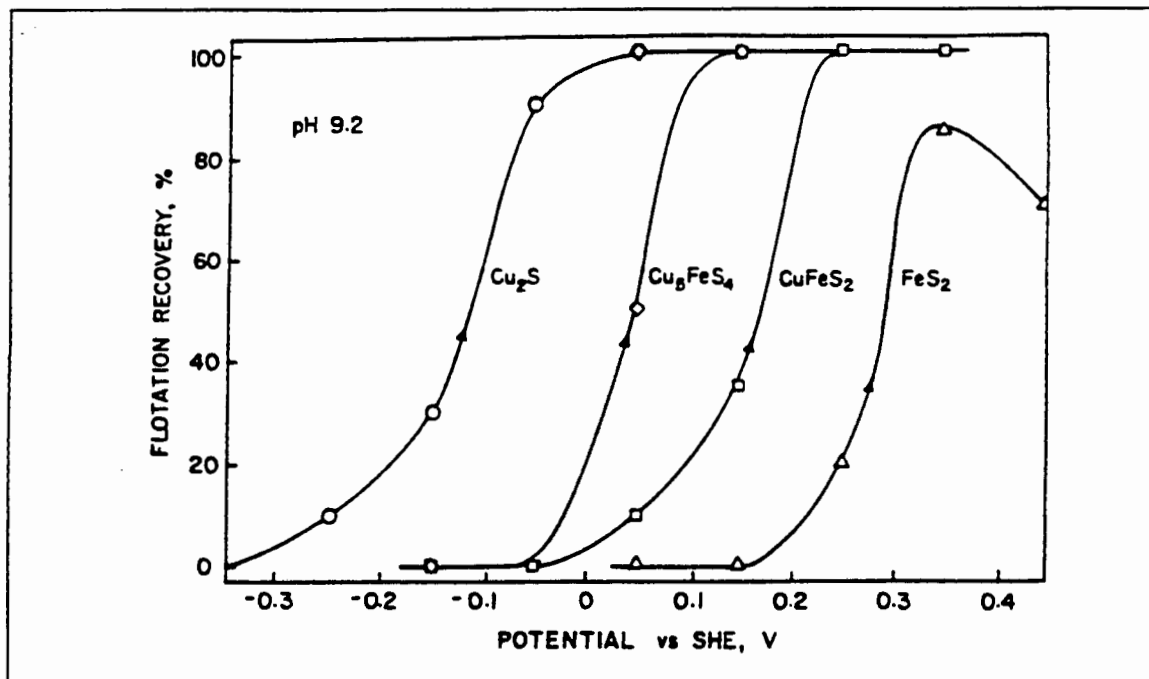


Figure 1.7: The relationship between flotation recovery and conditioning potential for chalcocite, bornite, chalcopyrite and pyrite with ethyl xanthate at pH = 9 [Richardson and Walker, 1985]

Eh affects flotation performance and different minerals have potentials above which flotation is successful. Figure 1.7, from Richardson and Walker [1985] shows that flotation is possible at much lower potentials with chalcopyrite than with pyrite.

1.4.2.1.1 PYRITE

Pyrite has a cubic structure built up of Iron (II), (Fe^{2+}) ions and disulphide, (S^{2-}) ions. Each Fe^{2+} ion is surrounded by six sulphur atoms in an octahedral arrangement and each S^{2-} ion is surrounded by another S^{2-} ions and three Fe^{2+} ions in a distorted tetrahedral configuration as shown in Figure 1.8.

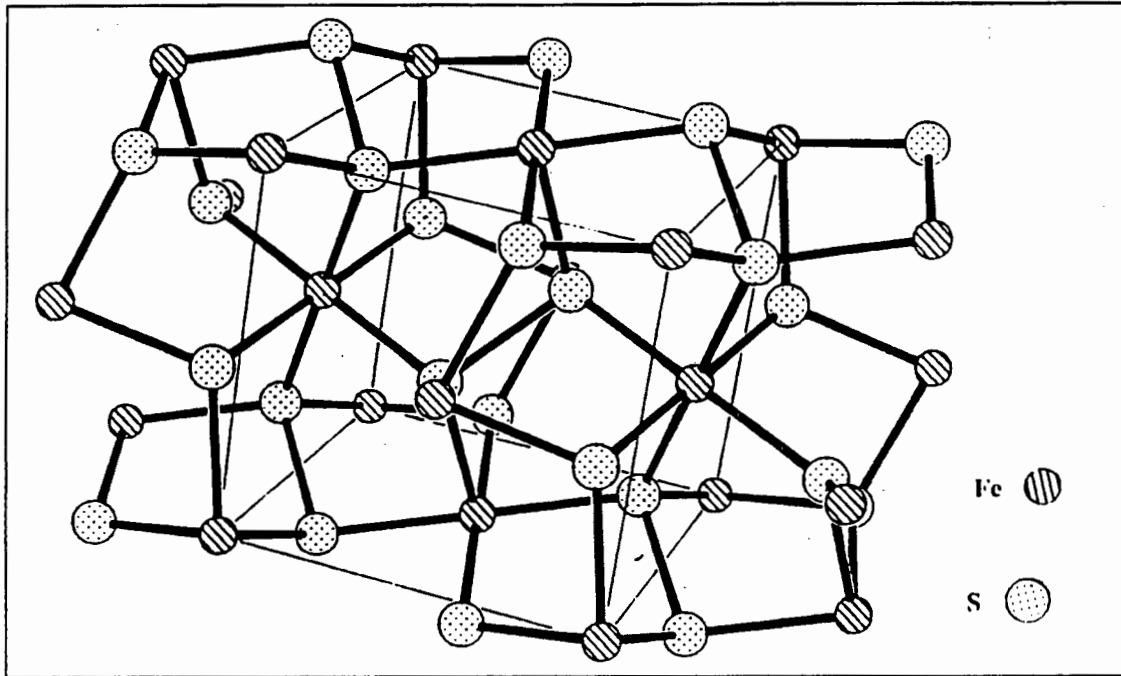
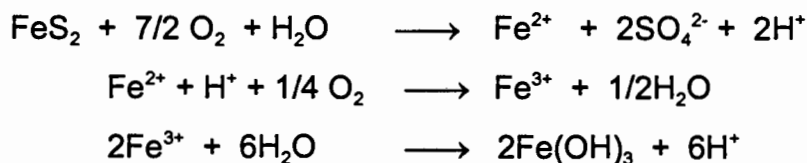


Figure 1.8: The crystal structure of pyrite [Persson, 1994]

It should be noted however that naturally occurring pyrite is more variable in composition and may have inclusions of other minerals relating to its depositional environment [Ball and Rickard, 1976; Wards, 1996]. The differing nature of pyrite samples from different deposits as well as the use of different methods and control of the sample preparation can result in different flotation behaviour being observed at 'similar' conditions [Chander, 1991].

Pyrite is easily oxidised in solution [Majima and Peters, 1969]. Unlike pyrrhotite, the oxidation of pyrite does not result in the formation of elemental sulphur, S^0 , but results in the formation of Fe^{2+} ions and can be described by



The products of the oxidation of pyrite are hydrophilic and inhibit flotation performance. This phenomenon was first reported by Gaudin [1957], who found that pyrite flotation, inhibited by oxidation could be restored after treatment with sodium sulphide. More recently Walker et al [1986], Dimou [1986] and

Kocabag et al [1990] showed the reduction of pyrite flotation performance after oxidation. Pritzker et al [1985] identified that the principal oxidation products at low pH (the conditions for their thesis) were Fe^{3+} and SO_4^{2-} ions.

Figure 1.9 from Kocabag [1990] shows the relationship of Eh and pH to the oxidation products of pyrite formed in water. The formation of Fe^{3+} and SO_4^{2-} ions at low pH is observed, but at slightly lower Eh, at 0.3 V, the iron is in the Fe^{2+} form.

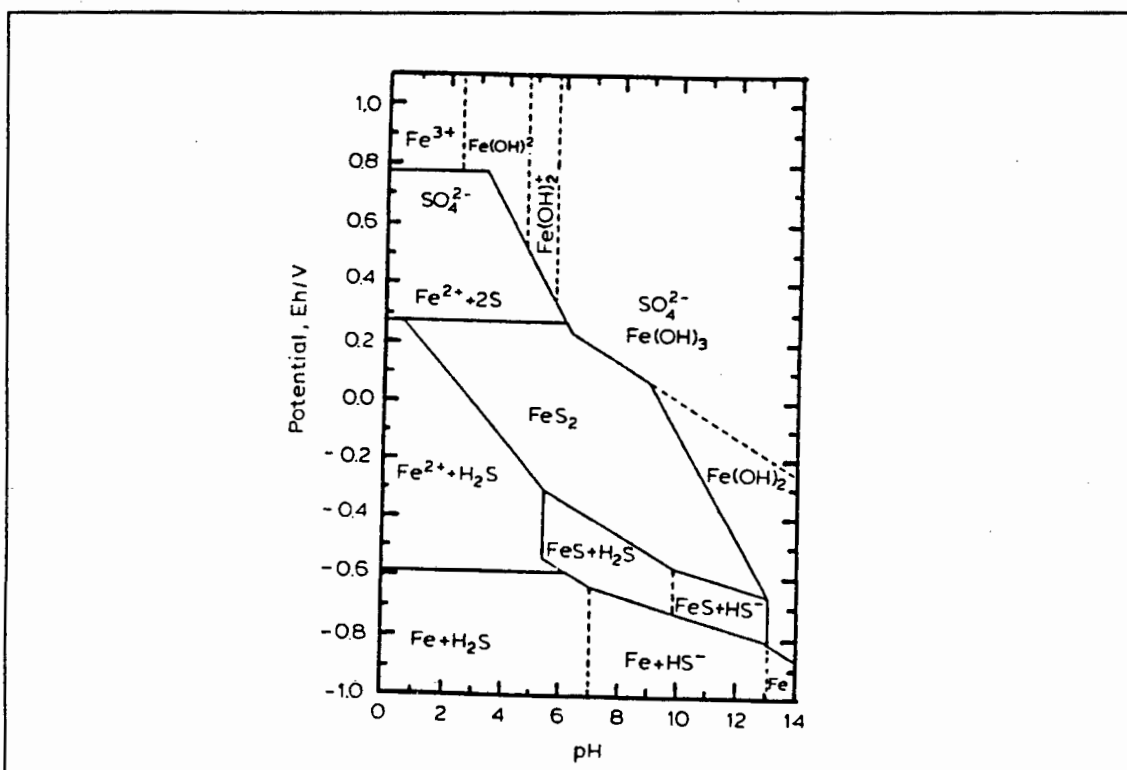


Figure 1.9: The Eh - pH diagram of pyrite in water [Kocabag, 1990]

The competitive role of the collector is to adsorb or react with the mineral surface, preventing the surface oxidation and creating a hydrophobic layer. Xanthate collectors in particular, achieve optimum performance in oxidising conditions (cf. Sec. 1.5.4).

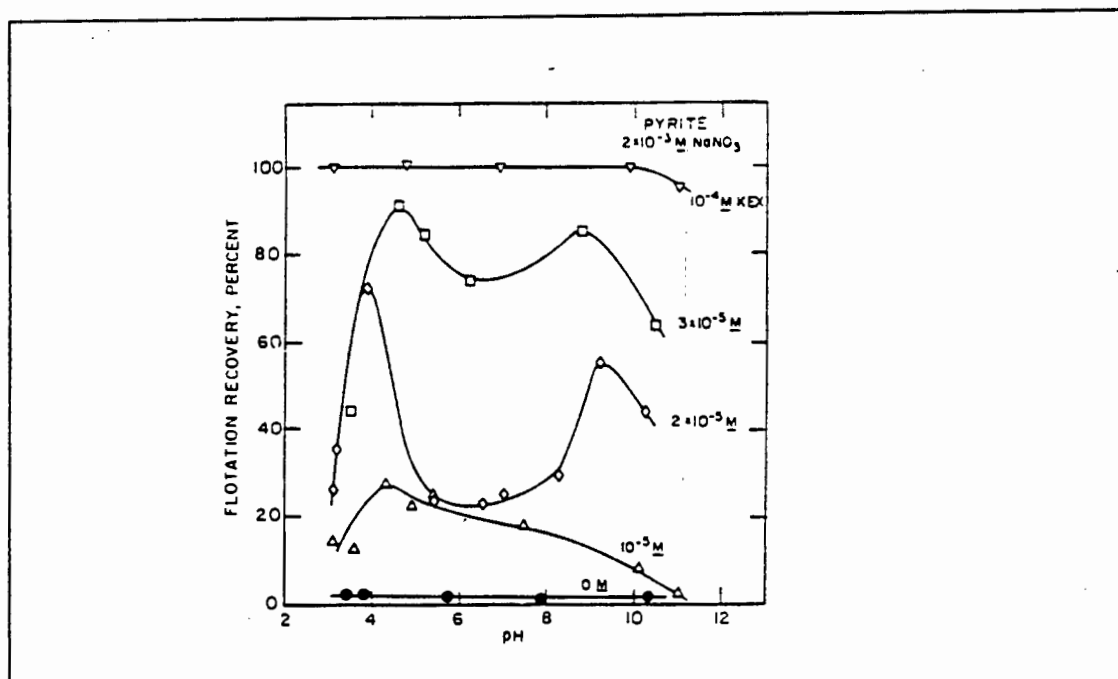


Figure 1.10: The flotation recovery of pyrite in a Hallimond Tube as a function of pH with various dosages of potassium ethyl xanthate (KEX) [Fuerstenau and Mishra, 1980]

Fornasiero and Ralston [1992] showed that the zeta potential of pyrite is strongly affected by the sample preparation, pH and atmosphere of preparation. As expected the point of zero charge (pzc) increases with oxidising conditions such as increasing exposure to oxygen and pH. These tests highlighted the sensitivity of pyrite to oxidising conditions.

Figure 1.10 from Fuerstenau and Mishra [1980] showed that the low flotation performance observed at neutral pH which coincides with the point of zero charge of pyrite at approximately pH = 6 could be compensated for by increasing collector addition.

1.4.3 ROLE OF COLLECTORS

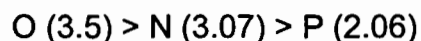
Collectors are classified according to the functional group (cf. Sec. 1.2.3.3.1). The behaviour of the collector is dependent on both the functional group and the alkyl chain [King, 1982].

1.4.3.1 THIOL COLLECTORS

Thiols refer to collectors containing a sulphur molecule that is not bonded to oxygen. The -SH group is known as the sulphydric, sulphydryl or mercapto group. This class of collectors is characterised by their high chemical activity towards metal ions, the absence of surface activity at the liquid - air interface and the absence of aggregation in solution (no formation of micelles) [Leja, 1982]. They are the largest group of collectors Crozier [1992] and are particularly effective for sulphide mineral flotation. Well known collectors in this group are: xanthates (X), dithiophosphates (DTP), dithiocarbamates (DTC), thionocarbamates, mercaptobenzothiazoles (MBT).

Thiol collectors are generally used as the alkali metal salts due to their high solubility and the low effect of the cation on the behaviour of the collector. The choice of cation is dependent on cost and application [Taggart, 1945].

The differences in behaviour of the collectors shown in Figure 1.11 are attributed to the differences in the structure and consequent behaviour of the "donor" oxygen, nitrogen and phosphorus atoms [Nagaraj, 1988]. The electronegativity of these elements on the Pauling scale, which affects both the bonding to the mineral surface and the interaction with water, decrease in the following order



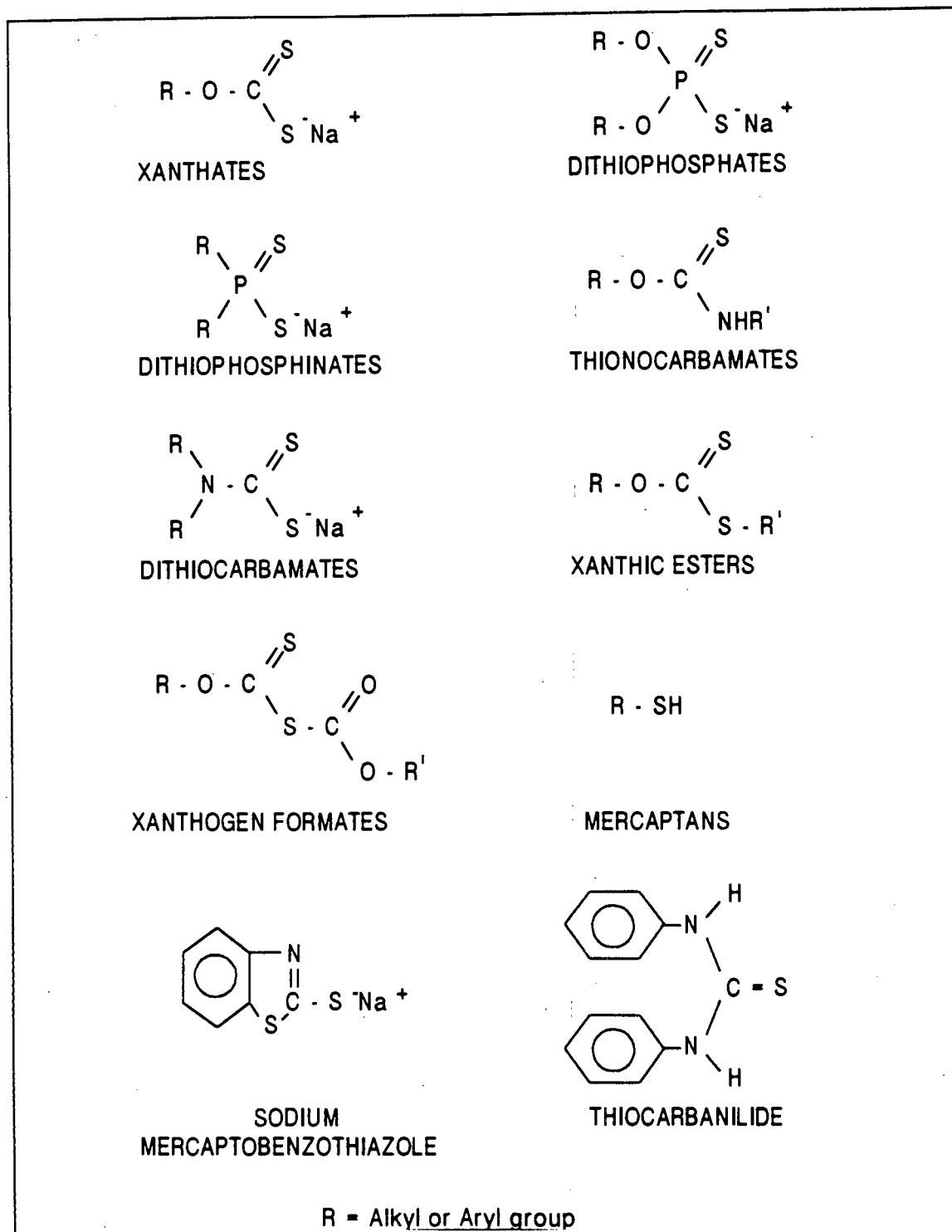


Figure 1.11: Examples of typical thiol collectors [Adkins and Pearse, 1992]

Oxygen has a lone pair of electrons and is the most polar atom of the three and tends to be an electron donor while nitrogen tends to be an electron acceptor. Thus the oxygen molecule in the dithiophosphate and xanthate molecules have strong electron withdrawing effects. This, combined with the phosphorus being more electropositive than the carbon in the xanthate, results in

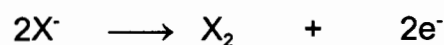
dithiophosphates being stronger acids and weaker, but more selective, collectors [Nagaraj, 1988]. In the case of dithiocarbamates, N is less electronegative than O and has a higher tendency to donate electrons, resulting in a stronger, less selective collector [Bhaskar Raju and Forsling, 1991], so that the following orders of collector strength and selectivity toward the sulphide mineral exist.

Collector Strength	DTC > X > DTP
Selectivity	DTP > X > DTC

This comparison holds for the formation of the metal thiolate on the mineral surface, however, collector oxidation may occur which will change the relationship. The dithiocarbamate and dithiophosphate have the potential for an additional alkyl group in the structure which would also contribute to a greater hydrophobicity than the xanthate, again for all other factors being equal and the collectors undergoing similar reactions. This comparison would hold in the case of all collectors forming the metal thiolate, but may not in the case of the xanthate forming the dithiolate.

The lower collecting strength of dithiophosphates or other short chain collectors can be compensated for by increasing the collector dosage, but too high a dosage is detrimental and for each system there is an optimum dosage Sutherland and Wark [1955].

Collector oxidation will occur if the potential of the system is higher than the oxidation potential of the thiolate to the dithiolate [Finkelstein and Poling, 1977], viz. for xanthates



The standard potential for the oxidation of ethyl xanthate to dixanthogen is -0.06 V and for the oxidation of diethyl dithiocarbamate to the dithiolate is 0.11 V [Finkelstein and Poling, 1972].

The alkyl affects the behaviour of the collector. Harris [1984] showed that the stability of xanthates in solution was affected by the alkyl group of the xanthate and the sequence of increasing stability was

methyl < ethyl < n-propyl < n-butyl < isopropyl

Harris [1984] reported that at pH = 4 the half life of PNBX, the xanthate collector used in this investigation was 0.84 hr. The decomposition was not measured in the presence of ore.

An increase in alkyl chain length decreases the concentration of collector needed for effective flotation and decreases the solubility of the metal salt formed [Taggart, 1945; Kakovsky, 1957].

The nature of the alkyl chain also affects the orientation of the collector molecules on the surface of the mineral and determines the closeness of packing, the cyclic alkyl chain forms an electron sink on the surface and will tend to lie horizontally on the mineral surface whereas the linear chains will tend to be perpendicular to the mineral surface Rosen [1989].

Measurements of contact angle have been used to compare the changes in hydrophobicity of dithiocarbamates, xanthates and mercaptans [Sutherland and Wark, 1955]. Although there are limitations to the information gained from such measurements (cf. Sec. 1.3.1.1), the contact angles illustrated the changing contributions of the alkyl chain to the mineral hydrophobicity. In the case of straight chain alkyl groups, the contact angle increased with increasing chain length. Batch flotation tests with xanthates of varying chain length have also shown this trend of increasing recoveries and grades with increasing alkyl chain [Dimou, 1986].

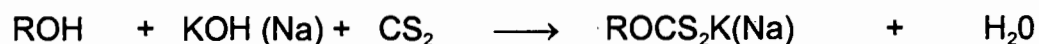
In the case of cyclic or cyclic derivative alkyl groups, the contact angle decreased below that of the butyl collector. In preliminary tests for this thesis,

batch flotation results of dithiocarbamates with different alkyl chains showed that lower recoveries and grades were obtained with the cyclohexyl than with the straight chain dithiocarbamates [Bradshaw et al, 1992].

1.4.3.1.1 XANTHATES

Xanthates, first patented in 1925 are the most widely used flotation collectors and account for over 80% of world usage of thiol collectors [Adkins and Pearse, 1992; Crozier, 1992].

Xanthates are the reaction products of alcohols, carbon disulphide and potassium or sodium hydroxide.



Xanthates undergo different reactions at different conditions as summarised by Cases et al [1993] and the possible pathways for oxidation and hydrolysis of xanthates are shown in Figure 1.12. The reaction pathways shown in Figure 1.12 do not give an indication of rate of reactions. In particular the rate of oxidation of xanthate to dixanthogen, although thermodynamically favourable, is slow. This reaction is catalysed by the presence of metal ions. There is also evidence to show that under certain conditions the formation of dixanthogen goes via the formation of the metal thiolate on the mineral surface [Montaldi et al, 1993; Leppinen et al, 1990; Meilczarski, 1986].

Figure 1.12 also shows that xanthates decompose via the hydrolysis reaction to xanthic acid and then to the original reactants, carbon sulphide and alcohol. The stability of xanthates in aqueous solutions depends on solution pH with the rate of decomposition decreasing with increasing pH [Fuerstenau, 1982; Harris, 1984].

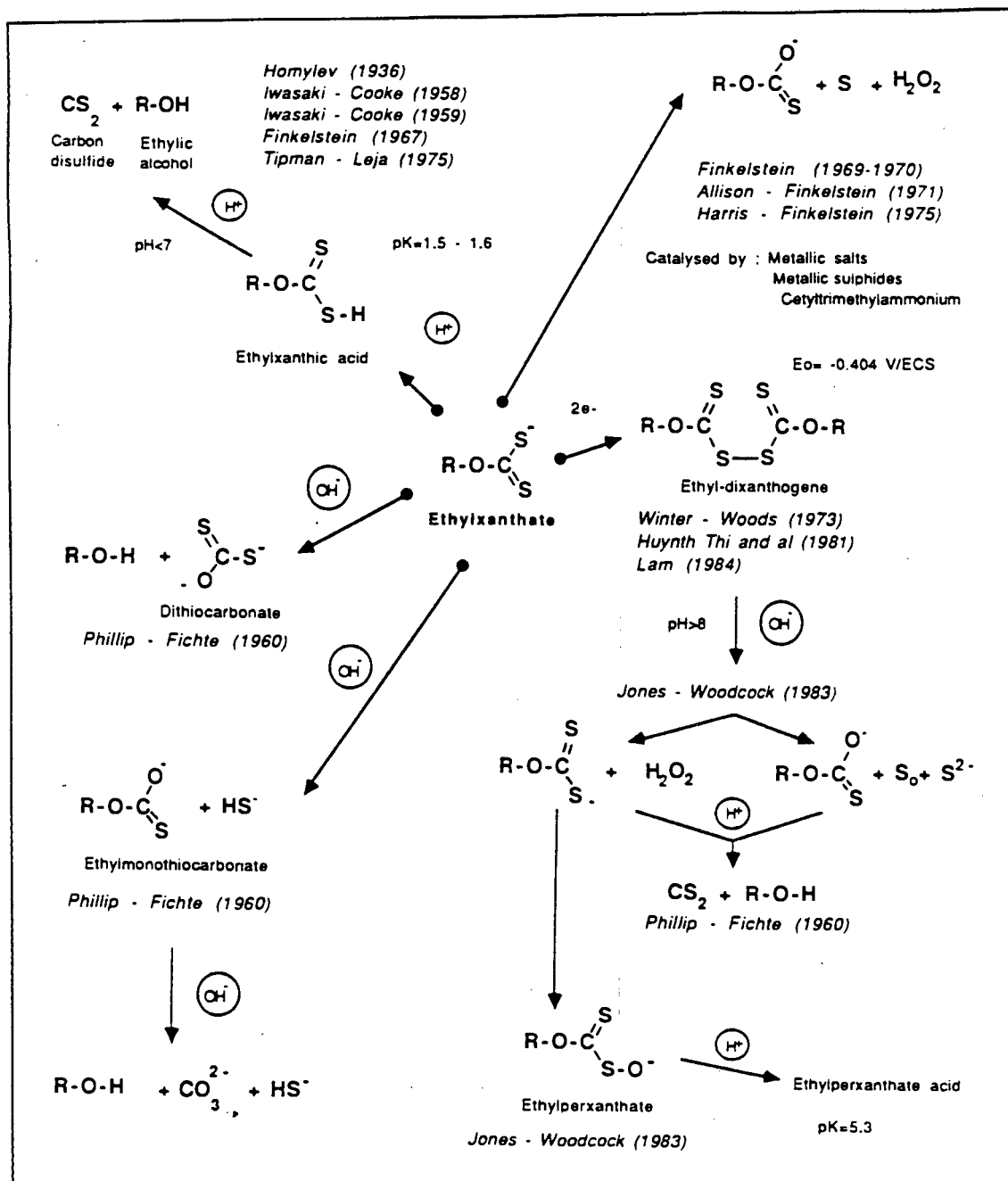


Figure 1.12: A summary of the hydrolysis and oxidation reactions of ethyl xanthate in aqueous solutions [de Donato et al, 1979]

The oxidation of xanthate ions to dixanthogen occurs in the presence of metallic sulphides and metal ions and these reactions are discussed in Section 1.4.5. Xanthate are themselves reducing agents and form the ferrous and cuprous salt in the presence of iron and copper respectively. In the case of the iron being present as Fe^{3+} , initially formed ferric xanthate is quickly reduced to ferrous xanthate [Sutherland and Wark, 1955, Kocabag et al, 1990].

1.4.3.1.2 DITHIOCARBAMATES

Dithiocarbamates are formed as reaction products between carbon disulphide and amines. They were discovered before 1850 and were recognised for their strong bonding properties with metals forming highly insoluble complexes [Thorn and Ludwig, 1962; Poling, 1976; Glembotsky et al, 1995]. Sodium diethyl dithiocarbamate was used extensively in the field of inorganic analysis. In 1945 dithiocarbamates were patented as fungicides and although they were reported as sulphide collectors by Taggart [1945], they were not widely used due to their high cost. Sutherland and Wark [1955] report that it was possible to use potassium di-amyl dithiocarbamate for the flotation of sulphide minerals without any activation. Although the formation of insoluble metal complexes made dithiocarbamates look promising as a class of sulphide collectors the high cost of manufacture reduced interest in their practical application [Poling, 1976].

Thorn [1962] report that the metal salts increase in stability with metal type, so that any metal of a dithiocarbamate complex will be displaced by another metal to the right of the following series.



Sutherland and Wark [1955] note that the adsorption of diethyl dithiocarbamate onto sulphide minerals is faster than that of ethyl xanthate. They attributed this finding to the lower solubility of the dithiocarbamate salts. Glembotsky [1988]; and Glembotsky et al [1995] investigated dithiocarbamates as a promising class of collectors for selective flotation of galena against pyrite and have tested dithiocarbamates industrially as pyrite depressants. The seemingly contradictory findings of successful pyrite flotation and depression using dithiocarbamates, albeit at different conditions, was also found in preliminary work for this thesis [Bradshaw et al, 1992]. The dithiocarbamate class of collectors was selected for investigation as the solubility products of the metal

salts are lower than those for the corresponding xanthates, viz. 8.6×10^{-17} and 4.9×10^{-9} for the zinc metal thiolates respectively Glembotsky et al [1995].

Jiwu et al [1984] reported the use of cyano diethyl dithiocarbamate for the flotation of copper sulphides. This particular collector was selected for its frothing and collecting properties. Dithiocarbamates have been used industrially in the flotation of complex copper - gold sulphides [Oudenne and de Cuyper, 1987]. A number of applications for dithiocarbamates have been patented [Hudson and Adamek, 1967; Adamek and Hudson, 1969; Falvey, 1969]. Dithiocarbamates are supplied and used industrially as liquids due to their low solubility [Senmin Handbook].

Dithiocarbamates have also been shown by Sutherland and Wark [1955] to be more effective collectors at lower dosages than xanthates with the critical pH also being significantly higher for dithiocarbamates.

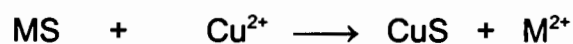
1.4.4 ROLE OF COPPER SULPHATE IN THE ACTIVATION OF PYRITE

Copper sulphate was first added to a pyrite plant in 1933 [Sutherland and Wark, 1955] and has since often been added to the pulp especially on many South African pyrite flotation plants. [Bushell and Krauss, 1962; Bushell, 1970; King, 1972, O'Connor et al, 1988 and O'Connor and Dunne, 1991]. The role of copper sulphate is, however, not clear and many conflicting theories have been proposed to explain the observed improvement in flotation performance when it is added to a flotation system.

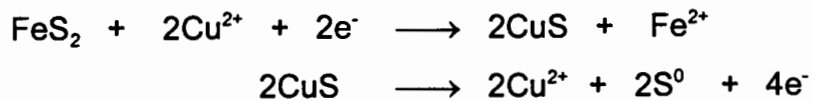
There is evidence to suggest that there are several potential mechanisms to explain activation and that these can dominate at different conditions. In some cases, copper sulphate was classified as a froth modifier in pyrite flotation [O'Connor et al, 1988], in others it was added to supposedly activate the mineral surface by the adsorption of copper ions, which enhanced the collector

adsorption, [Finkelstein and Allison, 1962; Leppinen, 1990; Leppinen et al, 1995; Nagaraj, 1995; Nagaraj and Brinen, 1995]. A third role proposed for copper sulphate is to complex out any residual cyanide [Lloyd, 1981; Bothelho de Sousa and Ross, 1990]. A fourth role proposed is for copper sulphate addition to increase the redox potential (ORP) of the pulp thereby increase the oxidising environment so as to make it more favourable for the oxidation of the thiol collectors. Nicol [1984] used electrochemical techniques to show that the presence of copper ions caused an anodic shift in the rest potential of pyrite which caused increased oxidation of the pyrite.

The replacement of the metal ions on the sulphide mineral surface by copper ions has been observed using scanning electron microscopy [Smart, 1991]. Stowe et al [1994] and Kim et al [1995] used TOF SIMS to detect the presence of copper ions on selected particles of sphalerite, galena, pyrrhotite and pyrite that reported to a zinc concentrate. The mechanism of activation of the sulphide mineral surface by ion exchange between copper ions and the cation of the mineral was reported to occur via an ion exchange process, viz. [Finkelstein and Allison, 1976; Leppinen, 1990; Nagaraj, 1995]



However other workers [Nicol, 1984; Mellgren et al, 1973; Leppinen et al, 1995], using various techniques, have proposed a different mechanism to explain the presence of copper on the surface of pyrite. Nicol [1984] used electrochemical techniques to show that the behaviour of pyrite differed to that of galena and pyrrhotite with respect to the addition of copper ions. Whereas with galena and pyrrhotite the cyclic voltammograms identified anodic peaks attributed to the formation of CuS with the addition of copper ions, these were not observed in the case of pyrite. However, in the presence of copper ions an anodic shift in the rest potential of pyrite was observed which indicated that the presence of copper ions caused an increase in the oxidation of the pyrite, viz.



so that the overall process is



Mellgren et al [1973] reported that the enthalpy change when copper ions were added to sphalerite corresponded thermochemically to the formation of CuS. In the case of pyrite, Mellgren et al [1973] reported that although copper ions were abstracted from the solution, no enthalpy change (ΔH) was detected.

Voigt et al [1994] and Leppinen et al [1995] independently investigated the activation of pyrite by copper sulphate using XPS techniques while Leppinen et al [1995] also used FTIR. In both cases, the XPS measurements showed that the iron - sulphur ratio did not change after copper activation and that the Cu 2p signal obtained showed that the copper ions adsorbed on the surface were in the +1 oxidation state rather than the +2 oxidation state. They observed the presence of copper xanthate and the absence of dixanthogen. The potentials were lower than those at which dixanthogen was observed in the case of no copper activation of pyrite in controlled non - oxidising conditions. Thus the activation of pyrite by copper sulphate changed the form of xanthate ions present from dixanthogen to copper (I) xanthate.

An alternative postulate of the role of copper sulphate in the flotation of pyrite, first proposed by Livshits and Dudenkov [1965], was that the copper ions complex with the xanthate to form colloidal hydrophobic precipitates. This would be likely particularly if the copper sulphate was added in excess or added at the same addition point as the xanthate in the conditioning tank in a flotation plant. Copper xanthate complexes can either destabilise the froth, as is expected from highly hydrophobic particles or can precipitate non - selectively on the mineral and gangue particles which would cause gangue particles to report to the froth and would thereby stabilise the froth [Harris, 1996].

Copper ions have also been shown to activate the non sulphide gangue minerals such as quartz and other oxide minerals, making them susceptible to collector adsorption [Fuerstenau and Palmer, 1976]. Evidence of the copper activation of pyroxene has been reported by Nagaraj and Brinen [1995] and of quartz by Chander [1991].

Wang et al [1989] also showed the initial unselective surface precipitation of copper hydroxide. They showed that the activation of the mineral surface occurred in a subsequent step where the mineral surface became equivalent to a copper sulphide mineral. This second step took time and if conditions were not favourable, did not occur, thus resulting in no activation of the mineral by the copper ions.

Activation of gangue with copper sulphate addition would result in a lower grade of flotation concentrate obtained. The increased froth stabilisation due to the increased gangue minerals recovered would increase the water recovery, which in turn would increase the mass pull and rate of recovery. The plant survey conducted by O' Connor et al [1988] of thirteen pyrite flotation plants showed that the principal opinion on the role of copper sulphate was that it resulted in froth stabilisation at an optimum dosage. The dosage of copper sulphate used by the flotation plants varied from nil to 160g/t. In general, higher dosages (over 60 g/t) of copper sulphate were added when xanthate collectors were used than when SMBT was used, the exception being at Buffelsfontein gold plant, where 100 g/t of copper sulphate was added with SMBT and Senkol 13 to process gold plant tailings. Note that the Buffelsfontein ore sample tested in this research programme is freshly mined low grade ore not gold plant tailings.

O' Connor et al [1988] showed that in batch tests copper sulphate increased rate of sulphur recovery, grades and water recovery. In three phase froth stability tests with fine pyrite (95% < 34 μm) and coarse pyrite (45% < 34 μm) added together with quartz (70% < 75 μm) it was shown that the decrease in

froth stability with copper sulphate addition was much larger in the tests with the coarse pyrite than with the tests with the fine pyrite. This was attributed to the froth stabilisation effect of the fine particles. High dosages of copper sulphate, viz. 357.5 g/t were added to get a measurable effect.

The pseudo depression of pyrite by copper sulphate and dithiocarbamate collectors was first reported by Sutherland and Wark [1955]. The decrease in flotation performance with copper sulphate addition to dithiocarbamate collectors in the flotation of pyrite was also investigated as a function of pH and dithiocarbamate type [Bradshaw et al, 1992]. It was shown that the extent of the decrease in flotation performance was dependent on the alkyl group of the collector and to a lesser extent on the pH.

1.4.5 COLLECTOR ADSORPTION ONTO MINERAL SURFACE

1.4.5.1 POSSIBLE THIOL - SULPHIDE ADSORPTION MECHANISMS

The predominant function of the collector is to selectively create a hydrophobic layer on the mineral surface thereby preparing it for successful collision with an air bubble. This can be done by a) Precipitation or b) Adsorption of a hydrophobic species on the mineral surface. In the case of precipitation, a solid phase with a 3 - dimensional lattice is formed. This can be initiated by homogeneous or heterogeneous nucleation. The effective species must be present on the surface and not in the bulk solution [Chander, 1988] for the mineral surface hydrophobicity to be affected.

The adsorption of the collector onto the mineral surface can be of a physical nature (physisorption) or of a chemical nature. With physisorption the collector does not interact with the mineral surface and is loosely held by Van der Waal's forces. The molecules largely retain their identity and the bonds are amorphous. The Gibbs free energy of adsorption is relatively low (below 25

kJ/mole) and the process is reversible [Persson, 1993]. Chemical bonds are much stronger, requiring a higher energy of adsorption, and are directional.

There are several modes of chemical interaction of the collector with the mineral surface. Chemisorption is where the collector interacts with the surface without movement of the metal ions from their lattice sites. This interaction has a covalent character. In this case adsorption is restricted to mono-layer coverage. The enthalpy change (ΔH) due to chemisorption is considerably larger than the heat of physisorption. Processes with ΔH values less negative than -25 kJ/mole are regarded as involving physisorption and values more negative than -40 kJ/mole are regarded as chemisorption. Surface chemical reaction is where this chemical interaction is accompanied by the movement of metal ions from their lattice sites. In this case multilayers may form. If this reaction occurs in the bulk solution a hydrophobic surface will only be established if there is bulk precipitation on the mineral surface [Chander, 1988].

Identification of the surface products and analysis of the reactions occurring is extremely sensitive to the conditions and purities of the samples used. Chander [1991] attributes differences in the results obtained by the different investigations to the following factors:

- (i) The inadequate methods of earlier surface characterisation.
- (ii) The history and depositional environment of the mineral sample.
- (iii) The methods and control of the sample preparation.
- (iv) Inadequate control of the experimental conditions.
- (v) The non-uniformity of formation of the surface products, both perpendicularly horizontally to the surface.

The interference of buffers with the pyrite surface has also been shown to enhance pyrite oxidation [Wang, 1995] and care must be taken when comparing results obtained from different investigations.

Leppinen et al [1995] note that they themselves have observed contradictory findings in two separate studies of the reaction between xanthates and pyrite. In the first case, iron xanthate compounds and diethyl dixanthogen were reported as surface products [Leppinen, 1990], whereas in the second case, only dixanthogen was reported [Leppinen, 1995]. The earlier study was done under open circuit conditions with pyrite a powder and in the presence of oxygen. The later study was under potential controlled conditions with the pyrite in the form of a massive plate in deoxygenated solutions.

Other compounds that may have been misinterpreted in various investigations have been reported by Winter [1975], who reports that the infrared spectrum for dixanthogen and sulphur dixanthate are identical except for rather weak peaks in the 300 - 600 cm^{-1} range and can be easily mistaken for one another. Finkelstein and Poling [1977] report the possible mistaken identity of the dithiolate by Wottgen and Berg [1968]. Wang [1995] points out the similarity of diethyl dixanthogen and ferric diethyl xanthate which may cause the presence of the ferric xanthate to be overlooked, particularly if it is in small quantities.

Adsorption of thiol collectors onto sulphide minerals involves the cathodic reduction of oxygen accompanied by the anodic oxidation of collectors [Woods, 1984]. This is known as the mixed potential mechanism. Sulphide minerals are semi-conductors which facilitate the electrochemical reactions occurring. The possible products of the anodic oxidation have been identified as chemisorbed collector, metal collector compounds and collector dithiolates. The electrochemical potential of the system and the thermodynamics of the respective reactions determine the identity of the surface products [Finkelstein and Goold, 1972; Finkelstein and Poling, 1977; Woods, 1984].

Yoon and Basilio [1993] summarise the following possible mechanisms of adsorption of thiol collectors onto sulphide minerals:

1.4.5.1.1. CHEMISORPTION

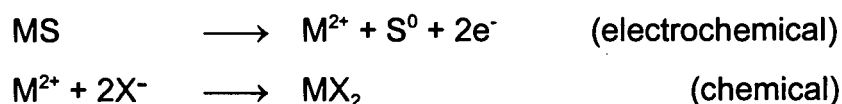
At potentials below those at which the metal thiol compound is formed a monolayer of the thiol oxidation product is formed [Woods, 1984]. This mechanism can be confirmed using voltammetry or spectroscopy and has been identified in the case of xanthate on copper, silver, chalcocite and galena [Leppinen et al, 1989]. In tests with ethyl xanthate and chalcocite, galena, and other minerals, Woods [1994] showed that the monolayer of chemisorbed species were better distributed on the mineral surface than the oxidised dithiolate multilayers which left some of the surface uncovered.

1.4.5.1.2. CATALYTIC OXIDATION

At suitable potentials the oxidation of the thiol to the dithiolate occurs. The presence of mineral catalyses the rate of this reaction which is otherwise slow. The mineral provides a passage for the transfer of electrons from the site where the collector is oxidised to the site where the oxygen is reduced, but does not take part in the reaction itself and the mineral surface is unaltered. This results in the formation of the dithiolate which is a neutral molecule. This is physisorbed and weakly held. This reaction predominates where the mineral does not readily liberate ions to form metal - thiol compounds. This mechanism has been identified in the case of the adsorption of xanthates onto pyrite, platinum, pyrrhotite, and gold where dixanthogen is formed [Woods, 1984]. Leppinen et al [1995] identified only dixanthogen on a massive pyrite plate under controlled conditions but when the pyrite was a powder and the conditions were more oxidising, iron xanthate compounds were identified [Leppinen, 1990]. This illustrates the possibility of other factors, such as the oxidising environment, determining which mechanism occurs between a particular collector and mineral. (cf. Sec. 1.4.5.2.3).

1.4.5.1.3. METAL - THIOL FORMATION (EC-MECHANISM)

In cases where mineral is easily oxidised or the formation metal - thiol compound is favoured, there is an electrochemical reaction (E) followed by a chemical reaction (C). This is known as a coupled electrochemical and chemical reaction [Nicholson and Shain, 1964].

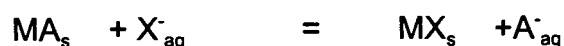


The mineral oxidation is controlled by the electrochemical potential (Eh) which determines the availability of metal ions and the chemical step is controlled by the stability constant (pK_{sp}) of the metal thiolate which determines whether the compound will be formed at those conditions.

They reported that the pK_{sp} values for thionocarbamates are approximately ten orders of magnitude higher than those of xanthates. Thus, metal thiol complexes are formed in the case of easily oxidised minerals, viz. chalcocite or galena, and in the case of the metal - collector complex having a large pK_{sp} value, viz. thionocarbamate.

1.4.5.1.4. METATHETICAL SUBSTITUTION

Taggart et al [1934] proposed the substitution on the oxidised mineral surface of the oxidation product by the thiol collector. Although this mechanism does not directly involve a charge transfer mechanism the oxidation products are formed by an electrochemical process.



where MA = The oxidised species on the mineral surface,
A = The oxidised anion.

Taggart et al [1934] first proposed that the magnitude of the solubility products of the metal xanthate and the oxidised sulphide species would determine the direction that the reaction would proceed.

Measurements of surface product have been correlated to their crystal structure and S - S distances [Persson, 1994]. They can be divided into three main groups depending on the type of sulphur in the compound: i) disulphide ions, (S_2^{2-}) ii) sheets or clusters of sulphur atoms, (polysulphur) and iii) sulphide ions, (S^{2-}) He correlated the surface products formed when xanthate collector is added to the length of the shortest S - S bond in the mineral, viz. the formation dixanthogen is proposed when the S-S bonds are less than 3.4 Angstroms. For bond lengths greater than 3.4 Angstroms, the formation of the metal thiolate is proposed. This rating may vary for other collectors with different oxidation potentials.

1.4.5.2. COMPARISON OF XANTHATES AND DITHIOCARBAMATES

1.4.5.2.1 GALENA

The surface products formed in investigations of the xanthate - galena system have been compared to those formed in the dithiocarbamate - galena system. Mellgren and Rao [1968] used thermochemical measurements to show that the reactions between both ethyl xanthate and ethyl dithiocarbamate with galena were similar to those occurring between the thiol collectors and the lead salt, viz. the formation of the corresponding lead thiolate. However, Yarar and Kitchener [1969] reported differences between the xanthate and dithiocarbamate systems with galena. At the conditions that ethyl xanthate oxidised to dixanthogen, ethyl dithiocarbamate did not oxidise to tetraethyl thiuram disulphide. There is also spectroscopic evidence to distinguish between the nature of the initial layer formed on the mineral surface and

subsequent layers in investigations of galena and xanthate [Shchukarev et al, 1994; Poling and Leja, 1963].

These findings disagree with the earlier work of Wottgen and Berg [1968] who found that the dithiolate was formed with diethyl dithiocarbamate and dibutyl dithiocarbamate with galena. Finkelstein and Poling [1977] note that their method using evaporation of the extract has been shown to give misleading results [Allison and Finkelstein, 1971].

Poling [1976] used electrochemical techniques to correlate the potential with surface products and he showed that the formation of the lead xanthate was more favourable than the dithiolate. He also showed that the lead dithiocarbamate was formed more readily than the lead xanthate.

Hu et al [1992] reported from their investigations of diethyl dithiocarbamate and galena that the surface reaction product was lead dithiocarbamate.

In general, taking all these investigations into consideration, the evidence suggests that the metal thiolate and not the dithiolate is formed in the case of the dithiocarbamates with galena.

1.4.5.2.2 COPPER SULPHIDES

Finkelstein and Poling [1977] reported the formation of only dixanthogen with chalcopyrite and that dixanthogen was the predominant product formed with covellite. Ackerman et al [1987a] report that dixanthogen is the species formed with chalcopyrite and that the metal thiolate is formed with bornite, chalcocite and covellite. They attribute the different reactions occurring to the differences in the mineral semi-conductor type. This was 'n' for chalcopyrite and 'p' for the other copper sulphides.

Leja [1982] reported that when xanthate was added to malachite the xanthate was completely abstracted from solution. This decreased the flotation performance and it was shown that the layers of surface products had "peeled" off the mineral. The nature of these layers was shown to be cuprous xanthate (CuX) and dixanthogen (X_2). Leppinen et al [1989] identified copper ethyl xanthate with chalcocite, while on chalcopyrite, copper ethyl xanthate was formed initially at low potentials with dixanthogen forming at more oxidising potentials.

Tests with di-ethyl dithiocarbamate and copper sulphides, covellite, tenorite and cuprite showed the formation and adsorption of various copper - thiolate complexes. No formation of the dithiolate was observed [Bhaskar Raju and Forsling, 1991; Mangalam and Khangaonkar, 1985].

1.4.5.2.3 PYRITE

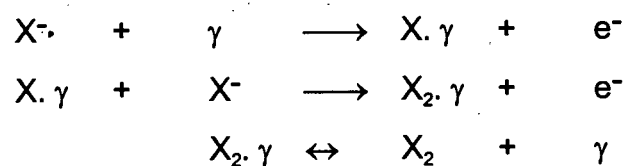
The reactions between pyrite and xanthate have been extensively investigated which has resulted in the reporting of conflicting results [Ball and Rickard, 1976]. On the one hand, only dixanthogen is observed and on the other, both iron xanthate and dixanthogen are observed. The debate was started in 1934 when Gaudin et al [1934] first reported the presence of both dixanthogen and ferric xanthate after having reported the presence of dixanthogen only. Possible reasons for this are discussed by Chander [1991] (cf. Sec. 1.4.5.1), and include the differing nature of the pyrite samples, the sample preparation, the control during experimentation and the methods of analysis.

The mechanism for dixanthogen formation with pure pyrite without the prior formation of the metal thiolate is reported to occur under carefully controlled conditions in the absence of oxygen via the catalytic oxidation mechanism [Yoon and Basilio, 1993; Leppinen, 1990].

However under less controlled conditions, and those more likely in a flotation environment, it has now been well established that dixanthogen is not the only product formed when xanthate is added to pyrite [Leja, 1973; Harris and Finkelstein, 1975; Finkelstein and Poling, 1977; Haung and Miller, 1978; Meilczarski, 1986; Wang and Forssberg, 1991; Fornasiero and Ralston, 1992; Montaldi et al, 1991; Hanson and Fuerstenau, 1993]. There is evidence that before the dixanthogen formation there is some xanthate - pyrite electrochemical interaction with the formation of a chemisorbed metal xanthate complex. This provides an anchor site for the larger scale physisorption of dixanthogen. This difference in surface composition has also been observed by Leppinen et al [1989]. In cases where this mechanism exists for dixanthogen formation with pyrite, the xanthate has been shown to be totally extracted from solution [Harris and Finkelstein, 1977].

Montaldi et al [1991] summarised the rate and reaction paths of adsorption of ethyl xanthate on pyrite at different pH as shown in Figure 1.13. At acidic conditions ethyl perxanthate and diethyl dixanthogen are dominant while at basic conditions ethyl monothiocarbonate is dominant.

This can be represented with the following reactions:



where $\gamma =$ Active site on the pyrite surface.

The reduction of oxygen that is associated with the thiol reaction is as follows



Figure 1.14 shows that the predominant form of the iron at low pH and high pe is the Fe^{2+} state. Note that the $pe = Eh \times (\text{Faraday constant} / 2.3 \times RT)$ which is equivalent to $Eh / 59$ (mV) at STP.

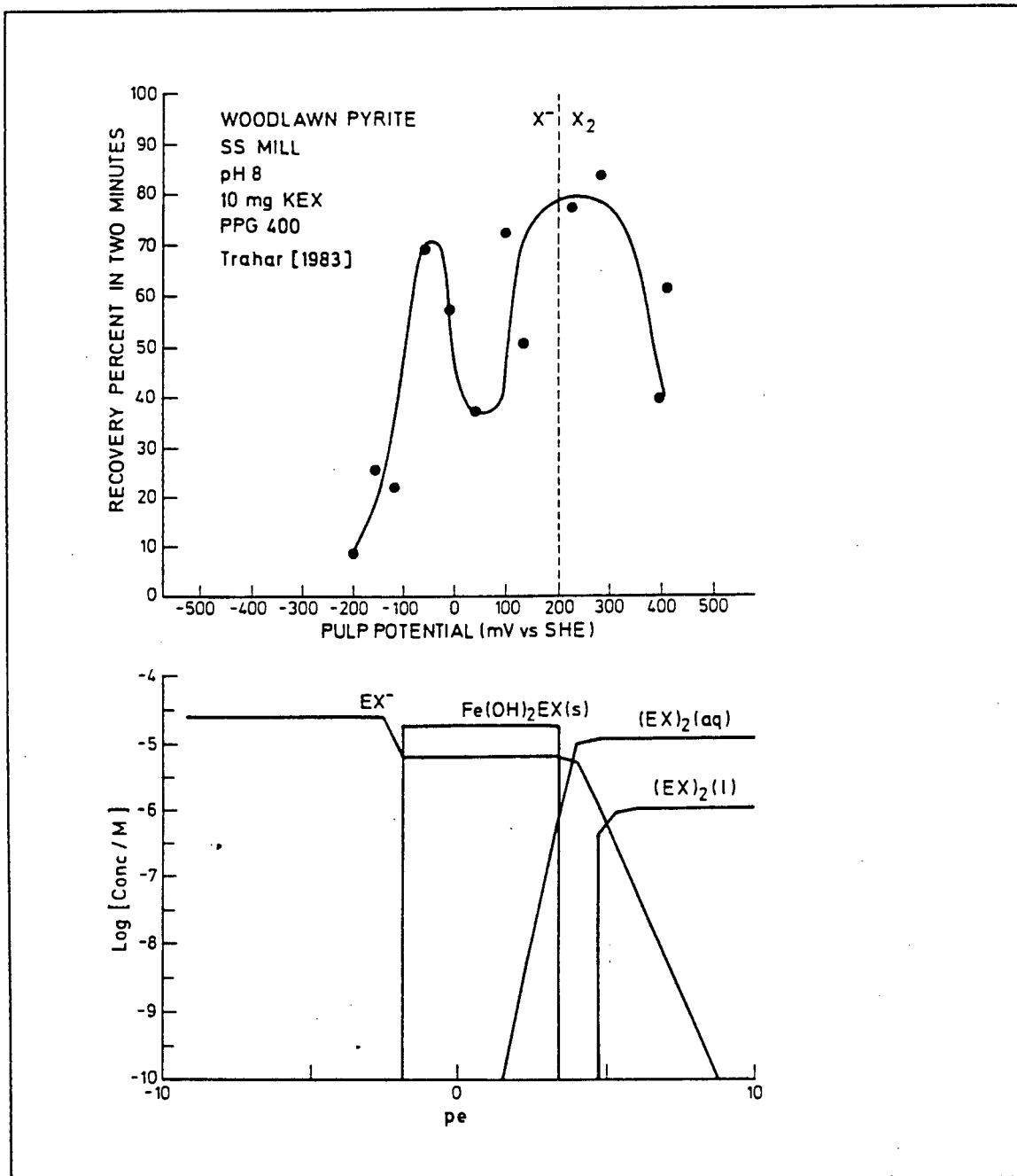


Figure 1.15: Relationship of species distribution for the Fe- X- H_2O system at a concentration of $[\text{Fe}] = 1.0 \times 10^{-3}$ moles/l and $[\text{EX}] = 2.5 \times 10^{-5}$ moles/l compared to pyrite flotation recovery from Trahar [1981], [Wang and Forssberg, 1991]

Figure 1.15 shows that flotation of pyrite occurs below the potential that dixanthogen occurs and this was correlated to species showing that some EX^- was present.

Pritzker et al [1985] showed thermodynamically that the dixanthogen formation was dependent on both the Eh and the concentration of xanthate added. At high pH it is possible for both ferric hydroxide and dixanthogen to exist.

Finkelstein and Poling [1977] in a comprehensive study of various thiol collectors and different sulphides at different conditions identified that the oxidation potential of xanthates (-0.127 V for PNBX) is much lower than for dithiocarbamates (-0.110 V for diethyl dithiocarbamate and 0.195 V for isopropyl dithiocarbamate). This indicated that a xanthate would form dixanthogen more readily than a dithiocarbamate would form its dithiolate, viz. thiuram disulphide. In their tests with pyrite the potential was high enough for the dithiolate to be formed in both cases viz. 0.545 V [Finkelstein and Goold, 1972]. It should be noted, however that the tests identifying the dithiolate as the surface product were done with di-ethyl dithiocarbamate at a pH of 11. No evidence of dithiolate formation was found in the follow up experiments [Harris, 1996] and, to the authors knowledge, no other evidence of dithiolate formation with dithiocarbamates has been observed.

1.4.5.3 MIXTURES OF THIOL COLLECTORS WITH SULPHIDE MINERALS

Various collector mixtures have been used in flotation practice to enhance flotation performance for a number of years [Taggart, 1945]. In particular blends of collectors and frothers have been used to reduced costs without loss in performance [Crozier and Klimpel, 1989; Leja, 1989]. Although the benefits have been reported for a wide range of collector mixtures (anionic, cationic and non-ionic), the mechanisms of enhancement with collector mixtures have not been clearly established.

On the one hand, better performance has been attributed to the summation of the differing contributions of the respective collectors [Mitrofanov et al, 1985], and, on the other, synergism, where the combined effect exceeds the sum of the parts, has been reported to occur as a result of collectors working together or interacting [Plaskin and Zaitseva, 1960].

This review is restricted to mixtures containing thiol collectors and used for the beneficiation of sulphide minerals. Xanthates are the most widely used of the pure collectors which is probably the reason that most of the reported cases of mixtures have xanthates as one of the components [Crozier, 1992; Adkins and Pearse, 1992].

Dithiophosphates are a class of thiol collector commonly added to other thiol collectors in mixtures to improve flotation performance and to this end are known as promoters. Many of the collector mixtures reported have dithiophosphates as a constituent collector, viz. [Plaskin et al, 1954; Wakamatsu and Numata, 1979; Mingione, 1984; Adkins and Pearse, 1992].

Plaskin et al [1954] investigated the combinations of ethyl xanthate and amyl xanthate as well as combinations of xanthates and diethyl dithiophosphates in the mass ratios of 2:1 for use in the flotation of arsenopyrite and galena. The improvement obtained was greater than a simple summation of the properties of the pure constituent collectors. The largest benefit was in the recovery of the coarse fraction (100 - 150 μm). In all cases the kinetics of recovery were improved with the use of mixtures. In the case of arsenopyrite flotation, no further improvement in recovery was obtained by increasing the dosage of the mixture, whereas the recovery obtained using the pure collectors was slightly enhanced. They attributed the improved flotation performance obtained with mixtures of collectors to the better adsorption characteristics on the non-homogenous mineral surface.

In a subsequent investigation, Plaskin and Zaitseva [1960] used microautoradiographic techniques to test the hypothesis that synergism resulted from improved adsorption of collector. Particles were abstracted from the flotation concentrate and immersed in dye and the radiographic impressions were scanned by microscope. They defined the "coefficient of variation" as a measure of uniformity of collector adsorption. In the case of pure xanthate, they noted that increasing the dosage did not increase the extent of surface coverage but increased the density of the already covered patches. In the case of the mixtures of xanthates the variation coefficient was decreased, so that surface coverage was increased and the patchy coverage of denser coverage was also reduced.

In his patent of dithiocarbamates, Falvey [1969] notes that the copper recoveries obtained with dithiocarbamates were further enhanced by using them in conjunction with other water soluble collectors such as xanthates, dithiophosphates or mecaptobenzothiazole.

Wakamatsu and Numata [1979] investigated the joint use of xanthates and dithiophosphates (mass ratio 50:50) for the flotation of galena using adsorption and bubble pick up tests. At low collector concentrations, coadsorption of collectors was observed whereas at higher collector dosage, competitive adsorption of the dithiophosphate occurred. There was a slight improvement in the bubble pick up of the galena observed in the case of mixtures relative to the pure collectors.

Crozier [1980] reports that flotation performance is enhanced with the use of mixtures of collectors which include one which is strong and not too selective and another which is weaker but more selective.

Mingione [1984] investigated the use of various mass ratios of dithiophosphates in combination with xanthates and sodium mecaptobenzothiazole and noted that there was an optimum ratio for specified applications. All mixtures of

sodium di-isobutyl dithiophosphate : sodium isopropyl xanthate achieved higher platinum group metal recoveries than the pure collectors and the highest recovery was obtained with the 80:20 mass ratio of sodium di-isobutyl dithiophosphate : sodium isopropyl xanthate.

Jiwu et al [1984] reported the use of cyano diethyl dithiocarbamate in conjunction with xanthates for the improved flotation performance of copper oxidised sulphides. The optimum mass ratio of cyano diethyl dithiocarbamate to sodium butyl xanthate was 12: 44. No mechanisms for the increase in grade and recovery were reported.

In batch flotation tests of a mixed copper ore with various mixtures of dithiophosphates, monothiophosphates and xanthates, Mitrofanov et al [1985] reported improved collection of fines due to the combination of the frothing properties of dithiophosphates and the "dry" froth produced by xanthates. The coarse particle recovery was credited to the xanthates.

Critchley and Riaz [1991] tested 0:100, 20:80, 33:66, 50:50, 66:33, 80:20, 100:0 mole ratio mixtures potassium ethyl xanthate and di-ethyl dithiocarbamate. and reported enhanced adsorption and microflotation of heazlewoodite with a ratio of 33:66 (1:2) potassium ethyl xanthate and di-ethyl dithiocarbamate. They proposed that enhanced overall extent of collector adsorption was the mechanisms for the synergistic enhancement of flotation performance.

Adkins and Pearse [1992] tested xanthate and dithiophosphate mixtures with various complex sulphide ores and showed that a 5% molar substitution of sodium isopropyl xanthate by sodium dicresyl dithiophosphate increased the mixed copper sulphide recovery and rate of recovery.

Vinogradova [1993] calculated the hydrodynamic effects of the adsorption coating of the mineral particle on the particle bubble collision and attachment.

She demonstrated that both physisorbed and chemisorbed coatings affected the attachment. At large distances the thinning of the interlayer was facilitated by the physically adsorbed collector, but at close approach this was affected by the chemically adsorbed collector.

Valdiviezo and Oliveira [1993] used surface tension measurements correlated to contact angle measurements for various ratios of ethyl xanthate and sodium oleate to show that synergism existed between the collectors and that the optimum ratio was a 3:1 mole ratio mixture of ethyl xanthate and sodium oleate. They also attributed the effects to a favourable arrangement of adsorbing species.

The benefits of using mixtures of collectors in place of pure collectors in flotation tests can be summarised as follows:

- 1) Improvement in rate of flotation [Plaskin et al, 1954; Adkins and Pearse, 1992].
- 2) Improvement in coarse particle recovery [Plaskin et al, 1954].
- 3) Reduction in dosage requirement [Plaskin et al, 1954].
- 4) Best results were obtained at an optimum ratio of constituents [Mingione, 1984; Critchley and Riaz, 1991; Valdiviezo and Oliveira, 1993].

1.5 PROPOSED MECHANISMS OF SYNERGISM

Based on the above discussion, the synergistic enhancement of flotation performance observed has largely been attributed to improved adsorption characteristics of the mixed collectors on the mineral surface as compared to those of the pure collectors.

Improved extent of adsorption has been proposed by Critchley and Riaz [1991]. The better orientation of the different collectors forming a more evenly dispersed surface film than that of pure collectors was proposed by Plaskin and Zaitseva [1960].

Woods [1994] showed that chemisorbed collector species were more evenly distributed on the mineral surface than physisorbed species. A mixture may result in a balance of better distributed and more strongly held chemisorbed species and more hydrophobic neutral physisorbed dithiolates, and this could result in the formation of a multilayer surface product that is more strongly attached to the mineral surface. For example, in this thesis, it can be hypothesised that with the use of xanthates and dithiocarbamates the metal thiolate could be formed by the dithiocarbamate which is chemically bound to the surface and dixanthogen is formed by the xanthate which is neutral and physisorbed, which would result in a more evenly spread, strongly attached collector.

This hypothesis is corroborated by Mellgren [1966] who also proposed that chemisorbed collector provides sites on the mineral surface for the subsequent adsorption of the more hydrophobic, neutral molecules (dixanthogen). The overall hydrophobic properties of the mineral are thereby increased.

The lower dosage recommended by several authors with mixtures of collectors may result from better distribution of the collectors to create the necessary 'hydrophobicity.'

The improved adsorption characteristics would result in improved flotability by increasing the bubble - mineral attachment tenacity which would result in less mineral detachment and elutriation. The frother - collector interactions may also be increased resulting in stronger mineral - bubble attachment.

1.6 RESEARCH OBJECTIVES

The objectives of this thesis are:

- 1) To investigate whether synergism, a phenomenon in which the combined effect exceeds the sum of the parts, as shown by enhanced sulphur grades and sulphur recoveries is observed when mixtures of PNBX and cyclohexyl DTC are used in the flotation of pyrite at pH = 4;
- 2) To ascertain whether the synergistic effects observed are a result of the effects in the froth zone or the pulp zone;
- 3) To investigate the effect of synergism on the efficiency of the mineral loading on the air bubble;
- 4) To investigate the effect of synergism on the surface reactions occurring between mixtures of collectors and pyrite using thermochemical and kinetic adsorption studies;
- 5) To investigate the effect of copper sulphate addition on the use of pure collectors and mixtures of PNBX and cyclohexyl DTC in the flotation of pyrite at pH = 4.

CHAPTER 2: BATCH FLOTATION TESTS

2.1 INTRODUCTION

The objective of this thesis was to establish whether a 90:10 mole ratio mixture of PNBX and cyclohexyl DTC gave a synergistic improvement of flotation performance when used as the collector in the flotation of pyrite at pH = 4. This particular collector mixture was selected due to its potential for use industrially. The observed results were compared to the predicted results obtained using the summation of the individual contributions of the constituent collectors at the same molar dosage.

Although mixtures of other ratios of PNBX and cyclohexyl DTC were also tested, the critical focus of this study was the 90:10 mixture of PNBX and cyclohexyl DTC (cf. Sec. 1.6). The determination of the optimum ratios of the collectors in the mixture was not the focus of the study. Batch flotation test results were used in conjunction with the results obtained using other techniques such as adsorption and bubble loading measurements to elucidate the mechanisms of this enhancement in flotation performance (cf. Ch. 3 and 4).

Tests with Buffelsfontein ore used the pure constituent dithiocarbamate and xanthate collectors as well as mixtures with different ratios of these constituent collectors. PNBX was used in the greater proportion in the mixtures of PNBX and cyclohexyl DTC tested. This was largely due to the higher cost of dithiocarbamate collectors. The 90:10 mole ratio mixture was tested at two dosages. This investigation was not aimed at optimising the ratios or dosages of collectors but rather at identifying and characterising any benefit on flotation performance obtained using a mixture of collectors in place of the pure constituent reagents.

Tests with St Helena ore compared the performance obtained with PNBX to that obtained with the 90:10 mole ratio mixture of PNBX and cyclohexyl DTC. The sequence of reagent addition was also tested with St Helena ore.

The flotation responses evaluated to characterise flotation performance were sulphur grade and sulphur recovery - both overall and by size - water and mass recoveries and the rate of sulphur recovery (using the Klimpel model [Klimpel, 1984]). Sulphur and mass recoveries were reported as percentages (%) of the initial sulphur and mass values. Water recoveries were reported in grams (g) as water was added continuously through the tests to maintain the level of the pulp - froth interface. Froth surface structures were analysed using digital image analysis for selected tests using Buffelsfontein ore.

2.2. EXPERIMENTAL PROCEDURES

2.2.1 FLOTATION TESTS

2.2.1.1 THE FLOTATION CELL

The flotation cell used in the batch flotation testwork was a modified 3 - litre Leeds laboratory cell. Although this has been shown to give reproducible results [Dell and Bunyard, 1972; Fickling, 1986, Stonestreet, 1991], the reproducibility was re-evaluated in the present work (cf. Sec. 2.3.1.1).

The impeller was fitted with a speed controller. The pulp level was controlled by a constant head device so as to have a froth height of 2.5 cm. The air flow was set at 6 l/min by means of a pressure regulator and a rotameter. Froth was removed manually at set time intervals as described in Section 2.2.2. Figure 2.1 shows the flotation cell.

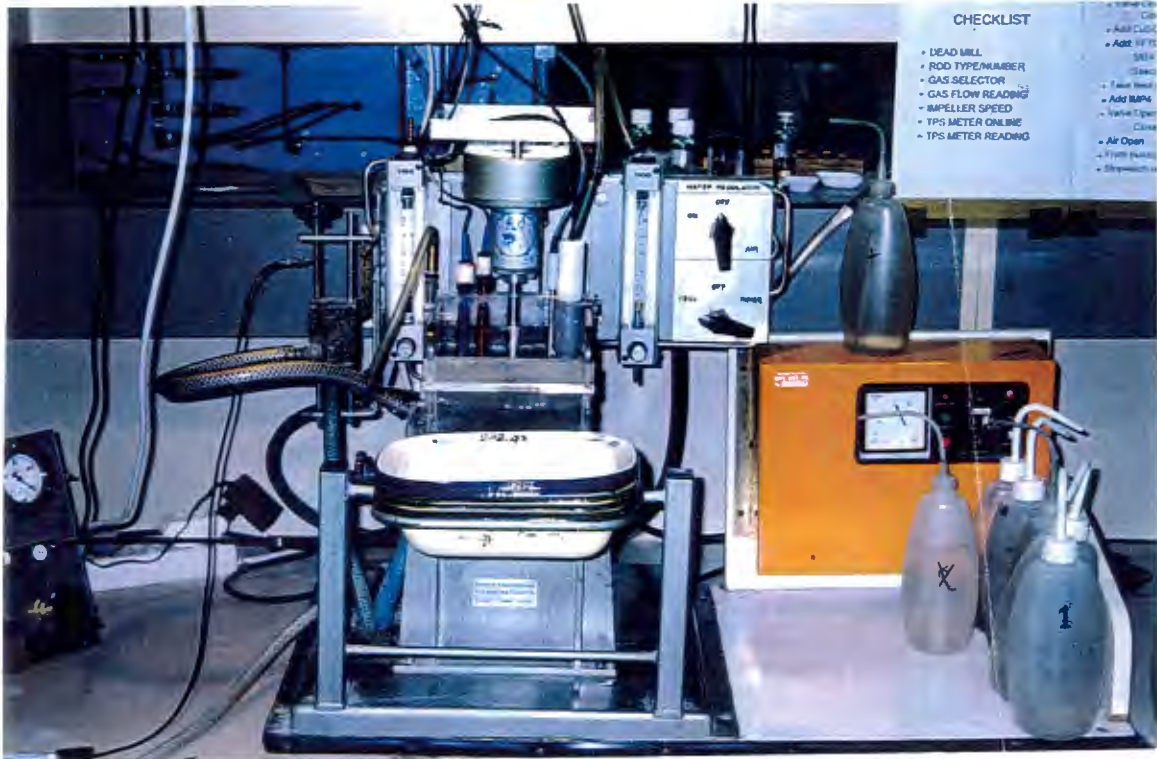


Figure 2.1: The modified Leeds flotation cell

2.2.1.2. ORE SAMPLES

Two ore samples were used in the batch flotation testwork. The first was a low grade ore from Buffelsfontein Gold Mine, near Stilfontein, North West Province, South Africa, with a grade of 0.83% sulphide sulphur (coded as B- in the results). The second was gold plant residue from a tailings dam at St Helena Gold Mine in the Welkom area, Free State, South Africa, with a grade of 1.27% sulphur (coded as SH- in the results).

The Buffelsfontein ore sample received was run of mine feed material crushed to below 2 mm and packed in 25 kg bags. Each bag was split into 1 kg samples using a rotary splitter. The ore was milled in a Sala stainless steel rod mill. The diameter and the length of the mill was 300 mm and the diameter of the rods were 25 mm. The mill charge was 25 rods. A milling curve was

determined in the usual manner in order to determine the milling time required to obtain a feed particle size distribution of 40% passing 75 μm (Appendix 2A). Each sample of ore was milled immediately prior to flotation.

Table 2.1: The sulphur distribution of the Buffelsfontein and St Helena ore samples

	St Helena Ore	Buffelsfontein Ore
Feed Grade (% Sulphur)	1.27	0.83
Fines	< 38 μm	< 25 μm
% Mass in Fraction	30.70	38.06
% Grade	1.70	0.52
Total Sulphur (mass x grade)	52.19	19.66
Middling	38 x 75 μm	25 x 75 μm
% Mass in Fraction	22.50	22.30
% Grade	2.40	0.90
Total Sulphur (mass x grade)	54.03	20.13
Coarse Range	> 75 μm	> 75 μm
% Mass in Fraction	46.90	39.64
% Grade	0.44	1.11
Total Sulphur (mass x grade)	20.78	44.21

The St Helena ore sample was received wet in a 200 litre drum and the particle size distribution was determined to be approximately 55% passing 75 μm . The average moisture content was measured and ore samples containing 1 kg of dry mass were prepared by using coning and quartering techniques [Kelly and Spottiswood, 1982], additional water was added and samples were stored in sealed containers. The mean sulphur grade was 1.27%.

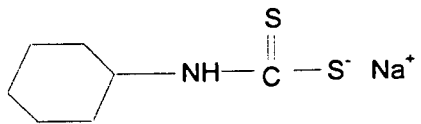
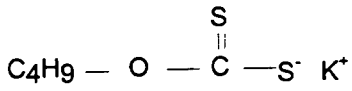
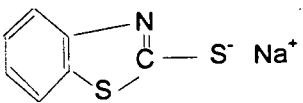
A mineralogical examination of both ores showed that quartz was the major gangue constituent. However in the Buffelsfontein ore the quartz:silicate matrix ratio was approximately twice as high as in the case of the St Helena ore. In the Buffelsfontein ore the silicate matrix was dominated by muscovite and chlorite with traces of pyrophyllite. The St Helena ore contains no muscovite, but pyrophyllite and chlorite are present in approximately equal amounts.

2.2.1.3. REAGENTS

2.2.1.3.1 COLLECTORS

Table 2.2 shows the structures of the collectors used in this study. The collectors were laboratory samples prepared and supplied by KARBOCHEM. All the collectors used were thiols. The dithiocarbamate samples were received as liquids, the active ingredients dissolved in a known volume of water, and the PNBX as a powder.

Table 2.2: Chemical structures and molecular weights of the collectors used in this investigation

Name	Abbreviation	Schematic of Structure	Molecular Weight (a.m.u.)
sodium cyclohexyl dithiocarbamate	oC6 DTC		199
potassium n-butyl xanthate	PNBX		188
sodium mecaptobenzothiazole	SMBT		189

The dithiocarbamate used was sodium cyclohexyl dithiocarbamate (oC6 DTC). This collector was selected as it had shown promise in a previous investigation [Bradshaw et al, 1992]. The xanthate selected was potassium n-butyl xanthate (PNBX), which is one of the most effective xanthate collectors for pyrite flotation

[Dimou, 1986]. Sodium mecaptobenzothiazole (SMBT) was used for the reproducibility tests, it being the standard collector used at Buffelsfontein Gold Mine.

The stability of the collectors was tested by measuring their half lives under controlled conditions at pH = 4. The rate of decrease of UV absorbance was measured at set wavelength, viz. 300 nm for PNBX and 280 nm for cyclohexyl DTC. Table 2.2 shows the half lives of the collectors used in this investigation. It can be seen that the cyclohexyl DTC is an order of magnitude more stable than the PNBX. Within the time of flotation both the collectors can be assumed to be chemically stable. Harris [1984] reported the half life of PNBX to be 0.8 hr at 25°C which was lower than that reported for this investigation. The higher half life observed in this investigation may be attributed to the differences in the water or impurities in the sample.

Table 2.3: The stability of the collectors used in this investigation at pH = 4

Collector	Half Life (mins)
di-n C3 DTC	950
oC6 DTC	650
PNBX	90

2.2.1.3.2 FROTHERS

The frother used for both ore samples was a proprietary frother, SK 6010, which was prepared and supplied by KARBOCHEM. The major constituent of this frother is tri-ethoxy butane (TEB).

2.2.1.3.3 pH CONTROL

The natural pH of the St Helena ore was between 5 and 6 and the natural pH of the Buffelsfontein ore was 7. Sulphuric acid and calcium hydroxide were used to control the pH as appropriate.

2.2.2 FLOTATION PROCEDURES

2.2.2.1 BATCH FLOTATION OF BUFFELSFONTEIN ORE (B-)

As described in Section 2.2.1.2, this ore sample was received as crushed material (< 2 mm) and was riffled and split into 1 kg samples. Immediately prior to flotation, each sample was milled as a slurry containing 60% solids for 10 minutes so as to achieve a final particle size of 60% < 75 μm as determined from the milling curve (Appendix 2A).

The ore was transferred to the flotation cell and water added to decrease the pulp density to 30% solids. The impeller speed was set at 1200 rpm. The pH was recorded, adjusted to 4 and the pulp conditioned for 10 mins. Copper sulphate (when used) was added at a dosage of 200 mmoles/t and the pulp conditioned for a further 5 mins. The frother was then added at a dosage of 92 ml /t. After the frother was added the pulp was conditioned for 1 min. The collector was then added and the pulp conditioned for a further 1 min. In the case of the mixtures of collectors, the pure constituent collectors were added simultaneously unless otherwise specified. Pure collectors and collector mixtures were compared at the same molar concentration. Mixtures were also constituted on a mole ratio basis. In these tests the standard molar dosage was 310 mmoles/t ore which was equivalent to 60 g/t of PNBX. The dosage of 465 mmoles/t was equivalent to 90 g/t of PNBX. The air was turned on and set to a rate of 6 l/min. The froth height of 2.5 cm was maintained by the level

controller throughout the test. An induction period of 45 secs was allowed before collection of concentrate commenced.

The froth scraping interval was 10 secs and 4 concentrates were collected at intervals of 1 min (0-1min), 2 mins (1-3 mins), 4 mins (3-7 mins) and 6 mins (7-13 mins). At the end of the flotation test, the air was turned off and the water recoveries measured. The froth characteristics, as visually observed, were described on the worksheets and the concentrates dried, weighed and analysed for sulphur. Mass and water recoveries were measured for each concentrate. For selected tests the surface froth structure was analysed using digital image analysis techniques (cf. Sec. 2.2.3.2).

2.2.2.2 BATCH FLOTATION OF ST HELENA ORE (SH-)

As stated in Section 2.2.1.2, this ore sample, of size fraction 55% passing 75 μm , was received wet. It was divided into 1.2 kg samples (dry mass 1 kg) and stored wet in sealed containers.

The ore was transferred to the flotation cell and water added to lower the pulp density to 30% solids. The impeller speed was set at 1400 rpm. The pH was recorded, adjusted to 4 and the pulp thus conditioned for 10 mins. Copper sulphate (when used) was added at a dosage of 200 mmol/t and conditioned for a further 5 mins. The frother was then added at a dosage of 40 μl /kg ore. After the frother was conditioned for 1 min, the collector was added and conditioned for 1 min. Pure collectors and collector mixtures were compared at the same molar concentration. In the case of the mixture of collectors, the pure constituent collectors were added simultaneously unless otherwise specified. Mixtures were also constituted on a mole ratio basis. The air was turned on and set to a rate of 6 l/min. The froth height was 2.5 cm. An induction period of 45 secs was allowed before collection of concentrate commenced.

The froth scraping interval was 10 secs and 5 concentrates were collected at intervals of 0.5 min (0-0.5 min), 0.5 min (0.5-1 mins), 2 mins (1-3 mins), 4 mins (3-7 mins) and 6 mins (7-13 mins). At the end of the flotation test, the air was turned off and the water recoveries measured. The froth characteristics, as visually observed, were recorded and the concentrates dried, weighed and analysed for sulphur. Mass and water recoveries were measured for each concentrate.

The redox potential of the system at pH = 4 was measured using a gold - calomel electrode [Rand and Woods, 1984; Labonté and Finch, 1988]. The potential of the system was between 0.V - 0.20 V, equivalent to -54 V - 24 V SHE (relative to a Standard Hydrogen Electrode). This was above the oxidation potential for xanthate to dixanthogen (cf. Sec. 1.4.3).

2.2.3 ANALYTICAL PROCEDURES

2.2.3.1 SULPHUR ASSAYS

The feed, concentrate and tailing samples were assayed for total sulphur using a LECO SC32 sulphur analyser. A detailed description of the procedure is given in Appendix 2B. In order to establish the reliability of these assays, nine replicate assays were done on typical feed, concentrate and tails samples. The results of these assays are shown in Appendix 2C.

The standard deviation for the tails assays of a sample with a mean sulphur assay of 0.0415% was 0.008%, so that the relative standard deviation was 18.84%. The mean sulphur assay of the feed sample was 0.67%, the standard deviation was 0.029% and the relative standard deviation was 4.35%. The mean sulphur assay of the concentrate sample was 33.44%, the standard deviation was 0.48% and the relative standard deviation was 1.42%. This shows that the low value of the tails assay resulted in it having a larger relative

standard deviation than the feed or concentrate and therefore was the largest potential source of error. The sulphur balances for each test are important as a measure of reliability of these assays.

2.2.3.2 DIGITAL IMAGE ANALYSIS OF FROTH SURFACE

For selected tests with Buffelsfontein ore the surface froth structure was analysed using digital image analysis. The details and methodology have been described by Moolman et al [1995] in which the use of these tests as well as other plant data to correlate the image data such as froth bubble size, colour, texture, stability and mobility with recovery and grade is described. The image analysis technique, in some tests, was used to ascertain whether differences in flotation performance could be directly attributed to the characteristics of the froth surface.

Grey level dependence matrix methods were used to extract features from digitised images of froths [Moolman et al, 1995]. The Non Number Uniformity (NNU) parameter which is a measure of the coarseness of the texture of the image was used to monitor the froth bubble size.

The froth mobility or froth speed was characterised using a digital function of the VHS camera, whereby the image in motion is blurred in proportion to the velocity of its motion. The more mobile the froth, the more pronounced the lines of motion on the images. This method of measuring froth speed was verified by comparison to measurements of the velocity of a piece of paper on the froth surface.

The froth stability was measured by monitoring the change in the highlights on the top surfaces of bubbles and bubble boundaries. For a stable froth the rate of bubble collapse is slow and there are fewer local changes in light intensity between frames.

2.2.4 EXPERIMENTAL DESIGN AND STATISTICAL ANALYSIS

2.2.4.1 FACTORIAL DESIGN OF EXPERIMENTS

For certain of the sets of tests in this thesis, factorial design methods were used to plan the experiments and to statistically evaluate the results. The tests with Buffelsfontein ore to compare the behaviour of the mixture and PNBX were done in one set of eight tests, viz. 2^3 , where three factors, viz. copper sulphate dosage, collector type and dosage, were each tested at two levels.

Table 2.3 shows the design matrix for the factorial design. In this example parameters A, B and C were tested at two levels, high (+) and low (-). All combinations of the levels of the parameters were tested in the eight tests. Each test was done with the levels allocated. Where the parameter was qualitative rather than quantitative, the levels were arbitrarily assigned.

This table was also used to analyse the results so as to determine the main effects of changing the level of the parameters as well as the interactions between these parameters.

Table 2.4: Design Matrix for a full factorial design, 2^3 (three parameters, each at two levels in eight runs)

RUN No.	VARIABLES			INTERACTIONS			
	A	B	C	AB	AC	BC	ABC
1	-	-	-	+	+	+	-
2	+	-	-	-	-	+	+
3	-	+	-	-	+	-	+
4	+	+	-	+	-	-	-
5	-	-	+	+	-	-	+
6	+	-	+	-	+	-	-
7	-	+	+	-	-	+	-
8	+	+	+	+	+	+	+

2.3. RESULTS

2.3.1 INVESTIGATION WITH BUFFELSFONTEIN ORE

The aim of these tests was to ascertain whether any enhancement in flotation performance was gained by using a mixture of PNBX and cyclohexyl DTC rather than pure PNBX. A comparison between the behaviour of pure PNBX and cyclohexyl DTC was first made. As explained above, the focus of this thesis was on the 90:10 mole ratio mixture of PNBX and cyclohexyl DTC although mixtures containing differing mole ratios of PNBX and cyclohexyl DTC were tested in order to gain more information about the mechanisms involved. Two dosages were tested to investigate the effect of dosage on flotation performance of the 90:10 mixture of PNBX and cyclohexyl DTC and pure PNBX. All operational parameters were constant throughout these tests (cf. Sec. 2.2.2.1). This investigation was not aimed at optimising the ratios or dosages of collectors but rather at establishing and characterising any benefit on flotation performance obtained using the 90:10 collector mixture in place of the pure constituent reagents.

2.3.1.1 REPRODUCIBILITY (Tests: B-R 1-8)

The aim of the reproducibility tests was to quantify the limits of changes that are significant by calculating the standard deviation of the various responses. The standard deviations calculated from these reproducibility tests were used to test the statistical significance of the effects investigated in this thesis. Possible sources of error include the ore variability, including the success of sampling, the consistency of the mill and flotation cell operation, the experimental technique of the operator, and the errors in weighing and in the sulphur assay results.

The reliability of the sulphur assays is discussed in Section 2.3.1, details are shown in Appendix 2D (i). The tails sulphur assay was the largest potential source of error due to the lower limits of detection of sulphur by the LECO, and had a larger relative standard deviation than the feed or concentrate.

The detailed reproducibility flotation tests are shown in Appendix 2D (ii). The tests with the Buffelsfontein ore used the standard batch flotation method used by the Buffelsfontein Gold Mine laboratory as described in Sec. 2.2.2.1. The collector used was SMBT at a dosage of 240 mmol/t (90 g/t), 200 mmol/t of copper sulphate was added and the pH = 4.

The objective of this section was to establish the reliability of the flotation test procedure used in this thesis. The reproducibility tests have established the standard deviations for each of the flotation responses, such as recovery and grade. These standard deviations compare well with reported tests using the modified Leeds cell, viz. the standard deviation of final recovery is 0.91% compared to 1% obtained by Stonestreet [1991]. The standard deviations obtained in these tests were used to ascertain the significance of the changes in flotation performance obtained when changes were made to the flotation operating parameters, such as the nature of the collector.

Statistical analysis using standard 'T' tests, with the 95 % confidence level termed significant (cf. Appendix 2D(ii)), showed that there was no significant difference between these two sets of tests with respect to the mass, water and final sulphur recoveries, grades or infinite time recoveries, R.

2.3.1.1.1. ANALYSIS BY SIZE OF REPRODUCIBILITY RESULTS

Analysis of recovery and grade by size was carried out for tests B-R 1-3. This data is shown in Table 2.5. Figure 2.2 shows that the initial recovery decreased with size fraction, with the recovery of the fines (< 25 μm)

substantially lower than that of the coarser particles viz. a mean of 60.8% for the $< 25 \mu\text{m}$ fraction compared to 86.5% for the $> 75 \mu\text{m}$ fraction. The differences of the different sizes in the final recovery were reduced relative to the differences of the initial sulphur recoveries, and all recoveries were over 84%. Table 2.5 shows that the standard deviation was higher for the initial recovery than for the final recovery. The decreased recovery is consistent with the expected reduction in collision efficiency [Ralston, 1994] (cf. Sec. 1.2.3.2.2).

Figure 2.3 shows the sulphur grade vs sulphur recovery by size after 1 and 13 mins respectively and that the grade of the fines material was substantially lower than for the other sizes. The grade was also reduced with time for all size fractions. The relatively high grade of the initial recovery (1 min) of the $> 75 \mu\text{m}$ material, viz. over 46%, shows that this sample was well liberated and most amenable to flotation. The relatively lower grades of the finer material show that there was a substantial recovery of the fine gangue material by entrainment.

The feed samples of the tests that were analysed by size were reconstituted. Figure 2.4 compares the reconstituted sulphur distribution to the measured sulphur distribution of the feed. Figure 2.4 shows that the sulphur grades were much higher in the coarse and medium size fractions than in the $< 25 \mu\text{m}$ fraction. This indicates that the size distribution of gangue material was lower than that of the pyrite and that the gangue minerals may be preferentially reduced in size during milling. The measured feed grade of the $> 75 \mu\text{m}$ size fraction was 1.1% sulphur, the $25 \times 75 \mu\text{m}$ fraction was 0.9% sulphur and the $< 25 \mu\text{m}$ fraction was 0.5% sulphur. Figure 2.4 demonstrates the low ore sample variability.

Table 2.5: Analysis by size of reproducibility tests B-R 1-3 (Buffelsfontein ore)

Test Number	Time	Sulphur Recovery (%)				Sulphur Grade (%)			
		Overall	< 25 μm	25x75 μm	> 75 μm	Overall	< 25 μm	25x75 μm	> 75 μm
Feed Grade						0.83	0.52	0.9	1.11
B-R 1	1 min	81.7	52.7	85.1	91.8	27.2	10.4	38.6	49.1
	13 min	95.4	93.0	95.5	97.1	15.1	7.9	27.8	23.8
B-R 2	1 min	78.8	66.3	80.8	78.2	30.5	13.7	36.9	49.2
	13 min	94.8	98.7	93.5	93.6	16.0	7.5	24.6	29.1
B-R 3	1 min	85.0	63.5	83.7	89.6	30.4	10.7	34.6	46.2
	13 min	96.6	89.1	93.0	100.0	17.2	6.4	26.7	27.3
Mean	1 min	81.8	60.8	83.2	86.5	29.4	11.6	36.7	48.2
Std Dev		3.10	7.18	2.19	7.30	1.88	1.82	2.01	1.70
Rel Std Dev (%)		3.79	11.81	2.64	8.44	6.39	15.73	5.47	3.54
Mean	13 min	95.6	93.6	94.0	96.9	16.1	7.3	26.4	26.7
Std Dev		0.93	4.83	1.32	3.20	1.06	0.77	1.62	2.68
Rel Std Dev (%)		0.97	5.16	1.41	3.31	6.57	10.51	6.15	10.04

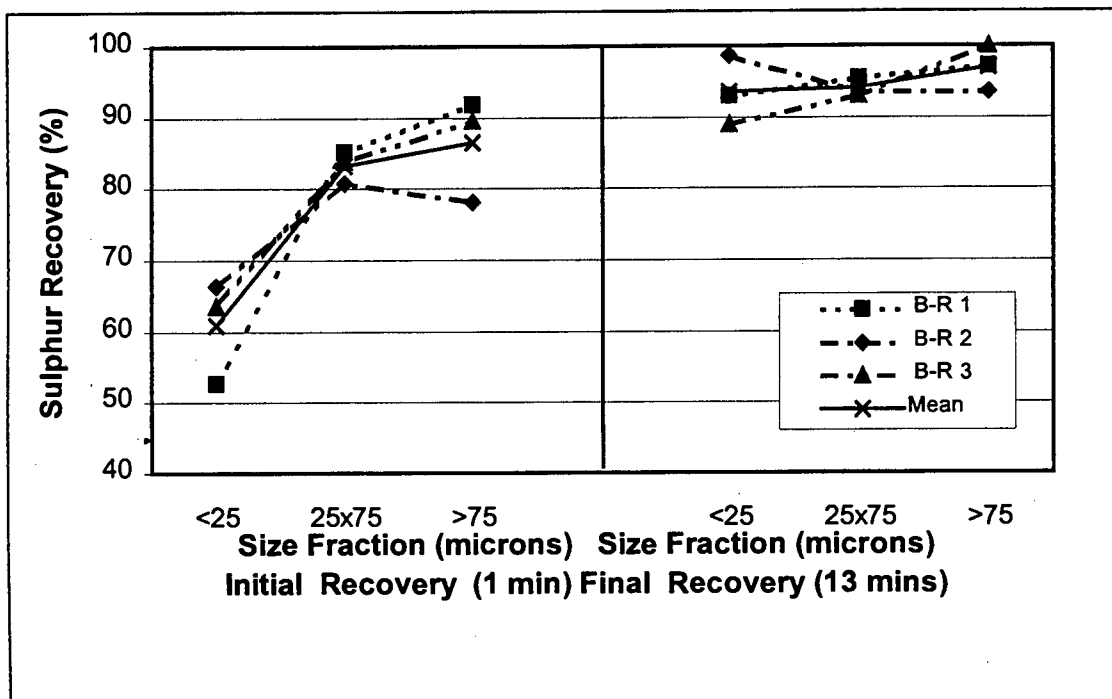


Figure 2.2: Sulphur recovery by size for reproducibility tests (B-R 1-3) using SMT as collector and 200 mmol/t copper sulphate (Buffelsfontein ore)

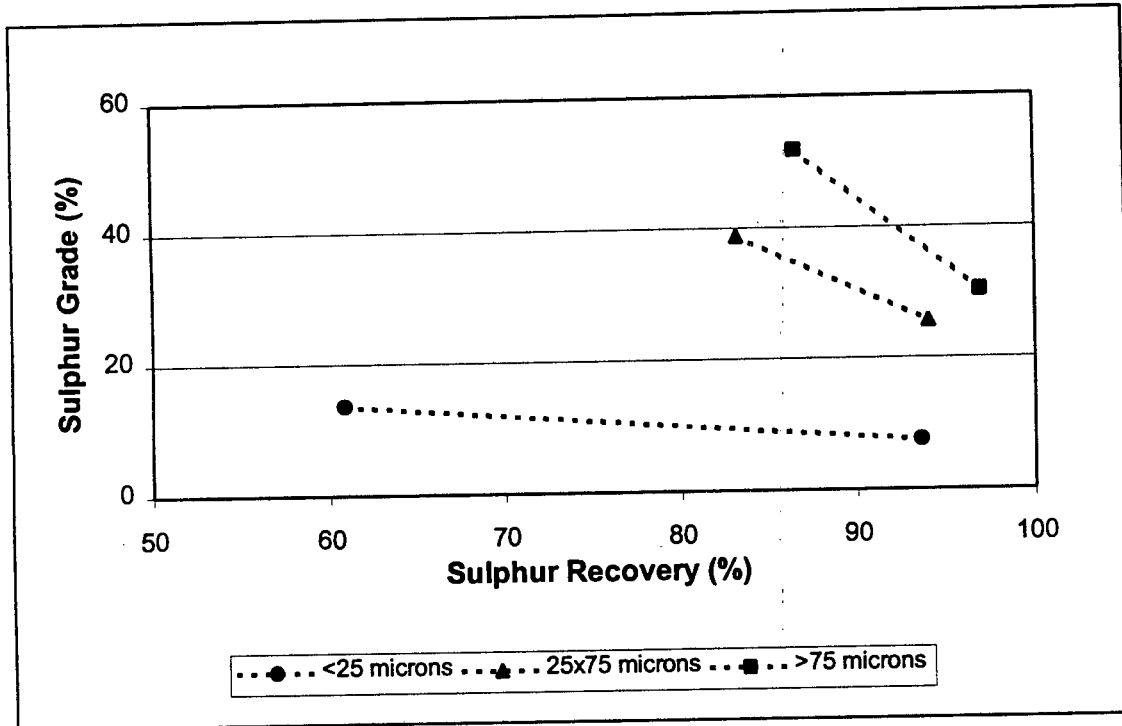


Figure 2.3: Mean sulphur grade vs sulphur recovery by size after 1 and 13 mins for the reproducibility tests (B-R 1-3) using SMBT as collector and 200 mmoles/t copper sulphate (Buffelsfontein ore)

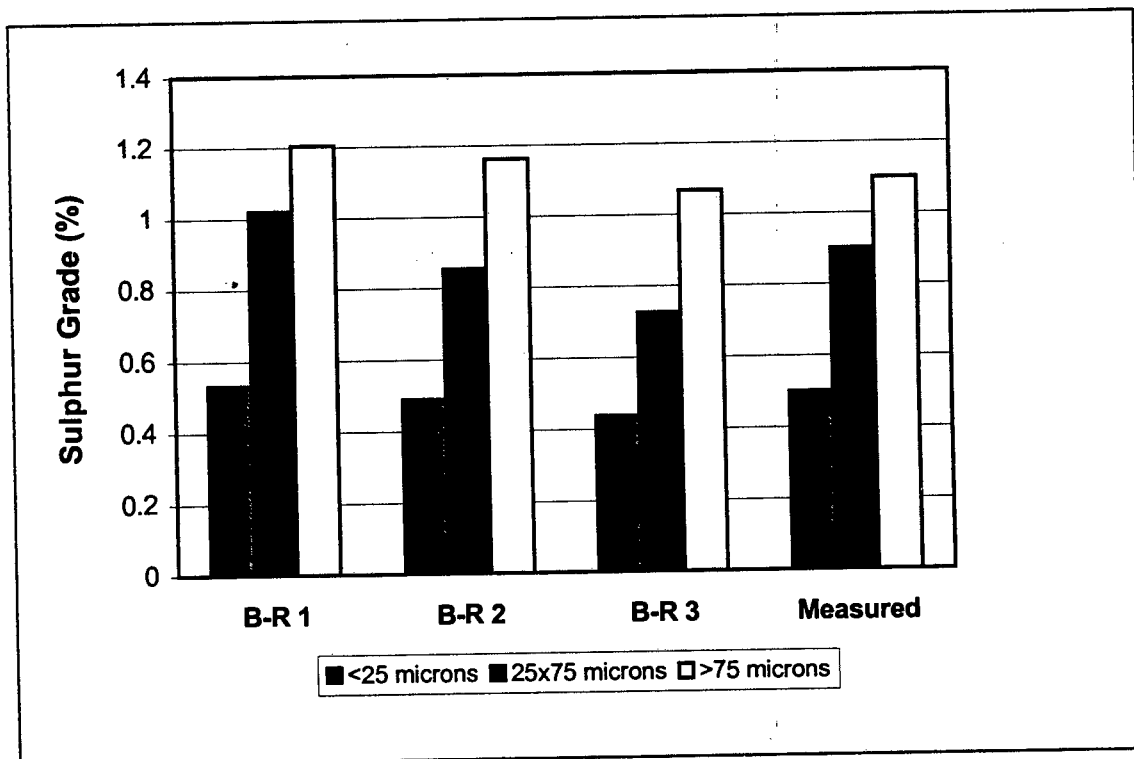


Figure 2.4: The calculated sulphur grades by size for the reconstituted feed samples compared to the measured feed grade (Buffelsfontein ore)

2.3.1.2 FLOTATION WITH PNBX AND CYCLOHEXYL DTC (TESTS B 9-12)

The aim of these tests was to characterise the differences in the flotation performance of pyrite at pH = 4, obtained using the thiol collectors, PNBX and cyclohexyl DTC, so that the contribution of the respective component collectors could be used in the interpretation of results obtained using the mixtures of these collectors (cf. Sec. 2.3.1.3). The collectors were both tested at a dosage of 310 mmol/t, which is equivalent to 60 g/t PNBX, with all other operational parameters kept constant.

The results of these tests and the results obtained using the mixtures (cf. Sec. 2.3.1.3) are summarised in Table 2.6, with full details given in Appendix 2E. The standard deviations calculated from the reproducibility tests are also shown so that a measure of the significance of the various differences can be gauged. The results obtained with the pure collectors, cyclohexyl DTC and PNBX are discussed under the following headings: Sulphur Grade vs Sulphur Recovery, Rate of Sulphur Recovery, Sulphur Recovery by Size, Water Recovery and Image Analysis of Froth Surface. The appropriate figures are included to highlight the relevant points.

The collectorless test (B-9) gave an indication of entrainment in that the mass yield was 3.4% with a sulphur recovery of 11.8%. The slight grade enrichment from 0.8% sulphur in the feed to 2.1% sulphur in the concentrate showed that at those conditions, there was some natural flotability of pyrite. Note that although the mineral recovery was significantly lower than that for the tests with collector present, the water and gangue recovery for this test was of the same order as that reported for the other tests reported in Table 2.6. The relationship between the gangue and sulphur recovery of the collectorless test is shown in conjunction with the gangue and sulphur recovery obtained with the pure collectors in Figures 2.9 and 2.10.

Table 2.6 Summary of results obtained with PNBX, cyclohexyl DTC and mixtures of PNBX and cyclohexyl DTC (Buffelsfontein ore)

Collector Type	Test Number	Collector Dosage (mmoles/t)	Klimpel Model Constants		Time	Mass Recovery (%)	Water Recovery (g)	Sulphur Recovery (%)				Sulphur Grade (%)			
			(k) (min ⁻¹)	(R) (%)				Overall	< 25 µm	25x75 µm	> 75 µm	Overall	< 25 µm	25x75 µm	> 75 µm
nil	B-9	nil	-	-	1 min	2.07	188.1	3.3	-	-	-	1.0	-	-	-
					13 min	3.39	322.4	11.8	-	-	-	2.1	-	-	-
oC6 DTC	B-10	310	4.63	97.8	1 min	2.45	125.7	77.1	68.2	78.7	74.7	25.6	8.7	36.9	47.2
					13 min	4.62	302.0	96.4	99.5	98.1	92.3	17.3	6.6	29.6	33.2
PNBX	B-11	310 ⁽²⁾	0.60	98.9	1 min	0.41	3.7	21.7	17.4	17.0	17.8	37.8	15.6	40.4	45.8
					13 min	3.08	114.2	85.9	79.3	69.2	92.8	20.1	7.7	22.5	38.8
95:5 ⁽¹⁾	B-12	310	1.68	94.2	1 min	1.07	8.2	49.8	33.3	67.8	42.1	35.2	16.4	45.5	51.1
					13 min	3.11	123.0	91.2	84.4	92.9	94.0	22.8	9.6	38.9	42.3
90:10	B-13	310	2.02	94.6	1 min	0.90	8.3	46.1	32.4	42.9	38.8	38.6	18.9	47.3	51.7
					13 min	3.28	131.5	93.1	91.2	95.0	92.2	21.4	8.5	30.4	42.2
85:15	B-14	310	2.69	94.9	1 min	1.27	14.9	62.8	51.8	65.5	95.1	37.5	16.4	44.8	52.6
					13 min	3.43	141.4	93.1	89.5	94.3	93.9	20.4	8.7	28.5	39.4
50:50	B-15	310	4.00	96.9	1 min	1.62	32.9	73.6	61.8	90.4	73.3	33.1	14.0	41.6	51.5
					13 min	3.55	171.4	95.8	90.5	99.8	87.1	19.6	8.3	30.4	38.6
PNBX	B-16	465 ⁽³⁾	0.62	82.1	1 min	4.53	2.4	24.3	20.9	36.0	22.2	39.0	15.8	43.0	49.2
					13 min	2.48	81.8	74.2	72.5	80.5	92.1	21.8	8.4	27.2	42.9
90:10	B-17	465	1.50	94.8	1 min	1.08	12.5	50.9	32.4	48.3	48.3	39.7	19.6	48.4	53.0
					13 min	3.89	134.8	92.3	81.1	96.3	95.6	20.0	8.5	30.1	43.7
Std Dev			1.2	0.9	1 min	0.17	15.94	3.41	6.30	3.14	7.91	2.18	1.82	2.01	1.70
					13 min	0.23	32.40	0.86	3.46	2.02	4.08	0.78	0.77	1.62	2.68

(1) Indicates mixture of PNBX:oC6 DTC

(2) Dosage equivalent to 60 g/t PNBX

(3) Dosage equivalent to 90 g/t PNBX

2.3.1.2.1 SULPHUR GRADE VS SULPHUR RECOVERY

Sulphur grade vs sulphur recovery curves are used to indicate the metallurgical performance of flotation, with increasing metallurgical performance represented by curves representing the highest grade - recovery combination. Figure 2.5 shows that the sulphur grade - sulphur recovery curve obtained using cyclohexyl DTC was higher than that obtained using PNBX. Initial grades obtained with PNBX were high, but this was at very low recovery.

It can also be seen from Figure 2.5 that at a sulphur recovery of 80%, a sulphur grade of 24.6% is obtained using cyclohexyl DTC compared to that of 21.4% obtained using PNBX. At a sulphur grade of 25% the sulphur recovery of 79.0% was obtained using cyclohexyl DTC compared to that of 67.5% obtained using PNBX. From Table 2.6 the standard deviation of sulphur recovery is 0.91% and the standard deviation of sulphur grade is 0.57%. The difference in the curves is greater than the limits of experimental error and the performance obtained with cyclohexyl DTC is thus qualitatively significantly higher than that obtained with PNBX.

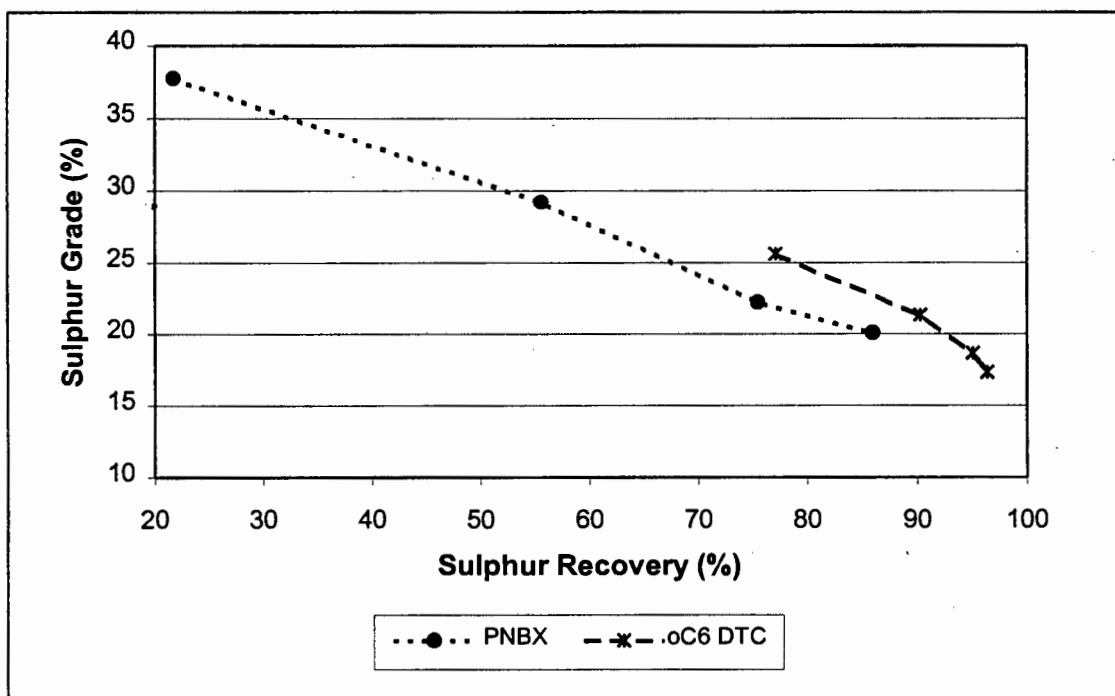


Figure 2.5: Sulphur grade vs sulphur recovery obtained using 310 mmoles/t PNBX and cyclohexyl DTC (Buffelsfontein ore)

2.3.1.2.2 RATE OF SULPHUR RECOVERY

The rate constants obtained from the Klimpel model are shown in Table 2.6. These show that the rate of recovery was much higher with cyclohexyl DTC than with PNBX, viz. 4.63 min^{-1} vs 0.60 min^{-1} . The difference in the infinite time recovery obtained with the two collectors was much smaller than the difference in rates, viz 97.8% sulphur vs 98.9% sulphur, thus validating the use of this model. The recovery after 1 minute is also an indicator of rate of recovery and Table 2.6 shows that whereas the sulphur recovery after 1 min obtained using cyclohexyl DTC was 77.1%, the recovery obtained using PNBX was 21.7%, thus reflecting the difference in the first order rate constants. The difference in recovery after 13 mins was lower, viz. 96.4% for cyclohexyl DTC compared to 85.9% for PNBX. These values are shown in Figure 2.29 in conjunction with the results obtained using a 90:10 mole ratio mixture of PNBX and cyclohexyl DTC.

2.3.1.2.3 SULPHUR RECOVERY BY SIZE

Figure 2.6 shows that the sulphur recovery of all size fractions is significantly higher with cyclohexyl DTC than with PNBX. The differences in overall sulphur recovery are much larger for the initial recoveries (1 minute) than those obtained for the final recoveries (13 minutes) as referred to in Sec. 2.3.1.2.2. Although the initial recovery of fines obtained with cyclohexyl DTC was slightly lower than the recovery of other size fractions, the final recovery was higher. This illustrates the lower collision efficiency expected with decreasing particle size [Ralston 1994]. The results suggest that over 13 mins, the additional time compensated for the lower collision efficiency and this was no longer a constraining factor.

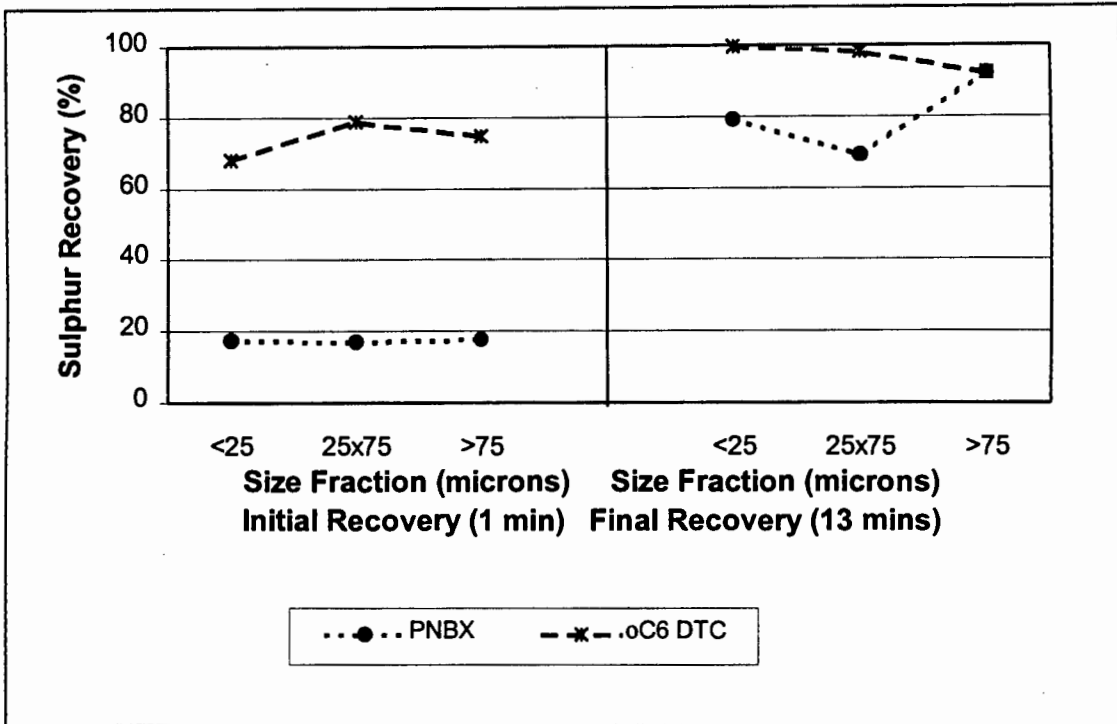


Figure 2.6: Sulphur recovery by size obtained using 310 mmoles/t PNBX and cyclohexyl DTC (Buffelsfontein ore)

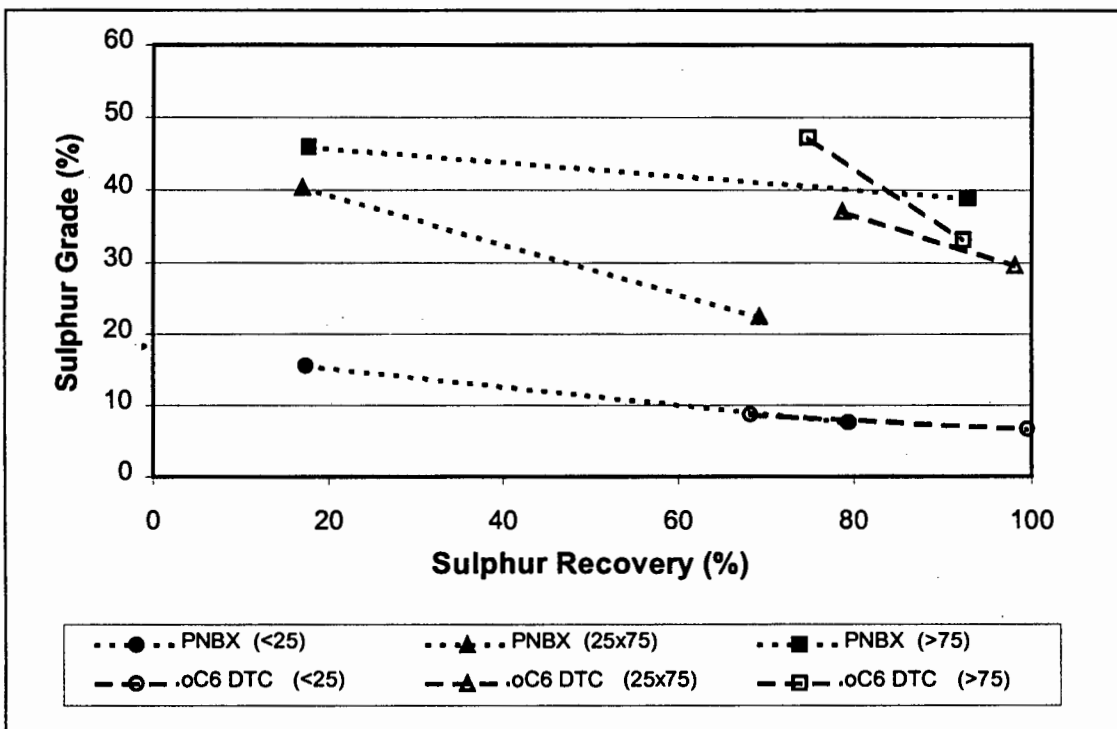


Figure 2.7: Sulphur grade vs sulphur recovery by size obtained using 310 mmoles/t PNBX and cyclohexyl DTC (Buffelsfontein ore)

Figure 2.7 shows that the increased fines recovery over 13 mins, relative to the coarser fractions was at a considerable grade penalty, viz. a sulphur grade of 8.7% for the $< 25 \mu\text{m}$ fraction compared to 47.2% and 36.9% respectively for the > 75 and $25 \times 75 \mu\text{m}$ fractions. In general, the highest grade material recovered was the initial $> 75 \mu\text{m}$ fraction for both the PNBX and cyclohexyl DTC collectors. The sulphur grade vs recovery curves for the $< 25 \mu\text{m}$ fraction showed a similar relationship for both the PNBX and cyclohexyl DTC, although the cyclohexyl DTC gave higher recoveries and lower grades. This indicated that the overall flotability of fine material was not changed and the differences in fine particle behaviour were related to the differences in mass pull, with increased non - selective recovery by entrainment in the case of cyclohexyl DTC. It can be seen that this was not the case for the other size fractions, with the increased sulphur recovery obtained with cyclohexyl DTC for the $25 \times 75 \mu\text{m}$ fraction being achieved at higher grade. The final recovery of the $>75 \mu\text{m}$ fraction was at a reduced grade but this may be attributed to the recovery of coarse composite particles.

2.3.1.2.4 WATER RECOVERY

Figure 2.8 compares the water recoveries obtained with cyclohexyl DTC, PNBX and with no collector addition. It can be seen that the highest water recovery was obtained in the case of no collector addition. The use of cyclohexyl DTC gave a slightly lower water recovery than that with no collector and the water recovery obtained using PNBX was substantially reduced to approximately one third of the others. High water recoveries are traditionally associated with high entrainment of fines, resulting in increased, although unselective, recovery of the fine fraction [Engelbrecht and Woodburn, 1975]. In the case of cyclohexyl DTC, the high water recovery was accompanied by the expected higher final recovery of the $< 25 \mu\text{m}$ material at decreased sulphur grades, as shown in Figure 2.7 and Table 2.6. This is consistent with the results obtained in the case of PNBX, where the lower water recovery resulted in the sulphur grade

obtained for the $< 25 \mu\text{m}$ material being higher than that obtained using cyclohexyl DTC although the relationship between sulphur grade and recovery was similar.

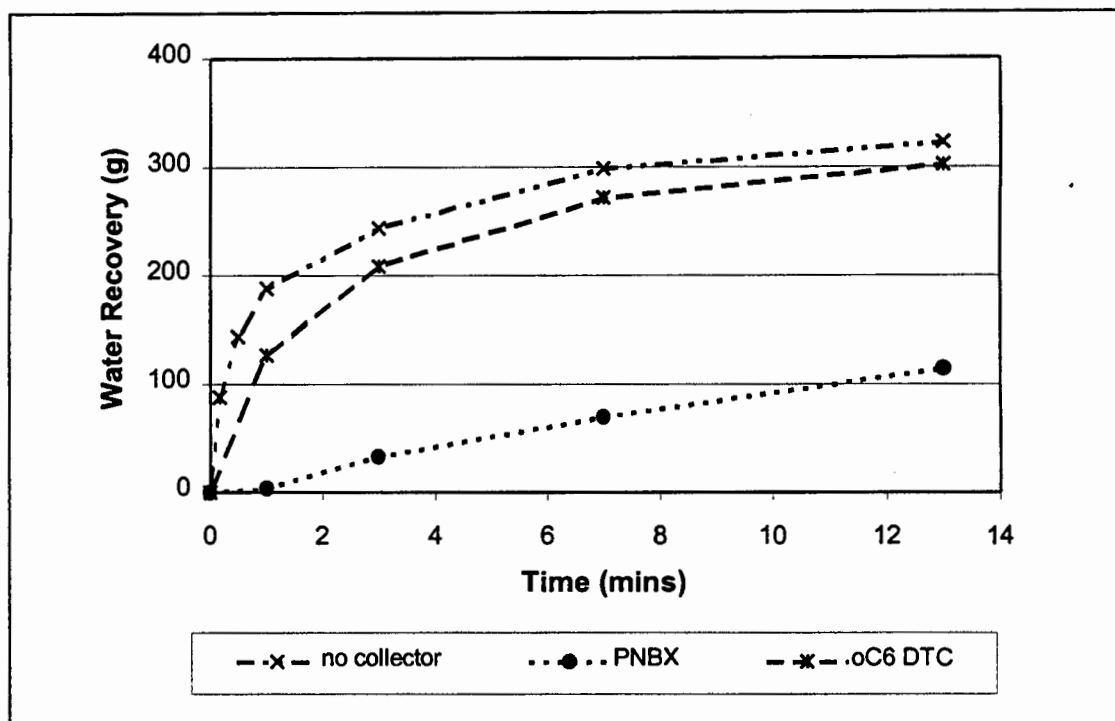


Figure 2.8: Water recovery vs time obtained using 310 mmol/t PNBX, cyclohexyl DTC and with no collector addition (Buffelsfontein ore)

In Figure 2.7, it was shown that, for the same recoveries, higher grades were obtained using cyclohexyl DTC rather than PNBX. The increased water recovery accompanying the increased sulphur recovery was without overall loss in grade in the case of cyclohexyl DTC due to the increased grade of the coarser fractions. This indicates that water recovery is not the only factor governing overall grade and that other factors, such as the froth drainage characteristics, also play a role in the overall grade obtained.

Figure 2.9 shows the difference in the relationship between the sulphur and recovery and the water recovery obtained for the two collectors and in the case of no collector addition.

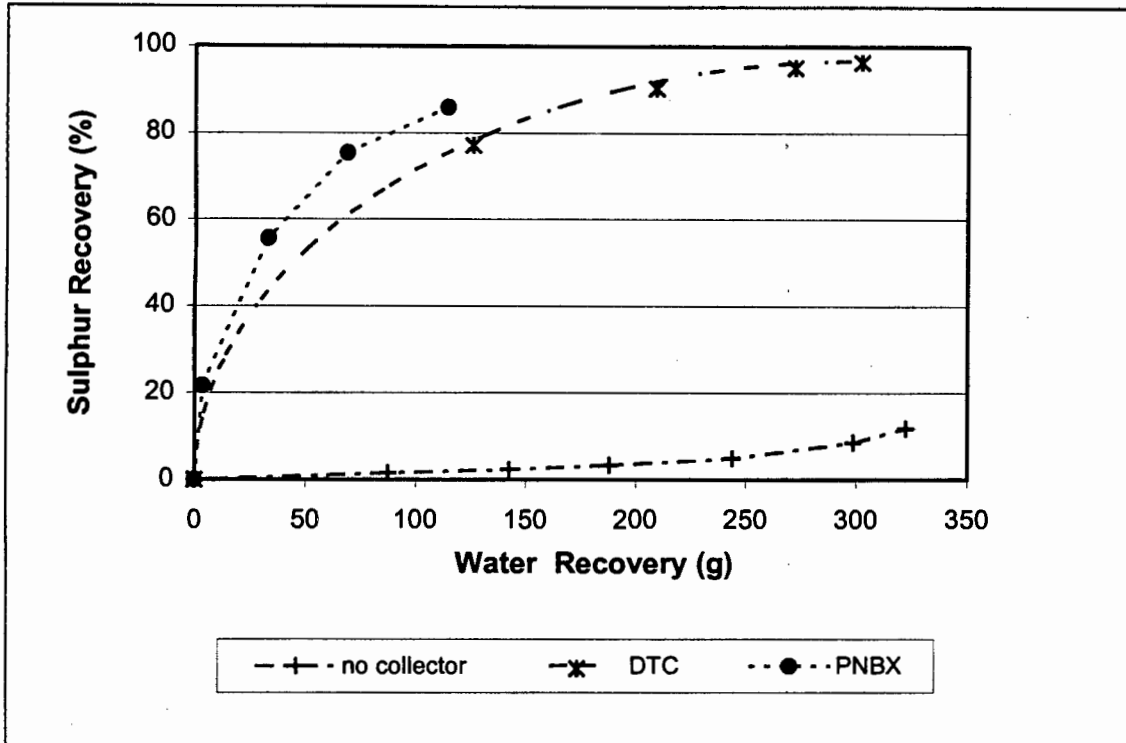


Figure 2.9: Sulphur recovery vs water recovery obtained using 310 mmole/t PNBX, cyclohexyl DTC and with no collector addition (Buffelsfontein ore)

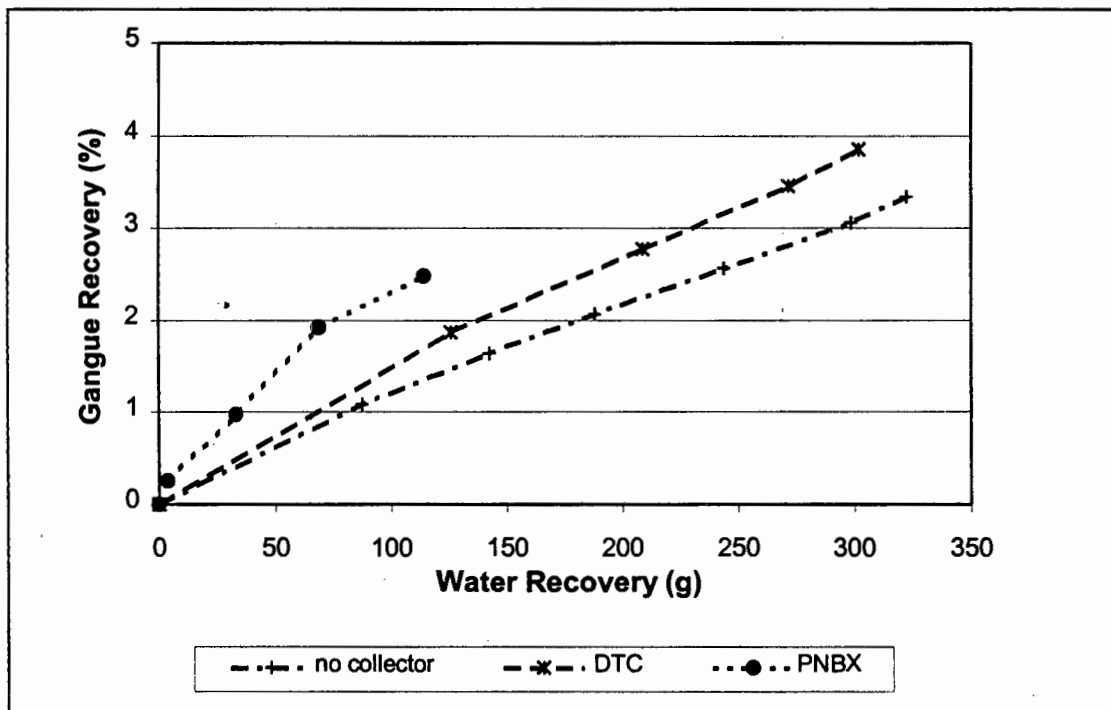


Figure 2.10: Gangue recovery vs water recovery obtained using 310 mmole/t PNBX, cyclohexyl DTC and with no collector addition (Buffelsfontein ore)

It can be seen that the use of PNBX results in a higher recovery of sulphur per mass of water, even though the overall water recovery was considerably lower than that of cyclohexyl DTC. It can also be seen that the recovery of sulphur is very low in the absence of collector.

Figure 2.10 shows the difference in the relationship between the gangue recovery and the water recovery obtained for the two collectors and in the case of no collector addition. As was the case for sulphur recovery, the gangue recovery was higher per mass of water recovered in the case of PNBX, indicating that the froth was poorly draining. This froth was also heavily laden and more viscous than that obtained with cyclohexyl DTC (cf. 2.3.1.2.5).

The highest water recovery was obtained in the absence of collector. The gangue recovery was lower for no collector addition than for cyclohexyl DTC, indicating that the entrainment was less, probably due to poorer froth characteristics.

2.3.1.2.5 IMAGE ANALYSIS OF SURFACE FROTH

The surface froth characteristics were analysed by image analysis in order to gain more information about the differences in flotation behaviour obtained for the different collectors and collector mixtures. The focus of the analysis was on the differences in characteristics and not on the absolute characteristics of the system. The relationship between these differences in surface froth characteristics and the metallurgical results is discussed. The parameters evaluated were froth surface bubble size, froth stability and froth mobility. It must be taken into account that the flotation tests were batch tests and there was a time lag before steady state was reached. For all the parameters measured steady state seems to be obtained after 4 mins.

Figure 2.11 shows that the change in average bubble size, as illustrated by the change in NNU (cf. Sec. 2.3.2), of the froth surface with time. It can be seen that the bubble size in the froth surface was considerably smaller in the case of cyclohexyl DTC. The small bubble size obtained with cyclohexyl DTC remained constant throughout the test whereas the bubble size obtained with PNBX was initially large and then decreased for the first 4 minutes before reaching a constant value until the end of the test. The lower bubble size obtained with cyclohexyl DTC corresponded to high water recovery (cf. Figure 2.8) and rate of sulphur recovery.

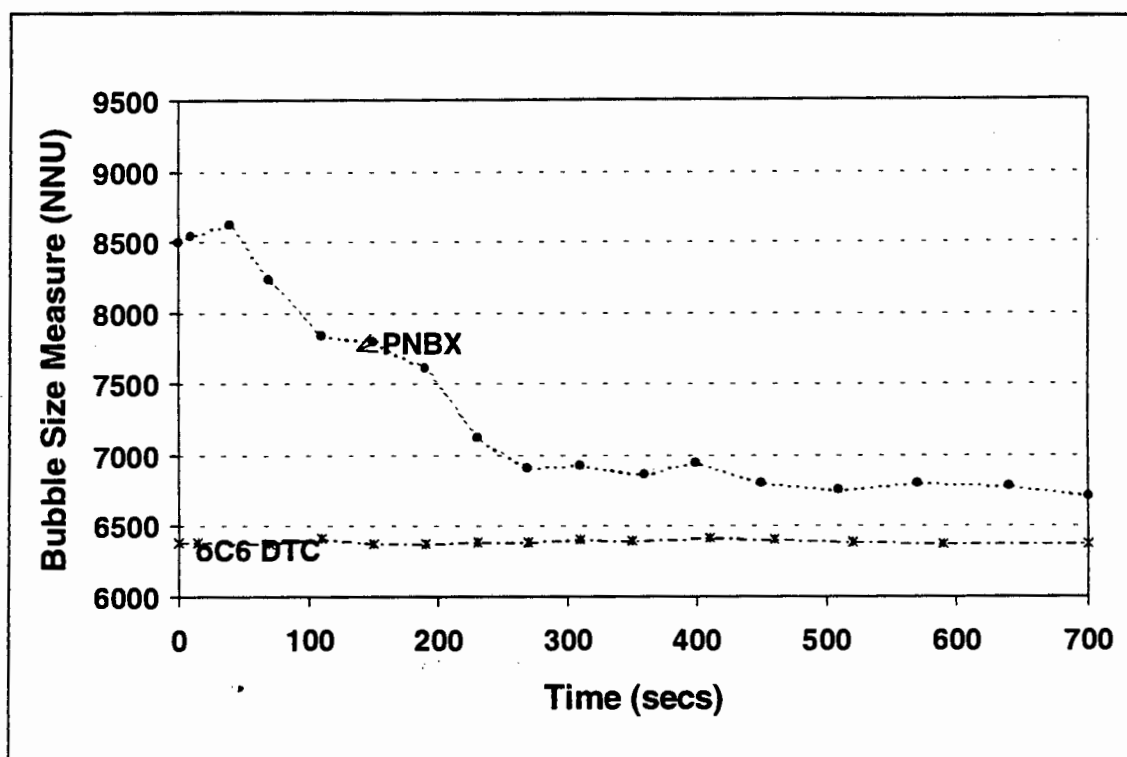


Figure 2.11 : The change in average bubble size of surface froth with time for tests using 310 mmol/t PNBX and cyclohexyl DTC (Buffelsfontein ore)

The froth instability was measured as the rate of change of froth structure and is shown in Figure 2.12. In the first 5 minutes the froth structure obtained with cyclohexyl DTC was less stable than the PNBX. This corresponded to the high water and mass recoveries and low grades obtained with cyclohexyl DTC.

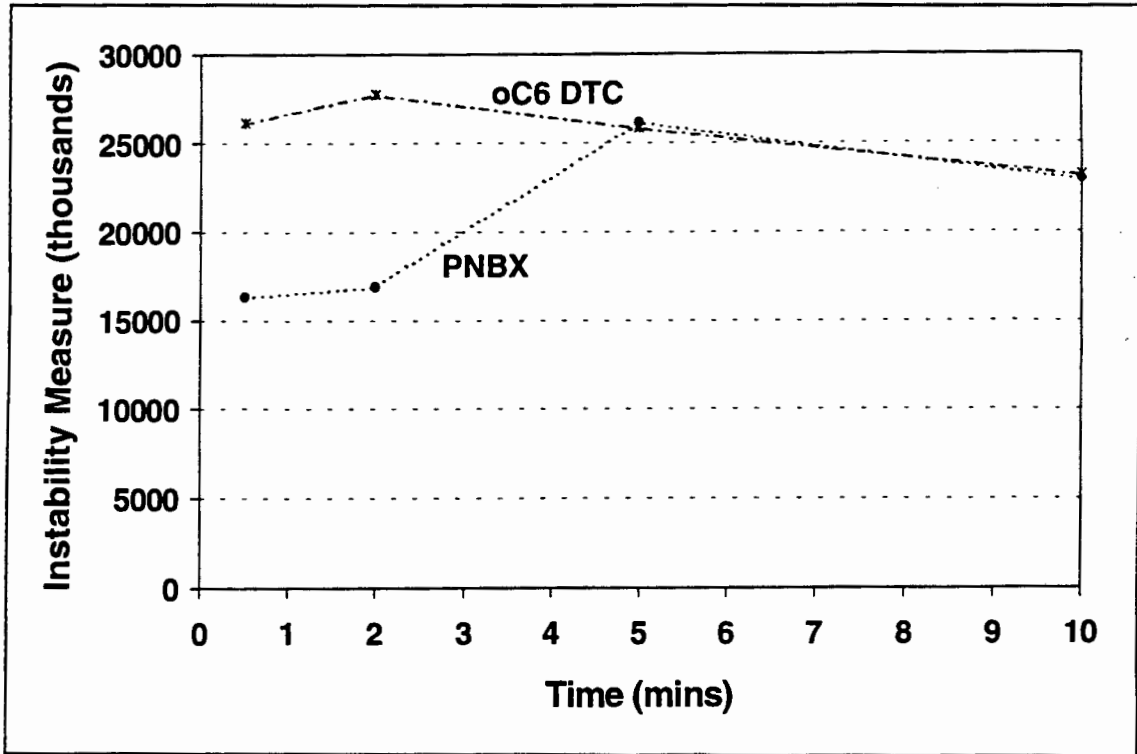


Figure 2.12: Instability feature measure for tests using 310 mmol/t PNBX and cyclohexyl DTC (Buffelsfontein ore)

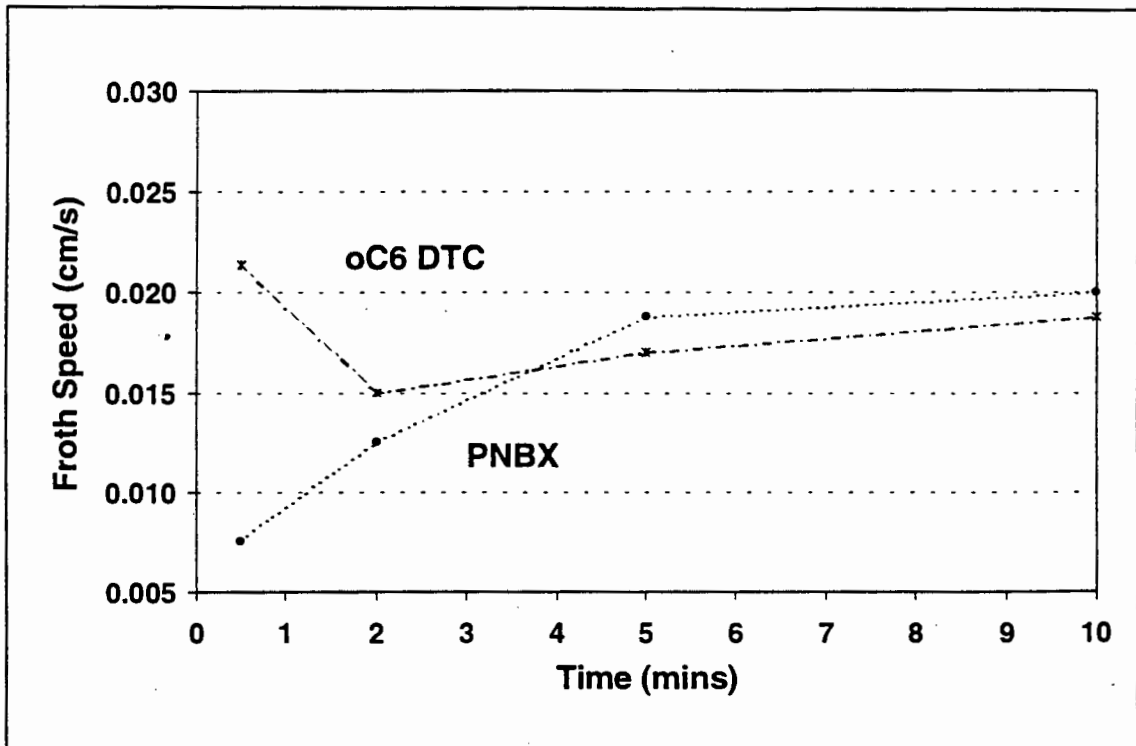


Figure 2.13: The froth speed of flotation tests using 310 mmol/t PNBX and cyclohexyl DTC mixture (Buffelsfontein ore)

The more stable froth obtained with PNBX corresponds to the lower water recoveries (cf. Figure 2.8) and higher sulphur and gangue recoveries per mass of water obtained for PNBX (cf. Figures 2.9 and 2.10). These froth characteristics are expected from a highly mineralised non - draining froth.

Figure 2.13 shows the froth speed of the two collectors. In the first two minutes a higher froth speed was measured with cyclohexyl DTC. This increased froth flow rate is accompanied by a higher water and gangue recovery after 13 mins. (cf. Figure 2.8 and 2.10). Lower speeds were initially observed with PNBX, which increased for the first 5 minutes, before reaching a constant level. This corresponds to decreasing bubble size and increasing froth instability over the same time.

This analysis showed that the varying metallurgical flotation performance obtained with the two collectors was accompanied by differences in surface froth behaviour. The higher grade and recovery obtained with cyclohexyl DTC was accompanied by a watery, mobile froth with small bubbles in the surface froth.

The use of cyclohexyl DTC gave a froth which was watery (cf. high water recovery in Figure 2.8), brittle (cf. higher instability in Figure 2.12) and fast moving (cf. Figure 2.13). This resulted in a well drained froth and, for the same sulphur recovery as that obtained for PNBX, the sulphur grade was also higher than that obtained for PNBX and the gangue recovery per unit water recovery was lower. If the results are compared with respect to flotation time, rather than with respect to water recovery, higher sulphur recoveries at lower sulphur grades are obtained with cyclohexyl DTC. In the case of PNBX, the much lower rate of flotation obtained was characterised by a viscous, less mobile froth with large bubble size.

The different froth characteristics and water recoveries obtained with the two collectors showed that the froth characteristics were strongly affected by the

nature of the collector. This illustrated the interactive nature of flotation parameters and that the effect of the nature of the collector was not limited to changing the degree of hydrophobicity of the mineral surface, affecting only the collection efficiency in the pulp zone, (cf. Sec. 1.2.2) but also had a significant effect on the characteristics of the froth. The additional water recovered with cyclohexyl DTC suggests that cyclohexyl DTC can be classified as having more frothing properties than PNBX. Jiwu et al [1984] reported that the choice of a dithiocarbamate reagent was due to its combined frothing and collecting properties.

The results of these flotation tests with pure collectors have established the boundary conditions for the evaluation of the mixtures of PNBX and cyclohexyl DTC. The measured flotation responses, such as water recovery, sulphur recovery or sulphur grade, obtained using the mixtures of collectors can be compared to a linearly predicted response obtained by combining the relative contributions of PNBX and cyclohexyl DTC in order to determine whether any synergistic behaviour occurs when mixtures are used.

2.3.1.3 EFFECT OF RATIO OF PNBX TO CYCLOHEXYL DTC IN COLLECTOR MIXTURE

The aim of these tests was to investigate the effect of the ratio of constituents in a PNBX and cyclohexyl DTC collector mixture. The dosage of all the mixtures was kept constant at 310 mmol/t and no copper sulphate was added to the flotation tests. The flotation performance obtained using pure PNBX and pure cyclohexyl DTC was compared to that obtained with mixtures of mole ratios of 95:5, 90:10, 85:15 and 50:50 of PNBX and cyclohexyl DTC. Higher xanthate concentrations were used in this series of tests, largely due to the high cost of dithiocarbamates. All the results obtained are shown in Table 2.6 (pg. 80) with full details in Appendix 2E.

2.3.1.3.1 SULPHUR GRADE VS SULPHUR RECOVERY

Figure 2.14 shows the grade vs recovery curves as a measure of flotation performance for these tests. It can be seen that any mole ratio substitution of cyclohexyl DTC for PNBX improved the flotation performance as shown by the higher grade vs recovery curves, where curves for all mixtures were higher than those for the pure constituents. The best performance, as shown by the highest grade vs recovery curve, was obtained for the 50:50 mole ratio of PNBX to cyclohexyl DTC. The lowest recovery was obtained with pure PNBX and the highest recovery, but the lowest grade, was obtained with pure cyclohexyl DTC.

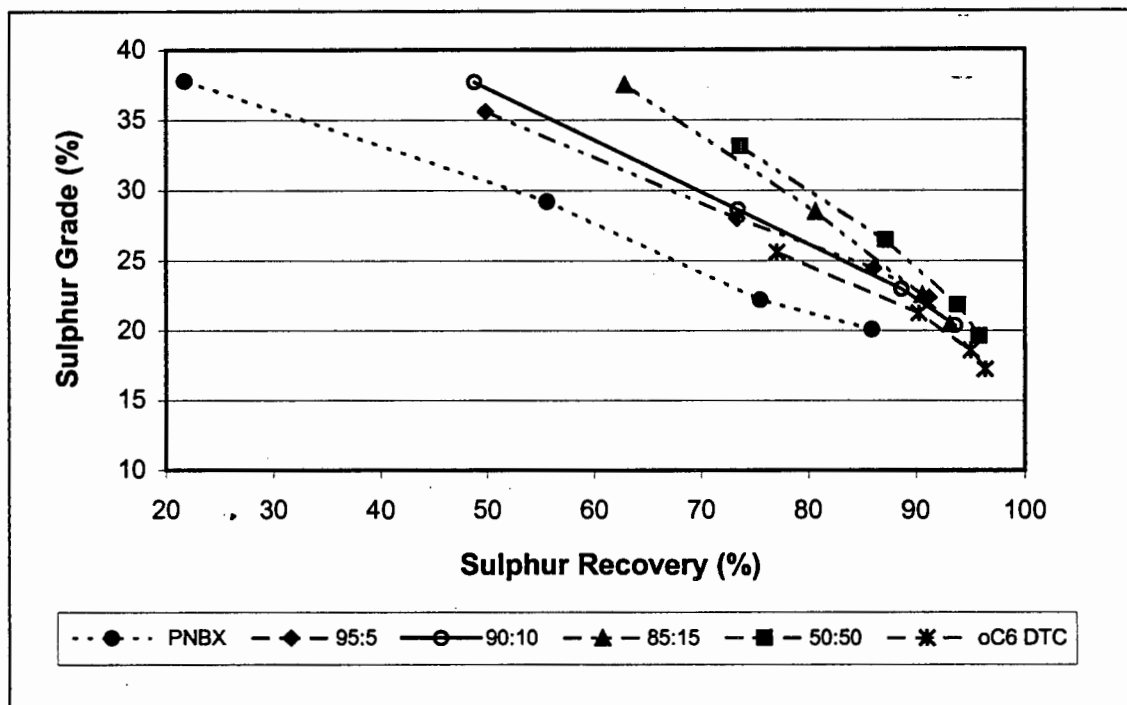


Figure 2.14: Sulphur grade vs sulphur recovery obtained using 310 mmol/t of collector containing varying ratios of PNBX and cyclohexyl DTC (Buffelsfontein ore)

In order to ascertain whether the improved flotation performance was not merely due to the linearly additive contribution of the individual collectors in the mixture, *measured* properties were compared to linearly additive *predicted* properties. This comparison is similar to the concept of excess property in

thermodynamics. Excess properties define the extent to which a mixture of fluids deviate in their behaviour from that predicted if the mixture properties were merely an additive function that depended on the amounts of each component present in the mixture. It would be similar in the present context to the difference between the *measured* and *predicted* values.

Figure 2.15 compares the measured sulphur grade with the predicted sulphur grade obtained at 80% sulphur recovery. It can be seen that the grade was highest for the 50:50 mole ratio of PNBX to cyclohexyl DTC. It is also clear that the sulphur grades are substantially increased above that expected from the linear contributions of the constituents, thus confirming that there is indeed a synergistic effect when collectors are mixed.

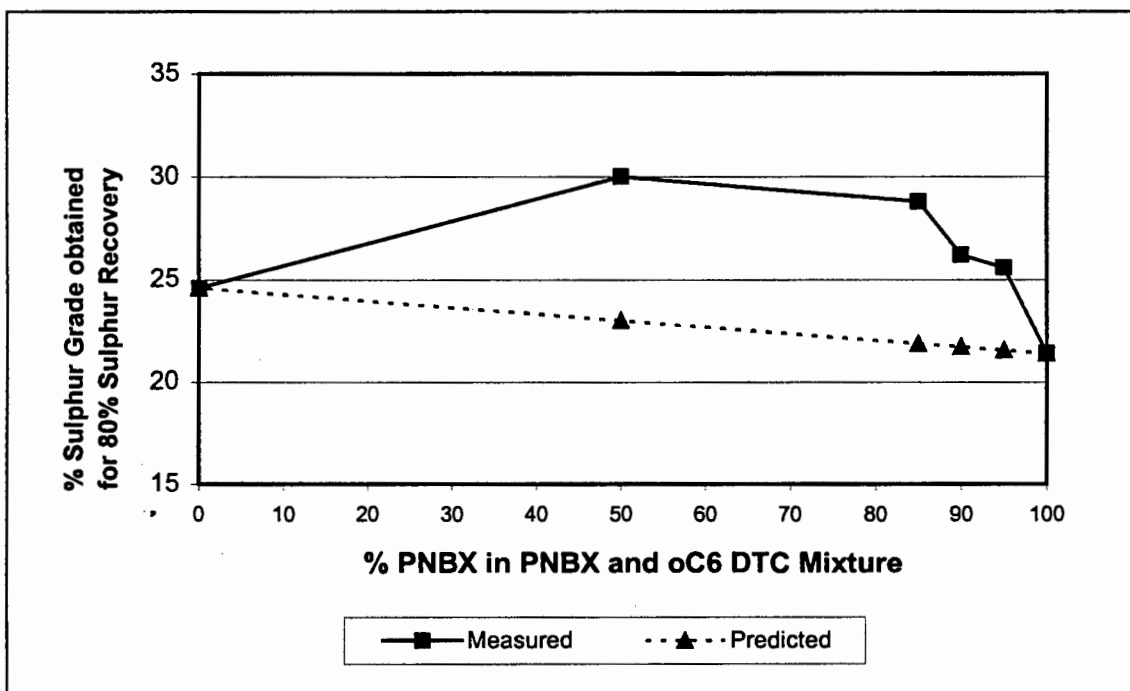


Figure 2.15: Comparison of measured vs predicted sulphur grades at 80% sulphur recovery obtained using 310 mmol/t of collector containing varying ratios of PNBX and cyclohexyl DTC (Buffelsfontein ore)

Figure 2.16 shows the measured and predicted sulphur recoveries at a sulphur grade of 25%. As was the case for the grades, all the recoveries obtained with the mixtures were greater than those predicted from the additive contributions clearly showing that there is synergism between the collectors.

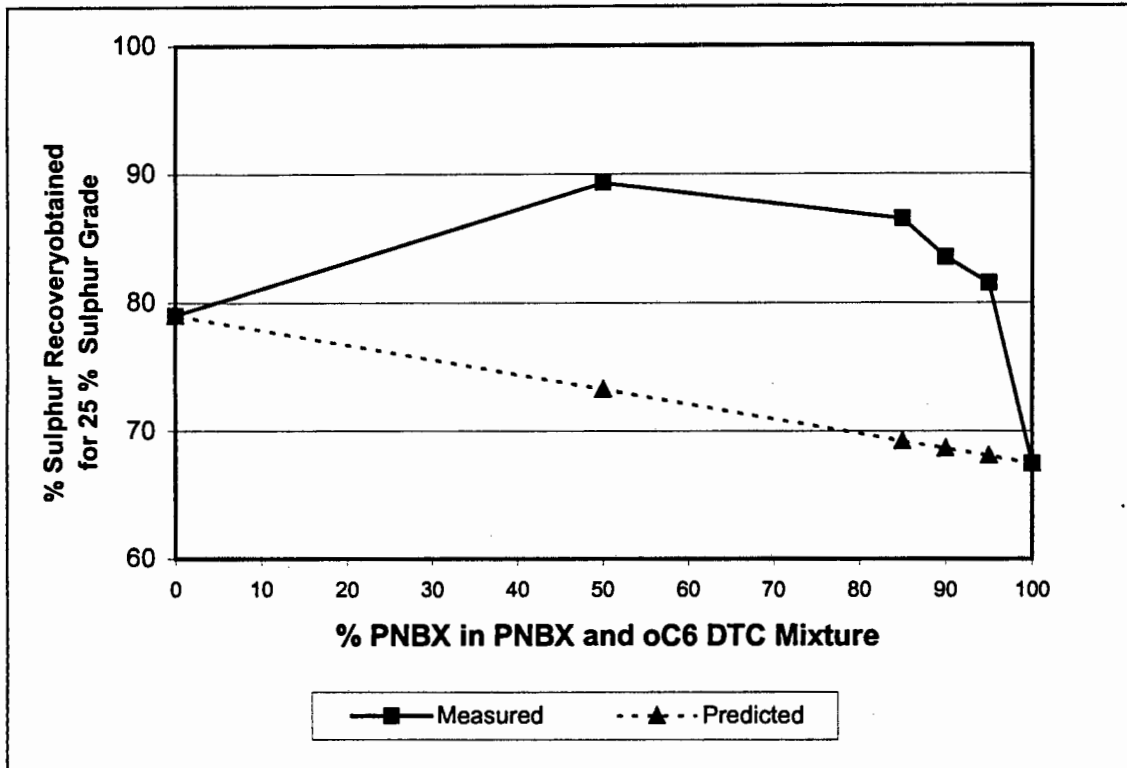


Figure 2.16: Comparison of measured vs predicted sulphur recoveries at 25% sulphur grade obtained using 310 mmoles/t of collector containing varying ratios of PNBX and cyclohexyl DTC (Buffelsfontein ore)

2.3.1.3.2 RATE OF SULPHUR RECOVERY

Figure 2.17 shows that the rate constant, k , was highest for cyclohexyl DTC and generally decreased with increasing content of PNBX. The lower value of k obtained for 90:10 mole ratio was not significant with respect to the standard deviation obtained for the reproducibility tests. The range in the infinite time recovery values, R , was between 94.5% and 98.9%. The rates were above those predicted from the additive contribution of the individual collectors and the infinite time recoveries were similar to those predicted.

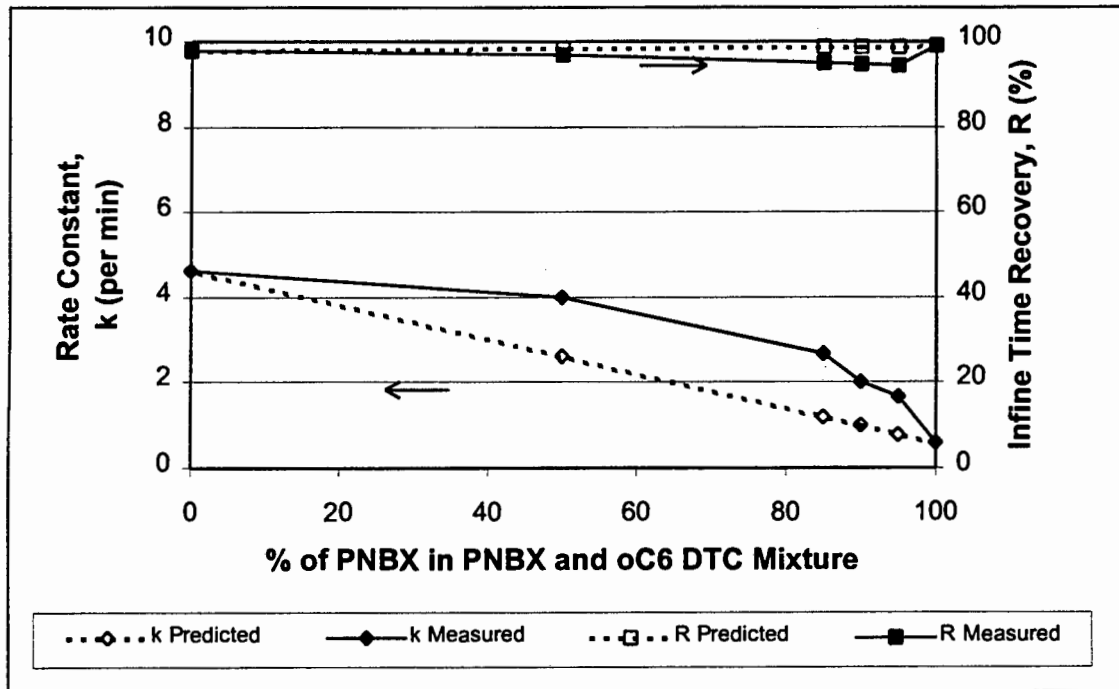


Figure 2.17: Comparison of measured vs predicted constants, k and R , from Klimpel obtained using 310 mmol/t of collector containing varying ratios of PNBX and cyclohexyl DTC (Buffelsfontein ore)

2.3.1.3.3 SULPHUR RECOVERY BY SIZE

Figure 2.18 shows the sulphur recoveries by size obtained after 1 min and after 13 mins as initial and final sulphur recoveries. The range in recoveries obtained with the different collector mixtures was much greater for the initial recoveries than for the final recoveries. Except for pure PNBX, the recovery for the middling fraction was higher than for the $< 25 \mu\text{m}$ and the $> 75 \mu\text{m}$ fractions. In general, the recovery in all size fractions increased with increase in proportion of cyclohexyl DTC in the mixture, the exceptions being the higher-than-expected mid-range recoveries of the 50:50 mixture and the 85:5 mixture. The fines recoveries increased with increase in proportion of cyclohexyl DTC in the mixture both for initial and final recoveries.

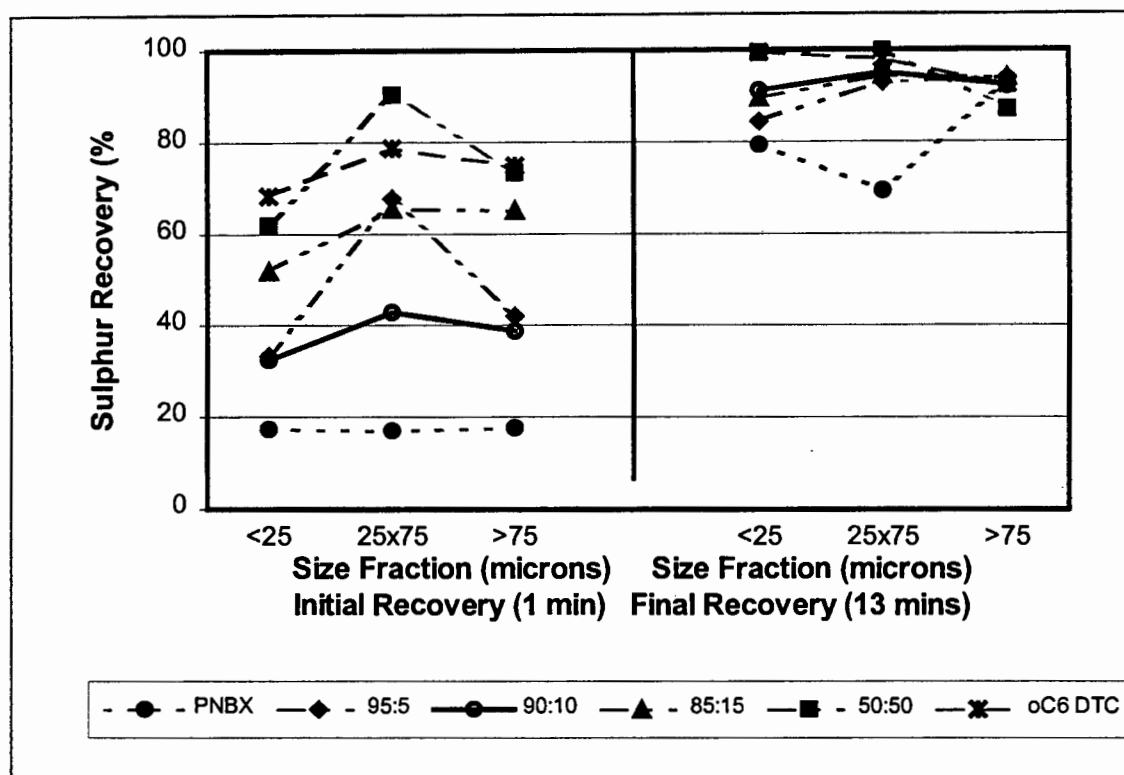


Figure 2.18: Sulphur recovery by size obtained using 310 mmol/t of collector containing varying ratios of PNBX and cyclohexyl DTC (Buffelsfontein ore)

Figures 2.19, 2.20 and 2.21 show the sulphur grade vs sulphur recovery for the < 25, 25 x 75 and > 75 μm fractions respectively. Figure 2.19 shows that the increased fines recovery shown in Figure 2.18 was at the cost of a grade penalty, and that the effect of the use of the mixtures on the overall sulphur grade vs recovery relationship was not quantitatively significant. In contrast to the results obtained for the overall flotation performance, the flotation performance of the < 25 μm fraction was not significantly improved by the use of mixtures. This phenomenon has also been reported by Finch and Dobby [1990], who showed that for the fine particle sizes, below 10 μm , increasing the particle hydrophobicity, as measured by reduced induction time, has less effect on the attachment efficiency than on the coarser fractions.

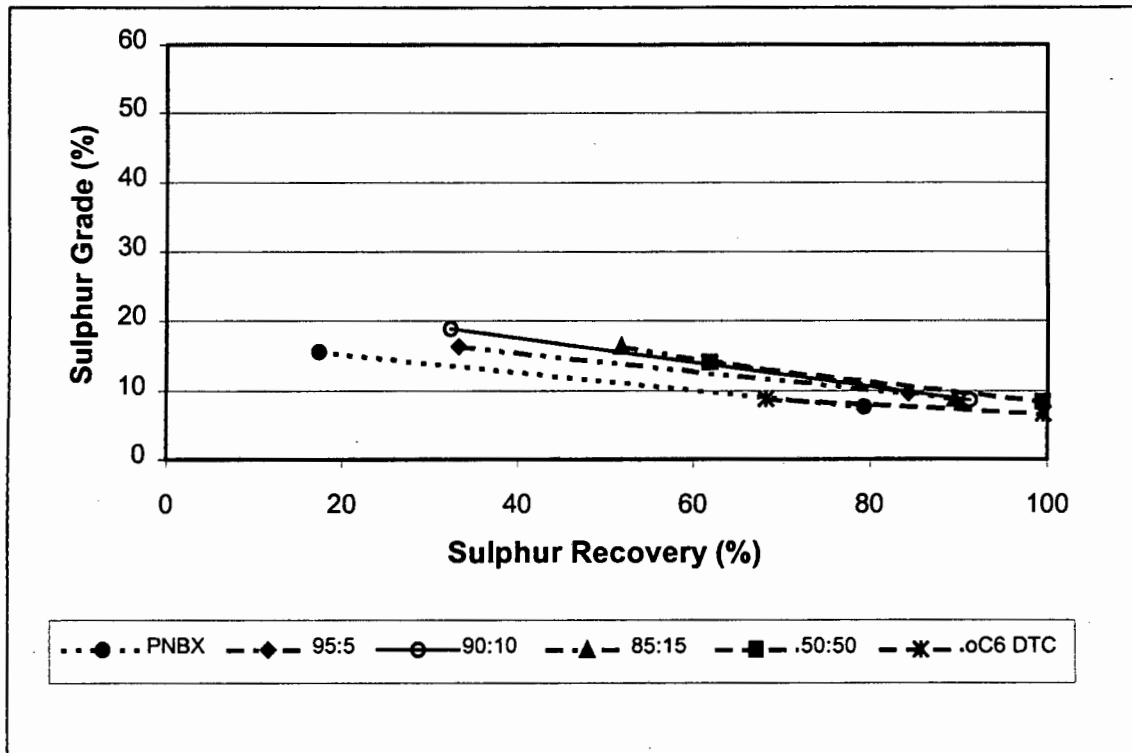


Figure 2.19: Sulphur grade vs recovery for < 25 μm size fraction obtained using 310 mmolles/t of collector containing varying ratios of PNBX and cyclohexyl DTC (Buffelsfontein ore)

Figure 2.20 shows that the sulphur grade vs sulphur recovery curves were higher for the mixtures in the 25 x 75 μm fractions. This showed that there was much less entrainment with the mixtures. The difference between the performance obtained with PNBX and the mixtures of collectors was significant in the light of the standard deviations obtained from the reproducibility tests.

Figure 2.21 shows that the sulphur grade vs recovery curves could be considered in two distinct groups. The first group, consisting of tests with pure PNBX and 95:5 and 90:10 mole ratio mixtures, was characterised by lower initial recoveries. The second group, consisting of pure cyclohexyl DTC and 85:15 and 50:50 mole ratio mixtures, was characterised by high initial recoveries and grades, although the grade with pure cyclohexyl DTC was lower. Overall the highest sulphur grade - recovery values were observed for the 85:15 mole ratio mixture. This can more likely be attributed to the recovery of composites than to entrainment due to the coarseness of the size.

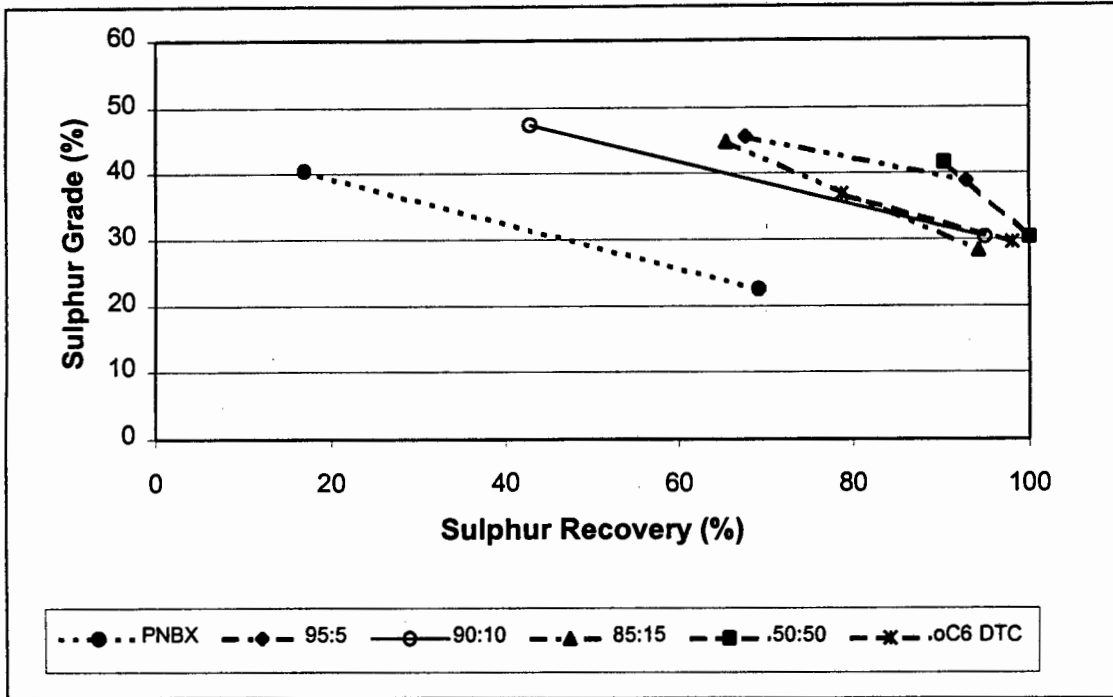


Figure 2.20: Sulphur grade vs recovery for 25 x 75 µm size fraction obtained using 310 mmoles/t of collector containing varying ratios of PNBX and cyclohexyl DTC (Buffelsfontein ore)

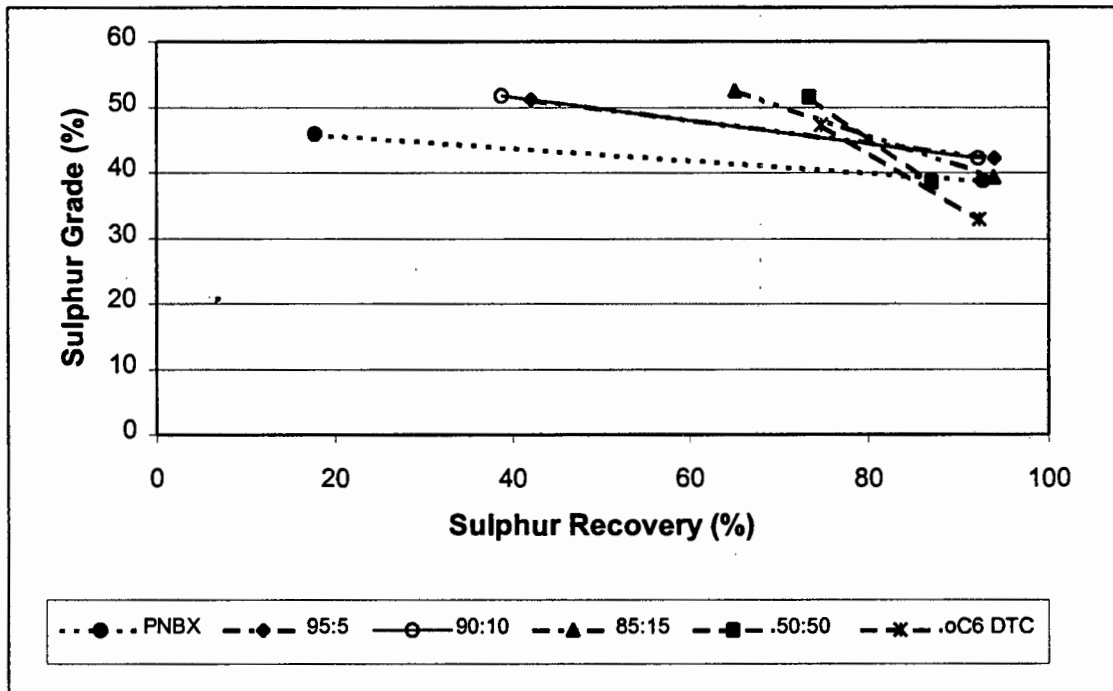


Figure 2.21: Sulphur grade vs recovery for > 75 µm size fraction obtained using 310 mmoles/t of collector containing varying ratios of PNBX and cyclohexyl DTC (Buffelsfontein ore)

2.3.1.3.4 WATER RECOVERY

Figure 2.22 shows that the water recovery increases with increasing proportion of cyclohexyl DTC, with that of pure cyclohexyl DTC being substantially higher than any of the mixtures.

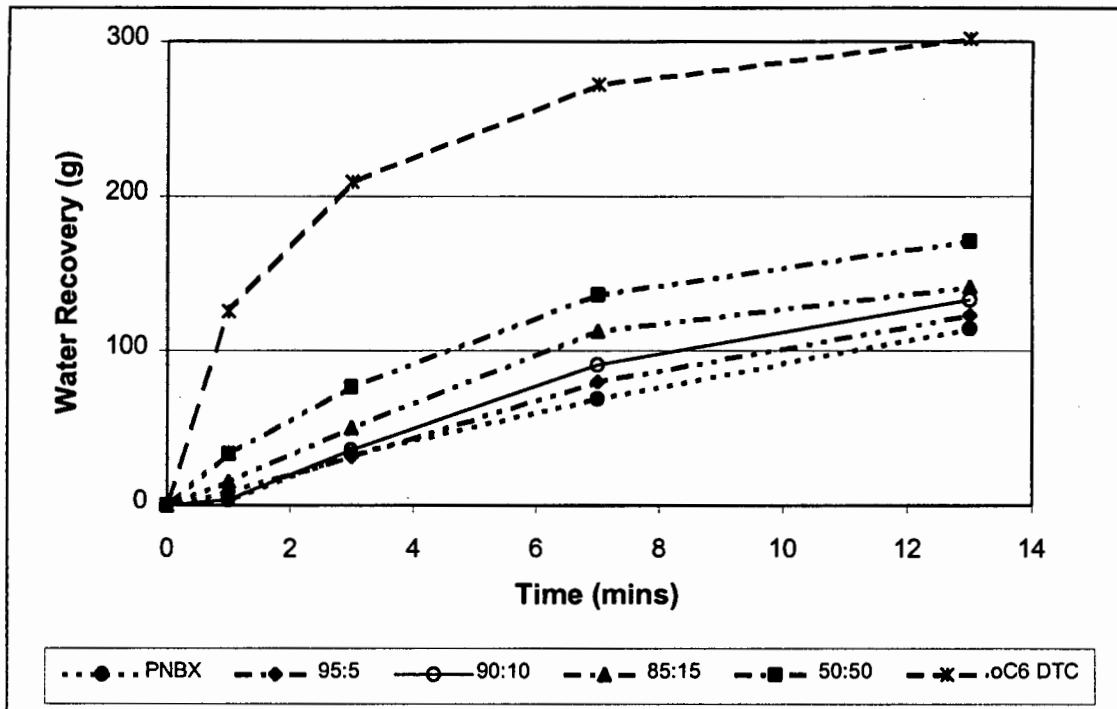


Figure 2.22: Water recovery vs time obtained using 310 mmol/t of collector containing varying ratios of PNBX and cyclohexyl DTC (Buffelsfontein ore)

Figure 2.23 shows the measured vs predicted water recovery (from additive contributions) obtained after 7 mins flotation time. It can be seen that the measured water recoveries do not differ significantly from the calculated water recoveries, although the deviation is slightly higher for the higher proportions of cyclohexyl DTC. There is, therefore, no measurable synergistic effect on the water recovery. Figures 2.24 and 2.25 show the relationship between the sulphur and gangue recovery respectively to the water recovery for the various mixtures. It can be seen that although both the sulphur and gangue recovery per mass of water is higher for the mixtures, the differences are greater for the sulphur recovery than for the gangue recovery.

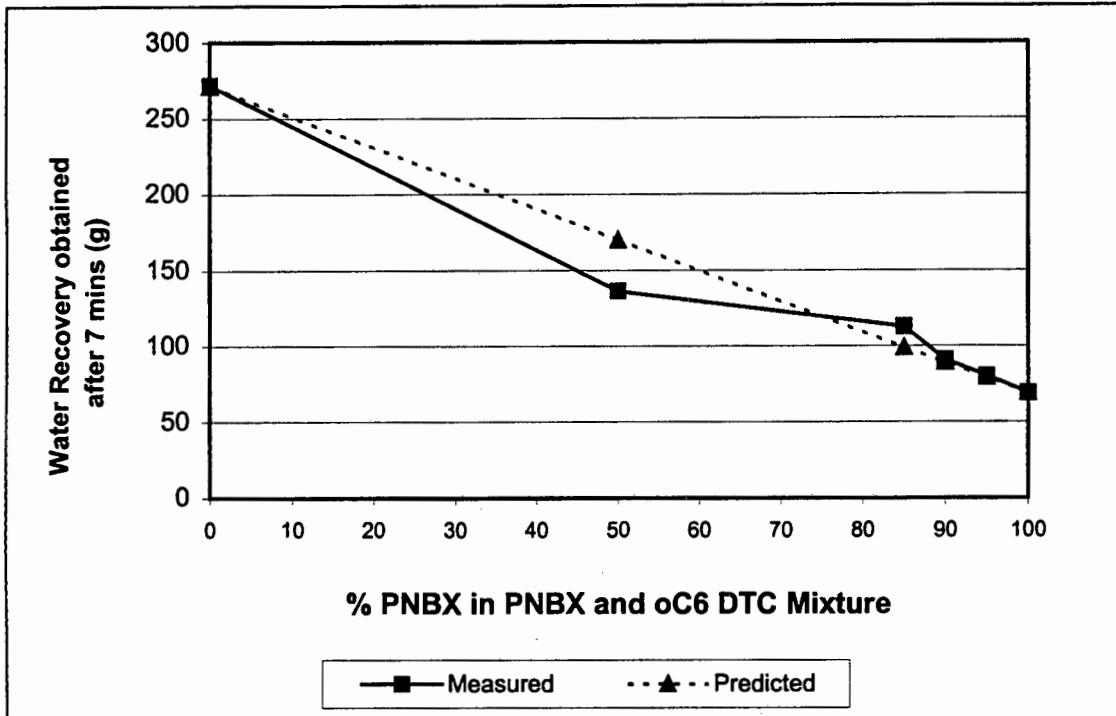


Figure 2.23: Comparison of measured vs predicted water recovery after 7 mins obtained using 310 mmoles/t of collector with varying ratio of PNBX and cyclohexyl DTC (Buffelsfontein ore)

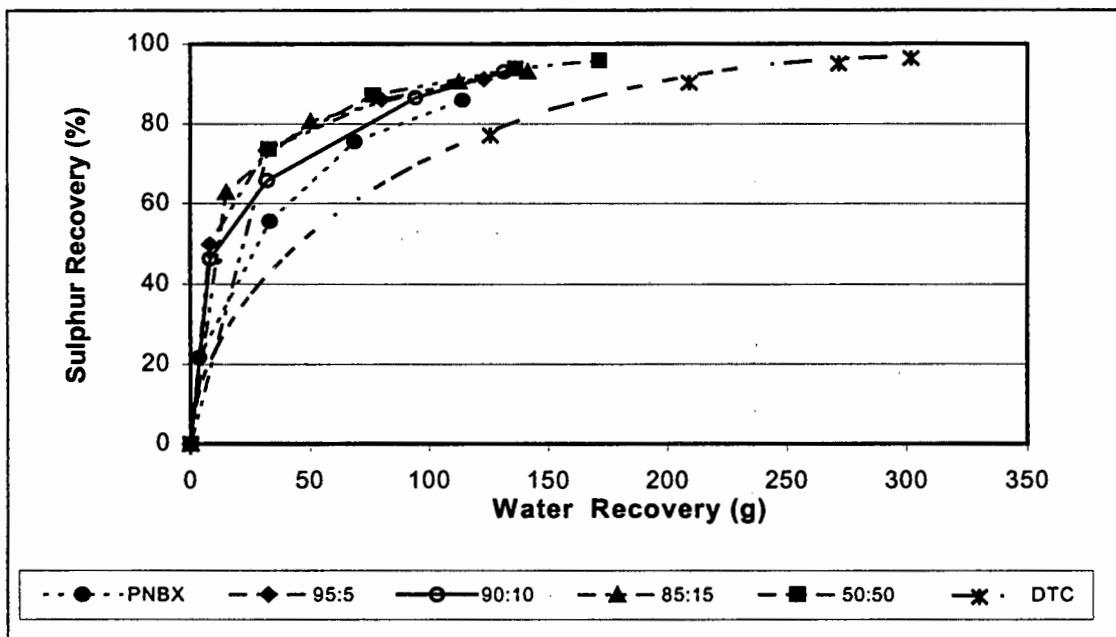


Figure 2.24: Sulphur recovery vs water recovery obtained using 310 mmoles/t of collector containing varying ratios of PNBX and cyclohexyl DTC (Buffelsfontein ore)

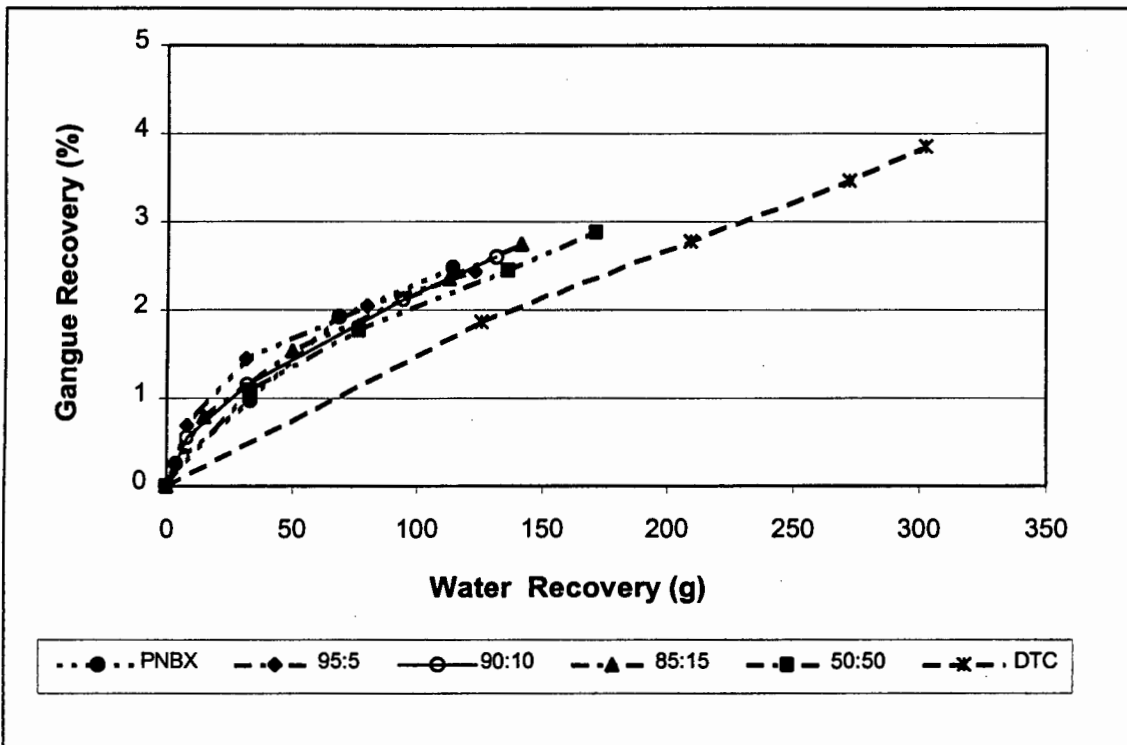


Figure 2.25: Gangue recovery vs water recovery obtained using 310 mmoles/t of collector containing varying ratios of PNBX and cyclohexyl DTC (Buffelsfontein ore)

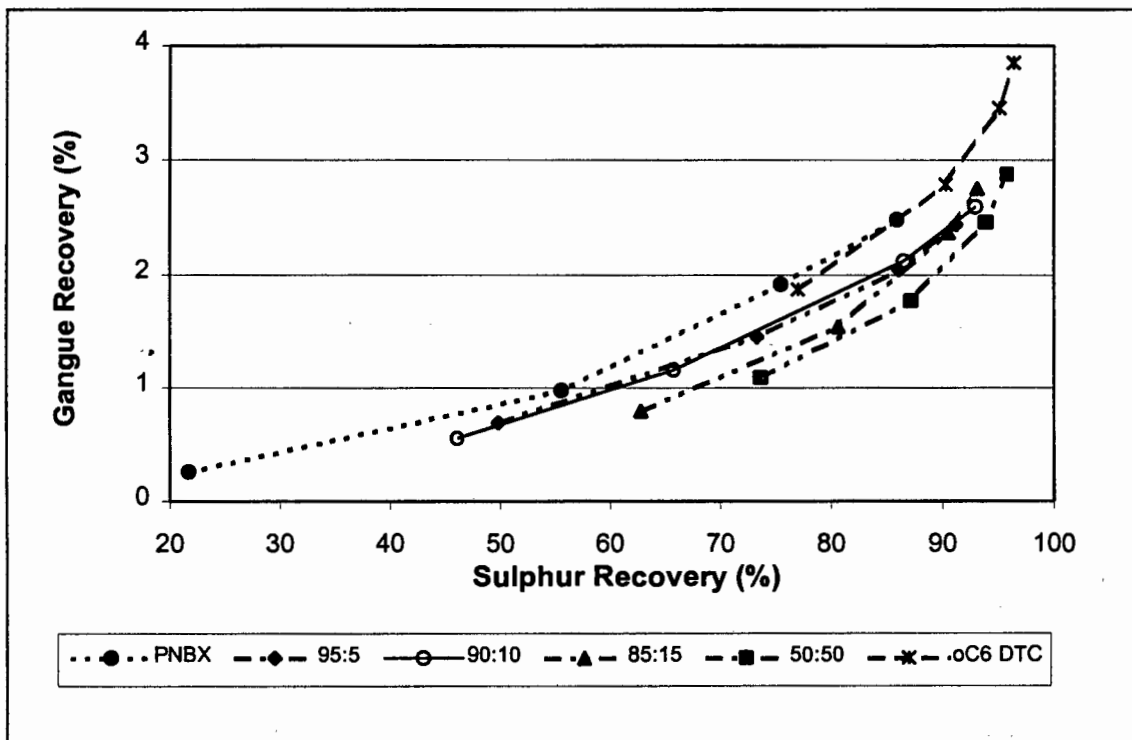


Figure 2.26: Gangue recovery vs sulphur recovery obtained using 310 mmoles/t of collector containing varying ratios of PNBX and cyclohexyl DTC (Buffelsfontein ore)

Figure 2.26 shows the gangue recovery vs sulphur recovery for the different mixtures and that all the mixtures recover less gangue at equivalent sulphur recoveries. It is noteworthy that the relationship between gangue and sulphur recovery is similar for both the pure PNBX and the cyclohexyl DTC, although sulphur recovery, at a fixed time, is much lower in the case of PNBX. In the case of PNBX, the high gangue recovery at fixed sulphur recovery with a low water recovery is attributed to the high froth viscosity and low froth mobility. In the case of cyclohexyl DTC, the high gangue recovery at fixed sulphur recovery is obtained with high water recovery with entrainment of fines. Lower gangue recoveries for fixed sulphur recovery obtained in the case of the mixtures indicate more selective flotation which may result from better draining froth characteristics.

For all the mixtures of PNBX and cyclohexyl DTC, the sulphur grade - recovery relationship is greater than that which is predicted by linearly interpolating the flotation performance obtained with the two pure collectors. There are indications that the improvement occurs in both the collection and froth zone. The increased final sulphur recoveries indicated improved collection efficiencies in the pulp zone. The improved grades, in spite of increased water and mass recovery, indicated that the froth drainage characteristics were improved in the froth zone. The best grade vs recovery was obtained with the 50:50 mixture of PNBX and cyclohexyl DTC.

2.3.1.4. EFFECT OF DOSAGE WITH PNBX AND THE 90:10 MIXTURE OF PNBX AND CYCLOHEXYL DTC

The aim of these tests was to investigate the effect of dosage on the flotation performance obtained using pure PNBX and the 90:10 mixture of PNBX and cyclohexyl DTC. Dosages tested were 310 mmoles/t and 465 mmoles/t which were equivalent to 60 g/t and 90 g/t PNBX respectively. These results are also shown in Table 2.6 (pg. 80) , together with the results obtained with the pure

collectors and the mixtures with other ratios of constituents. Detailed results are given in Appendix 2E.

2.3.1.4.1 SULPHUR GRADE VS SULPHUR RECOVERY

Figure 2.27 shows that the sulphur grades and sulphur recoveries obtained with the 90:10 mixture were higher, at both dosages, than those obtained with the pure PNBX. The effect of increasing the dosage from 310 mmoles/t to 465 mmoles/t was much lower than the difference in the grade vs recovery curves observed when comparing the 90:10 mixture and pure PNBX.

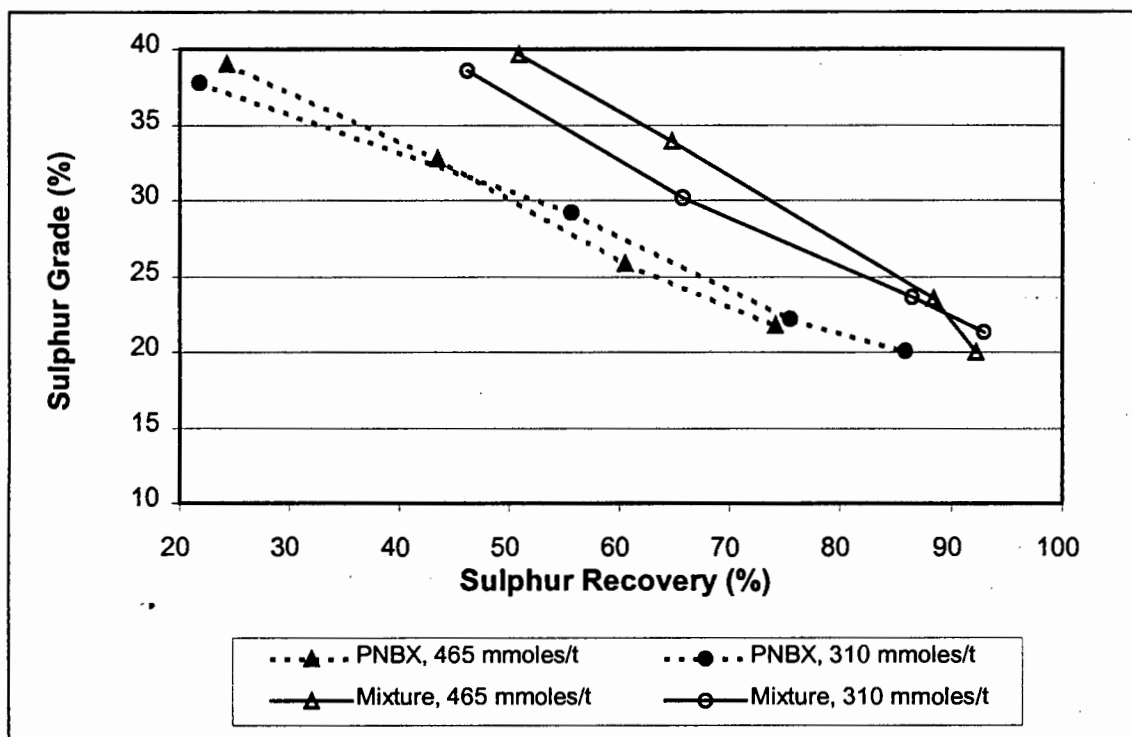


Figure 2.27: Sulphur grade vs sulphur recovery obtained using 310 mmoles/t and 465 mmoles/t of PNBX and the 90:10 mixture of PNBX and cyclohexyl DTC (Buffelsfontein ore)

2.3.1.4.2 RATE OF SULPHUR RECOVERY

Figure 2.28 shows that, for both the mixture and PNBX, the rate constant, k , increased slightly as the dosage increased from 310 mmoles/t to 465 mmoles/t. The equilibrium rate constants, R , decreased with increase in dosage. The predicted value for the rate constant, k , of the mixture, as obtained from the linear summation of the contributions of the individual collectors, was lower than the rate constant, k , actually obtained.

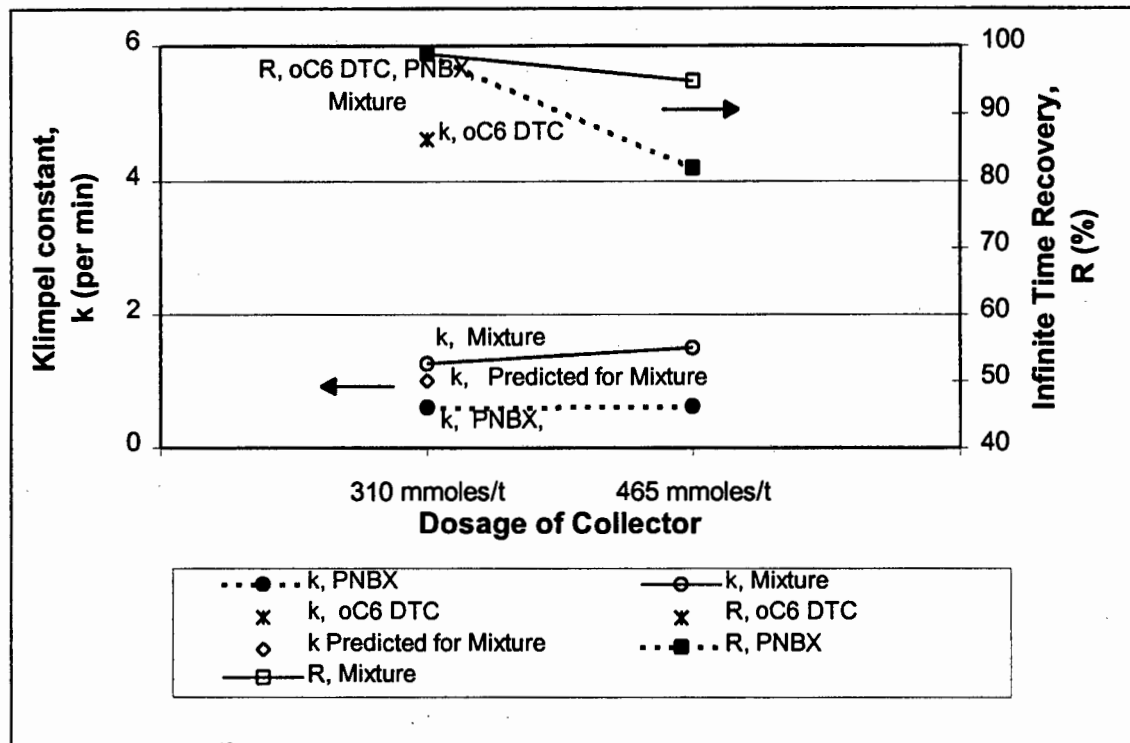


Figure 2.28 Constants, k and R , from Klimpel obtained using pure PNBX, pure cyclohexyl DTC and the 90:10 PNBX:cyclohexyl DTC mixture with a dosage of 310 mmoles/t and 465 mmoles/t (Buffelsfontein ore)

2.3.1.4.3 SULPHUR RECOVERY BY SIZE

Figure 2.29 shows that the initial sulphur recovery of all size fractions obtained with the mixture was higher than obtained with PNBX. In the case of the mixture, for both dosages, the initial fines recovery was lower than the 25 x 75 and > 75 μm fractions. The final fines recovery obtained with the lower dosage of the mixture increased relative to the other fractions in the final recovery.

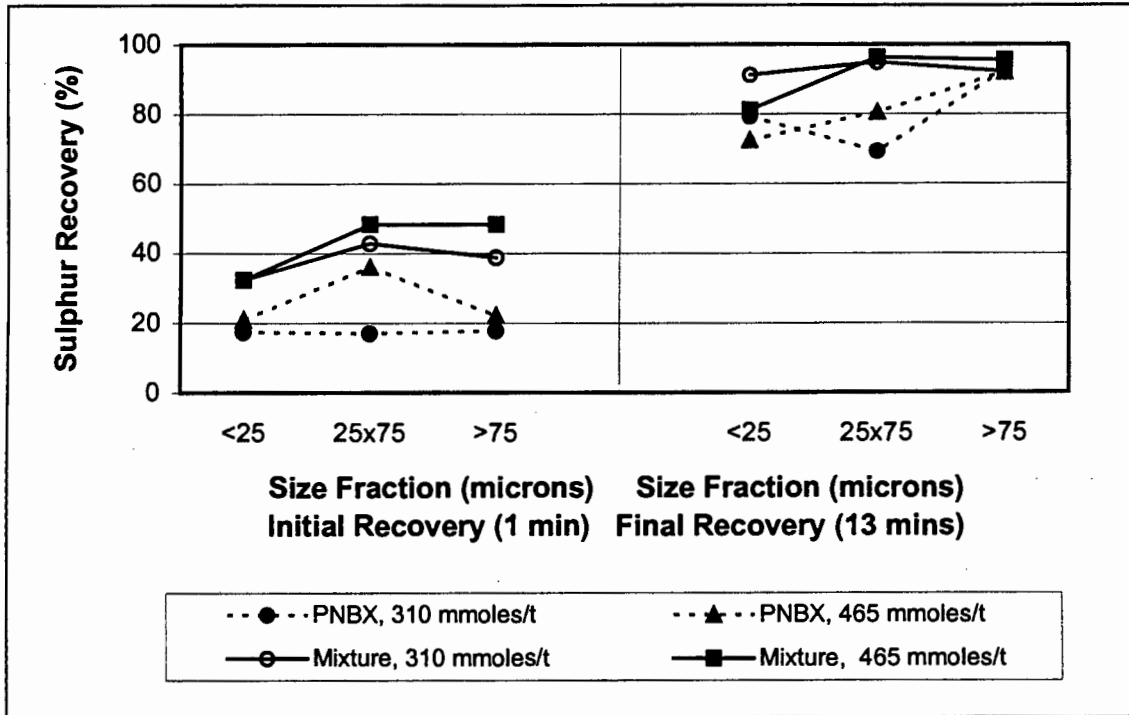


Figure 2.29: Sulphur recovery by size obtained using dosages of 310 mmoles/t and 465 mmoles/t of PNBX and the 90:10 mixture of PNBX and cyclohexyl DTC (Buffelsfontein ore)

Figures 2.30 and 2.31 show the effect of dosage on the relationship between sulphur grade vs sulphur recovery, by size, for PNBX and the 90:10 mole ratio mixture of PNBX and cyclohexyl DTC respectively. It can be seen that in the case of PNBX, the grades at fixed recovery of the middling and coarse size fractions (i.e. $> 25 \mu\text{m}$) was much greater than that of the fines in general and also increased with increasing dosage.

In the case of the 90:10 mixture, the comparative improvement was much less for all of the size fractions when the dosage increased from 310 mmoles/t to 465 mmoles/t.

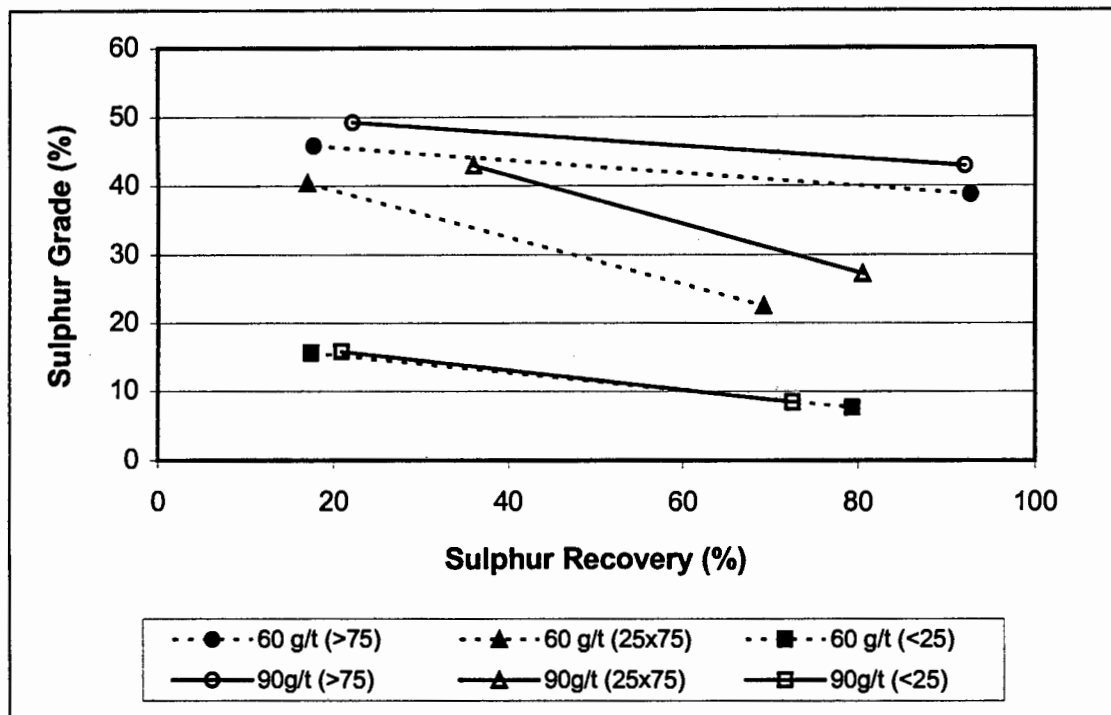


Figure 2.30: Sulphur grade vs sulphur recovery by size obtained using 310 mmol/t and 465 mmol/t of pure PNBX (Buffelsfontein ore)

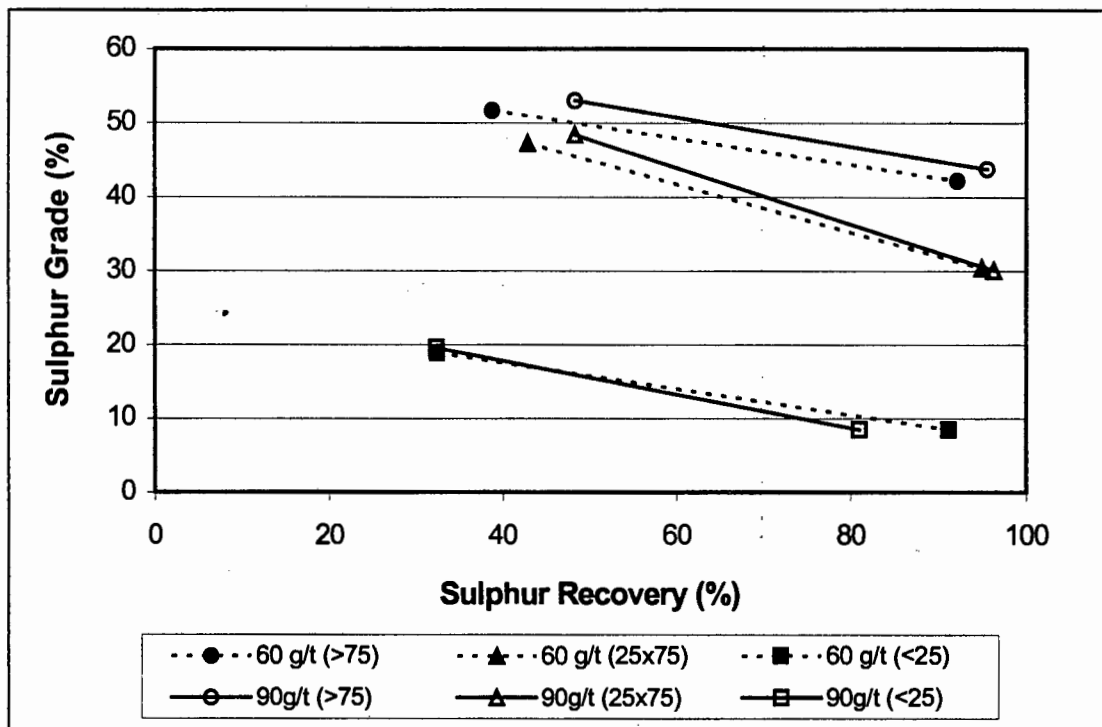


Figure 2.31: Sulphur grade vs sulphur recovery by size obtained using 310 mmol/t and 465 mmol/t of the 90:10 mixture of PNBX and cyclohexyl DTC (Buffelsfontein ore)

2.3.1.4.4 WATER RECOVERY

Figure 2.32 shows that the effect of collector dosage on water recovery was greater with the PNBX than with the 90:10 mixture. Higher water recoveries were obtained with the mixture at both the dosages.

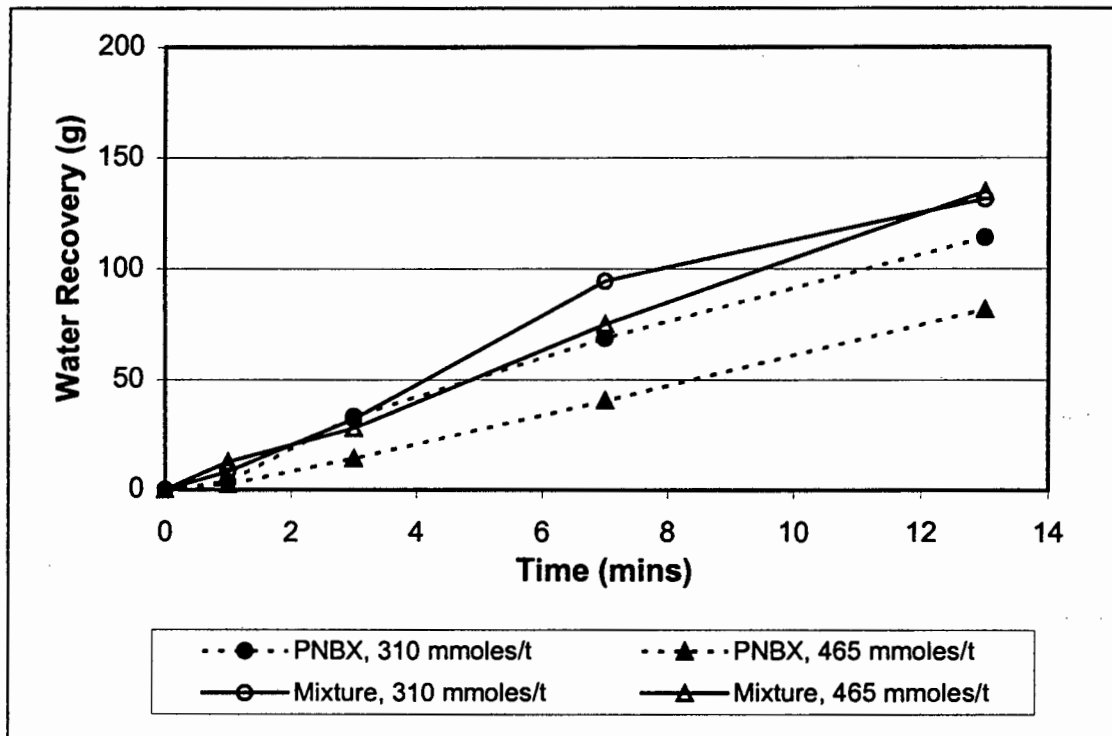


Figure 2.32: Water recovery vs time obtained using 310 mmol/t and 465 mmol/t PNBX and the 90:10 mixture of PNBX and cyclohexyl DTC (Buffelsfontein ore)

Figures 2.33 and 2.34 show the relationship between the sulphur and gangue recovery to the water recovery respectively for the pure PNBX and for the 90:10 mixture for both dosages. It can be seen that the sulphur recovery per mass of water is slightly higher for the mixture, but that the increasing dosage had little effect on the trends obtained for either the pure PNBX or the 90:10 mixture. In the case of gangue recovery, neither the change in collector type or collector dosage changed the trend of gangue recovery per mass of water recovered.

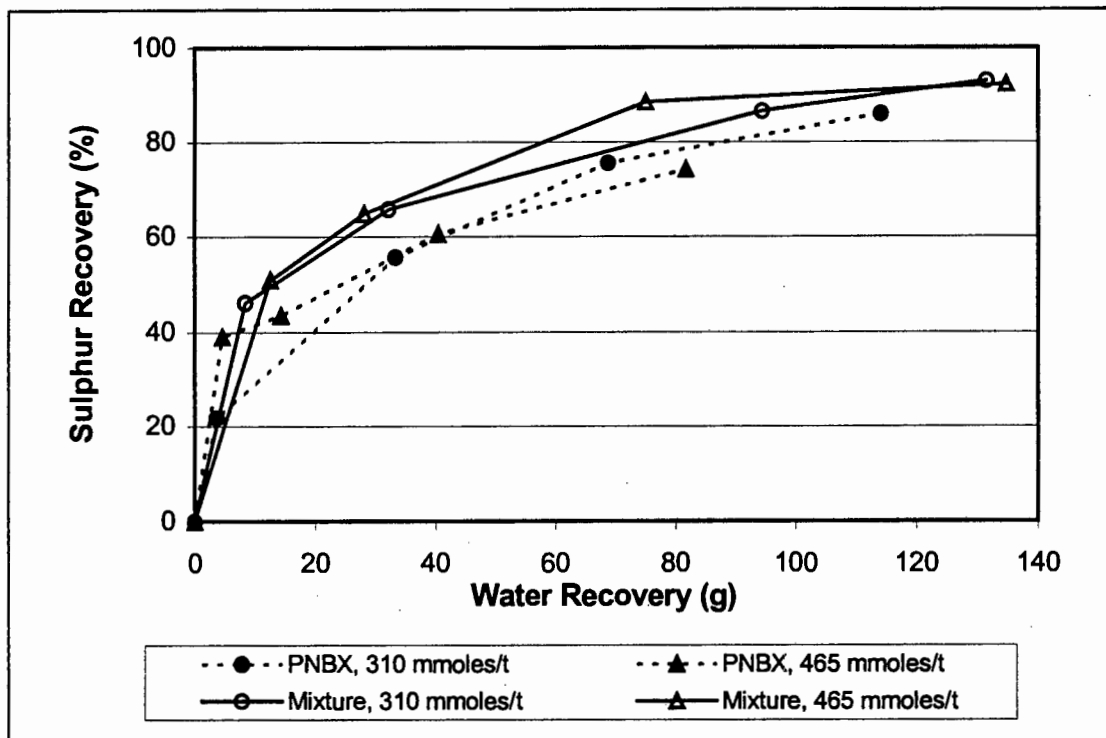


Figure 2.33: Sulphur recovery vs water recovery obtained using 310 mmoles/t and 465 mmoles/t PNBX and the 90:10 mixture of PNBX and cyclohexyl DTC (Buffelsfontein ore)

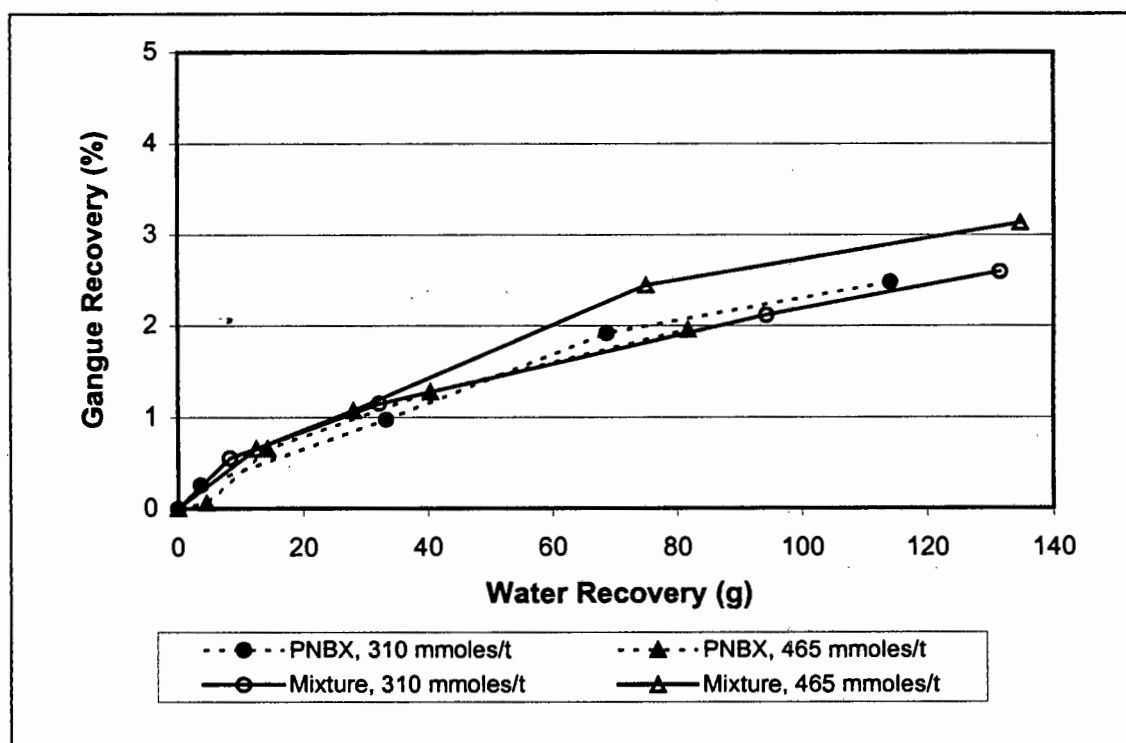


Figure 2.34: Gangue recovery vs water recovery obtained using 310 mmoles/t and 465 mmoles/t PNBX and the 90:10 mixture of PNBX and cyclohexyl DTC (Buffelsfontein ore)

2.3.1.4.5 IMAGE ANALYSIS OF THE SURFACE FROTH

Image analysis was used to compare the surface froth characteristics obtained with the 90:10 mixture of PNBX and cyclohexyl DTC with those obtained with pure PNBX. The emphasis of this analysis was on the difference between the characteristics rather than on the characteristics themselves. The dosage of both collectors was 310 mmol/t. The surface froth structure was analysed for average bubble size, froth stability and mobility of surface froth.

Figure 2.35 shows the change in average bubble size of surface froth with time. It can be seen that initial bubble size is similar for both the PNBX and the 90:10 mixture, viz. large. After 3 mins, the mixture of collectors, produced larger bubbles than PNBX. These tests have a high froth solids concentration, and low water recovery which is associated with stable froths and with large bubbles.

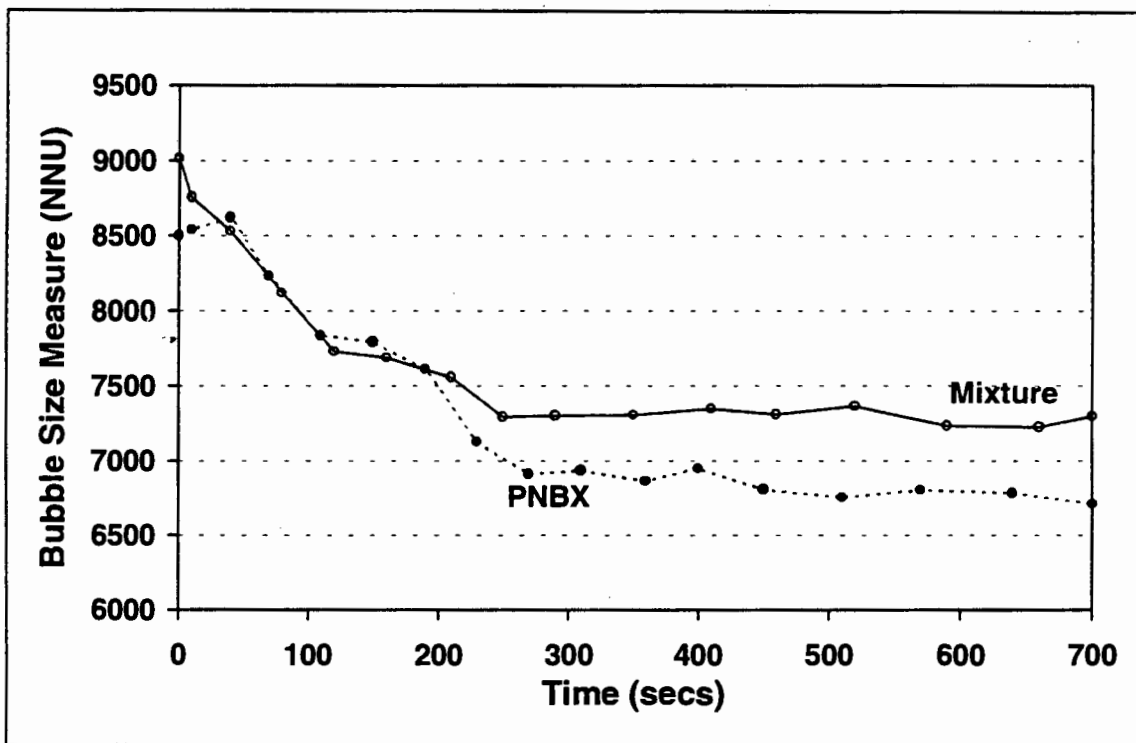


Figure 2.35 : The change in the bubble size of surface froth with time for tests using PNBX and the 90:10 mixture of PNBX and cyclohexyl DTC at a dosage of 310 mmol/t (Buffelsfontein ore)

The froth instability, measured as the rate of change of froth structure, is shown in Figure 2.36. The mixture of collectors produced a more stable froth than PNBX throughout the flotation test, although for both collectors the froth was least stable after 5 mins. This was in contrast to the constantly unstable froth observed with cyclohexyl DTC (cf. Figure 2.12).

Figure 2.37 shows the froth speed obtained with the mixture and with PNBX. The froth speed was much higher for the 90:10 mixture than for the pure PNBX, and was more similar to that obtained with pure cyclohexyl DTC (cf. Figure 2.13). This was accompanied by increased water recovery (cf. Figure 2.32). This highlighted the extent of the effect of only 10 mole percent substitution of PNBX by cyclohexyl DTC on the froth speed.

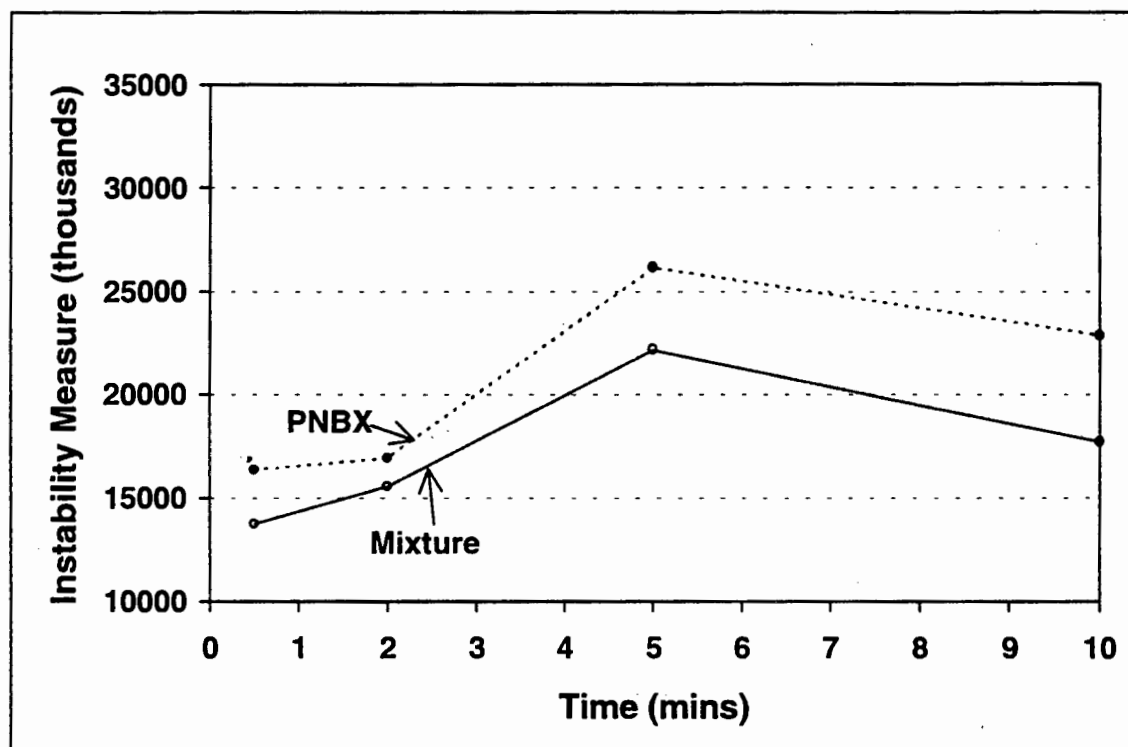


Figure 2.36: Instability feature measure for tests using PNBX and the 90:10 mixture of PNBX and cyclohexyl DTC at a dosage of 310 mmoles/t (Buffelsfontein ore)

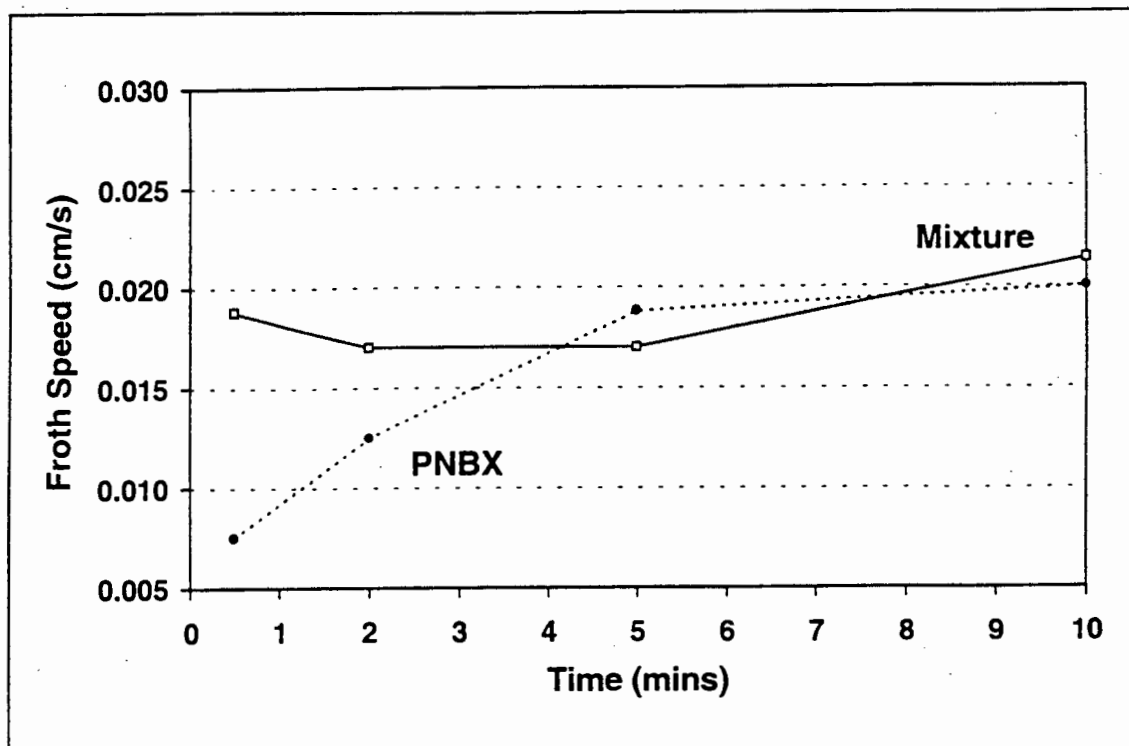


Figure 2.37: The froth speed of flotation tests using PNBX and the 90:10 mixture of PNBX and cyclohexyl DTC at a dosage of 310 mmol/t (Buffelsfontein ore)

2.3.1.4.6 STATISTICAL ANALYSIS

Table 2.7 shows the statistical analysis of the results obtained using the 90:10 mixture of PNBX and cyclohexyl DTC and pure PNBX at varying collector dosages. These tests were carried out as part of a factorial design of experiments and are assessed as such. The differences in responses (effects) are compared to the variance from the reproducibility tests (σ^2 , square of standard deviation), and using ANOVA techniques to get the 'F' values, the statistical significance of each effect was checked. Thus effects evaluated graphically and discussed in Section 2.3.1.4 can also be evaluated statistically.

Table 2.7 is split into four parts for ease of interpretation. Table 2.7.1 shows the different responses (i.e. rate, recovery etc.) extracted from Table 2.6 (pg. 80). Table 2.7.2 shows the percentage change in the different responses resulting from the changes in parameter levels indicated (i.e. the effect of

changing collector type on recovery, grade etc.). The standard deviation (σ), calculated from the reproducibility tests, is also shown. Table 2.7.3 shows the 'F' factors obtained by comparing the effect to the variance, where the residual error or variance (σ^2) is obtained from the standard deviation. Table 2.7.4 shows the significance of the 'F' values obtained from standard statistical tables. It must be noted that 8 reproducibility tests were done and thus the number of degrees of freedom was 7. A significance of over 95% is considered high enough on which to make a decision. As shown on the table, the 'F' factor for 95% confidence with 7 degrees of freedom on the reproducibility tests and 1 degree of freedom on the effect is $F_{95,1,7} = 5.59$. All effects which obtained an 'F' factor above this level are termed significant. In Table 2.7.4, (***) denotes a highly significant effect of over 99%, (**) denotes a significant effect of between 95% and 99%, (*) denotes a slightly significant effect of between 90% and 95% and (~) denotes no significant difference.

It can be seen that the statistical assessment is strongly influenced by the standard deviations or variance of the system. Factors which achieved the highest effects were not necessarily the factors which were most significant, viz. the effect of changing collector type was greatest on water recovery, but the standard deviation of the water recovery was also high, so the 'F' value was relatively low. The highest 'F' factors were obtained for the effect of collector type on initial and final recovery.

The statistical comparison of the difference in effects obtained with PNBX and the 90:10 PNBX and cyclohexyl DTC mixture confirmed that the use of the collector mixture in place of pure PNBX improved the sulphur recoveries highly significantly (> 99%), both at 1 min and at 13 mins. The use of the mixture resulted in an increase in rate constant, but this was not significant due to the high standard deviation. This was also the case with the increase in water recovery where the large difference was reduced to a slightly significant effect (90 - 95%).

Table 2.7: Statistical evaluation of differences obtained with PNBX and the 90:10 mixture of PNBX and cyclohexyl DTC (Buffelsfontein Ore)

2.7.1 Results extracted from Table 2.6

Collector Type	Test Number	Collector Dosage (mmoles/t)	Klimpel Model Constants		Mass Recovery (%)	Water Recovery (g)	Sulphur Recovery		Sulphur Grade	
			(k) (min ⁻¹)	(R) (%)			1 min (%)	13 min (%)	1 min (%)	13 min (%)
PNBX	B16	465	0.62	82.1	2.48	81.8	24.3	74.2	39.0	21.8
PNBX	B11	310	0.60	98.9	3.08	114.2	21.7	85.9	37.8	20.1
90:10 ⁽¹⁾	B17	465	1.50	94.8	3.89	134.8	50.9	92.3	39.7	20.0
90:10	B13	310	1.27	96.7	3.28	131.5	46.1	93.0	38.6	21.4

2.7.2 Percentage change in response (Effect) due to changing parameter level

SINGLE EFFECTS										
Collector Type (PNBX vs Mixture)	0.78	5.5	0.81	35.2	25.5	12.6	0.8	-0.3		
Dosage (60 g/t vs 90 g/t)	0.13	-9.4	0.01	-14.6	3.7	-6.2	1.2	-0.2		
INTERACTIONS										
Collector/Dosage	0.11	7.5	0.61	17.9	1.1	5.5	-0.1	-1.6		
Std Dev	2.58	0.9	0.22	32.4	3.2	0.9	2.2	0.8		

2.7.3 'F' Factors from ANOVA (NOTE: F_{99,1,7} = 12.5; F_{95,1,7} = 5.59; F_{90,1,7} = 3.59)

SINGLE EFFECTS										
Collector Type (PNBX vs Mixture)	0.40	30.5	11.90	6.4	138.1	214.7	0.1	0.1		
Dosage (60 g/t vs 90 g/t)	0.00	96.9	0.00	1.1	2.9	52.0	0.3	0.0		
INTERACTIONS										
Collector/Dosage	0.00	6.2	6.70	1.6	0.3	40.9	0.0	3.9		

2.7.4 Significance of effect (NOTE: *** = > 99%, ** = 95 x 99%, * = 90 x 95%, ~ = < 90%)

SINGLE										
Collector Type (PNBX vs Mixture)	~	***	**	*	***	***	~	~		
Dosage (60 g/t vs 90 g/t)	~	***	~	~	~	***	~	~		
INTERACTIONS										
Collector/Dosage	~	**	**	~	~	**	~	*		

(1) Indicates mixture of PNBX:oC6 DTC

The increase mass recovery was significant (95 - 99%) with the use of the 90:10 mixture. It was notable that the penalty in initial or final grade accompanying the increased recoveries was not significant.

It can be seen from the 'F' values that, with the exception of the increase in initial sulphur grade, the changes in responses due to increasing dosage were all lower than the effects due to changing collector type.

The significant interactions between dosage and collector type were on the final sulphur grade, where increased dosage of the mixture decreased the grade whereas increased dosage of PNBX increased the grade. This result indicates that the use of the mixture is recommended at lower dosages.

The statistical evaluation has confirmed that the beneficial effect of using the 90:10 mixture of PNBX and cyclohexyl DTC in place of pure PNBX is greatest on the sulphur recovery and that the grade penalty is not significant.

2.3.2 INVESTIGATION WITH ST HELENA ORE

The aim of these tests was to evaluate the behaviour obtained using a 90:10 mixture of PNBX and cyclohexyl DTC mixture relative to that obtained with pure PNBX with a second low grade pyrite sample with a view to investigating to what extent the results shown with Buffelsfontein ore are ore specific. The ore used was from St Helena Gold Mine, a gold leach residue material.

Table 2.1 compared the sulphur distribution of the St Helena ore to the Buffelsfontein ore. The total sulphur (mass in size fraction x grade) is shown to illustrate the differences in sulphur content and distribution in the different size fractions. It can be seen that the sulphur grade of the St Helena ore (SH) was significantly higher than that of the Buffelsfontein ore (B), viz. 1.27% sulphur vs 0.83% sulphur. The additional sulphur in the St Helena Residue Material was

present in the middling (25 x 75 μm) and fine (< 25 μm) size fractions. Despite having a lower overall grade, the Buffelsfontein Low Grade ore contained double the amount of sulphur in the > 75 μm range.

2.3.2.1 REPRODUCIBILITY (Tests: SH-R 1-4)

The reproducibility tests are represented as SH-R 1-4, (St Helena ore - Reproducibility tests, numbers 1-4). The collector used in the reproducibility tests was PNBX (potassium n-butyl xanthate) at the conditions described in Section 2.2.1. The mean recovery was 81.6% (standard deviation = 1.9%) and mean grade was 26.8% (standard deviation = 0.8%). The standard deviation obtained for the water recoveries was higher than for the other parameters. Details of these tests are shown in Appendix 2D (iii). These values are used in the ANOVA and 'T' tests to evaluate the significance of the benefits of the mixture.

2.3.2.2 COMPARISON OF PNBX TO THE 90:10 MIXTURE OF PNBX AND CYCLOHEXYL DTC

These tests compared the flotation performance obtained using a 90:10 mole ratio mixture of PNBX and cyclohexyl DTC to PNBX at the same molar dosage of 400 mmol/t. The comparisons were made at pH = 4 with no copper sulphate addition. Table 2.9 summarises these results and full details are given in Appendix 2E. Figure 2.38 shows that the sulphur grade vs sulphur recovery curve obtained with the mixture of collectors is only slightly higher than that obtained with pure PNBX. The effect is not as high with St Helena ore as that obtained with Buffelsfontein ore. The effect on rate of flotation can be seen from Table 2.9, by comparing results obtained for tests SH-5 with SH-8. The rate constant, k , calculated using the Klimpel model increased with the use of the mixture as did the initial sulphur, mass and water recovery.

Table 2.8: Summary of flotation results with PNBX and the 90:10 mixture of PNBX and cyclohexyl DTC (St Helena Ore)

Collector Type	Test Number	Klimpel Model Constants		Time	Mass Recovery (%)	Water Recovery (g)	Sulphur Recovery (%)	Sulphur Grade (%)
		(k) (min ⁻¹)	(R) (%)					
PNBX	SH-5	2.68	91.0	1 min	2.2	40.3	59.1	33.1
				13 mins	5.7	165.0	88.2	19.3
90:10 Mixture ⁽¹⁾	SH-6	3.38	91.7	1 min	2.5	38.8	65.3	34.5
				13 mins	5.5	115.7	89.6	21.3
90:10 Mixture ⁽²⁾	SH-7	3.74	91.3	1 min	2.7	54.5	67.4	31.9
				13 mins	5.8	171.4	89.5	20.0
90:10 Mixture ⁽³⁾	SH-8	3.02	91.6	1 min	2.5	45.3	62.5	32.9
				13 mins	5.8	167.8	89.1	20.2
90:10 Mixture ⁽⁴⁾	SH-9	3.05	91.0	1 min	2.5	45.0	62.5	32.9
				13 mins	5.7	155.6	88.7	20.5

(1) oC6 DTC addition before PNBX addition

(2) PNBX addition before oC6 DTC addition

(3) Simultaneous addition

(4) Collectors premixed

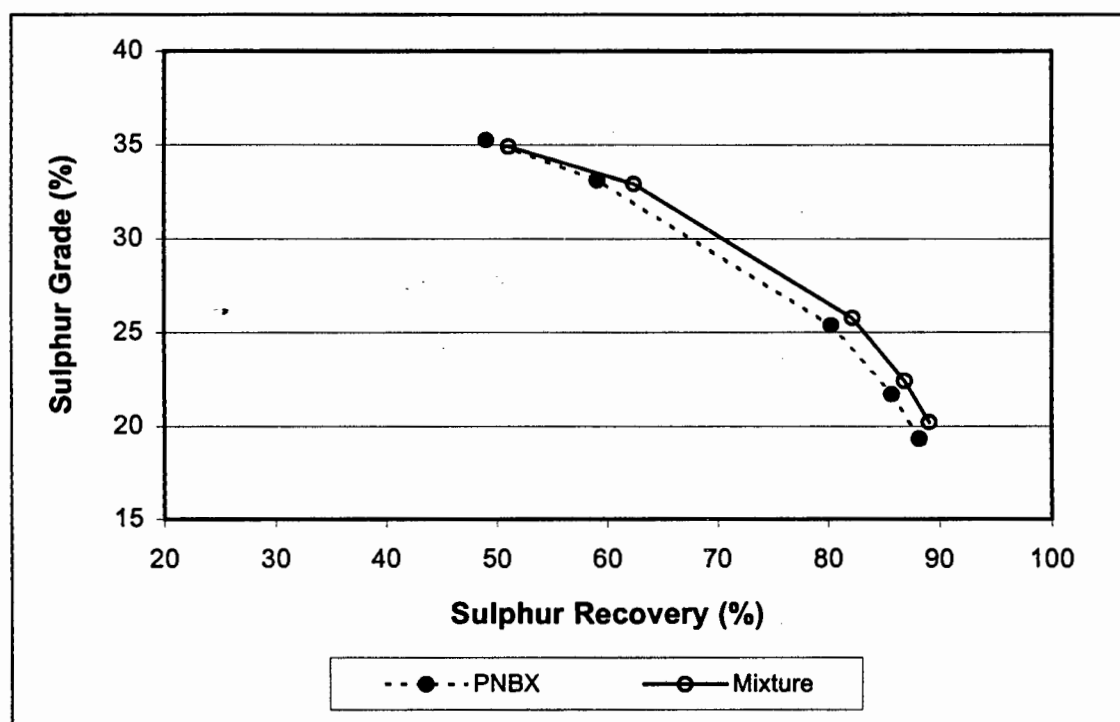


Figure 2.38: Sulphur grade vs sulphur recovery obtained using 400 moles/ PNBX and a 90:10 mole ratio mixture of PNBX and cyclohexyl DTC (St Helena ore)

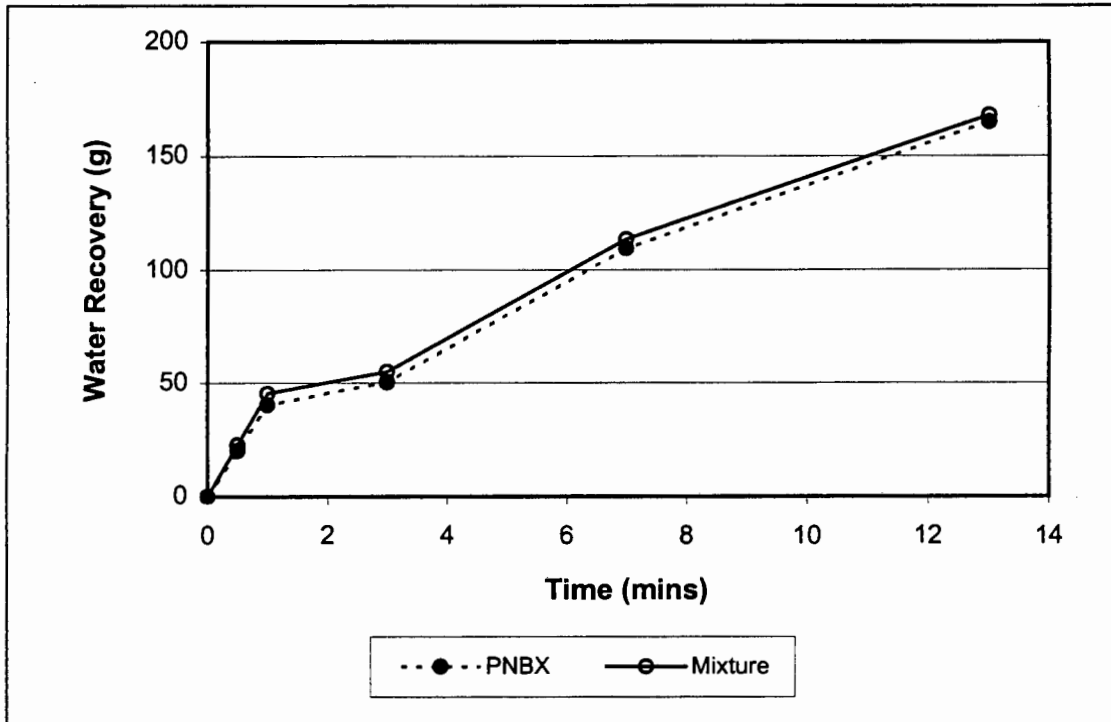


Figure 2.39: Water recovery vs time obtained using 400 moles/t PNBX and a 90:10 mole ratio mixture of PNBX and cyclohexyl DTC (St Helena ore)

Figure 2.39 shows that the water recovery was not increased with the use of the mixture. This finding was in contrast to the increased water recovery obtained using the 90:10 mole ratio mixture of PNBX and cyclohexyl DTC with Buffelsfontein ore (cf. Fig. 2.32).

Table 2.9 shows the statistical assessment of the results obtained with the 90:10 mixture and pure PNBX. The same method of analysis was used for the results with St Helena ore as with Buffelsfontein ore (cf. Sec. 2.3.1.4.6). It can be seen that although there are differences in the responses due to changing collector type, these are not significant due to the relatively high residual error or variance.

Table 2.9: Statistical evaluation of differences obtained with PNBX and the 90:10 Mixture (St Helena Ore)**2.11.1 Results extracted from Table 2.10**

Collector Type	Test Number	Collector Dosage (mmoles/t)	Klimpel Model Constants		Mass Recovery (%)	Water Recovery (g)	Sulphur Recovery		Sulphur Grade	
			(k) (min ⁻¹)	(R) (%)			1 min (%)	13 min (%)	1 min (%)	13 min (%)
PNBX 90:10 ⁽¹⁾	SH-5	400	2.68	91.0	5.70	165.0	59.1	88.2	33.1	19.3
	SH-8	400	3.02	91.6	5.80	167.8	62.5	89.1	32.9	20.2

2.11.2 Percentage change in response (Effect) due to changing parameter level

EFFECT	(k)	(R)	Mass Recovery (%)	Water Recovery (g)	Sulphur Recovery 1 min (%)	Sulphur Recovery 13 min (%)	Sulphur Grade 1 min (%)	Sulphur Grade 13 min (%)
Collector Type (PNBX vs Mixture)	0.34	0.60	0.10	2.80	3.36	0.89	-0.20	0.88
Std Dev	0.70	2.23	0.25	14.89	4.95	1.91	0.38	0.81

2.11.3 'F' Factors from ANOVA (NOTE: $F_{99,1,3} = 34.1$; $F_{95,1,3} = 10.1$; $F_{90,1,3} = 5.54$)

EFFECT	(k)	(R)	Mass Recovery (%)	Water Recovery (g)	Sulphur Recovery 1 min (%)	Sulphur Recovery 13 min (%)	Sulphur Grade 1 min (%)	Sulphur Grade 13 min (%)
Collector Type (PNBX vs Mixture)	0.24	0.07	0.16	0.04	0.46	0.22	0.28	1.18

2.11.4 Significance of effect (NOTE: * = > 99%, ** = 95 x 99%, * = 90 x 95%, ~ = < 90%)**

EFFECT	(k)	(R)	Mass Recovery (%)	Water Recovery (g)	Sulphur Recovery 1 min (%)	Sulphur Recovery 13 min (%)	Sulphur Grade 1 min (%)	Sulphur Grade 13 min (%)
Collector Type (PNBX vs Mixture)	~	~	~	~	~	~	~	~

(1) Indicates mixture of PNBX:oC6 DTC

These tests have shown that although there is a difference in flotation performance indicating a slight improvement of performance the benefit of the mixture is not as significant as that observed for the Buffelsfontein ore. The dosage of collector was not optimised. It is thus possible that the optimum mixture composition may be different and thus be ore specific.

2.3.2.3 THE EFFECT OF SEQUENCE OF REAGENT ADDITION

The aim of these tests was to ascertain whether there was any difference in flotation behaviour obtained when the method of addition of collectors was varied. The results of these tests are shown in Table 2.8 and details are shown in Appendix 2E. Figure 2.40 shows that the best results were obtained when cyclohexyl DTC was added first, this method yielding the highest grade vs recovery curve. In all other tests, including the tests with Buffelsfontein ore, the constituent collectors were added simultaneously.

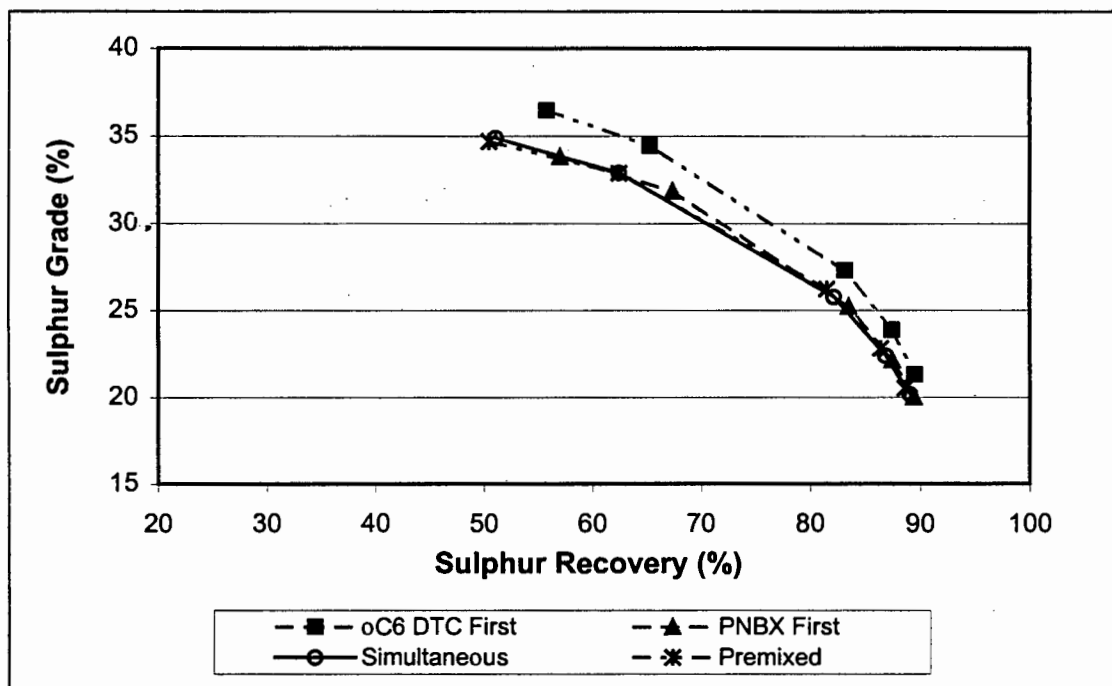


Figure 2.41 shows that the water recovery obtained when cyclohexyl DTC was added first was lower than for all other tests. These tests showed that adding cyclohexyl DTC first, reduced the water recovery and increased the grades obtained with the mixture. The tests with Buffelsfontein ore showed that the higher the ratio of cyclohexyl DTC in the collector mixture, the higher the water recoveries that were obtained. When cyclohexyl DTC was added before PNBX, more collector would be adsorbed onto the mineral surface, and less available in solution to act as a frother. This is corroborated by the result that when PNBX was added first, the rate of sulphur recovery, the water and mass recovery was highest, and the grade lowest.

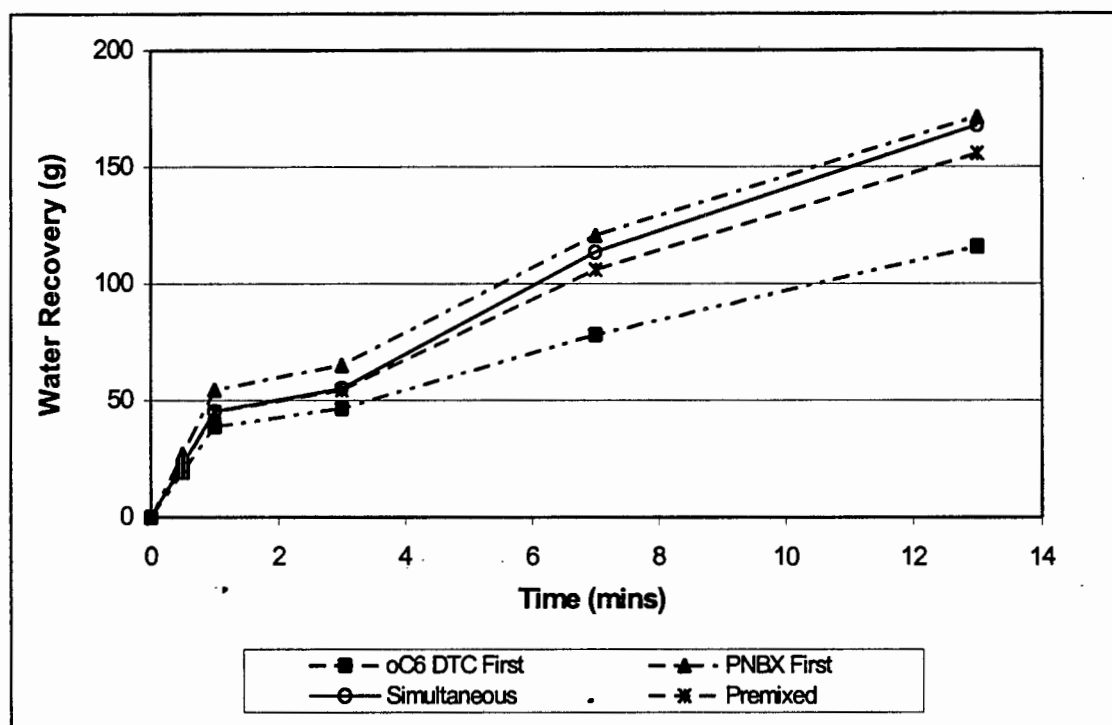


Figure 2.41: Water recovery vs time obtained using differing methods of addition of the 90:10 mole ratio mixture of PNBX and cyclohexyl DTC (St Helena ore)

2.4 DISCUSSION

The aim of this part of the study was to analyse the changes in the batch flotation test responses with a view to ascertaining whether the effects observed when mixtures of collectors were used were merely linearly additive, with respect to the amount of each component in the collector mixture, or, whether in fact a synergistic interaction between the collectors has occurred, ie. to determine whether the "combined effect exceeds the sum of the parts" (Oxford dictionary definition of synergism). The overall sulphur recoveries, the sulphur grades and the rates of recovery obtained with the mixtures of collectors were greater than the values predicted from the molar contributions of the component collectors, demonstrating the synergistic interactions between the collectors in the mixtures (cf. Figures 2.15, 2.16 and 2.17). In contrast, the water recovery obtained was almost equivalent to the linear contribution of the cyclohexyl DTC and PNBX (cf. Figure 2.23).

Reproducibility tests were done to obtain the standard deviation for the various flotation responses and these values were used to quantify the significance of the changes occurring. The standard deviation for the final recovery of flotation tests with Buffelsfontein ore, obtained for 8 tests, was 0.86% (cf. Table 2.6) which was lower than that obtained by previous researchers with the same cell [Stonestreët, 1991] and with the original Leeds flotation cell [Dell and Bunyard, 1972].

The changes in flotation performance resulting from the use of the different pure collectors and collector mixtures can be best assessed in the context of the various flotation sub-processes (cf. Sec. 1.1, Figure 1.2).

The role of the collector in flotation is to adsorb onto the mineral surface to create the necessary hydrophobicity which makes the mineral particle amenable to attachment to the air bubble in the event of bubble - particle collision. In the case of successful attachment occurring after the mineral -

bubble collision, the attached mineral is transported by the bubble through the pulp phase to the froth phase. Detachment or elutriation of the mineral can occur at the pulp - froth interface. In the froth phase, if the conditions are suitable, water drainage returns the hydrophilic gangue material, which has been entrained, back into the pulp and the valuable mineral is collected via the launder.

It follows that the mineral particles cannot be removed from the froth phase unless they have first been collected by the bubbles in the pulp phase, or the pulp collection zone. In the case of no elutriation or mineral detachment, the overall recovery is equal to that of the pulp phase. An increase in the overall mineral recovery resulting from the change in the nature of the collector could result from either more successful collection in the pulp collection zone, or, from a decrease in mineral detachment by elutriation due to increased tenacity in the mineral - bubble attachment.

The grade of the mineral obtained from the flotation process is determined by the success of the froth phase in facilitating removal of entrained gangue material without the loss of attached mineral particles. There is an optimum froth stability required to achieve this. If the froth is too stable the gangue does not drain back into the pulp and the grade is low. If the froth is not stable enough, froth collapse will cause the loss of mineral from the froth back into the pulp phase, thus reducing recovery.

There were differences in the flotation performance obtained with the pure PNBX and pure cyclohexyl DTC as shown by the differences in the sulphur recovery, sulphur grade, rate of recovery and water recovery.

In the case of cyclohexyl DTC, the sulphur recovery was higher for all size fractions than that obtained with PNBX. The rate of recovery was also considerably higher and this was accompanied by a higher water recovery and recovery of gangue. This resulted in the final sulphur recovery obtained (after

13 mins) being achieved at a lower grade of sulphur than that obtained with PNBX. The surface froth speed was also greater in the case of cyclohexyl DTC.

For the equivalent sulphur recovery for both collectors, however, in the case of the cyclohexyl DTC, the sulphur grade was higher and there was less gangue, viz. for 80% sulphur recovery, the sulphur grade obtained with cyclohexyl DTC was 24.5% compared to 21.5% obtained with PNBX. Although the sulphur and gangue recoveries were higher with respect to time in the case of cyclohexyl DTC, the sulphur and gangue recoveries with respect to water recovery were lower than those obtained with PNBX.

The differences in the relationship between sulphur and gangue recoveries to the water recoveries can be attributed to the differences in the froth characteristics obtained with the two collectors. In the case of cyclohexyl DTC the froth was runny and non - mineralised with small bubbles. The surface froth instability measure showed that the froth obtained with cyclohexyl DTC was less stable, as characterised by a higher rate of change in intensity of the image due to collapsing bubbles, than that obtained with PNBX for the first 5 mins. Harris [1984] reported that froth stability is generally improved with reduction in bubble size, but in the case of cyclohexyl DTC, the froth was less stable even though the bubble size was smaller than with PNBX. This can be attributed to the considerably lower mineralisation of the froth caused by the high water content which resulted in a brittle, unstable froth.

The froth characteristics in the case of PNBX varied more with respect to time than those for cyclohexyl DTC, showing the effect of decreasing mineralisation as the test progressed. After 5 mins, the bubble size decreased which corresponded to a lower froth stability in the case of PNBX. The trend of reduced stability corresponding to lower bubble size was similar to the trend observed with cyclohexyl DTC. The higher relationship of sulphur and gangue

to water recovery (cf. Figures 2.9, 2.10) is consistent with the froth being more mineralised, less efficiently drained and slower moving.

Jiwu et al [1984] noted that dithiocarbamates showed good “frothing” properties and used cyanoethyl dithiocarbamate successfully in the flotation of sulphide minerals with lower frother dosages. “Frothing ability” of cyclohexyl DTC suggests that a portion of the collector was present in solution and that not all the collector was adsorbed onto the mineral surface. In contrast to suggestions of dithiocarbamates remaining in solution, xanthate abstraction from solution has been reported to continue until total depletion [Harris and Finkelstein, 1977].

The reasons for the differing flotation performance obtained with the two different thiol collectors, cyclohexyl DTC or PNBX, can result from different surface reactions occurring between cyclohexyl DTC and PNBX and the pyrite surface. This is further investigated and discussed in Chapter 4, where the adsorption characteristics of cyclohexyl DTC and PNBX are investigated.

In the batch flotation tests the flotation performance was compared with collectors at the same molar dosage and the dosage was not varied or optimised. Hence the relative performance of these two collectors may have been affected by varying the dosage of collector. There are indications that cyclohexyl DTC may also have been as effective at lower dosages due to the nature of the metal thiolate salt formed on the mineral surface [Sutherland and Wark, 1955]. The frother dosage and type also affects flotation performance and collector behaviour. This may not have been at an optimum for the collector types and dosages selected for this investigation [Lekki and Laskowski, 1975; Cilliers et al, 1991;]. In order to optimise these the method of Lekki and Laskowski [1975] is recommended where various dosages of collector and frother are tested to obtain recovery and grade contours in order to determine the conditions that achieved the highest recoveries and grades (cf. Sec. 1.2.3.3.7).

Mixtures of PNBX and cyclohexyl DTC with molar ratios of 50:50; 85:15; 90:10 and 95:5 were tested with Buffelsfontein ore. From the differing flotation performance obtained with the cyclohexyl DTC and PNBX it would be expected that the use of mixtures of collectors would result in flotation responses corresponding to combination of properties. The results, however, have shown that the sulphur grade - recovery relationship is enhanced for all the mixtures of PNBX and cyclohexyl DTC. The measured increases in recovery, grade and rate of flotation were above those which were predicted by linearly interpolating the flotation performance obtained with either of the two pure collectors (cf. Figures 2.15, 2.16 and 2.17). Improved flotation recoveries have also been reported by Plaskin et al [1954] and Adkins and Pearse [1992] for the xanthate - dithiophosphate systems.

The best sulphur grade - recovery performance was obtained with the 50:50 mixture of PNBX and cyclohexyl DTC and the 90:10 ratio of PNBX and cyclohexyl DTC which was the focus of this thesis, was not the optimum ratio of collectors. The existence of the optimum ratio of constituents for specific applications to achieve maximum synergistic enhancement in flotation performance has been reported by Mingione [1984], Critchley and Riaz [1991], Valdiviezo and Oliveira [1993]. The distribution and orientation of the different collectors at the optimum ratio has been hypothesised to result in a more even surface layer and increased hydrophobicity of the mineral surface. The 90:10 mixture enjoyed the focus of attention here because of the interest in the effect of a very small amount of one or other collector. This resulted in a more perceptive study of synergism. It parallels phenomena such as the excess properties for mixtures in thermodynamics where small amounts of one or other component reveal the most important information.

The improvement in the recovery can be attributed to improved "hydrophobicity" or "flotability" resulting in improved collection efficiency in the pulp phase. This possibility is further investigated in Chapter 3 by determining the bubble loading characteristics of the pyrite with the different collectors. The improved

attachment is hypothesised to result from the differing adsorption and improved surface product on the mineral surface. The reaction pathways of PNBX and cyclohexyl DTC are investigated in Chapter 4.

In a comparison of the sulphur recovery by size and sulphur recovery vs sulphur grade by size it is notable that the improvement obtained with the use of the mixtures is greatest in the middling range (25 x 75 μm). Plaskin et al [1954] reported the improvement in coarse particle recovery (100 x 150 μm) with the use of xanthate and dithiophosphate mixtures. The low increase in the flotation performance of the < 25 μm material with mixtures is possibly due to the collision efficiency of the fine particles being so low in general that this becomes the overriding factor in fine particle collection. Finch and Dobby [1990], for example, showed that increasing the hydrophobicity, as measured by reduced induction time, has less effect on the attachment efficiency of the fine particle sizes (below 10 μm) than on the coarser fractions.

The improved grades obtained with mixtures of collectors, in spite of increased water and mass recovery, indicated that the froth drainage characteristics were improved in the froth zone. The change in water recovery resulting from changes in the ratio of cyclohexyl DTC in the collector mixture did not show any synergistic effects, but was proportional to the amount of cyclohexyl DTC in the collector mixture (cf. Figure 2.22).

The analysis of the surface froth showed that the froth was more stable in the case of the mixtures of collectors. The froth was least stable with pure cyclohexyl DTC. For all three collector types, the high froth instability corresponded to the presence of smaller bubbles and low mineralisation. The froth speed was much higher for the 90:10 mixture than for the pure PNBX, and was similar to that obtained with pure cyclohexyl DTC. This was accompanied by increased water recovery (cf. Figure 2.32). This highlighted the extent of the effect of the 10 mole percent substitution of PNBX by cyclohexyl DTC on the froth characteristics obtained. Whereas the surface froth obtained using the

mixture had similar bubble size and stability features to those obtained with PNBX, the froth mobility was similar to that achieved with cyclohexyl DTC, even though the mixture only contained 10% of cyclohexyl DTC.

The collector, which is added to the pulp to affect mineral hydrophobicity may also affect the froth characteristics thus illustrating the interactive nature of parameters in the flotation process and highlighting the difficulty in evaluating one parameter at a time.

It was notable that the performance of the 90:10 mole ratio mixture did not improve when the dosage of collector added increased. This was in contrast to the performance obtained with pure PNBX where the recovery of the 25 x 75 μm fraction and the > 75 μm fraction increased by increasing the dosage of PNBX, although there was no significant effect on the fines (> 25 μm) recovery. The reduction in dosage requirement has also been reported by Plaskin et al [1954] and Adkins and Pearse [1992] for xanthate - dithiophosphate mixtures.

The dosage effect resulted in the difference in flotation performance observed between the 90:10 mixture and PNBX at the higher dosage of 465 mmoles/t being lower than the difference at the lower dosage of 310 mmoles/t with Buffelsfontein ore.

Tests investigating the sequence of addition showed that when cyclohexyl DTC was added first the water recovery was lower and the sulphur grade was higher for the same sulphur recovery. A possible explanation for this behaviour caused by changing the sequence of addition is that the extent to which cyclohexyl DTC affects the froth is dependent on the amount of collector remaining in solution. Adding PNBX first, may result in less cyclohexyl DTC being adsorbed on the pyrite surface thus more cyclohexyl DTC remaining in solution, available to interact with the frother and this sequence achieved the higher water recovery. Adding cyclohexyl DTC first, results in an increase in the extent of cyclohexyl DTC adsorption and lowers the concentration of

cyclohexyl DTC in solution. This results in a lower water recovery and lower grades and recoveries. This explanation is consistent with the observation that more water is recovered with increasing proportion of cyclohexyl DTC in the mixture. The above hypothesis assumes competitive adsorption onto restricted sites as proposed by Wakamatsu and Numata [1979] and Zaal and Bryson [1992].

An alternative explanation to the reduced water recovery in the case of cyclohexyl DTC being added first is that the increased hydrophobicity of the mineral surface could have resulted in the destabilisation of the froth [Harris, 1984].

For both ore samples, the 90:10 mole ratio mixture of PNBX and cyclohexyl DTC, achieved higher overall flotation performance as demonstrated by sulphur recoveries and rates, with no loss in grades, than that of either of the individual components. The extent of this enhancement was lower for the St Helena ore than for the Buffelsfontein ore.

2.5 CONCLUSIONS

The reproducibility of the procedure was good and the effects measured were statistically evaluated with respect to the standard deviations calculated from these tests.

The batch flotation tests with pure cyclohexyl DTC and PNBX, at a dosage of 310 mmol/t, showed that the flotation performance was better with cyclohexyl DTC, as shown by higher recoveries and grades, but that the froth was unstable, mobile and watery.

Synergistic enhancement of flotation performance above that which was linearly predicted from the contributions of the component collectors, as shown by improved sulphur grade vs sulphur recovery, was achieved using mixtures of PNBX and cyclohexyl DTC. An increase in sulphur recovery indicated that the particle collection in the pulp was enhanced. An increase in grade as well as the changes in water recovery and surface froth behaviour indicated that the froth zone was also affected. This illustrated the interactive nature of flotation parameters.

Table 2.10 Summary of flotation responses affected and the possible industrial implications of the use of the mixture of collectors in place of the pure collectors at a dosage of 310 mmol/t

Parameter	Effect	Implication
Rate of Recovery	Increased synergistically	Increase circuit throughput
Grade	Increased synergistically	Increase circuit efficiency
Fines Recovery	Increased synergistically	Increased Fines and Water
Water Recovery	Increased in proportion to concentration of constituents	Froth mobility without addition of copper sulphate

The flotation performance of the $< 25 \mu\text{m}$ fraction was not significantly improved with the use of mixtures, although the recovery increased but at a grade penalty. The largest increase in performance resulting from the use of mixtures was in the $25 \times 75 \mu\text{m}$ fraction. The highest sulphur grade vs sulphur recovery curve was obtained for the 85:15 mixture of PNBX and cyclohexyl DTC.

Increasing the dosage of the 90:10 mole ratio mixture of PNBX and cyclohexyl DTC from 310 mmol/t to 465 mmol/t with the Buffelsfontein ore did not increase the sulphur grade vs recovery of any of the size fractions. In the case of PNBX, the sulphur grade vs sulphur recovery of the $25 \times 75 \mu\text{m}$ fraction increased.

Adding cyclohexyl DTC before the PNBX, reduced the water recovery and increased the sulphur grades. The increase in performance due to the use of mixtures of collectors was much more significant in the case of Buffelsfontein ore than in the case of St Helena Ore. This may have been due to the high dosage of collector, or due to the synergistic effect being ore specific.

CHAPTER 3: BUBBLE LOADING TESTS

3.1 INTRODUCTION

The attachment of mineral particles to air bubbles is a critical sub-process in flotation. This sub-process, viz. bubble loading or particle collection, may be strongly affected by the condition of the mineral surface and the reaction products formed by the collector surface of the mineral. Bubble loading is defined in this thesis as the mass of mineral collected per bubble or per bubble surface area. The measurement of bubble loading requires the measurement of the bubble size as well as the measurement of the mass of mineral recovered by flotation and not entrainment. This was achieved with the use of an apparatus incorporating a flow-through microflotation cell developed for this study.

It was hypothesised that the differences observed in batch flotation tests using different collectors and collector mixtures could be due to differences in the particle - bubble attachment efficiency (cf. Sec. 1.3.2.4) and that the extent of the loading of bubbles with particles could explain the batch flotation results.

The aim of the work described in this chapter was thus to measure the bubble loading of the pyrite onto bubbles at equivalent conditions to the batch flotation tests and to use this information to ascertain whether the improvement in flotation performance observed when mixtures of collectors were used could be attributed to an increase in the extent of bubble loading.

3.2 EXPERIMENTAL DETAILS

3.2.1 APPARATUS AND SAMPLES

3.2.1.1 FLOW - THROUGH MICROFLOTATION CELL

This apparatus, developed to enable the measurement of the mineral loading of the bubbles is shown in Figure 3.1.



Figure 3.1: The flow - through microflotation cell

Figure 3.2 shows a schematic of the apparatus. The pulp was prepared (cf. Sec. 3.2.1.2) and recirculated using a peristaltic pump. The air was introduced

into the pulp through a syringe at a controlled flow rate and pressure. Mineral particles collected by the bubbles were carried to the launder and deposited there as the bubbles broke on reaching the liquid - air interface. By measuring the mass of mineral (cf. Sec. 3.2.2.1) and the bubble size (cf. Sec. 3.2.2.2) it was possible to calculate the loading of the mineral onto the bubble.

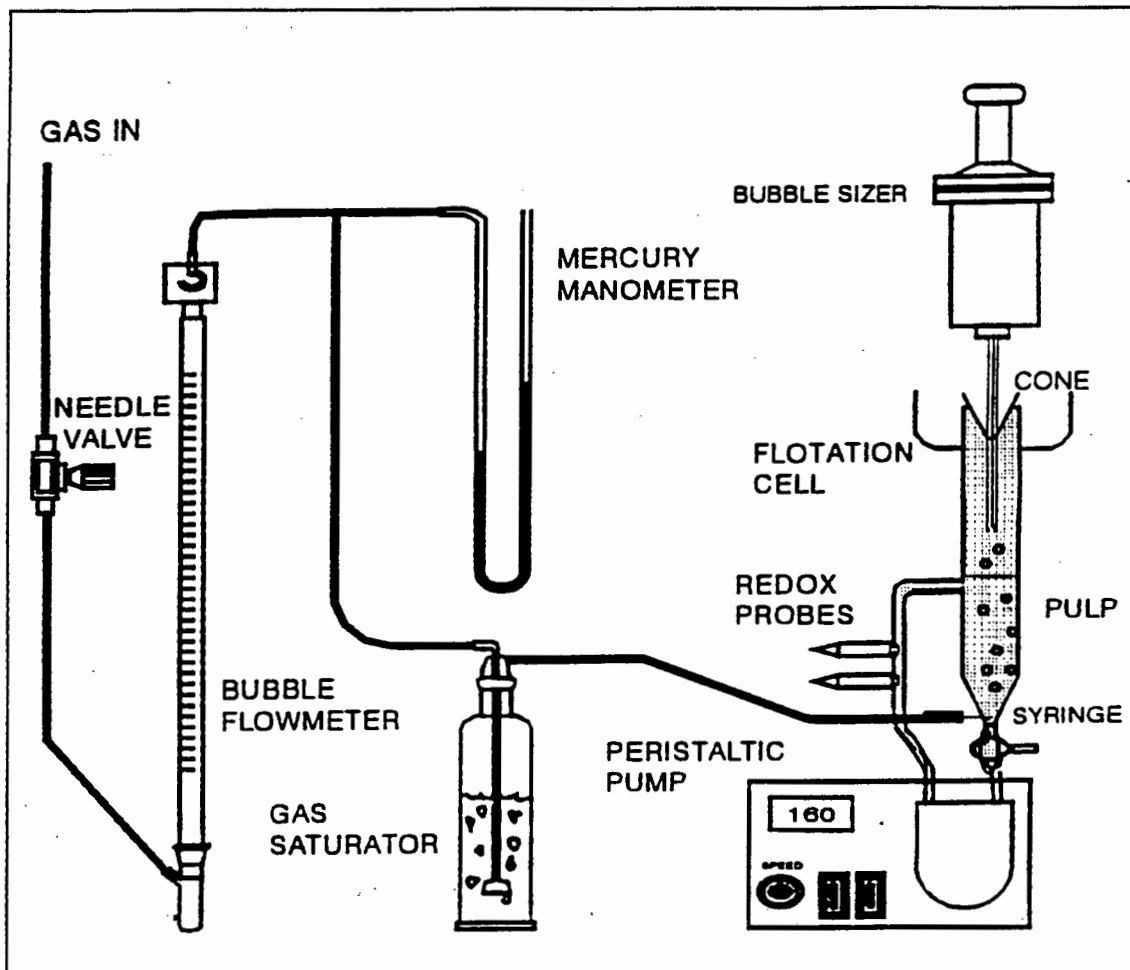


Figure 3.2: A schematic of the flow - through microflotation cell

3.2.1.2 BUBBLE SIZER

The bubble sizer was developed at the University of Cape Town by Randall et al, [1989]. A schematic is shown in Figure 3.3. The bubbles to be measured are drawn through a capillary tube with a belled end and pass between two pairs of photo-cell-diode detectors. As the bubbles pass the detectors they are monitored as a change in light intensity. From the velocity and frequency of the

interfaces passing the detectors and the total volume of air collected the distribution of the bubbles is obtained.

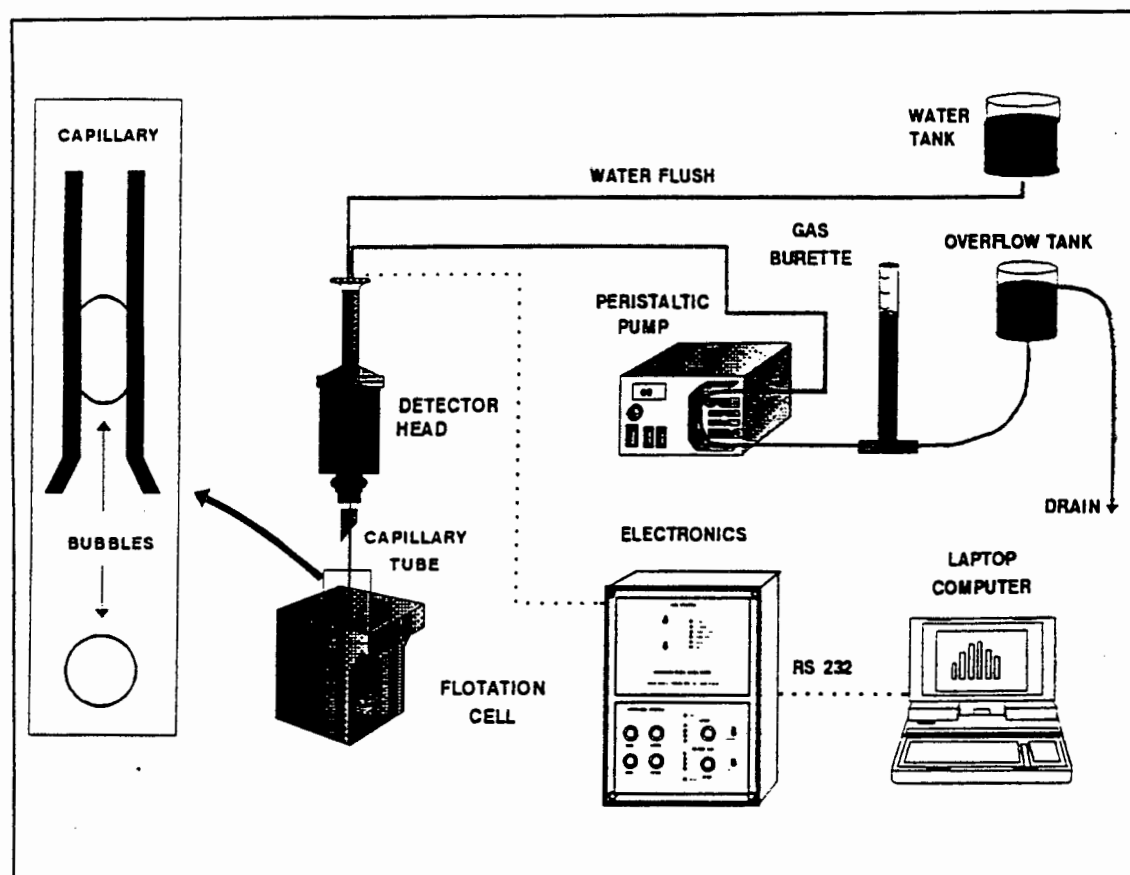


Figure 3.3: The UCT bubble sizer

3.2.1.3 MINERAL SAMPLE

The mineral sample used was Durban Roodepoort Deep gravity-concentrated pyrite. This mineral sample was also used in the thermochemical and kinetic adsorption measurements. The purity of this sample was 96% pyrite. The mineral sample was screened and samples of the following size distribution were used: 25 x 53 μm , 53 x 75 μm , 75 x 106 μm and > 106 μm . Prior to use, the pyrite surface was cleaned by sonification in a 0.1 molar solution of HCl in an Elma ultrasonic bath (model T 310). This was the sample preparation method recommended by Smart [1991] to remove surface oxidised material. The cleaned pyrite was washed copiously with de-ionised water to remove any traces of the dissolved oxidised material.

3.2.1.4 REAGENTS / COLLECTORS

The reagents used for these tests were cyclohexyl dithiocarbamate (oC6 DTC) and potassium n-butyl xanthate (PNBX). These were the same samples that were used for the batch flotation and adsorption tests (cf. Sec. 2.2.1.3.1).

3.2.2 PROCEDURES

3.2.2.1 MEASUREMENT OF BUBBLE LOADING

For each test, a 2 g sample of pyrite was weighed and added to 50 ml of de-ionised water. The pulp was treated in the ultrasonic bath for 10 mins, washed and filtered to remove surface oxidised material. The ore was then added together with 100 ml de-ionised water to the microflotation cell. A peristaltic pump set at 130 rpm (flow rate 1.8 l/min) was used to circulate the pulp. The pH was set to 4 using H_2SO_4 and the redox potential was monitored with a gold electrode (with a calomel standard) throughout the experiment. The reagents were added and the pulp was conditioned. The cell was then carefully topped up with de-ionised water and the cone was then put in place. Air was introduced through a syringe at the base of the cell, at a set flowrate (8 ml/min), pressure (40 mm Hg) and previously determined bubble size distribution. The mean bubble size was measured with a UCT Bubble Sizer in a separate measurement. Loaded bubbles rose through the cell and moved into the collection zone past the cone where the flotation product was deposited into the launder. After a set time interval of 30 secs, the syringe was removed and the flotation product collected and weighed. Air flow rate and bubble size readings were re-measured after collection of the flotation product. The bubble loading was calculated from the mass of mineral recovered and the bubble size measured as mass per bubble or as mass per bubble surface area. The bubble loading was also calculated as a function of bubble volume [Szatłowski and Freyberger, 1985] (cf. Sec. 3.3.1.2).

In order to ensure the reproducibility of the technique it was critical to ensure that the following parameters were carefully controlled:

(i) **The preparation of the pyrite:** The surface of the pyrite required cleaning but, after some procedures viz. leaching at $\text{pH} = 2$, was prone to sheer flocculation. Best results were achieved using a mild leach (10% HCl) and sonification for 10 mins to prepare the mineral surface.

(ii) **The air line pressure:** This affected the lag time between the air being connected and the air bubbles rising through the pulp. The lag time was inversely proportional to the pressure. In order to obtain good reproducibility the air line pressure was kept constant.

(iii) **The bubble size:** Below a critical size, which depended on the size fraction of the pyrite, [Szatlowksi and Freyberger, 1985] the bubbles became overloaded and were unable to rise until either collision with another bubble or until some of the mineral particles became detached. For the $75 \times 106 \mu\text{m}$ size fraction of pyrite the critical bubble size was 1.17 mm, for the $53 \times 75 \mu\text{m}$ size fraction of pyrite this was 0.82 mm and for the $45 \times 53 \mu\text{m}$ fraction of pyrite this was 0.62 mm. This also affected the reproducibility and in order to obtain reproducible results the bubble size was kept above the critical bubble size for each size fraction.

3.2.2.2 MEASUREMENT OF BUBBLE SIZE

The capillary tube of the bubble sizer was positioned in the pulp with the capillary at a set point. The capillary was flushed out before collection started. Bubbles were collected until the total volume of air collected was approximately 2 ml. The data was evaluated for consistency by comparing the number of period readings to the number of velocity readings. The reading was rejected if the discrepancy was greater than 15%.

3.3 RESULTS

3.3.1 REPRODUCIBILITY

3.3.1.1 BUBBLE SIZE MEASUREMENT

Table 3.1 shows the summary of results obtained with the bubble sizer. Detailed results are shown in Appendix 3A. 52 runs were done on 4 different days to establish reproducibility of the system. As has been found previously, by O' Connor et al, [1990], the reproducibility was well within the 95% confidence limits. Within each run there was a consistent bubble size distribution produced as shown by the variance of bubble sizes in each run.

The bubble size was measured in the bubble loading apparatus, before and after, the bubble loading tests. In the development of the system an attempt was made to carry out the bubble sizing and loading measurements simultaneously but the reproducibility was poor due to the very low mass of mineral collected.

Table 3.1: Reproducibility of bubble size data

		Mean Bubble Diameter Db (mm)	Variance Within Each Run	Mean Bubble Surface Area (mm ²)	Total Surface Area (mm ²)	Total No. of Bubbles in Time Interval of 30 secs
Reproducibility Tests (50 Runs)	Mean (mm)	0.96	0.29	3.14	5888.9	1868.7
	Std Dev	0.02	0.03	0.15	698.7	219.4
	Rel Std Dev (%)	2.17	11.14	4.63	11.9	11.7
Measurements for Bubble Loading Tests (3 Runs)	Mean (mm)	1.24	0.36	5.26	15758.5	2997
	Std Dev	0.02	0.01	0.21	943.5	109
	Rel Std Dev (%)	1.61	3.90	3.99	5.99	3.64

The mineral bubble loading of the system can be used as a measure of the particle flotability (cf Section 1.3.2.3). This can be described in various ways and Table 3.3 shows how the values on Table 3.2 are calculated.

3.3.1.2 BUBBLE LOADING MEASUREMENT

Table 3.2 shows the results of 8 tests indicating that the system was capable of producing reproducible results.

Table 3.2: Reproducibility results with 2 g pyrite of 75 x 106 μm size fraction and a dosage of 1.4×10^{-2} mmoles PNBX / 2 g pyrite

Test Number	Overall Mass Recovery (%)	(1) Average Mass per Bubble (mg)	(2) Number of Particles per Bubble	(3) Average Mass per Surface Area (g/m^2)	(4) Actual Loading As a Fraction of Total Possible Loading (%)
1	65.2	0.435	111	82.71	26.8
2	56.8	0.379	97	72.07	23.3
3	66.8	0.446	114	84.81	27.4
4	68.1	0.455	116	86.45	28.0
5	59.6	0.398	102	75.62	24.5
6	65.9	0.439	112	83.58	27.0
7	70.6	0.471	120	89.60	29.0
8	67.5	0.450	115	85.67	27.7
Mean	65.1	0.434	111	82.56	26.7
Std Dev	4.6	0.031	8	5.84	1.9
Rel Std Dev (%)	7.1	7.074	7	7.07	7.1

For these tests, a 2g sample of pyrite from the 75 x 106 μm size fraction was used with 1.4×10^{-2} mmoles of PNBX as collector at pH = 4. Table 3.3 shows the relationships and calculations required for each column in Table 3.2 with typical values of the various parameters.

The average mass loaded per bubble, shown in column (1), was the mass recovery divided by the number of bubbles measured in the time interval. The number of particles per bubble, shown in column (2), was calculated from the number of particles in the mass collected per bubble assuming a cubic structure for pyrite [Kelly and Spottiswood, 1982]. The average mass per surface area, shown in column (3), was calculated from the mass recovered per bubble surface area available in the measured time interval. The actual loading as a

fraction of the total possible loading, shown in column (4), was calculated from the maximum load that a bubble of that size would be able to lift to the surface in terms of the buoyancy forces [Szatkowski and Freyberger, 1985]. A collectorless test was done to quantify the extent of entrainment for the system. The overall recovery for the collectorless test was 8.6%. This was taken into account for the other tests.

Table 3.3: A sample calculation of bubble loading data (cf. Test Number 1, Table 3.2)

Pyrite:	Size fraction		75 x 106 μm	
	Mean diameter	d_p	0.092 mm	
	Density	ρ	5.04 g/cm ³	
	Mass of particle	M_p	3.9x10 ⁻⁶ g	
	Surface area of particle (calc)	A_{sp}	5.07x10 ⁻² mm ²	
	Contact area of particle	A_p	8.46x10 ⁻³ mm ²	
	Time Interval	t	30 secs	
Bubble:	Mean diameter	d_b	1.24 mm	
	Surface area per bubble	A_b	5.25 mm ²	
	Volume of bubble	V_b	1.3 mm ³	
	Number of bubbles in time interval	N_b	2997	
	Total bubble surface area in time interval	A_t	1.576 x 10 ⁵ mm ²	
Overall mass recovery		R	1.35 g in 30 secs	
(1) Average mass per bubble	M_b	R/N_b	0.435 mg	
(2) Number of particles per bubble	N_{pb}	M_b/M_p	111	
(3) Mass per bubble surface area	M_{sa}	R/A_t	82.71 g/m ²	
(4) Actual loading as a fraction of total possible loading of bubble ($d_b = 1.2$ mm)	M_{fl}	M_b/M_{max}	26.8%	
where	M_{max}	$V_b/\rho - \rho_{air}$		

3.3.2 THE EFFECT OF MINERAL PARTICLE SIZE ON BUBBLE LOADING

The aim of these tests was to determine the effect of mineral diameter (d_p) on the bubble loading measured in this system. Table 3.4 shows the results of tests done using 1.4×10^{-2} mmoles PNBX / 2 g pyrite at pH = 4, with the pyrite

split into the following size fractions: < 38 μm , 38 x 53 μm , 53 x 75 μm , 75 x 106 μm , 106 x 150 μm and > 150 μm .

Table 3.4: The effect of particle size on bubble loading of pyrite with a dosage of 1.4×10^{-2} mmoles PNBX / 2 g pyrite

Size Fraction of Pyrite (μm)	Test Number	Overall Mass Recovery (%)	(1) Average Mass Loaded per Bubble (mg)	(2) Number of Particles per Bubble	(3) Average Mass per Surface Area (mg/m ²)	(4) Actual Loading As a Fraction of Total Possible Loading (%)
< 38	9	15.6	0.100	1273	18.98	6.2
38 x 53	10	32.5	0.208	426	39.54	12.8
53 x 75	11	54.0	0.346	251	65.70	21.3
75 x 106	12	65.1	0.425	111	82.58	27.0
106 x 150	13	65.8	0.422	38	80.05	26.0
> 150	14	88.0	0.564	19	107.06	34.7

Figure 3.4 shows the effect of particle size on the mass collected per bubble as well as the number of particles collected per bubble. It can be seen that bubble loading increased with increase in particle size for all the size fractions tested.

The collection efficiency has been defined as the product of the collision efficiency (E_c), the attachment efficiency (E_a) and the detachment efficiency (E_d) [Finch and Dobby, 1990] (cf. Sec. 1.2.2). The collision efficiency increases with increase in particle size [Ralston, 1994, Schulze, 1989]. The attachment efficiency increases with decreasing particle size and increasing contact angle or hydrophobicity [Ralston, 1994]. The detachment efficiency of the mineral particles increases with increase in particle size and turbulence or hydrodynamics of the system [Jowett; 1979, Woodburn et al, 1971 and Finch and Dobby, 1990]. These factors contribute to the existence of a flotation domain with upper and lower limits of particle size in any particular system.

The results shown in Table 3.4 and Figure 3.4 demonstrate the lower particle size limit for this system and the decrease in mass per loaded bubble with

decrease in size fraction can be attributed to the decreased collision efficiency (E_C) and / or the attachment efficiency (E_A) [Schulze, 1989; Hewitt et al, 1994], (cf. Sec. 1.2.2).

The fact that the highest recovery was obtained for the $> 150 \mu\text{m}$ fraction shows that the upper limit had not been reached in this system and confirms the quiescent nature created in the microflotation cell. Woodburn et al, [1971] showed that the detachment of the mineral from the bubble is dependent on the turbulence of the system and the critical size for detachment would be lower in a mechanical flotation cell than in the quiescent environment of a column.

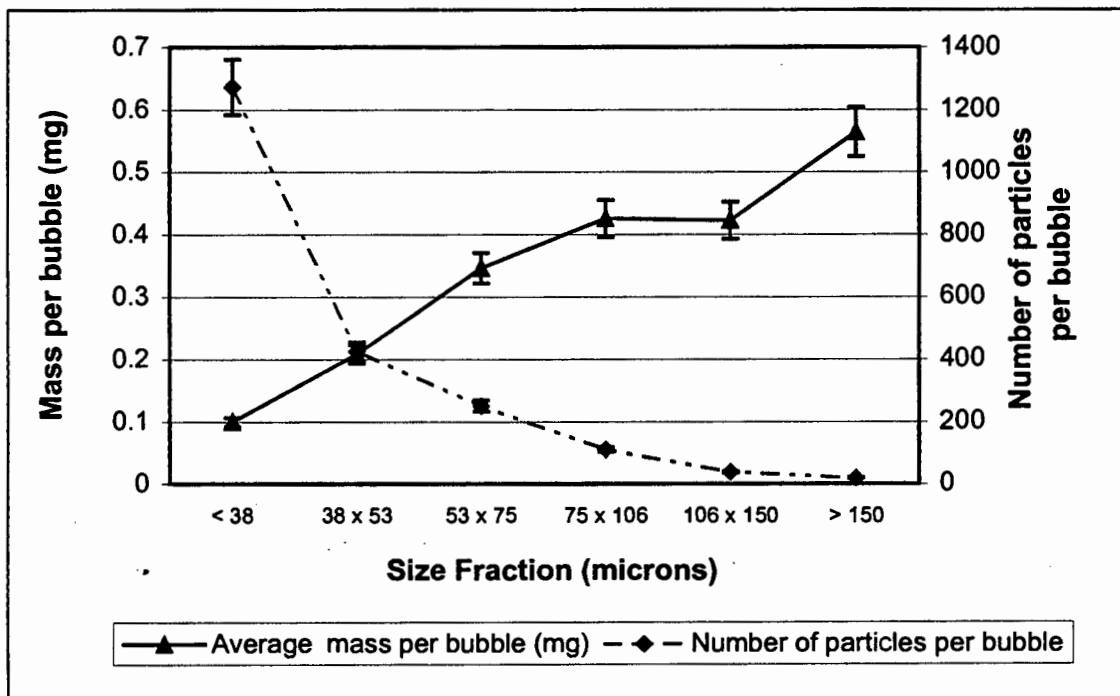


Figure 3.4: The effect of particle size on the mass and number of pyrite particles collected per bubble with a dosage of 1.4×10^{-2} mmoles PNBX / 2 g pyrite

Previously reported values by for pyrite by Imaizumi and Inoue [1985] showed that the optimum particle size range was between 25 and 100 μm . However, Jowett [1980] showed that the upper limit for pyrite in another system was over 200 μm which highlights the specificity of these types of measurements. The results of these tests were however intrinsically consistent and thus the reproducibility and the relative values are of greatest importance.

In these tests excess collector was added to ensure adequate surface coverage for all size fractions, viz. in excess of 5 times pseudo monolayer coverage for the < 38 μm fraction and above 24 pseudo monolayers for the > 150 μm fraction. This assumed the cross sectional surface area of the collector molecule to be approximately 37 Å [Bhaskar Raju and Forsling, 1991].

Drysmala et al [1992] reported that the particle size of pyrite should be over 61 μm for the results not to be masked by entrainment in a Hallimond tube. The implications of this are that the results obtained for the finer fractions in these tests, may have included some entrainment and the true bubble loading was lower than reported.

3.3.3 THE EFFECT OF COLLECTOR TYPE ON BUBBLE LOADING

The aim of these tests was to ascertain whether changing the collector type affected the bubble loading. Collectors and conditions were selected so that results could be used to determine whether the batch flotation results, obtained at equivalent conditions, could be interpreted in terms of bubble loading. Selected collectors were pure PNBX, pure cyclohexyl DTC and the 90:10 mole ratio mixture of PNBX and cyclohexyl DTC. The size fraction of the pyrite was 53 x 75 μm and the tests were done at pH = 4. The collector dosage was constant for all collectors at 1.4×10^{-2} mmoles / 2 g pyrite.

Table 3.5 and Figure 3.5 show that the bubble loading obtained with the mixture was significantly higher than that obtained with pure PNBX or cyclohexyl DTC. It is noteworthy that the ratio of PNBX to cyclohexyl DTC was 90:10, and that a small substitution of C6 DTC had such a marked effect. Table 3.5 also shows the significance of the difference in bubble loading due to the use of the mixture in place of the pure collector which was evaluated using standard 'T' tests with the standard deviation obtained from the reproducibility

tests (cf. Table 3.2).

Table 3.5: The effect of collector type on bubble loading by pyrite with a dosage of 1.4×10^{-2} mmoles collector / 2 g pyrite

Collector Type	Test Number	Overall Mass Recovery (%)	Average Mass per Bubble (mg/bubble)	Difference in loading (Mixture - Pure) (mg/bubble)	Significance of Difference Obtained
PNBX	15	35.5	0.237	0.175	>99.5%
oC6 DTC	16	49.0	0.327	0.090	95 - 99%
Mixture(1)	17	61.8	0.412		

(1) Indicates 90:10 mole ratio mixture of PNBX and cyclohexyl DTC

It can be seen that the loading obtained with the mixture was higher than that obtained with either of the pure collectors. The bubble loading obtained with the mixture was not a linear summation of the contributions of the individual components in the mixture and thus showed that there was a synergistic interaction between the collectors.

3.4 DISCUSSION

The aim of the bubble loading tests was to ascertain whether the use of mixtures of collectors in place of the pure collectors resulted in increased bubble loading and to thereby gain further understanding of the mechanisms which are occurring in the batch flotation tests which could result in the observed synergistic increase in grades and recoveries. The increased sulphur recoveries that were obtained in the batch flotation tests when mixtures of collectors were used indicated that collection zone characteristics were improved (cf. Sec. 2.4). Figure 2.15 in Chapter 2 showed that the highest flotation performance was obtained using the mixture of collectors as shown by the highest sulphur grade vs sulphur recovery curve.

In order to make the results from the two investigations, viz. batch flotation and bubble loading comparable, the conditions were set as similar as possible for both sets of tests. However there are inherent differences between the bubble loading and batch flotation tests which affect the comparison of the results obtained. The most notable being the absence of a froth phase and of a turbulent environment in the former case. Table 3.6 summarises the conditions used in the batch flotation and bubble loading tests (cf. Sec. 2.2.2.1). Both sets of tests were done at pH = 4.

Table 3.6: A comparison of the conditions for bubble loading and batch flotation tests

Parameter	Batch Flotation Tests	Bubble Loading Tests
Ore Source	Buffelsfontein - flotation feed	Durban Roodepoort Deep-gravity conc.
Ore Sample size	1 kg	2 g
Total volume pulp	3 litres	100 ml
Pulp Density	30%	2%
Particle Size of Ore	60% < 75 μm	53 x 75 μm
Percentage pyrite in ore	1.50%	96%
Collector dosage	20.8×10^{-3} mmoles /g pyrite	7×10^{-3} mmoles /g pyrite
Frother	2.92 $\mu\text{l/kg}$ ore	nil
Froth Phase	2.5 cm	nil
Collection zone	Turbulent	Quiescent
Energy Input	High	Low

The most significant differences between the two systems include:

(i) **The particle size distribution, which was much wider in the case of the batch flotation tests.** The particle size of the Buffelsfontein ore used in the batch flotation tests was 60% < 75 μm whereas the size fraction of the Durban Roodepoort Deep pyrite was 53 x 75 μm . The fines present in the case of the batch flotation tests would have a lower collision and attachment efficiency (cf. Sec. 1.2.2 and Figure 3.4) and may lower the overall results obtained in the batch flotation tests, relative to the results obtained in the bubble loading tests. This would imply though that the batch flotation tests represent a conservative

result.

(ii) **The presence of a gangue in the case of the batch flotation tests.** The Buffelsfontein ore was 1.5% pyrite (0.83% sulphur, cf. Table 2.8) whereas the Durban Roodepoort Deep material used in the bubble loading tests was 96% pyrite. The implications of the presence of gangue are that in the batch flotation tests overall performance is a function of both sulphur recovery and sulphur grade whereas performance in the bubble loading tests can be measured in terms of one parameter only, viz. mass loaded per bubble.

(iii) **The presence of frother and the effect of the froth zone.** In the batch flotation tests, frother was added to create the froth. In the froth zone, there is the potential for material collected by the bubbles in the pulp to be lost by elutriation. The implications of this are that the benefits of increased bubble loading in the pulp collection zone of the flotation process can be lost due to poor froth characteristics. This may result in the batch flotation recoveries being lower than the bubble loading recoveries. The batch flotation tests showed that the nature of the collector affected the froth characteristics (cf. 2.4).

It can be seen by comparing Figures 3.5 and 3.6 that in both the batch flotation and the bubble loading tests, the use of the mixture has achieved the best results. This shows that the improvement in bubble loading characteristics obtained using the mixture of PNBX and cyclohexyl DTC was translated into an improvement in the batch flotation performance. Hence even the presence of a froth in the batch flotation tests did not significantly reduce the overall synergistic effect observed in bubble loading.

(iv) **The batch flotation test conditions are more turbulent with a much higher energy input than in the case of the flow through microflotation cell.** Flotation performance is also affected by the hydrodynamics of the system and the increased turbulence would increase the collision efficiency and also increase the detachment efficiency [Finch and Dobby, 1990]. Again this

effect would be expected to reduce the difference between the mixture and the pure reagents in the case of the batch flotation tests.

The batch flotation tests also showed that the froth characteristics were better draining and more mobile in the case of the mixture which resulted in higher sulphur grades being achieved than with the pure collectors (cf. Sec. 2.3.1.4.5). This suggests that although improved bubble loading may be the primary effect, it is not the only factor that was affected by the nature of the collector. Possibly, increased bubble loading is responsible for the improved recovery obtained and improved froth characteristics are responsible for the increased grade.

The reason for the increased bubble loading when mixtures of collectors were used may be attributed to the change in nature of the surface products on the pyrite which may make the particles more hydrophobic. This is discussed more fully in Chapters 2 and 4.

3.5 CONCLUSIONS

These tests have shown that the loading of the mineral onto the bubble is a function of particle size and collector type. The upper particle size limits of the flotation domain where recovery was reduced with increase in particle size were not reached in these tests. The use of a 90:10 mole ratio collector mixture of PNBX and cyclohexyl DTC in place of pure PNBX resulted in a significantly increased bubble loading of 0.175 mg / bubble. The bubble loading results were consistent with the batch flotation tests with respect to the synergistic effect of mixtures of collectors. The increased bubble loading is, itself, the outcome of a more fundamental process - the increased hydrophobicity of the mineral particle which may be the result of the collector - mineral adsorption reactions and this phenomenon is investigated in Chapter 4.

CHAPTER 4: INVESTIGATION OF THE ADSORPTION OF COLLECTORS ONTO PYRITE

4.1. INTRODUCTION

The hydrophobicity of the mineral surface is a critical factor in the success of the flotation process. This can be achieved through the collector - mineral surface reactions (cf. Sec. 1.4). Changes in the nature and characteristics of these surface reactions and resulting surface products can substantially affect the flotation behaviour. The batch flotation and bubble loading tests showed that the use of a mixture of collectors in place of the pure constituent collectors resulted in improved performance of both the overall process and the particle collection process. The aim of the tests described in this chapter was to ascertain whether this enhanced performance was due to improved hydrophobicity of the mineral surface resulting from different surface reactions.

The adsorption of reagent onto mineral surfaces is an exothermic process and the measurement of ΔH_{ads} can be used to determine the strength of adsorption of the reagent as well as to distinguish between reactions occurring between different reagents and minerals [Mellgren, 1966; Mellgren et al, 1973 and Haug and Miller, 1978]. The aim of the thermochemical measurements was to ascertain differences in the heat released on addition to pyrite at pH = 4 with PNBX, cyclohexyl DTC and the 90:10 mole ratio mixture of PNBX and cyclohexyl DTC in order to distinguish between the reactions occurring. The interpretation of these results was made using the known reactions of xanthate and pyrite at pH = 4 [Montaldi et al, 1991] (cf. Sec. 1.4.5.2.3).

The kinetic adsorption and solubility product measurements were made to assist with the interpretation of the thermochemical results. However, it should

be noted that these were not in-depth investigations themselves, but rather were aimed at gaining a preliminary insight into the mechanisms occurring. Measurements of the kinetics of the adsorption of PNBX and cyclohexyl DTC onto pyrite gave a comparison of the rate and extent of adsorption of the different collectors. Measurements of the solubility products of the respective ferrous - thiol salts can be used to distinguish between the stability of the respective ferrous salts formed and are an indicator of the likely collector - mineral surface reactions. Yoon and Basilio [1993] reported that the pK_{sp} values of the thionocarbamate metal salts were approximately ten orders of magnitude higher than those for xanthates indicating the formation of the metal thiolate and not the dithiolate [Yoon and Basilio, 1993] (cf. Sec. 1.4.4).

4.2. EXPERIMENTAL DETAILS

4.2.1 MINERAL SAMPLE

The ore sample, used for all the tests described in this chapter, was the 53 x 75 μm size fraction of Durban Roodepoort Deep gravity-concentrated pyrite. This mineral sample was also used in the bubble loading tests. The sample was 96% pyrite as determined from the sulphur and iron assays. The surface area of the pyrite was 0.108 m^2/g , as measured using BET with argon.

4.2.2 REAGENTS

The collectors used for these tests were cyclohexyl dithiocarbamate (oC6 DTC) and potassium n-butyl xanthate (PNBX). These were the same samples that were used for the batch flotation and bubble loading tests (cf. Sec. 2.2.1.3 and Table 2.2). In specified tests, Mohr's salt, $(\text{NH}_4)_2\text{Fe}(\text{SO}_4)_2 \cdot 6\text{H}_2\text{O}$, was used as an alternative source of Fe^{2+} ions. This particular salt was used due to the presence of the ammonium ion ($(\text{NH}_4)_2^{2+}$) in the molecule, which stabilised the

iron in the ferrous state (Fe^{2+}). Cases et al [1993] report the formation of dixanthogen from sodium ethyl xanthate and Mohr's salt only after 2 days.

Assuming the cross sectional surface area of the thiol molecules to be 37 \AA^2 [Bhaskar Raju and Forsling, 1991], the number of moles required for pseudo-mono-layer coverage of 4 g of pyrite is 1.9×10^{-3} mmoles. At an addition rate of 2.31×10^{-6} moles/min, this would occur after the addition of approximately 48 secs (which equates to 0.27 ml of reagent). The concentration of collector in solution was calculated using the Beer Lambert Law, viz.

$$A = \epsilon b C_m$$

where

- A = Adsorbance of clear solution at set wavelength,
- ϵ = Molar extinction coefficient,
- b = Path length of radiation (cm^{-1}),
- C_m = Molar concentration ($\text{moles}^{-1} \text{cm}^{-1}$).

The adsorbance of the filtered solution was read at fixed wavelength on a Carey UV spectrophotometer adsorbance at set wavelength viz. 280 nm for the cyclohexyl DTC and 300 nm for the PNBX.

Table 4.1 The molar extinction coefficients of the collectors

Collector	Wavelength (nm)	Measured Extinction Coefficient (ϵ)
PNBX	300	1.626×10^3
oC6 DTC	280	0.940×10^3

4.2.3 APPARATUS AND PROCEDURES

4.2.3.1 THERMOCHEMICAL MEASUREMENTS

4.2.3.1.1. APPARATUS

A TRONAC 1250 calorimeter was used to measure the enthalpy change (ΔH) of the reactions occurring. Figure 4.1 shows this equipment. It consisted of a stirred reaction chamber fitted with a microburette positioned in a 50 litre water bath. The heat released during collector addition was recorded using a flat bed recorder and a computer. Data was analysed using software supplied by TRONAC. The heat flux required to maintain a constant temperature inside the reactor was measured. The temperature inside the reaction chamber was kept constant at 25 °C to within 2×10^{-5} °C of the bath temperature. Isothermal measurements were made whereby heat was removed at a constant rate by the Peltier cooler or added by the control heater as required to keep the temperature constant.

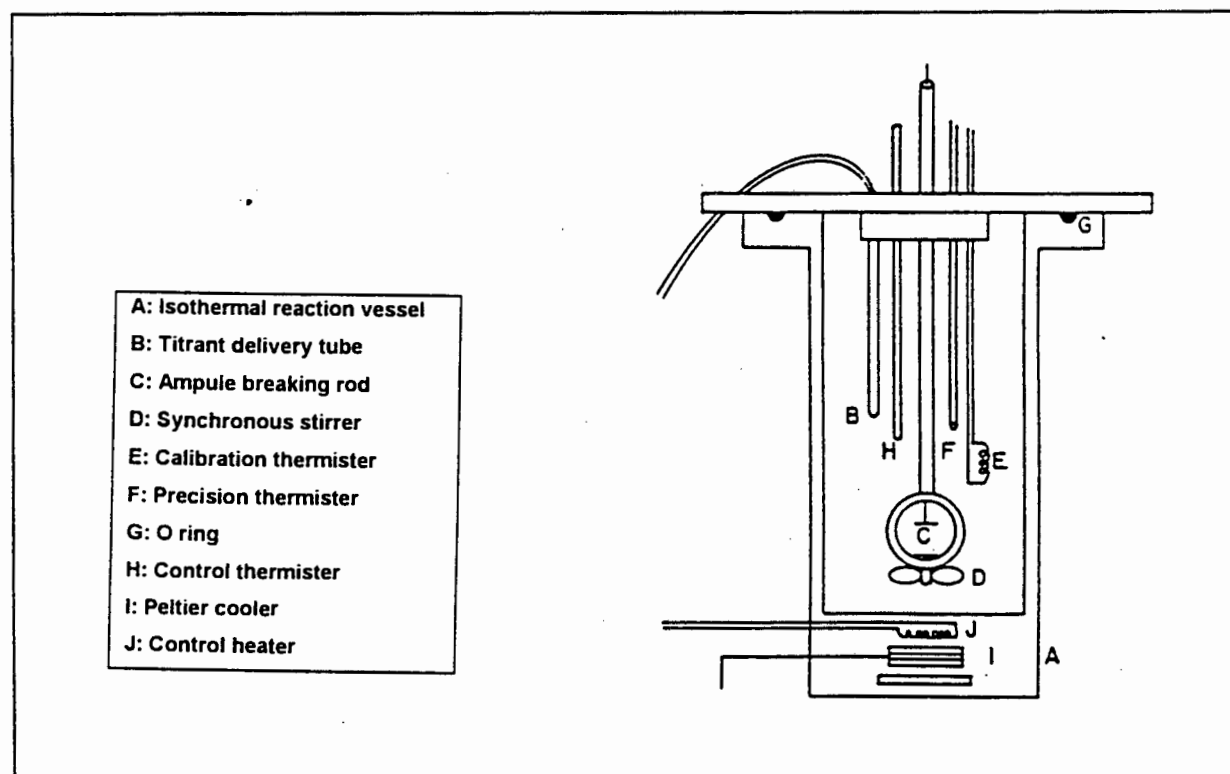


Figure 4.1: The Microcalorimeter used in the Testwork (Haung and Miller, 1978)

4.2.3.1.2 PROCEDURE

The pyrite sample (4 g) was weighed and prepared by sonification in 100 ml of 0.1 molar solution of HCl for 10 mins. This treatment removed and dissolved any surface oxidation products. The pyrite was then washed, filtered and added to the reaction chamber together with 25 ml of de-ionised water. In the case of $(\text{NH}_4)_2\text{Fe}(\text{SO}_4)_2 \cdot 6\text{H}_2\text{O}$, 25 ml of a 0.2 molar solution was added to the reaction chamber. The pH was measured and the reaction chamber was positioned in the calorimeter. At the conditions of the experiment the iron in the pyrite was assumed to be in the Fe^{2+} oxidation state (cf. Sec. 1.4.5.2.3).

The motor-driven microburette was filled with collector of concentration 0.007 moles/l and positioned with the reaction chamber in the calorimeter. Once the temperature of the reaction chamber and collector in the microburette stabilised at 25 °C the calorimeter was calibrated. The microburette turned on automatically to commence the titration and the collector was added to the ore in the stirred reaction chamber at a rate of 0.333 ml/min for 6 minutes so that, in 6 mins, 2 ml or 1.4×10^{-2} mmoles was added. The progressive change in heat generated as collector was added, was measured. The calibration of the system was checked after the experiment.

4.2.3.2 KINETIC MEASUREMENTS

4.2.3.2.1 APPARATUS

The experiments were done in a baffled reactor to ensure good mixing. The dimensions of the reactor were height = 150 mm, diameter = 95 mm and there were 4 x 9.5 mm baffles each of height = 100 mm. The impeller was driven by a 38 W Heidolph Variable Speed Motor. The reactor was covered stirred beaker and nitrogen was bubbled through the pulp for some tests. An ink tracer was used to determine the best point of collector addition. The rate of

change of collector concentration was monitored using the absorbance reading from the UV spectrophotometer and inferred adsorption onto the mineral surface was calculated.

4.2.3.2.2 PROCEDURE

The ore (4 g) was weighed and prepared by sonification in 50 ml de-ionised water for 10 mins. The ore was then washed, filtered, added to the cell and made up to 400 ml. 0.5 ml phthalate buffer was added and the pH set to 4 and conditioned. The cell and impeller design ensured good mixing and the point of reagent addition was chosen to ensure that the system was well mixed and that the adsorption of collector was not limited by the transfer in solution to the pyrite surface. 2.5×10^{-3} mmoles/g pyrite of the reagent was added with a micro syringe at time zero. 5 ml aliquots were removed with a pipetman at set time intervals for 22 mins and immediately filtered with a millipore filter attached to a syringe. The absorbance of the clear solution was read at fixed wavelength on a Varian UV spectrophotometer (280 nm for cyclohexyl DTC and 300 nm for PNBX). From the rate of decrease in absorbance the molar uptake of collector by the pyrite surface was calculated.

4.2.3.3 SOLUBILITY MEASUREMENTS OF FERROUS SALTS

4.2.3.3.1 APPARATUS

These experiments were done in a covered stirred reactor with nitrogen bubbled through the pulp. The absorbance of the filtered solution was read at fixed wavelength on the UV spectrophotometer (280 nm for cyclohexyl DTC and 300 nm for PNBX).

4.2.3.3.2 PROCEDURE

2.5×10^{-3} mmoles of specified collector was added to 100 ml of de-ionised water at pH = 4 at 27 °C. 2.5×10^{-3} mmoles of $(\text{NH}_4)_2\text{Fe}(\text{SO}_4)_2 \cdot 6\text{H}_2\text{O}$ was added until a precipitate was formed. The precipitate was then washed in de-ionised water and added to a fresh sample of de-ionised water. The reactor was covered and stirred. After 1 hour the concentration of collector was measured in solution and the solubility product of each salt was calculated from the concentration in de-ionised water in the presence of the solid ferrous thiolate complex, viz.

$$K_{sp} = -\log [\text{Fe}^{2+}] [\text{Th}]^2$$

where Th = Thiolate ion, either X⁻ or DTC.

4.3. RESULTS

4.3.1 THERMOCHEMICAL TESTS

Table 4.2 shows all the results obtained for the thermochemical tests. Blank titrations using only collector and de-ionised water showed that the heat of dilution, or more specifically the heat of mixing, was negligible. 'ΔH Steady State' refers to the heat flux corresponding to the point when the first plateau or steady state was achieved, as shown in Figure 4.2 (plateau DE). 'Q' refers to the total heat released in each test, viz. the area under the curve in Figure 4.2, as given by the area BDEF.

Tests 1 and 2 were the reproducibility tests in which cyclohexyl DTC was used as the collector with 4 g pyrite. Test 3 was done to with PNBX so that the enthalpy values obtained with cyclohexyl DTC and PNBX could be compared. Tests 4 and 5 were done using PNBX and cyclohexyl DTC with ferrous

sulphate in place of pyrite in order to test the role of pyrite at these conditions. The semi-conducting nature of pyrite has been shown to influence the oxidation of xanthate to dixanthogen [Yoon and Basilio, 1993]. All other conditions were kept constant and the iron was assumed to be in the ferrous state (Fe^{2+}) in all tests. The difference between Tests 4 and 3 and Tests 5 and 1 show the effect of the nature of pyrite on the thiol collectors PNBX and cyclohexyl DTC respectively.

Tests 6 and 7 were done at pH = 3.3 and 5.6 respectively to check the dependence on pH of the reaction between cyclohexyl DTC and pyrite. Tests 8 and 9 were done using the 90:10 mole ratio mixture of PNBX and cyclohexyl DTC in order to compare the behaviour of the collector mixture to that of the pure collector.

Table 4.2: Summary of thermochemical measurements of the reactions between thiol collectors and pyrite or ferrous sulphate

Collector Type	Test Number	Fe^{2+} ion source	pH Change during Test	Measured Enthalpy Change	
				ΔH Steady State (kJ/mole)	Q (Total Heat) (J)(2)
oC6 DTC	1	4.0 g pyrite	4.6 - 7.3	-68.2	-0.69
oC6 DTC	2	4.0 g pyrite	4.2 - 7.7	-67.4	-0.62
PNBX	3	4.0 g pyrite	3.7 - 6.8	-69.5	-0.90
PNBX	4	5×10^{-3} moles Fe^{2+}	-4.2	-43.9	-0.38
oC6 DTC	5	5×10^{-3} moles Fe^{2+}	3.8 -	-66.8	-0.66(3)
oC6 DTC	6	4.0 g pyrite	3.3 - 4.6	-63.5	-0.78
oC6 DTC	7	4.0 g pyrite	5.5 - 7.5	-46.7	-0.38
Mixture(1)	8	4.0 g pyrite	3.6 - 4.6	-90.0	-1.68
Mixture(1)	9	4.0 g pyrite	3.5 - 5.8	-73.0	-1.10

(1) Mixture refers to 90:10 mole ratio mixture of PNBX and cyclohexyl DTC

(2) Total amount of collector added was 1.4×10^{-5} moles (except Tests 5 and 6, where 1.75×10^{-5} moles was added)

(3) Heat includes adsorption and precipitation

4.3.1.1 REPRODUCIBILITY TESTS WITH CYCLOHEXYL DTC

Figure 4.2 shows that the results of Tests 1 and 2 were essentially identical and indicate that the reproducibility was very good. The period AB denotes that the system was at equilibrium and represents the base line at the start of the experiment. BC shows the duration of collector addition. BD represents the response of the calorimeter to the heat developed during the period to reach the steady state period shown by DE. E represents the point at which no further reaction appeared to occur, notwithstanding continued reagent addition. EF is the response of the calorimeter during the period in which it was returning to the new base line, F corresponding to the point of no further heat release. Hence the area under the curve BDEF represents the total heat generated during reagent addition and is referred to as 'Q' in Table 4.1. G indicates the base line at the end of the tests. The difference between the baselines AB and G shows that the enthalpy of the system after the collector was added was higher than that before the collector addition. This is due to the increased volume that is being stirred in the reaction chamber. For these tests the steady state values of ΔH (DE) were -68.2 and -67.4 kJ/mol respectively and the values for the total ΔH (BDEF) for the tests were -0.69 and -0.62 J respectively. A heat of adsorption greater than 40 kJ/mole can be associated with chemisorption [Pearson, 1994].

The steady state ΔH value of -68.2 kJ/mole measured for the cyclohexyl DTC adsorption onto pyrite corresponds to that for the diethyl dithiocarbamate / pyrite system reported by Mellgren et al [1973]. They showed that the initial heat of adsorption was approximately -69.9 kJ/mole and that this decreased with subsequent addition of collector. Mellgren and Rao [1968] reported that the heat of oxidation of diethyl dithiocarbamate to tetraethylthiuram disulphide by iodine was -54.4 kJ/mole compared to -78.2 for the oxidation of ethyl xanthate to dixanthogen.

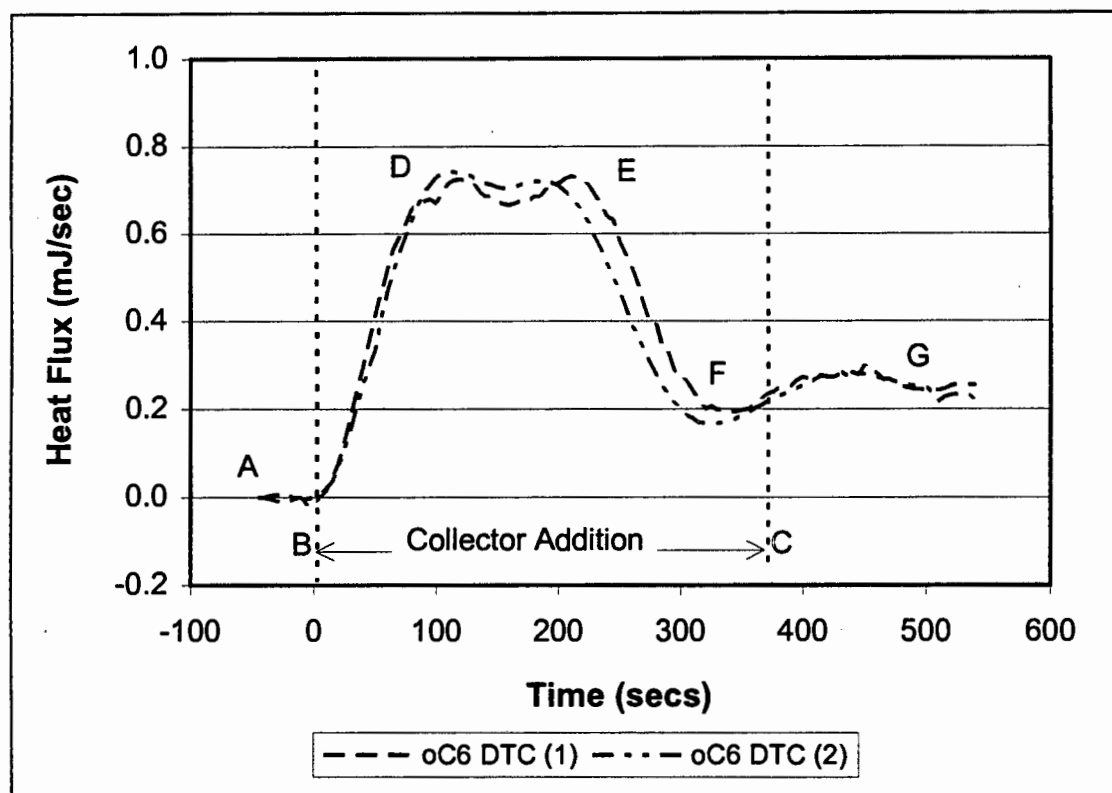


Figure 4.2: Reproducibility of the heat flux recorded when 1.4×10^{-2} mmoles of cyclohexyl DTC was added to 4 g pyrite

4.3.1.2 COMPARISON BETWEEN CYCLOHEXYL DTC AND PNBX WITH PYRITE

The aim of these tests was to ascertain whether there was a difference in surface reactions as demonstrated by a difference in the heat of adsorption of the two collectors, cyclohexyl DTC and PNBX, when they were added to pyrite under identical conditions. The set conditions were equivalent to those for the bubble loading and batch flotation tests so that the thermochemical results could be used to assist in interpreting the bubble loading and batch flotation results.

Figure 4.3 shows the heat of adsorption of cyclohexyl DTC and PNBX onto pyrite (Tests 1, and 3). For both reagents the initial steady state ΔH values were similar (i.e. DE), viz. -68.2 kJ/mole for the cyclohexyl DTC and

-69.5 kJ/mole for the PNBX. For pseudo-mono-layer coverage (mlc) of the pyrite surface by the collectors, based on 37 \AA^2 per molecule and the pyrite surface area of $0.108 \text{ m}^2/\text{g}$, 1.9×10^{-3} mmoles of collector would be required. For both collectors the value of ΔH per mole of collector added did not change after the point of pseudo-mono-layer coverage had been reached. In the case of cyclohexyl DTC the reaction stopped after the addition of 0.93×10^{-5} moles (E), as indicated by the subsequent decrease in the value of the heat flux (EF). In the case of PNBX the value of the heat flux, ΔH , reached a second maximum (HI) soon after collector addition stopped, before decreasing to the baseline.

It is noteworthy to mention that with cyclohexyl DTC, at point E, the reaction terminates as indicated by a decrease in heat release despite continued collector addition and that the subsequent reaction that occurs in the case of PNBX, (HI), does not occur with the cyclohexyl DTC.

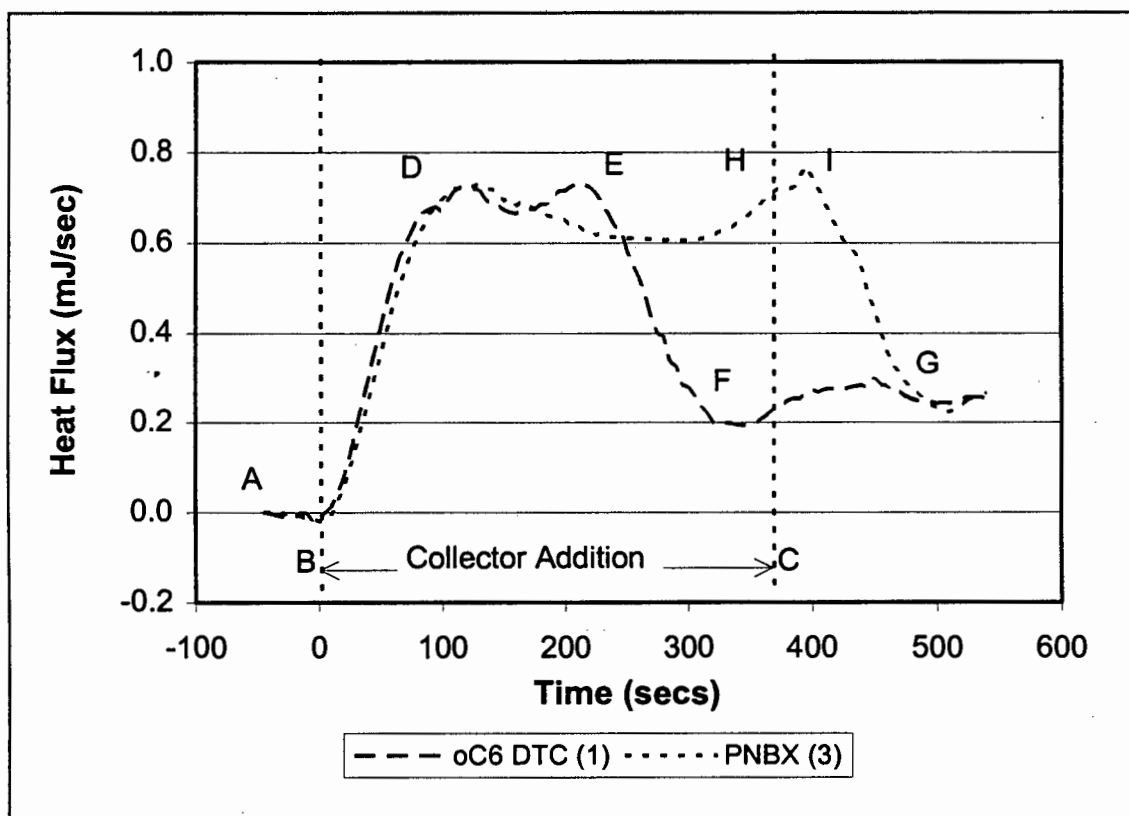


Figure 4.3: A Comparison of the heat flux recorded when 1.4×10^{-2} mmoles of cyclohexyl DTC and PNBX was added to 4g pyrite

The two peaks observed in the case of PNBX correspond to the initial formation of ferrous xanthate and subsequent formation of dixanthogen (cf. Sec. 4.4). In the case of cyclohexyl DTC, only one peak was observed. This suggested that only the ferrous thiolate was formed between cyclohexyl DTC and the pyrite surface and that no second oxidation reaction to form the dithiolate occurred. This is consistent with the kinetic adsorption results discussed in 4.3.2.

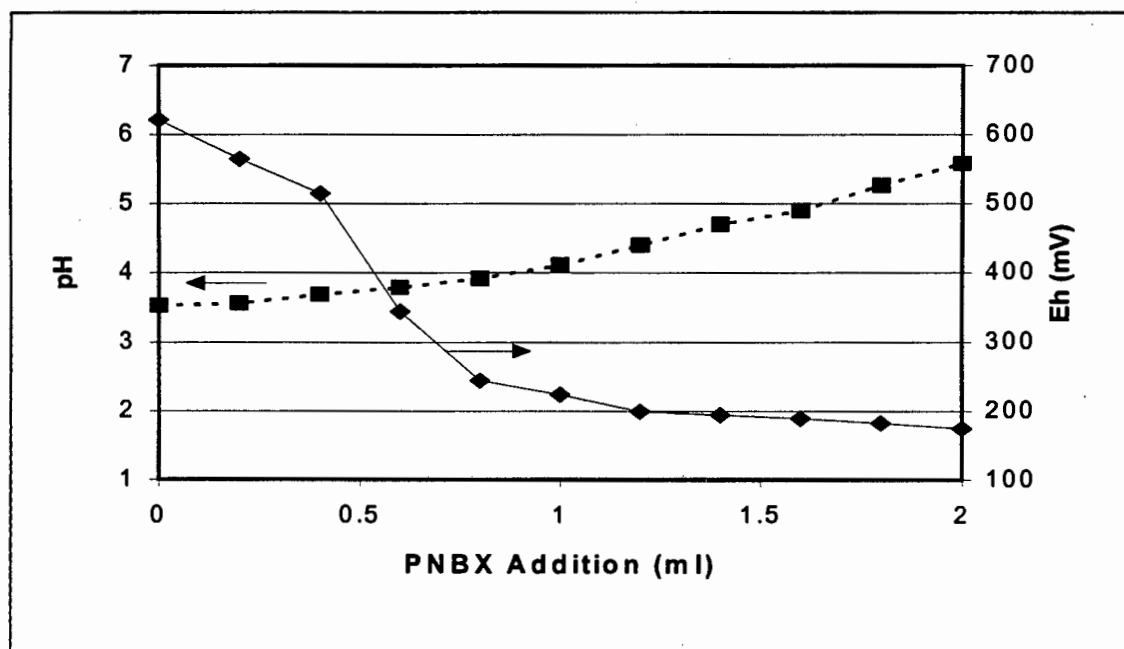


Figure 4.4: The change in pH and Eh recorded when 1.4×10^{-2} mmoles of PNBX was added to 4 g pyrite in 0.2 ml aliquots

Figure 4.4 shows the Eh and pH change occurring during the addition of 0.2 ml aliquots of PNBX to 4 g of pyrite at pH = 4 in 25 ml water. The Eh remained above 150 mV, which was above the oxidation potential of PNBX viz. -127 mV [Finkelstein and Poling, 1977], which indicated that the conditions for the oxidation of xanthate to dixanthogen were favourable (cf. Sec. 1.4.5.2.3).

4.3.1.3 COMPARISON BETWEEN CYCLOHEXYL DTC AND PNBX WITH FERROUS IONS

The aim of these tests was to establish the role of the ferrous ions in the pyrite in the reaction with the collector by replacing pyrite with $(\text{NH}_4)_2\text{Fe}(\text{SO}_4)_2 \cdot 6\text{H}_2\text{O}$

as a source of ferrous ions in the aqueous and not the solid form. This was to test whether the second exothermic reaction occurring between PNBX and pyrite was due to the formation of dixanthogen. The formation of dixanthogen requires the semi - conducting nature of pyrite to provide the electron transfer for the reduction of oxygen and this would not be available with the ferrous sulphate [cf. Sec. 1.4.5.2.3].

Figure 4.5 shows the heat released when cyclohexyl DTC and PNBX were titrated into a freshly prepared solution of $(\text{NH}_4)_2\text{Fe}(\text{SO}_4)_2 \cdot 6\text{H}_2\text{O}$ (Tests 4 and 5). The Fe^{2+} ions were added as $(\text{NH}_4)_2\text{Fe}(\text{SO}_4)_2 \cdot 6\text{H}_2\text{O}$ as the salt stabilised the iron in the ferrous ion state and prevented the oxidation from ferrous ions to ferric ions.

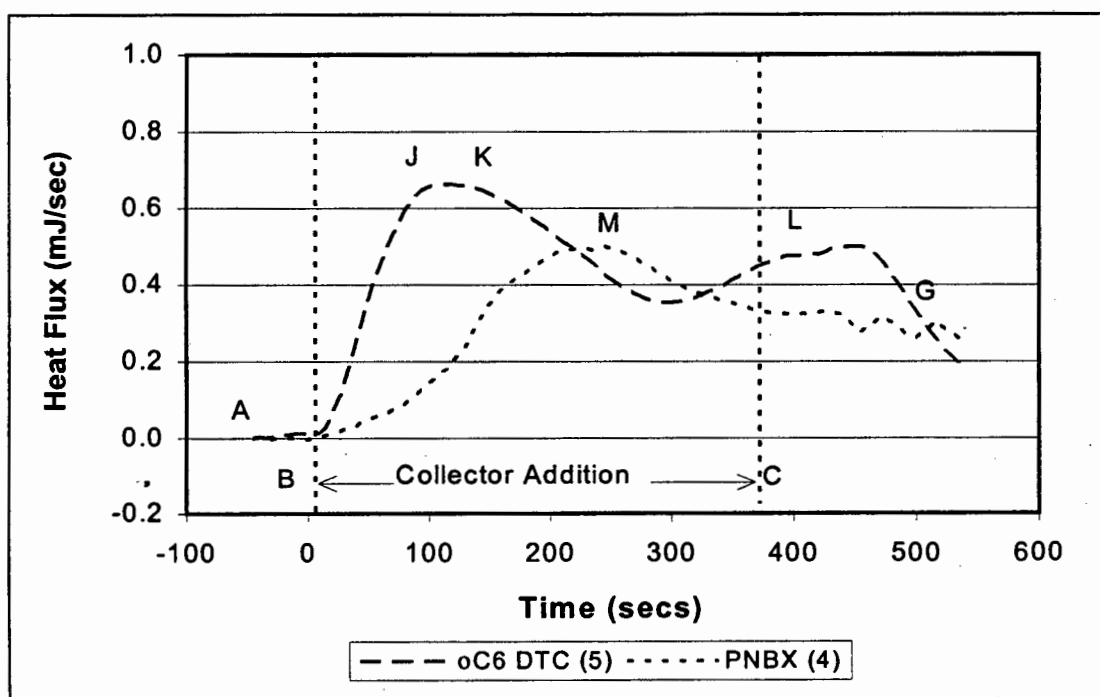


Figure 4.5: Comparison of the heat flux recorded when 1.75×10^{-2} mmoles of cyclohexyl DTC and PNBX was added to $(\text{NH}_4)_2\text{Fe}(\text{SO}_4)_2 \cdot 6\text{H}_2\text{O}$

A comparison of Figures 4.2 and 4.5 showed that the steady state heat flux (ΔH) values for the initial reaction of cyclohexyl DTC with Fe^{2+} ions and pyrite were similar, viz. -68.2 kJ/mole with pyrite and -66.8 kJ/mole with the Fe^{2+} ions. The ΔH peak associated with L corresponds to the precipitation of the ferrous -

thiolate complex which was visually observed in this experiment. The addition of PNBX to Fe^{2+} ions gave a much lower initial ΔH value (M) in the case of the Fe^{2+} ions, viz. -69.5 kJ/mole with pyrite vs -43.9 kJ/mole with Fe^{2+} ions. A comparison of Figure 4.3 and Figure 4.4 showed that the additional reaction occurring between the PNBX and pyrite (HI in Figure 4.2), which was attributed to the oxidation of xanthate to dixanthogen, is not due to any interactions with dissolved Fe^{2+} ions and does not occur in the presence of Fe^{2+} ions only.

4.3.1.4 THE EFFECT OF pH ON CYCLOHEXYL DTC WITH PYRITE

The aim of these tests was to establish whether the reaction termination at point E for Tests 1 and 2 shown in Figure 4.1 and Figure 4.2 was dependent on pH, since Montaldi et al [1991] reported that the number of potential adsorption sites (active sites) on the pyrite surface was dependent on the concentration of H^+ ions (pH).

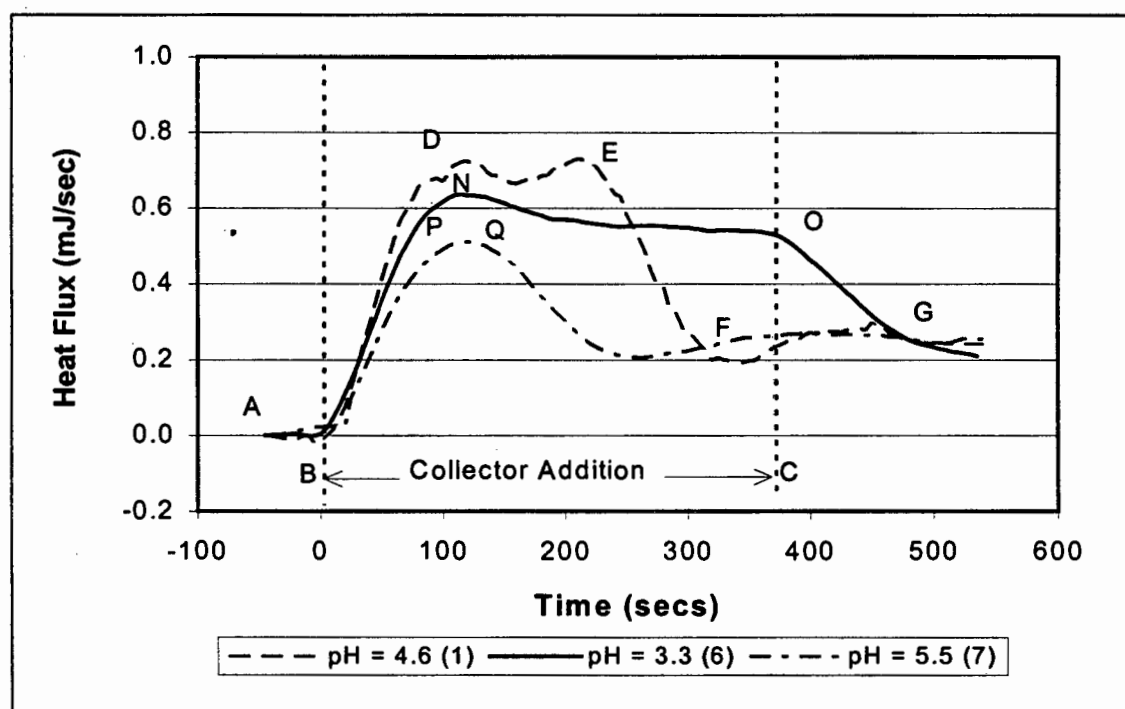


Figure 4.6: The effect of pH on the heat flux recorded when 1.4×10^{-2} mmoles of cyclohexyl DTC was added to 4 g pyrite

Figure 4.6 shows the effect of pH on the extent of reaction between cyclohexyl DTC and pyrite (Tests 1, 6 and 7). In Test 1 (Figure 4.2 and Figure 4.6), where the starting pH was 4.6, the reaction terminated after 200 secs, in Test 6 where the starting pH was 3.3, the reaction continued until the reagent addition was completed and in Test 7, where the starting pH was 5.5, the reaction terminated before the plateau was reached. It can be clearly seen that the reaction is strongly dependent on pH and appears to terminate when the pH gets too high.

4.3.1.5 THE EFFECT OF THE 90:10 MIXTURE OF PNBX:CYCLOHEXYL DTC WITH PYRITE

The aim of these tests was to ascertain whether there was a difference in the reactions occurring on the pyrite surface with the mixture of collectors as opposed to the pure collectors.

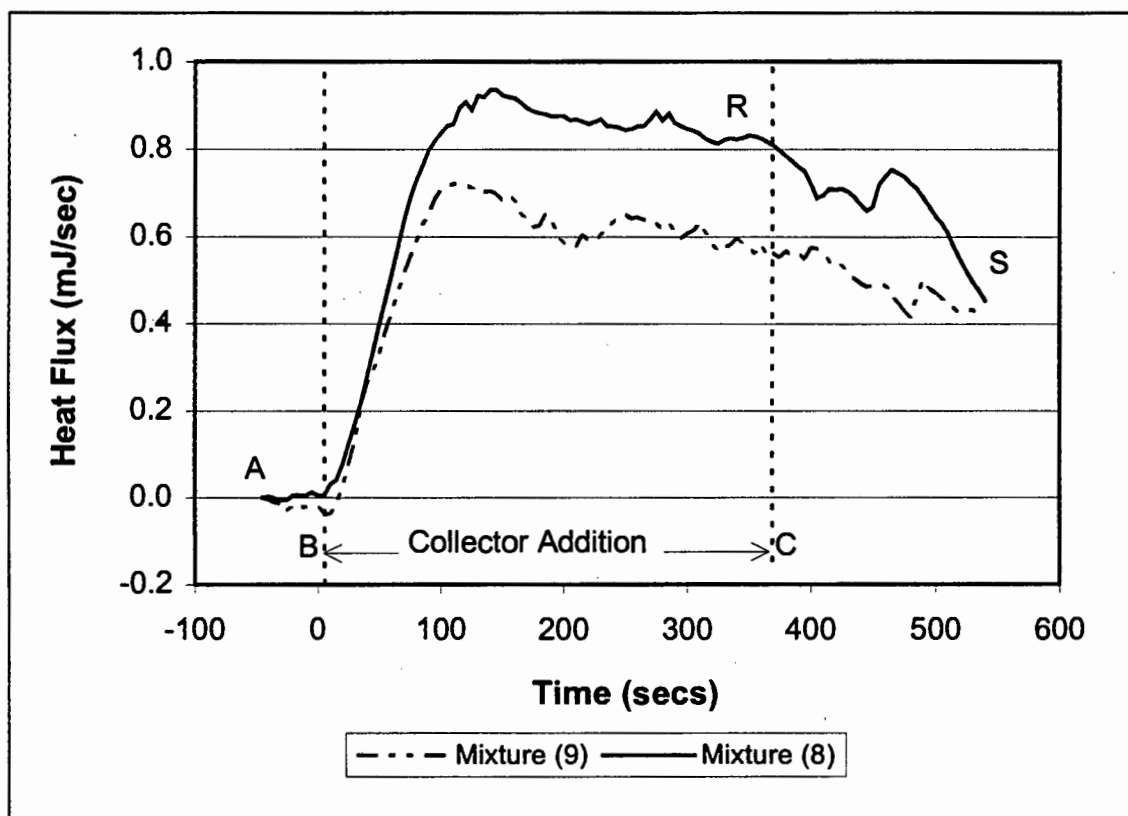


Figure 4.7: The heat flux recorded when 1.4×10^{-2} mmoles of a 90:10 mixture of PNBX and cyclohexyl DTC was added to 4g pyrite

Figure 4.7 shows the ΔH values obtained when two tests with the 90:10 mole ratio mixture of PNBX and cyclohexyl DTC were done (Tests 8 and 9). The mixture of collectors was formulated so as to ensure that the total molar addition rate was kept constant at 7×10^{-6} moles/min which was the same as for the pure collectors.

The reproducibility between the two tests using the mixture was not as good as that for the pure collectors, viz. -90.0 and 73.3 kJ/mol at steady state and the Q values were 1.7 and 1.1 J respectively. A greater ΔH value was measured in the case of Test 8 for which the pH increase was lower than for Test 9, viz. from 3.6 to 4.6 as opposed to from 3.5 to 5.8. In both cases significantly more heat was released with the mixture than for the pure reagents and the heat released continued after reagent addition stopped as shown by the period RS in Figure 4.7, compared to the period EFG in the case of cyclohexyl DTC (Figure 4.2) and the period following IG in the case of PNBX (Figure 4.3). The pH change was also lower for the mixtures than for the pure reagents.

4.3.1.6 SUMMARY OF THERMOCHEMICAL RESULTS

The thermochemical tests have shown that cyclohexyl DTC and PNBX undergo the same initial reactions with pyrite at pH = 4. The heat released was 69.5 and 68.2 kJ/mole. This is indicative of the formation of the metal thiolate which is chemisorbed onto the pyrite.

In the case of PNBX there is a further reaction which is interpreted as being the oxidation of the adsorbed xanthate ions to dixanthogen. The oxidation reaction depends on the presence of pyrite and does not occur when ferrous ions are added as a salt in solution.

In the case of cyclohexyl DTC, the second reaction, attributed to collector oxidation, does not occur despite continued reagent addition. This may be due

to the strong stability of the ferrous dithiocarbamate initially formed (cf. Sec. 4.3.3). The extent of reaction between cyclohexyl DTC and pyrite was shown to be dependent on the pH.

When mixtures are used there was an increase in the enthalpy values which indicated that there was a stronger mineral surface reaction. This may result from the increased extent of oxidation of xanthate to dixanthogen caused by the presence of the dithiocarbamate. It also may be caused by a stronger bond forming between the mixture of collectors and the mineral surface due to the interactions of the pure collectors.

4.3.2 KINETIC ADSORPTION MEASUREMENTS

The aim of these tests was to compare the kinetic adsorption characteristics of cyclohexyl DTC and PNBX with pyrite at pH = 4. Sutherland and Wark [1955] have reported that the kinetics of adsorption are faster with dithiocarbamates than with xanthates. There is controversy in the literature concerning the adsorption kinetics of xanthate onto pyrite. Harris and Finkelstein [1975] were the first to report that xanthate abstraction from solution continues until xanthate depletion and is not limited by surface coverage. Montaldi et al [1991] report that the adsorption of ethyl xanthate onto pyrite fits second order kinetics with the rate of reaction dependent on the concentration of the active sites on the pyrite surface as well as the concentration of collector. Haung and Miller [1978] found that the rate of adsorption of PAX was approximately 0.5 order kinetics and was controlled by the electrochemical discharge.

Figure 4.8 shows the adsorption of PNBX, cyclohexyl DTC and the 90:10 mole ratio mixture of PNBX and cyclohexyl DTC onto pyrite as a function of time. It can be seen that the rate of adsorption of cyclohexyl DTC onto pyrite was more rapid than that of PNBX. The PNBX adsorption continues until reagent depletion, (2.5×10^{-6} moles / g pyrite adsorbed) whereas the cyclohexyl DTC

adsorption reached equilibrium (2.0×10^{-6} moles / g pyrite adsorbed). The equilibrium extent of adsorption was not related to mono-layer coverage, which would have occurred within the first minute after the adsorption of 4.75×10^{-3} mmoles / g pyrite (cf. Sec. 4.3.1.2 and mlc in Fig. 4.8). The equilibrium extent of adsorption of cyclohexyl DTC showed that the number of moles adsorbed in the kinetic adsorption tests was approximately equal to the number of moles reacted before the termination of heat release in the thermochemical tests, viz after 2×10^{-6} mmoles / g pyrite.

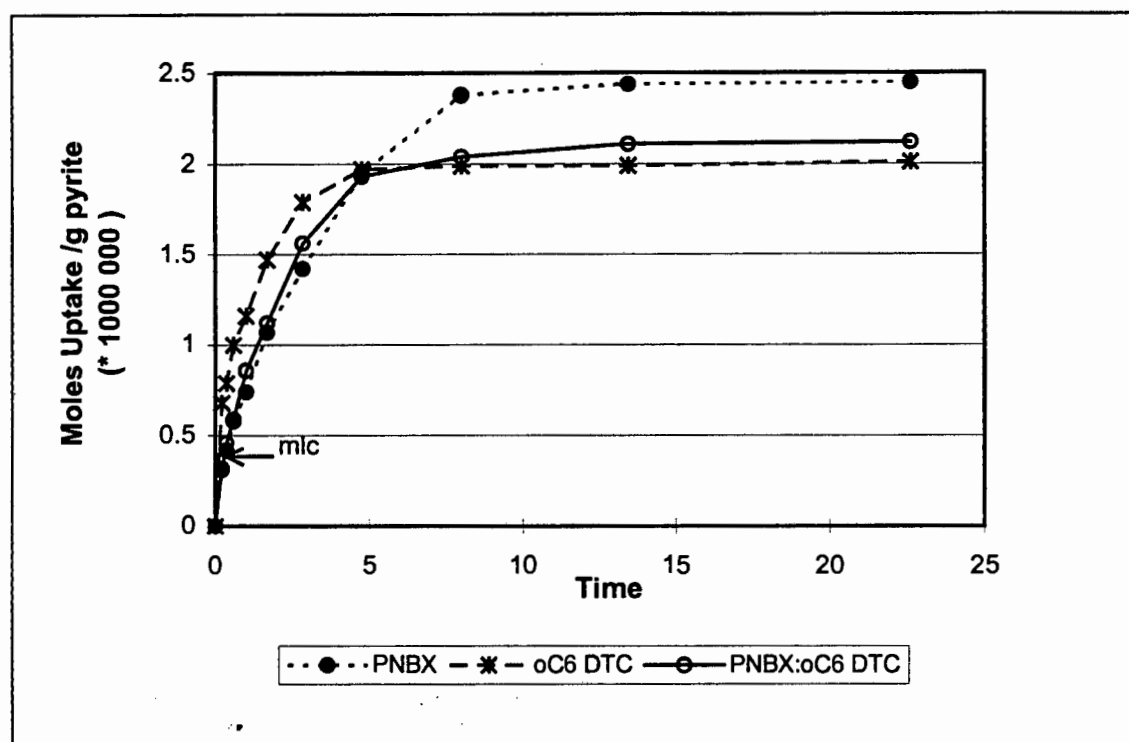


Figure 4.8: The rate of adsorption of PNBX, cyclohexyl DTC and the 90:10 mole ratio mixture of PNBX and cyclohexyl DTC onto pyrite

The adsorption of the mixture was monitored by the reduction of the absorbance peak at 300 nm, i.e. the rate of adsorption of the xanthate in the mixture was monitored. The concentration of the 10% molar substitution of cyclohexyl DTC was very low and the peak at 280 nm was masked by the peak at 300 nm so that it was not possible to monitor the change in concentration of the cyclohexyl DTC. It can be seen that the rate of PNBX uptake in the mixture

as indicated by the adsorption of the xanthate at 300 nm, was not significantly changed. Note that the overall concentration of xanthate in the mixture was 90% of that for the pure collector addition.

The adsorption isotherm was modelled as a first order process. Table 4.3 shows the rate constant and confidence limits of the first order rate constants for the first 0.36 min and for the first 5 mins. Reproducibility tests with cyclohexyl DTC showed that the standard deviation of the first order rate constants was 3.8%.

Table 4.3: The first order rate constants for PNBX and cyclohexyl DTC and the 90:10 mole ratio mixture of PNBX and cyclohexyl DTC

Collector Type	First Order Rate Constant (0.36 mins)		First Order Rate Constant (5 mins)	
	k (min ⁻¹)	R ²	k (min ⁻¹)	R ²
PNBX	0.52	97.5	0.38	99.4
oC6 DTC	1.08	92.6	0.31	92.8
Mixture (1)	0.64	98.9	0.39	99.7

(1) Mixture refers to 90:10 mole ratio mixture of PNBX and cyclohexyl DTC

For the first 0.36 min, the rate constant obtained in the case of the cyclohexyl DTC was more than double that obtained with PNBX, viz 1.08 min⁻¹ vs 0.52 min⁻¹. The rate of depletion of PNBX in the mixture was not significantly faster than that in the case of pure PNBX. This indicated that the rate of adsorption of PNBX was not increased by the presence of cyclohexyl DTC, showing no synergism in the rate of adsorption of collector onto the pyrite surface.

4.3.3 SOLUBILITY PRODUCT MEASUREMENTS

The solubility product (pK_{sp}) of the respective metal salts has been used by several authors in conjunction with other measurements, such as FTIR and

cyclic voltammetry, to gain further insights into the interactions between the thiol collectors and the pyrite surface. [Yoon and Basilio, 1993; Fuerstenau and Mishra, 1980 and Raju and Forsling, 1991] (cf. Sec. 1.4.5). Yoon and Basilio [1993] showed that the lower the solubility of the metal salt, the more favourable the formation of the metal thiolate on the mineral surface according to the Paneth - Horovitz principle (cf. Sec. 1.4.1.4)

The aim of these tests was to measure the solubility products (pK_{sp}) of the ferrous salts formed with cyclohexyl DTC and PNBX in order to compare and categorise them according to the method described by Basilio and Yoon [1993] and thus to determine which reaction mechanism is indicated (cf. Sec. 1.4.4).

The ferrous salts of cyclohexyl DTC and PNBX were prepared according to the procedure detailed in Section 4.2.4.2 and the results are shown in Table 4.4

Table 4.4: The solubility products (pK_{sp}) of ferrous - thiol salts

	Ferrous salt	
	oC6 DTC	PNBX
Absorbance	0.278	142.80
Concentration of Thiolate ion	4.11E-07	8.69E-03
Concentration of Fe^{2+}	2.05E-07	4.34E-03
$[Fe^{2+}][Th^-]^2$	3.46E-20	3.28E-07
pK_{sp}	19.46	6.48

The results reported in this table shows similar values to those obtained for similar salts by other authors, viz. $pK_{sp} [Fe(C_2X)_2] = 7.2$ [Kakovski, 1957], $pK_{sp} [Cu (DTC)_2] = 24$ and $pK_{sp} [Cu (DTC)] = 12.5$ [Raju and Forsling, 1991].

The solubility product (pK_{sp}) of the ferrous salt with PNBX was significantly lower than that for the dithiocarbamate salts. Using the hypothesis proposed by Basilio and Yoon [1993] that decreased solubility of the metal salt indicates the formation of the metal thiolate, in combination with the thermochemical and kinetic tests, it is proposed that different surface reactions occur with pyrite.

The dithiolate is indicated with the xanthate but the metal thiolate is indicated with the dithiocarbamates.

4.4. DISCUSSION

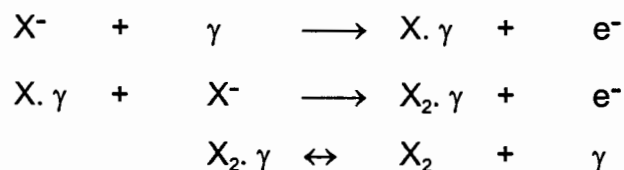
The objective of the adsorption tests was to ascertain whether the differences observed in the flotation behaviour tests (cf. Chapter 2) and the bubble loading tests (cf. Chapter 3) obtained with PNBX, cyclohexyl DTC and the 90:10 mole ratio mixture of PNBX and cyclohexyl DTC could be attributed to differences in the hydrophobicity of the pyrite, resulting from differences in the adsorption reactions between the pyrite surface and the respective collectors.

Dithiocarbamates and xanthates are both thiol collectors, with the same ionic, or polar head of the molecule (cf. 1.4.3.1, Fig. 1.9). The differences in the respective structures, however, affect aspects of the behaviour of the collectors. The effect of the nitrogen atom in the dithiocarbamate molecule is to create a collector which bonds more strongly than xanthate to the mineral surface [Nagaraj, 1988]. This has been reported to result in increased stability and lower solubility of the corresponding metal - thiolate salts [Thorn, 1962; Poling, 1976; Glembofsky, 1995].

The extent of the solubility of the metal - thiolate salt has been correlated by Yoon and Basilio [1993], to the occurrence of the electrochemical - chemical coupled reaction between the collector and the mineral surface, resulting in the formation of the metal thiolate as the mineral surface product. They showed that the solubility products for the xanthate metal salts were approximately ten times lower than the salts formed with the equivalent dithionocarbamate collectors so that in the case of dithionocarbamate collectors (cf. Sec. 1.4.3.1, Figure 1.11), the metal thiolate was formed and in the case of xanthates, the dithiolate was formed.

The standard potential for the oxidation of ethyl xanthate to dixanthogen has been reported as -60 V and for the oxidation of diethyl dithiocarbamate to its respective dithiolate (thiuram disulphide) was reported as 110 mV [Finkelstein and Poling, 1977]. The difference in oxidation potential indicates that the oxidation of dithiocarbamates would be less favourable than the oxidation of xanthates. To the authors knowledge, the potential of the oxidation of cyclohexyl DTC to the dithiolate has not been reported and it is not known whether the dithiolate will be formed at the conditions used in this study. However, in tests with dithiocarbamates and other sulphide minerals only the metal thiolate has been identified (cf. Sec. 1.4.5.2) [Mangalam and Khangaonkar, 1985; Bhaskar Raju and Forsling, 1991; Hu et al, 1992]. In the case of xanthates with pyrite, dixanthogen is reported as the species formed. It has now been well established that, under flotation conditions, dixanthogen is not the only product formed when xanthate is added to pyrite but that before the dixanthogen formation there is some xanthate - pyrite electrochemical interaction with the formation of a chemisorbed metal xanthate complex (cf. 1.4.5.2.3) [Leja, 1973; Harris and Finkelstein, 1975; Finkelstein and Poling, 1977; Huang and Miller, 1978; Mielczarski, 1986; Leppinen et al, 1989; Wang and Forssberg, 1991; Fornasiero and Ralston, 1993; Montaldi et al, 1991; Hanson and Fuerstenau, 1993].

Montaldi et al [1991] summarised the rate and reaction paths of adsorption of ethyl xanthate on pyrite at pH = 4. These can be represented by the following surface reactions:



where γ = active site on the pyrite surface.

The thermochemical tests showed that both PNBX and cyclohexyl DTC undergo the first reaction, viz. the formation of the metal thiolate. In the case of PNBX, a second reaction is observed which has been attributed to the oxidation of xanthate to dixanthogen. This second reaction does not occur in the case of cyclohexyl DTC, indicating the formation of the metal thiolate only.

The second peak attributed to the formation of dixanthogen was dependent on the presence of pyrite and was not formed when ferrous sulphate was used. This was evidence of the requirement of the electron transfer facility at the surface and was another indirect confirmation of the second peak being due to dixanthogen formation.

The value of ΔH obtained in the case of the PNBX, viz. -69.5 kJ/mole, was lower than the heat measured by Rao [1972] for the potassium ethyl xanthate / pyrrhotite system, viz -78.2 kJ/mole when the pyrrhotite was unactivated. When the pyrrhotite was activated with copper sulphate the heat measured was similar to that obtained in this investigation, viz. -69.9 kJ/mole. A heat of oxidation of potassium ethyl xanthate to dixanthogen by iodine of -78.2 kJ/mole is reported by Mellgren [1966]. Haung and Miller [1978] measured the heat released when potassium amyl xanthate was added to pyrite. They obtained values of -122.2 and -132.5 kJ/mole at pH = 4 with different buffers and interpreted this as the combined heat of oxidation of the potassium amyl xanthate to dixanthogen and the formation of water. The differences between the findings of Haung and Miller [1978] and those of this investigation may result from the effect of the buffer or from the difference in pyrite sample [Ball and Rickard, 1976; Wards, 1996] and mineral sample preparation.

The extent of the reaction of the cyclohexyl DTC with pyrite was shown to depend on pH which indicated that the presence of active sites on the pyrite was dependent on pH. This was also demonstrated by Montaldi et al [1991].

The kinetic tests showed that cyclohexyl DTC adsorbs faster onto pyrite than the PNBX but that the adsorption of cyclohexyl DTC reaches equilibrium whereas the adsorption of PNBX continues until reagent depletion. The amount of cyclohexyl DTC adsorbed was the same in the kinetic tests and the thermochemical tests. This finding is added evidence to support the formation of the metal thiolate in the case of cyclohexyl DTC and the dithiolate in the case of PNBX.

The batch flotation tests showed that higher water recoveries were obtained in tests with increased cyclohexyl DTC addition which is consistent with a portion of the cyclohexyl DTC remaining in solution to contribute to the frothing properties of the system. The good frothing properties of dithiocarbamates have also been noted by Jiwu et al [1984] who used cyanoethyl dithiocarbamate successfully in the flotation of sulphide minerals with lower frother dosages.

Using the interpretation proposed by Basilio and Yoon [1993] that the higher the pK_{sp} , the higher the probability of the formation of the metal thiolate, the solubility product measurements are also consistent with the formation of the metal thiolate in the case of the cyclohexyl dithiocarbamate and the dithiolate in the case of the PNBX. The pK_{sp} of cyclohexyl DTC was 19.46 vs 6.48 for PNBX which indicated that the dithiocarbamate is more likely to form the metal thiolate than the xanthate.

The results from these three sets of tests indicate that at the conditions of the batch flotation tests, the xanthate, PNBX, is likely to form dixanthogen but the dithiocarbamate, cyclohexyl DTC, may not form the respective dithiolate, but rather the ferrous dithiocarbamate complex.

The techniques used in this chapter are indirect methods, aimed at gaining an insight into the nature of the surface products. More sophisticated methods are recommended such as TOF SIMS, XPS or FTIR would be necessary to shed

more light on this question but the use of these techniques was beyond the scope of this thesis.

The thermochemical measurements with the mixture of PNBX and cyclohexyl DTC gave an increased enthalpy change which indicated the presence of a stronger mineral surface interaction. This may result from the increased oxidation of xanthate to dixanthogen caused by the presence of the dithiocarbamate. It also may be caused by a stronger bond forming due to synergistic behaviour between the mixed collector and the mineral surface due to the interactions of the pure collectors. Again direct methods of analysis would be required to confirm the nature of these surface products.

The kinetic measurements showed no increase in rate of adsorption of xanthate with the 10% molar substitution of cyclohexyl dithiocarbamate, showing that there was no synergistic enhancement in rate of adsorption of xanthate onto pyrite.

The following mechanism is proposed for the enhancement of flotation performance observed when a mixture of PNBX and cyclohexyl DTC is used. The cyclohexyl DTC adsorbs more rapidly than the PNBX and forms the metal thiolate on the surface of the pyrite. This may increase the extent of dixanthogen formation with PNBX (cf. thermochemical measurements). Dixanthogen is a neutral molecule which is physisorbed, however the presence of ferrous cyclohexyl DTC which is chemically bonded, may increase the strength of collector attachment to the mineral surface. This may decrease induction time, thus increasing the rate of flotation, or increase the tenacity of the overall bubble - particle attachment, resulting in less elutriation and thus higher grade.

4.5 CONCLUSIONS

The thermochemical measurements demonstrated the differences in the reactions between PNBX and cyclohexyl DTC and the pyrite surface. The heat changes when PNBX was added to pyrite has corresponded to the established mechanisms of the initial formation of the ferrous - thiolate followed by the formation of dixanthogen. In the case of the dithiocarbamate, only the formation of ferrous - thiolate was indicated. Dixanthogen was not formed with PNBX when ferrous sulphate was used in place of the pyrite illustrating the requirement of the semiconducting nature of pyrite for the electron transfer to form dixanthogen.

The results from the kinetic adsorption tests were consistent with the formation of dixanthogen in the case of PNBX but not in the case of cyclohexyl DTC in that the extraction of PNBX continued until reagent depletion whereas the extraction of cyclohexyl DTC reached equilibrium.

The measurements of the solubility products showed that the metal thiolate salt formed in the case of cyclohexyl DTC was considerably less soluble than that formed with xanthate which indicated the preferential formation of the metal thiolate and not the dithiolate with pyrite.

The increased heat change obtained when the mixture of PNBX and cyclohexyl DTC was used indicated the occurrence of additional reactions or complex formation. The increased hydrophobicity of this product could be used to explain the synergistic behaviour observed in the bubble loading and batch flotation tests. Although the findings of these tests are consistent with the literature they do not provide final definitive evidence of the surface products formed and thus confirmation of the mechanisms occurring.

CHAPTER 5: THE ROLE OF COPPER SULPHATE

5.1. INTRODUCTION

Copper sulphate is added to the pulp in many pyrite flotation plants. [Bushell, 1962; King, 1972; O' Connor et al 1988; Bothelho de Sousa and Ross, 1990 and O' Connor and Dunne, 1991]. The role of copper sulphate is not clear and there are many conflicting theories proposed to explain the observed effects (cf. Sec. 1.2.2.3.4). In some cases, copper sulphate is classified as a froth modifier [O' Connor et al, 1988], in others it is proposed that the adsorption of copper ions onto the mineral surface enhances collector adsorption [Leppinen, 1990; Nagaraj, 1995]. A third possible role is for the copper sulphate to complex with any remaining cyanide on the mineral surface of residual ores [Lloyd, 1981; Bothelho de Sousa and Ross, 1990]. A fourth role is to increase the redox potential (ORP) of the pulp thereby creating a more favorable environment for the oxidation of the thiol collectors.

This chapter investigates the role of copper sulphate in the flotation of pyrite at pH = 4 and to elucidate the interactions of copper sulphate with the pure collectors and the 90:10 mole ratio mixture of PNBX and cyclohexyl DTC, as referred to in the figures and tables as 'Mixture'. The evaluation was made using batch flotation tests and bubble loading tests.

5.2. BATCH FLOTATION TESTS

5.2.1 INVESTIGATION WITH BUFFELSFONTEIN ORE

The aim of the batch flotation tests with Buffelsfontein ore was to investigate the effect of copper sulphate addition on batch flotation performance of pyrite at pH = 4 obtained with PNBX, cyclohexyl DTC and the 90:10 mixture of PNBX and cyclohexyl DTC at a constant dosage of 310 mmoles/t. Table 5.1 shows the results of these tests as well as the results obtained in the absence of copper sulphate addition (cf. Sec. 2.3.1, Table 2.6). Detailed results are shown in Appendix 5A.

5.2.1.1 SULPHUR GRADE VS SULPHUR RECOVERY

Figure 5.1 shows that the effect of copper sulphate addition with PNBX was to increase the sulphur recovery but with a grade penalty, so that the overall relationship between sulphur grade and sulphur recovery did not change. This shows that the flotability of pyrite relative to the gangue had not changed. The effect of copper sulphate addition with cyclohexyl DTC was to considerably reduce both sulphur grade and sulphur recovery. The effect of copper sulphate addition with the 90:10 mole ratio mixture of PNBX and cyclohexyl DTC was to reduce grades at similar recoveries and thereby lower the overall flotation performance obtained.

5.2.1.2 RATE OF SULPHUR RECOVERY

Figure 5.2 shows the constants, k and R , calculated using the Klimpel model (cf. 1.2.2.1). It can be seen that copper sulphate addition increased the rate constants obtained with both the pure PNBX and the mixture of collectors but reduced the rate constant obtained with cyclohexyl DTC.

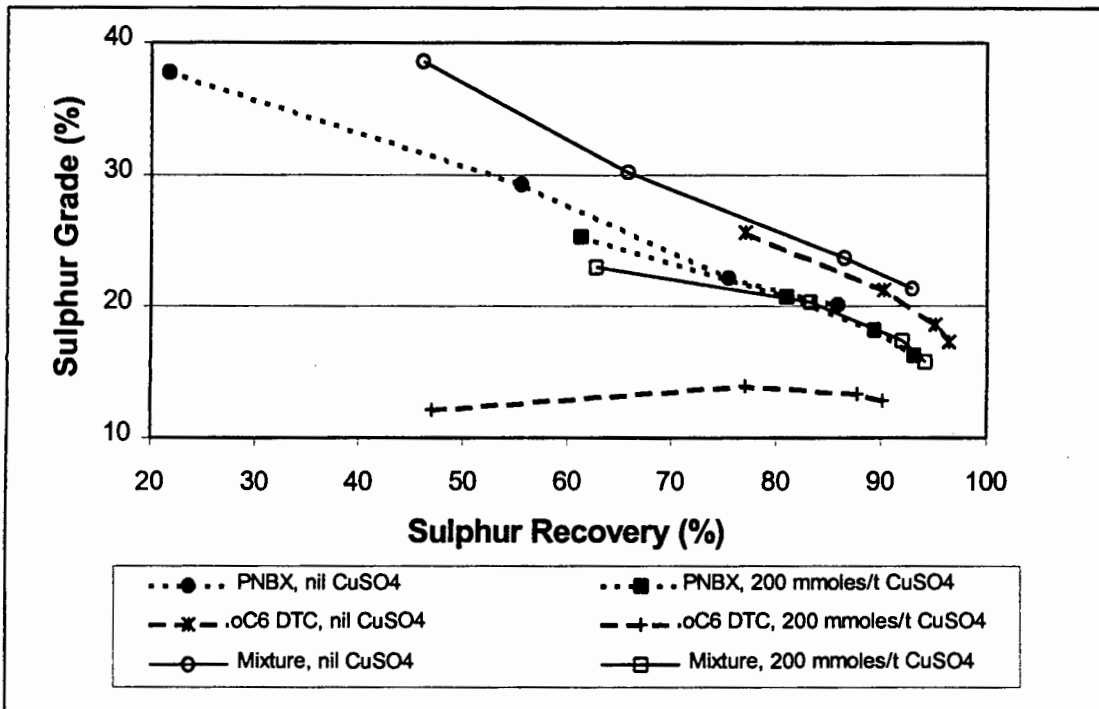


Figure 5.1: Sulphur grade vs sulphur recovery obtained using PNBX, cyclohexyl DTC and the 90:10 PNBX:cyclohexyl DTC mixture at 310 mmoles/t with nil and 200 mmoles/t copper sulphate addition (Buffelsfontein Ore)

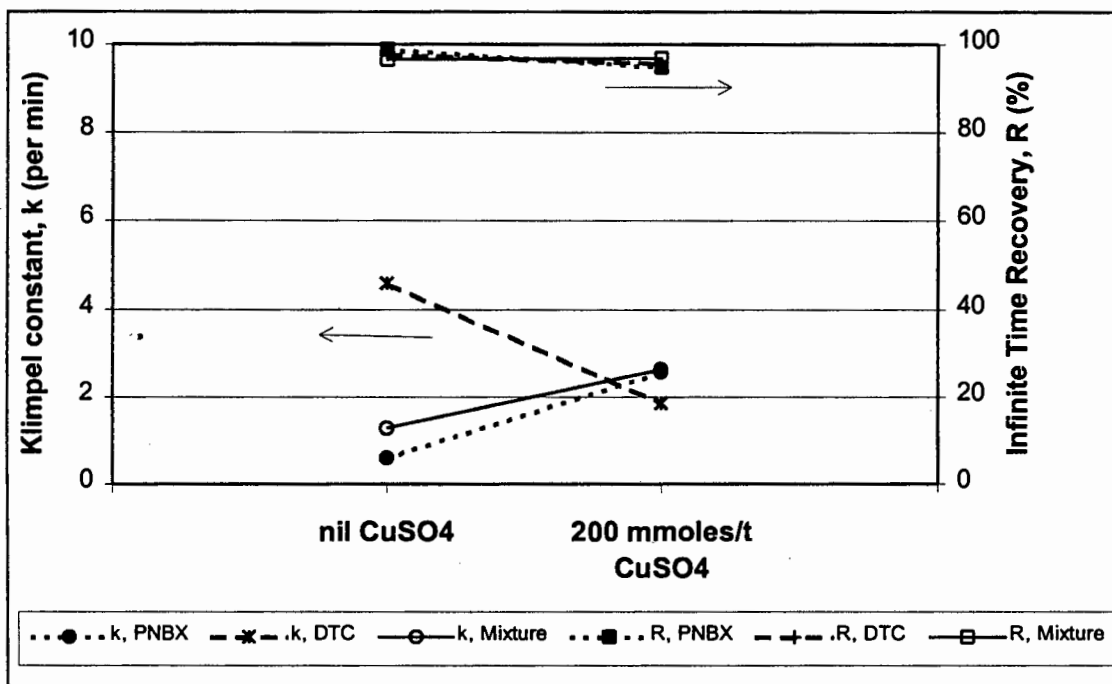


Figure 5.2: Constants, k and R, from Klimpel obtained using PNBX, cyclohexyl DTC and the 90:10 mixture of PNBX and cyclohexyl DTC at 310 mmoles/t with nil and 200 mmoles/t copper sulphate addition (Buffelsfontein Ore)

Table 5.1 Summary of results to show the effect of copper sulphate addition with a collector dosage of 310 mmoles/t (Buffelsfontein ore) (cf. Table 2.6)

Collector Type	Test Number	CuSO ₄ Dosage (mmoles/t)	Klimpel Model Constants		Time	Mass Recovery (%)	Water Recovery (g)	Sulphur Recovery (%)				Sulphur Grade (%)			
			(k) (min ⁻¹)	(R) (%)				Overall	<25 µm	25x75 µm	>75 µm	Overall	<25 µm	25x75 µm	>75 µm
oC6 DTC	B-10	nil	4.63	97.8	1 min	2.45	125.7	77.1	68.2	78.7	74.7	25.6	8.7	36.9	47.2
					13 min	4.62	302.0	96.4	99.5	98.1	92.3	17.3	6.6	29.6	33.2
oC6 DTC	B-18	200	1.70	94.7	1 min	2.85	208.1	21.9	54.3	46.6	31.4	11.3	4.8	26.5	36.7
					13 min	5.17	385.1	90.1	87.8	83.2	98.7	12.8	5.1	26.2	29.0
PNBX	B-11	nil	0.60	98.9	1 min	4.14	3.7	21.7	17.4	17.0	17.8	37.8	15.6	40.4	45.8
					13 min	3.08	114.2	85.9	79.3	69.2	92.8	20.1	7.7	22.5	38.8
PNBX	B-19	200	2.56	94.8	1 min	1.76	5.7	61.3	51.8	65.5	65.0	25.3	7.9	31.2	48.2
					13 min	4.15	199.9	93.1	89.5	94.3	93.9	16.3	6.3	24.4	34.2
Mixture ⁽¹⁾	B-13	nil	1.27	96.7	1 min	0.90	8.3	46.1	32.4	42.9	38.8	38.6	18.9	47.3	51.7
					13 min	3.28	131.5	93.0	91.2	95.0	92.2	21.4	8.5	30.4	42.2
Mixture	B-20	200	2.61	96.8	1 min	2.14	96.5	62.8	39.8	39.2	76.8	23.0	7.6	32.1	48.8
					13 min	4.66	261.9	94.2	82.6	83.9	99.8	15.8	5.6	24.1	36.5
Std Dev			1.2	0.9	1 min	0.17	15.94	3.41	6.30	3.14	7.91	2.18	1.82	2.01	1.70
					13 min	0.23	32.40	0.86	3.46	2.02	4.08	0.78	0.77	1.62	2.68

(1) Indicates 90:10 mole ratio mixture of PNBX:cyclohexyl DTC

The infinite time recoveries were reduced with the addition of copper sulphate except for the mixture, which was hardly affected.

5.2.1.3 SULPHUR RECOVERY BY SIZE

Figure 5.3 shows that the initial sulphur recovery of all size fractions is highest with the use of cyclohexyl DTC with no copper sulphate addition and lowest for PNBX with no copper sulphate addition. In the cases of PNBX and the 90:10 mole ratio mixture of cyclohexyl DTC and PNBX, copper sulphate addition increased the initial coarse sulphur recovery more than the other size fractions. The increase in final sulphur recovery was much less. In the case of cyclohexyl DTC, copper sulphate addition reduced the initial coarse sulphur recovery more than the other size fractions. The difference in the final sulphur recoveries by size obtained for the different collectors was lower than the difference after 1 min.

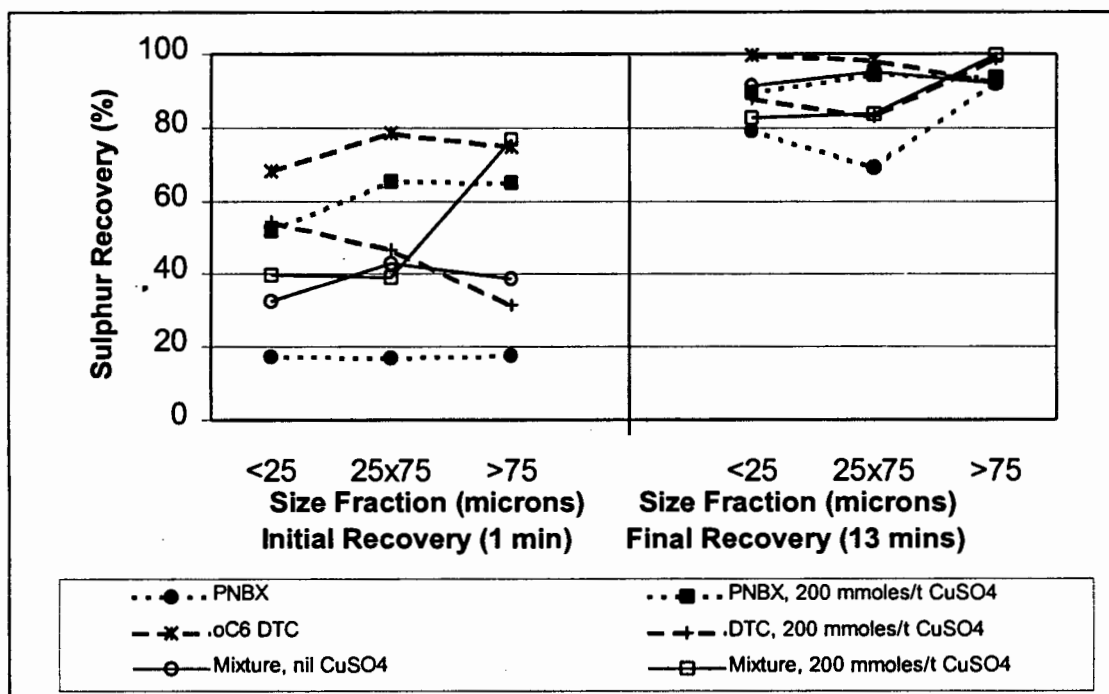


Figure 5.3: Sulphur recovery by size obtained using PNBX, cyclohexyl DTC and the 90:10 PNBX:cyclohexyl DTC mixture at 310 mmoles/t with nil and 200 mmoles/t copper sulphate addition (Buffelsfontein Ore)

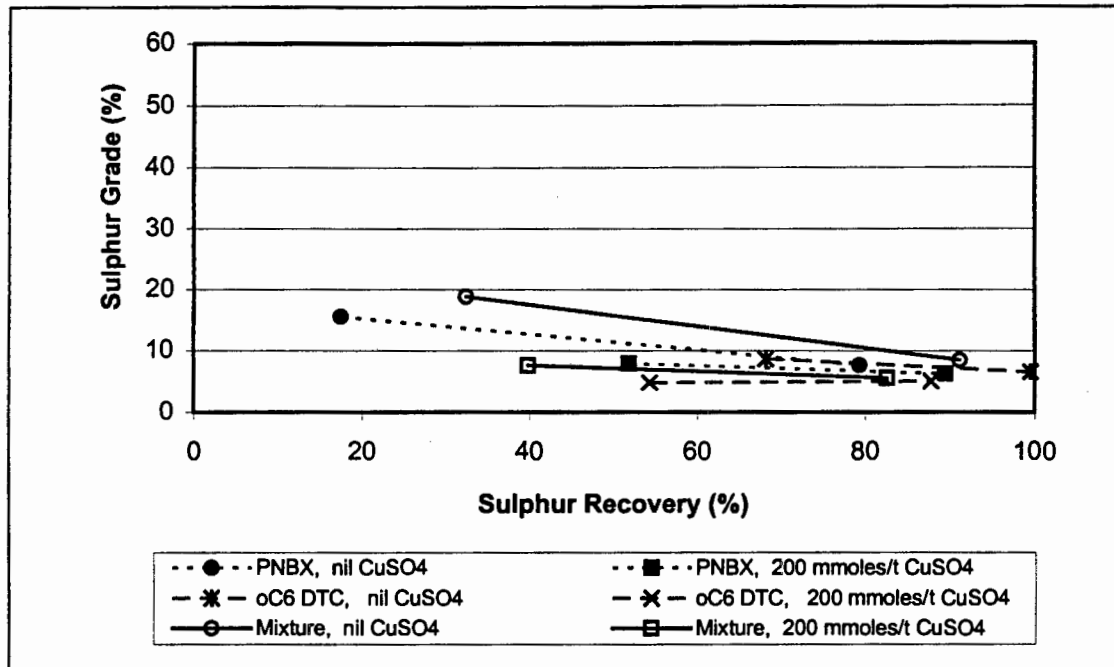


Figure 5.4: Sulphur grade vs sulphur recovery for < 25 μm size fraction obtained using PNBX, cyclohexyl DTC and the 90:10 PNBX:cyclohexyl DTC mixture at 310 mmoles/t with nil and 200 mmoles/t copper sulphate addition (Buffelsfontein Ore)

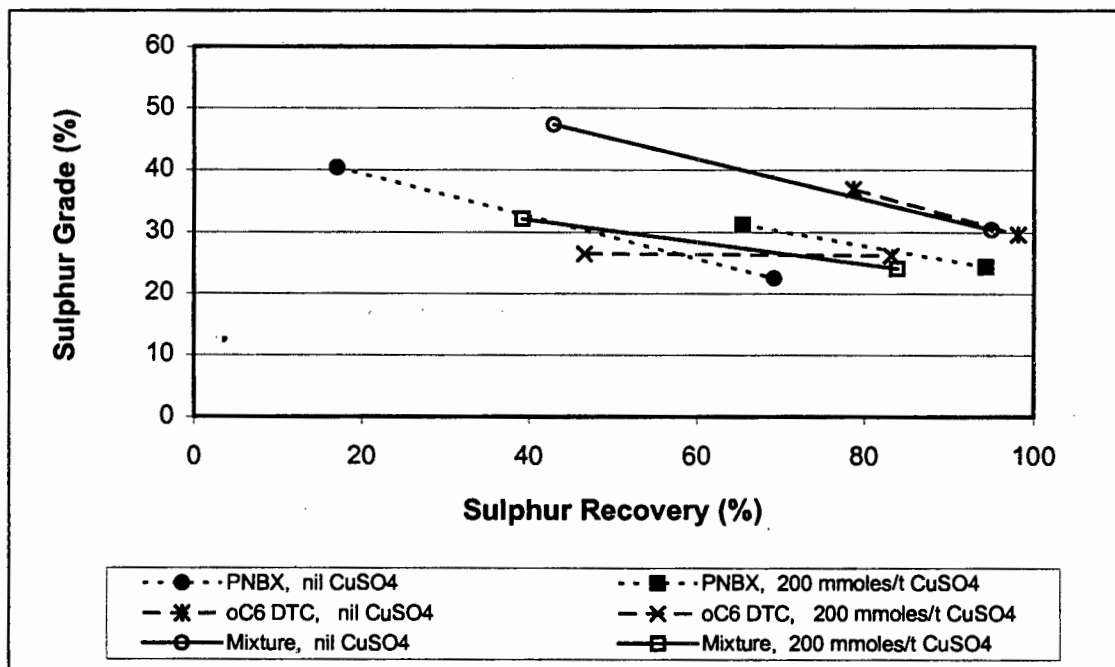


Figure 5.5: Sulphur grade vs sulphur recovery for 25 x 75 μm size fraction obtained using PNBX, cyclohexyl DTC and the 90:10 PNBX:cyclohexyl DTC mixture at 310 mmoles/t with nil and 200 mmoles/t copper sulphate addition (Buffelsfontein Ore)

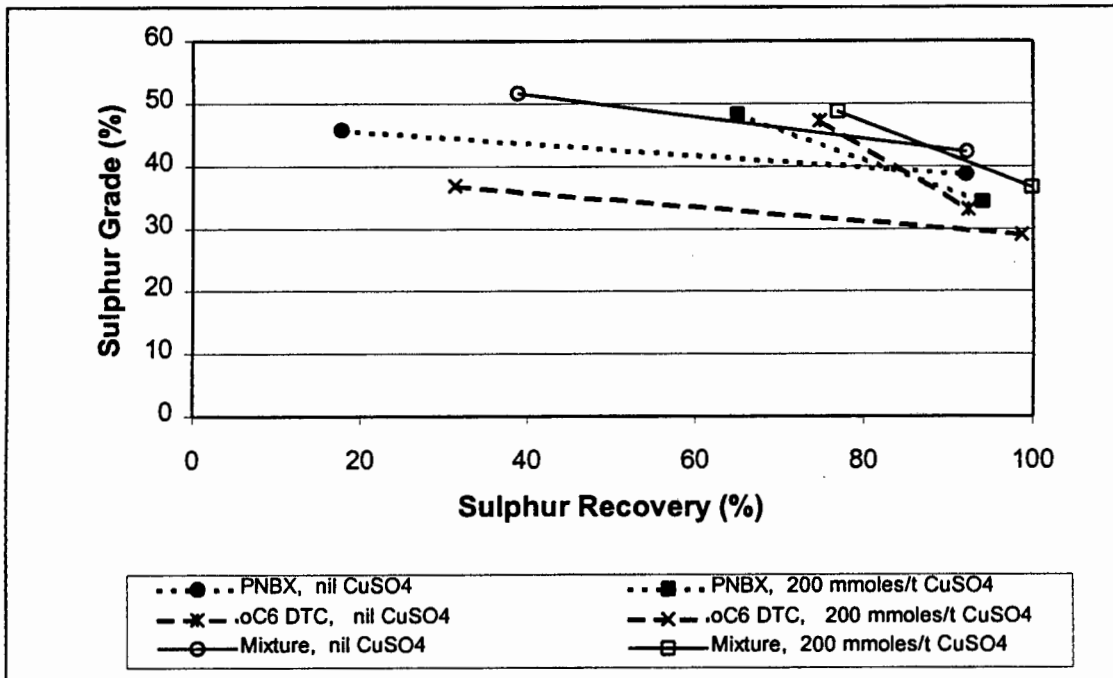


Figure 5.6: Sulphur grade vs sulphur recovery for > 75 μm size fraction obtained using PNBX, cyclohexyl DTC and the 90:10 PNBX:cyclohexyl DTC mixture at 310 mmoles/t with nil and 200 mmoles/t copper sulphate addition (Buffelsfontein Ore)

The increase in coarse particle recovery obtained with the addition of copper sulphate was also reported by Allison et al [1982]. Figures 5.4, 5.5 and 5.6 show the relationship between sulphur grade and sulphur recovery by size for the < 25 μm , 25 x 75 μm and > 75 μm size ranges respectively.

With the exception of the initial grade of the >75 μm material obtained with PNBX and the mixture, all grades were reduced by the addition of copper sulphate. The grade of the < 25 μm material was particularly low. There was less difference in the sulphur grade vs recovery curves for the < 25 μm size fraction for the different collectors, than for the other size fractions.

For all size fractions, the 90:10 mixture of PNBX and cyclohexyl DTC, without copper sulphate addition gave the highest overall sulphur grade vs recovery curve, although in the case of the >75 μm fraction, the sulphur grades were higher in the absence of copper sulphate addition and the sulphur recoveries higher with the addition of copper sulphate. The decreased grades in all size

fractions with the addition of copper sulphate suggests that mechanisms other than entrainment may be responsible for the increased recovery of gangue with copper sulphate addition. Possible mechanisms for the increased gangue recovery include the activation of gangue by the copper ions [Nagaraj and Brinen, 1995].

5.2.1.4 WATER RECOVERY

Figure 5.7 shows that, for all collector types, the water recovery was considerably increased by adding copper sulphate. The water recovery was highest with cyclohexyl DTC, and this was further increased with copper sulphate addition. The increase in water recovery did not result in an increase in fines recovery (cf. Figure 5.3), but it did result in a decrease in the grade of fines recovered (cf. Figure 5.4). This indicated that entrainment of fine gangue increased with copper sulphate addition. Copper sulphate addition did not increase the mass recovery to the same extent as the water recovery (cf. Table 5.1) and this produced a froth of lower solids density.

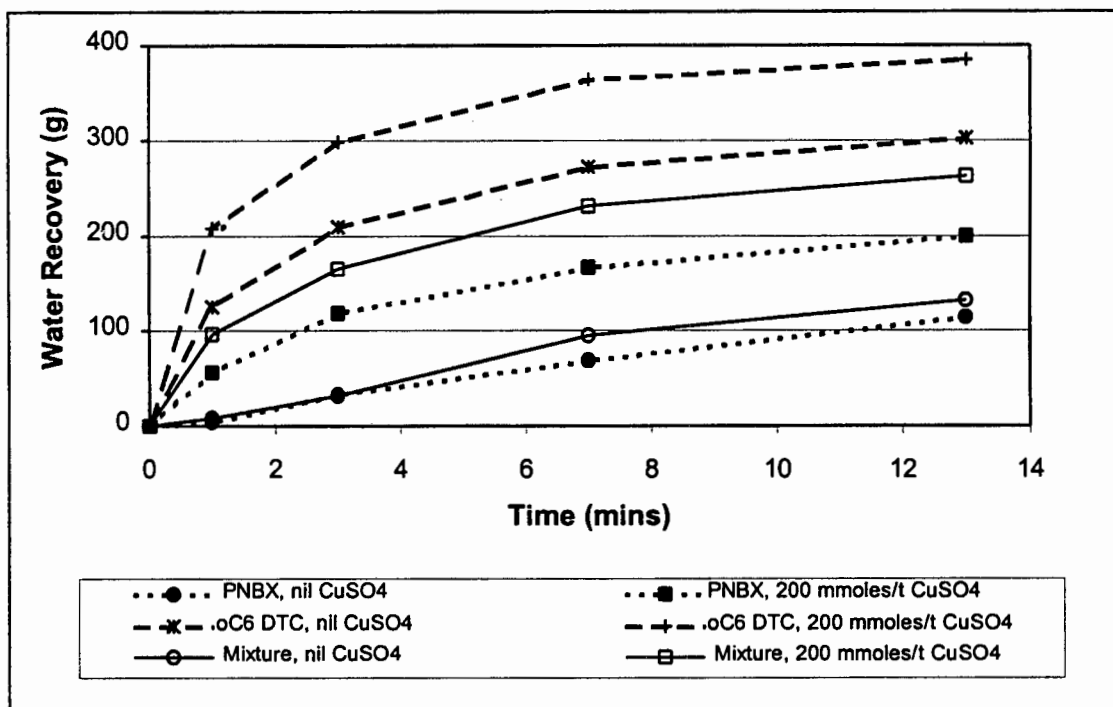


Figure 5.7: Water recovery vs time obtained using PNBX, cyclohexyl DTC and the 90:10 PNBX:cyclohexyl DTC mixture at 310 mmoles/t and nil and 200 mmoles/t copper sulphate addition (Buffelsfontein Ore)

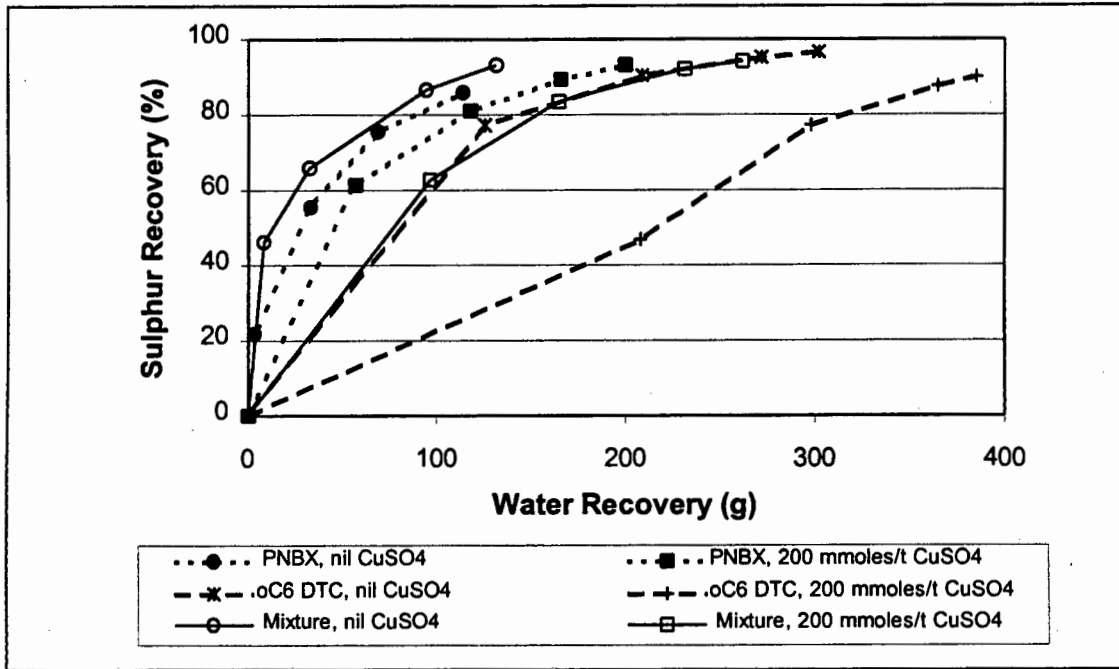


Figure 5.8: Sulphur recovery vs water recovery obtained using PNBX, cyclohexyl DTC and the 90:10 PNBX:cyclohexyl DTC mixture at 310 mmoles/t and nil and 200 mmoles/t copper sulphate addition (Buffelsfontein Ore)

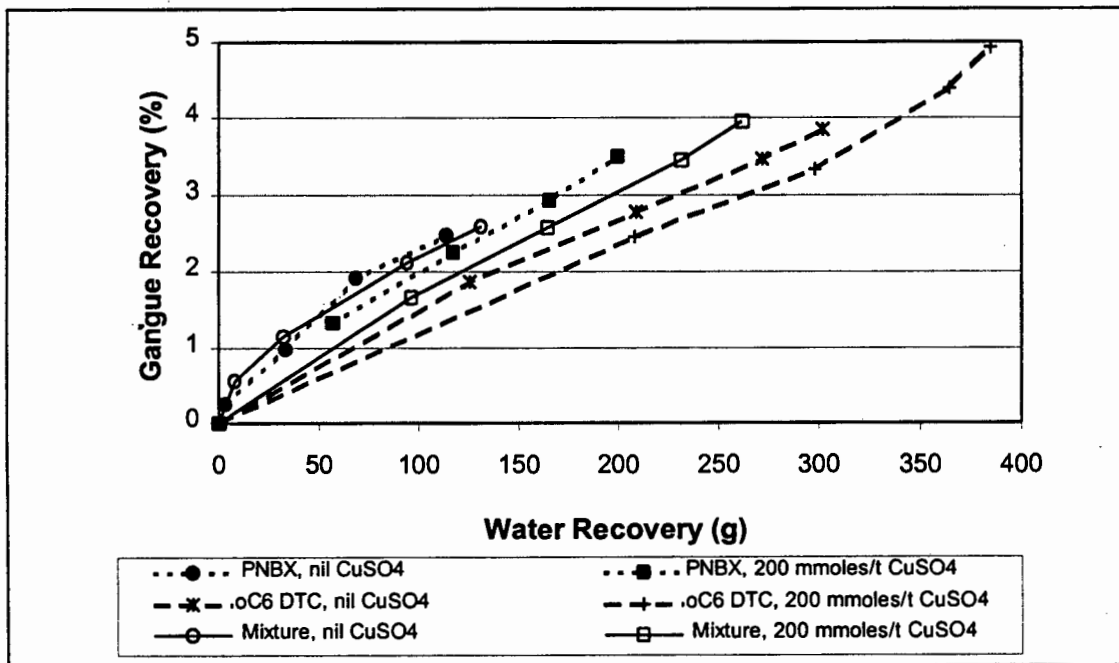


Figure 5.9: Gangue recovery vs water recovery obtained using PNBX, cyclohexyl DTC and the 90:10 PNBX:cyclohexyl DTC mixture at 310 mmoles/t and nil and 200 mmoles/t copper sulphate addition (Buffelsfontein Ore)

The increase in water recovery in the case of copper sulphate addition was accompanied by a change in surface froth structure (cf. Sec. 5.2.1.5).

Figures 5.8 and 5.9 show the relationship between sulphur and gangue recovery to water recovery respectively. For all collectors tested, and especially in the case of cyclohexyl DTC, the sulphur recovery per mass of water was higher in the absence of copper sulphate, although the rate of sulphur recovery was higher with copper sulphate addition. This indicated that the increased water recovery resulted in an increase in the rate of sulphur recovery, but with decreased efficiency of sulphur recovery. The overall gangue recoveries were higher with the addition of copper sulphate which accounts for the decrease in sulphur grade with copper sulphate addition. The relationship of gangue recovery to water recovery was slightly lower for all collectors with the addition of copper sulphate but this may not be significant due to the low overall gangue recovery. The gangue recovery increases linearly with water recovery and did not asymptote as in the case of the sulphur recovery.

5.2.1.5 IMAGE ANALYSIS OF FROTH SURFACE

Digital image analysis was used to analyse the effect of copper sulphate addition and collector type on the average bubble size, froth stability and mobility of the surface froth (cf. Sec. 2.2.2.3).

Figure 5.10 shows the change in average bubble size of surface froth with time. It can be seen that for the first 5 mins the effect of copper sulphate addition on bubble size is greater than the effect of collector type and smaller bubbles are observed with copper sulphate addition, irrespective of collector type. After 5 mins, the collector type becomes the dominant effect on the bubble size of the surface froth and the largest bubbles were associated with tests using the mixture of PNBX and cyclohexyl DTC rather than pure PNBX.

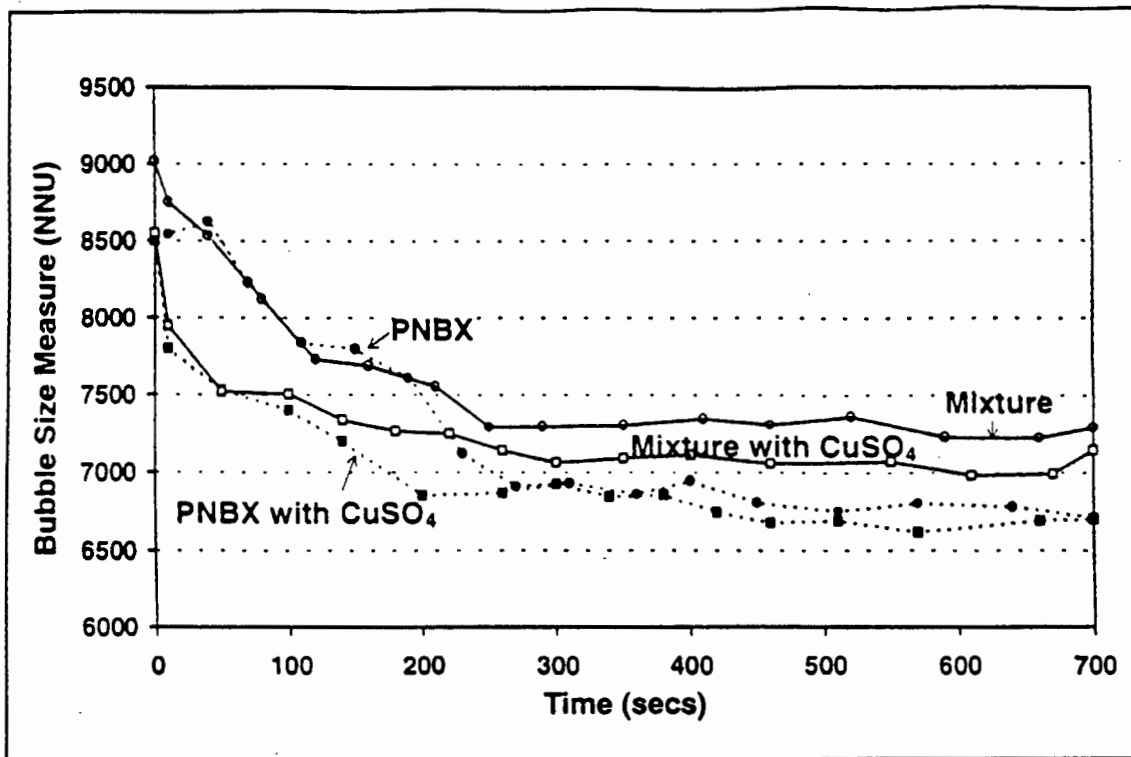


Figure 5.10: The change in average bubble size of surface froth with time for tests using PNBX and the 90:10 PNBX:cyclohexyl DTC mixture at 310 mmolles/t and nil and 200 mmolles/t copper sulphate addition (Buffelsfontein Ore)

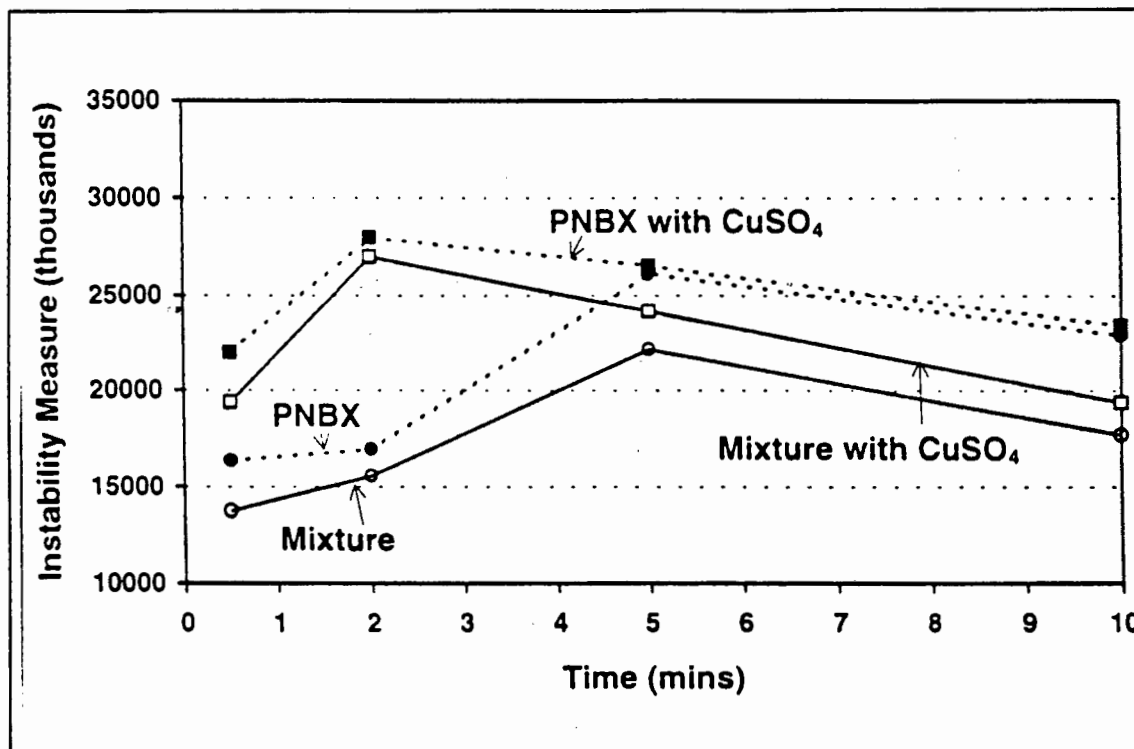


Figure 5.11: Instability feature measure for tests using PNBX, cyclohexyl DTC and the 90:10 PNBX:cyclohexyl DTC mixture at 310 mmolles/t and nil and 200 mmolles/t copper sulphate addition (Buffelsfontein Ore)

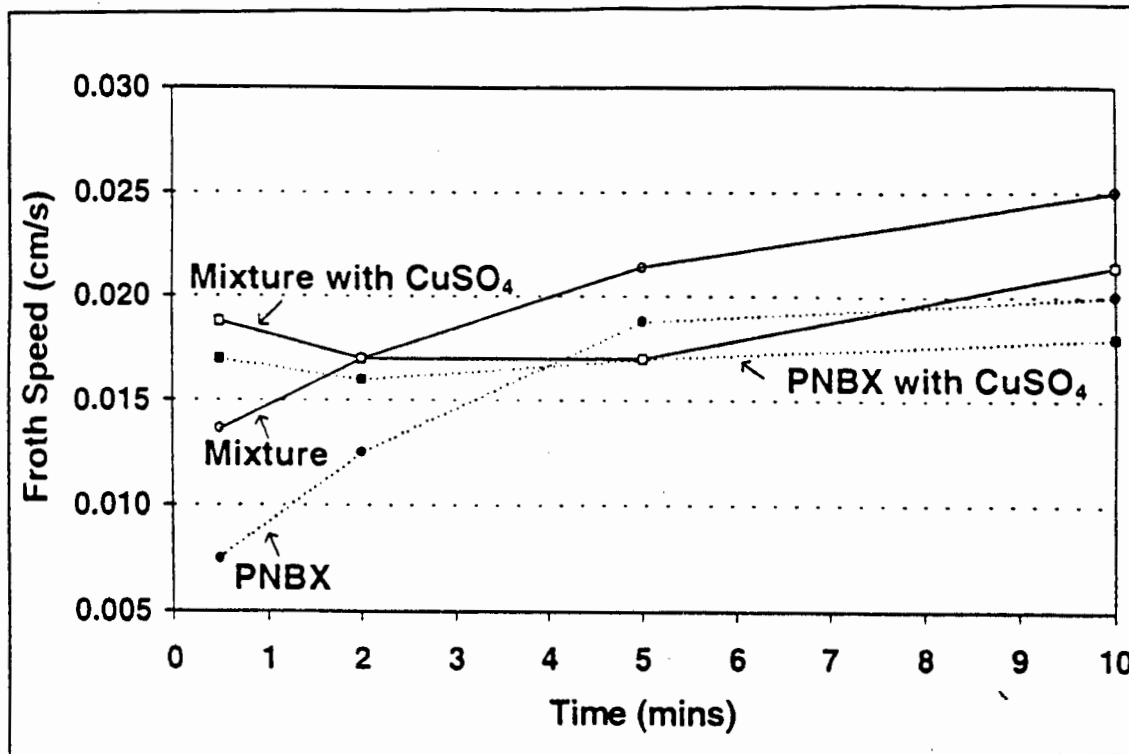


Figure 5.12: The froth speed of flotation tests using PNBX, cyclohexyl DTC and the 90:10 PNBX:cyclohexyl DTC mixture at 310 mmoles/t and nil and 200 mmoles/t copper sulphate addition (Buffelsfontein Ore)

The froth stability, as measured by the rate of change of froth structure, is shown in Figure 5.11. Again, for the first five minutes, copper sulphate addition was the overriding influence, and the surface froth was less stable with copper sulphate addition for both the pure PNBX and for the mixture of PNBX and cyclohexyl DTC. After 5 mins the most stable froths were those obtained with the mixture, irrespective of copper sulphate addition. In the case of no copper sulphate addition the froth surface was least stable after 5 mins whereas when copper sulphate was added the stability improved after 2 mins.

Figure 5.12 shows froth mobility as represented by the froth speed. In the first 2 mins the highest mobility was observed in the tests with copper sulphate addition with that of pure PNBX being much lower than the others. This trend changed after 5 mins with the mixture of PNBX and cyclohexyl DTC in the absence of copper sulphate addition producing the fastest moving surface froth.

The analysis of the surface froth in these tests showed that both the collector type and addition of copper sulphate had a strong effect on the surface froth structure. It must be noted though that these were batch flotation tests and the initial froth characteristics were during the time before the operation at steady state. In a plant environment, these differences may not be observed due to the continuous operation at steady state. The best mineralogical results were obtained with test B-13, obtained using the 90:10 mole ratio mixture of PNBX and cyclohexyl DTC without copper sulphate addition (cf. Figure 5.1) and this correlated to the froth structure that had the largest froth bubble size, the highest stability and the greatest mobility.

5.2.1.6 STATISTICAL ANALYSIS

Table 5.2 shows the statistical analysis of the results obtained using the PNBX:cyclohexyl DTC mixture and PNBX with copper sulphate addition of nil and 200 mmol/t (cf. Figure 5.1).

Table 5.2 is split into four parts for ease of interpretation. Table 5.2.1 shows the different responses (i.e. rate, recovery etc.) extracted from Table 5.1. Table 5.2.2 shows the percentage change in the different responses resulting from the changes in parameter levels indicated. The standard deviation (σ), calculated from the reproducibility tests is also shown (cf. Table 2.6). The residual error or variance (σ^2), is obtained from the standard deviation. Table 5.2.3 shows the 'F' factors obtained by comparing the effect to the variance. Table 5.2.4 shows the significance of the 'F' values obtained from standard statistical tables. Note that 8 reproducibility tests were used so the degrees of freedom was 7. A significance of over 95% is considered high enough on which to make a decision. As shown on the table $F_{95,1,7} = 5.59$ which is the 'F' factor for 95% confidence. All effects which obtained a 'F' factor above this level are termed significant. In Table 5.2.4, (***) denotes a highly significant effect of over 99%, (**) denotes a significant effect of between 95% and 99%,

(*) denotes a slightly significant effect of between 90% and 95% and (~) denotes no significant difference.

Table 5.2 and Table 2.7 (Sec 2.3.1.4.6) both assess the effect of changing collector type from PNBX to the 90:10 mixture as the first parameter. The results are similar, but not identical, largely due to the confounding nature of the copper sulphate addition. In both cases the initial and final recoveries were increased with the use of the mixture in place of pure PNBX. The increase in water recovery obtained in the case of the mixture was more significant in the case of the tests with copper sulphate addition, viz. 95 x 97.5% from Table 5.2.4 vs 90 x 95% from Table 2.7.4 and the increase in mass pull was less significant, viz. < 90% from Table 5.2.4 vs 95 x 97.5 % from Table 2.7.4.

The effect of copper sulphate addition on flotation performance was much more significant than the effect of collector type, as seen by the larger 'F' factors in Table 5.2.3. The increase on initial and final grade was highly significant, but this was at an equally highly significant decrease in grade. This resulted in the overall performance being better without copper sulphate addition, despite these increases in recoveries and grades. The effect on rate of recovery was not significant due to the high standard deviation (cf. Sec. 2.3.1.16).

The interaction between collector type and copper sulphate addition was also highly significant for sulphur recovery (initial and final) and to a lesser extent for water recovery. This was due to the copper sulphate addition having a larger effect on the recoveries obtained with PNBX than on those obtained with the 90:10 mixture.

Table 5.2: Statistical evaluation of the effects of copper sulphate addition and collector type on flotation performance (Buffelsfontein Ore)

5.2.1 Results extracted from Table 5.1

Collector Type	Test Number	CuSO ₄ Dosage (mmoles/t)	Klimpel Model Constants		Mass Recovery (%)	Water Recovery (g)	Sulphur Recovery		Sulphur Grade	
			(k) (min ⁻¹)	(R) (%)			1 min (%)	13 min (%)	1 min (%)	13 min (%)
PNBX	B-11	nil	0.60	98.9	3.08	114.2	21.7	85.9	37.8	20.1
PNBX	B-19	200	2.56	94.8	4.15	199.9	61.3	93.1	25.3	16.9
Mixture ⁽¹⁾	B-13	nil	1.27	96.7	3.28	131.5	46.1	93.0	38.6	21.4
Mixture	B-20	200	2.61	96.8	4.66	261.9	62.8	94.2	23.0	15.8

5.2.2 Percentage change in response (Effect) due to changing parameter level

SINGLE EFFECTS										
Collector Type (PNBX vs Mixture)	0.36	-0.1	0.36	39.7	13.0	4.1	-0.8	0.1		
CuSO ₄ addition (nil vs 200 mmoles/t)	1.65	-2.0	1.23	108.1	28.2	4.2	-14.1	-4.4		
INTERACTION										
Collector Type / CuSO ₄ Addition	-0.31	2.1	0.16	22.4	-11.5	-3.0	-1.6	-1.2		
Std Dev	2.58	0.9	0.22	32.4	3.2	0.9	2.2	0.8		

5.2.3 'F' Factors from ANOVA (NOTE: F_{99,1,7} = 12.5; F_{95,1,7} = 5.59; F_{90,1,7} = 3.59)

SINGLE EFFECTS										
Collector Type (PNBX vs Mixture)	0.10	0.0	2.30	8.1	35.6	22.7	0.1	0.0		
CuSO ₄ addition (nil vs 200 mmoles/t)	1.90	4.4	27.60	60.3	168.3	23.9	41.9	31.8		
INTERACTION										
Collector Type / CuSO ₄ Addition	0.01	4.9	0.40	2.6	27.8	12.2	0.5	2.4		

5.2.4 Significance of effect (NOTE: *** = > 99%, ** = 95 x 99%, * = 90 x 95%, ~ = < 90%)

SINGLE EFFECTS										
Collector Type (PNBX vs Mixture)	~	~	~	**	***	***	~	~		
CuSO ₄ addition (nil vs 200 mmoles/t)	~	*	***	***	***	***	***	***		
INTERACTION										
Collector Type / CuSO ₄ Addition	~	*	~	~	***	**	~	~		

(1) Indicates 90:10 mole ratio mixture of PNBX:cyclohexyl DTC

5.2.2 INVESTIGATION WITH ST HELENA ORE

These tests compared the effect of 200 mmoles/t of copper sulphate addition on the flotation performance obtained with PNBX and on that with the 90:10 mole ratio mixture of PNBX and cyclohexyl DTC at a collector dosage of 400 mmoles/t. The effect of the point of copper sulphate addition was also tested. The copper sulphate was added before the collector addition, between the addition of cyclohexyl DTC and PNBX and after both collectors. In all cases the cyclohexyl DTC was added before the PNBX. Table 5.3 shows the results obtained using pure PNBX to those obtained using the mixture of PNBX and cyclohexyl DTC. The detailed results are shown in Appendix 5B.

Table 5.3: Summary of results with varying the dosage and point of 200 mmoles/t copper sulphate addition to the reagent suite (St Helena Ore)

Collector Type	Test Number	CuSO ₄ Dosage (mmoles/t)	Klimpel Model Constants		Time	Mass Recovery (%)	Water Recovery (g)	Sulphur Recovery (%)	Sulphur Grade (%)
			(k)	(R)					
			(min ⁻¹)	(%)					
PNBX	SH-5	nil	2.68	91.0	1 min	2.23	40.3	59.1	33.1
					13 mins	5.70	165.0	88.2	19.3
PNBX	SH-10	200	3.64	89.1	1 min	2.63	60.6	61.5	32.8
					13 mins	6.19	197.2	88.4	20.0
Mixture ⁽¹⁾	SH-8	nil	3.02	91.6	1 min	2.49	45.3	62.5	32.9
					13 mins	5.79	167.8	89.1	20.2
Mixture	SH-11	200 ⁽²⁾	3.56	91.9	1 min	2.83	69.8	67.0	30.9
					13 mins	6.71	245.2	90.5	17.6
Mixture	SH-12	200 ⁽³⁾	3.68	91.8	1 min	2.93	77.9	67.7	29.9
					13 mins	6.93	269.7	90.6	16.9
Mixture	SH-13	200 ⁽⁴⁾	2.92	94.6	1 min	2.74	53.0	63.4	31.0
					13 mins	6.88	183.3	91.5	17.8

(1) Indicates 90:10 mole ratio mixture of PNBX:cyclohexyl DTC

(2) CuSO₄ addition before collector addition (First)

(3) CuSO₄ addition between PNBX and cyclohexyl DTC addition (Second)

(4) CuSO₄ addition after collector addition (Third)

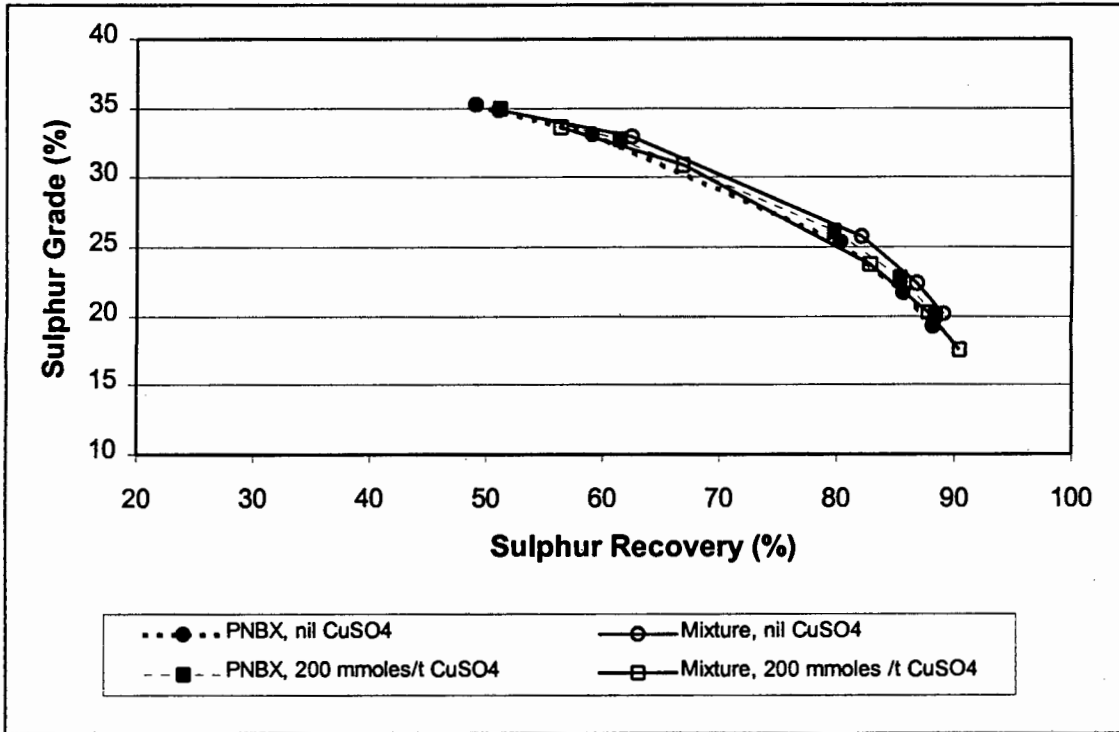


Figure 5.13: Sulphur grade vs sulphur recovery obtained using 400 moles/t PNBX and a 90:10 mole ratio mixture of PNBX and cyclohexyl DTC with copper sulphate addition of nil and 200 mmoles/t (St Helena Ore)

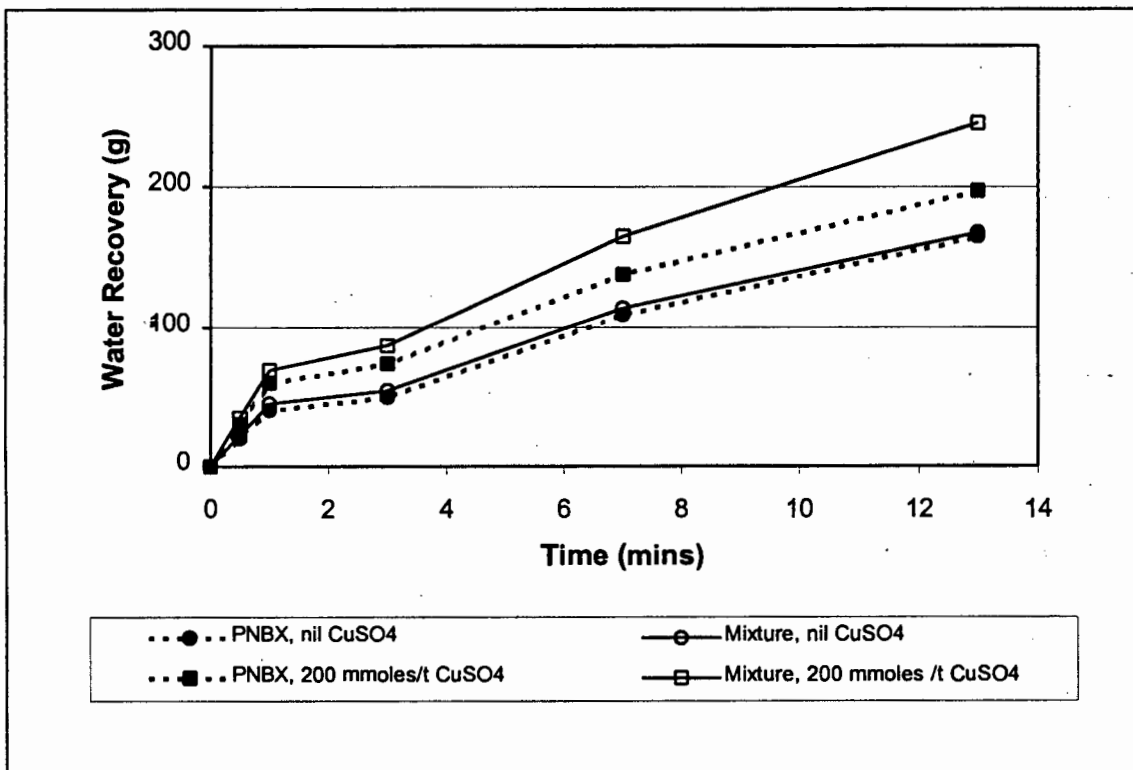


Figure 5.14: Water recovery vs time obtained using 400 moles/t PNBX and a 90:10 mole ratio mixture of PNBX and cyclohexyl DTC with copper sulphate addition of nil and 200 mmoles/t (St Helena Ore)

Figure 5.13 shows that although the difference in the curves is not significant, the highest sulphur grade vs recovery relationship is obtained with the mixture of collectors and no copper sulphate addition. The addition of copper sulphate increased sulphur recovery but at a sulphur grade penalty shown in Figure 5.13.

Figure 5.14 shows the effect of copper sulphate addition on water recovery. For both PNBX and the mixture of PNBX and cyclohexyl DTC, the water recovery was increased by copper sulphate addition. The high water recoveries with copper sulphate addition account for the grade penalty.

Table 5.4 shows the statistical assessment of the effect on flotation performance of adding the cyclohexyl DTC to the PNBX collector and also of the copper sulphate addition to the reagent suite. It can be seen that the results obtained with St Helena ore were much less significant than those found with Buffelsfontein ore, which was the same finding as that obtained in the tests with no copper sulphate addition (cf. Table 2.9, Sec. 2.3.2.2). The increase in water recovery obtained with the addition of copper sulphate was the only significant result. This was accompanied by a slightly significant decrease in the initial sulphur grade for both the use of the mixture and for the addition of copper sulphate.

Figures 5.15 and 5.16 show the effect of adding the copper sulphate to the PNBX:cyclohexyl DTC mixture at different points of the test. The copper sulphate was added before the collector addition, between the addition of cyclohexyl DTC and PNBX and after both collectors. In all cases the cyclohexyl DTC was added before the PNBX. Table 5.3 shows these results.

Figure 5.15 shows that the point of copper sulphate addition caused little difference in the sulphur grade vs recovery relationship. Figure 5.16 showed that there was a lower water recovery when copper sulphate was added after the reagents but this had little effect on performance.

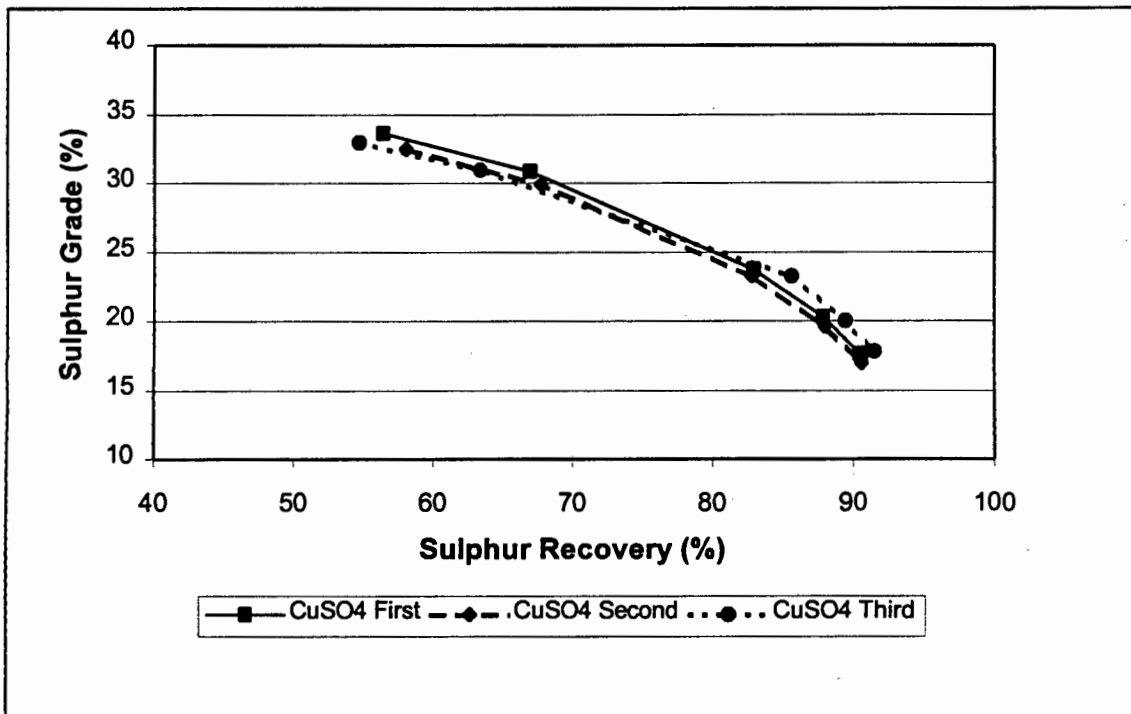


Figure 5.15: Sulphur grade vs sulphur recovery for different points of 200 mmolles/t copper sulphate addition on the performance of the 90:10 mole ratio mixture of PNBX and cyclohexyl DTC (St Helena Ore)

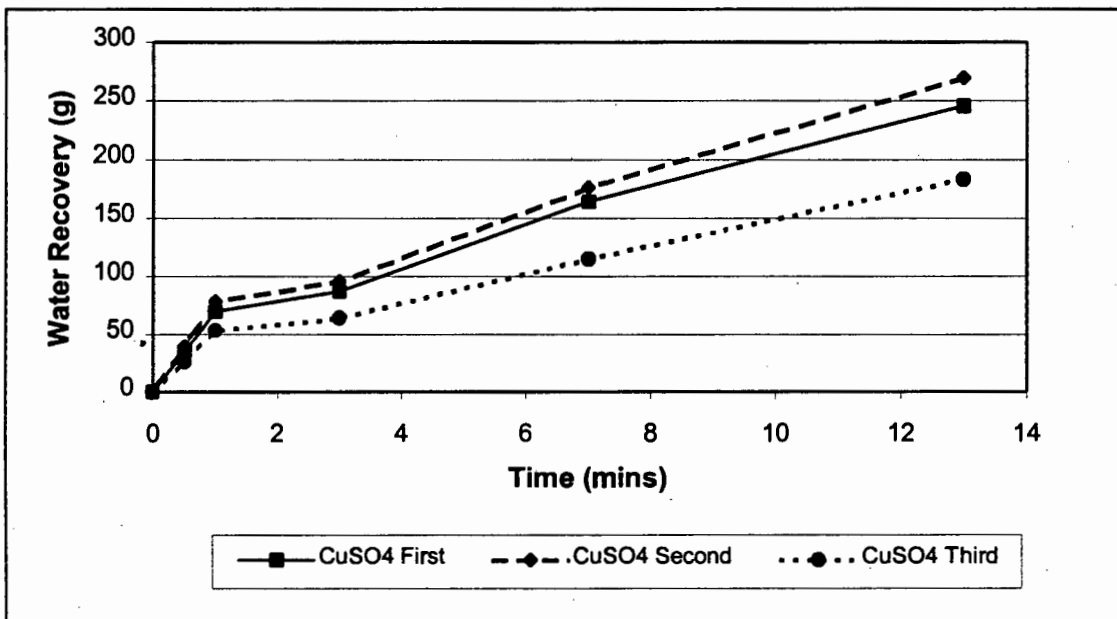


Figure 5.16: Water recovery vs time for different points of 200 mmolles/t copper sulphate addition on the performance of the 90:10 mole ratio mixture of PNBX and cyclohexyl DTC (St Helena Ore)

Table 5.4: Statistical evaluation of the effects of copper sulphate addition and collector type on flotation performance (St Helena Ore)

5.4.1 Results extracted from Table 5.3

Collector Type	Test Number	CuSO ₄ Dosage (mmoles/t)	Klimpel Model Constants		Mass Recovery (%)	Water Recovery (g)	Sulphur Recovery		Sulphur Grade	
			(k) (min ⁻¹)	(R) (%)			1 min (%)	13 min (%)	1 min (%)	13 min (%)
PNBX	SH-5	nil	2.68	91.0	5.70	165.0	59.1	88.2	33.1	19.3
PNBX	SH-10	200	2.97	90.0	6.19	197.2	61.5	88.4	32.8	20.0
Mixture ⁽¹⁾	SH-8	nil	3.02	91.6	5.80	167.8	62.5	89.1	32.9	20.2
Mixture	SH-11	200	3.56	91.9	6.71	245.2	67.0	90.5	30.9	17.6

5.4.2 Percentage change in response (Effect) due to changing parameter level

SINGLE EFFECTS										
Collector Type (PNBX vs Mixture)	0.47	1.3	0.31	25.4	19.5	1.5	-1.0	-0.8		
CuSO ₄ addition (nil vs 200 mmoles/t)	0.42	0.4	0.70	54.8	11.9	0.8	-1.2	-0.9		
INTERACTION										
Collector Type / CuSO ₄ Addition	0.13	0.7	0.21	22.6	1.1	1.2	-0.8	-1.7		
Std Dev	0.70	2.23	0.25	14.89	4.95	1.91	0.38	0.81		

5.4.3 'F' Factors from ANOVA (NOTE: F_{99,1,3} = 34.1; F_{95,1,3} = 10.1; F_{90,1,3} = 5.54)

SINGLE EFFECTS										
Collector Type (PNBX vs Mixture)	0.40	0.3	1.50	2.9	0.8	0.6	7.3	0.9		
CuSO ₄ addition (nil vs 200 mmoles/t)	0.40	0.0	7.70	13.6	0.5	0.2	9.6	1.3		
INTERACTION										
Collector Type / CuSO ₄ Addition	0.10	0.1	0.70	2.3	0.0	0.1	4.7	4.2		

5.4.4 Significance of effect (NOTE: *** => 99%, ** = 95 x 99%, * = 90 - 95 %, ~ = < 90%)

SINGLE EFFECTS										
Collector Type (PNBX vs Mixture)	~	~	~	~	~	~	*	~		
CuSO ₄ addition (nil vs 200 mmoles/t)	~	~	*	**	~	~	*	~		
INTERACTION										
Collector Type / CuSO ₄ Addition	~	~	~	~	~	~	~	~		

(1) Indicates 90:10 mole ratio mixture of PNBX:cyclohexyl DTC

St Helena ore was a residual material, and copper sulphate addition is reported to enhance the flotation of residual material by complexing with any remaining cyanide [Lloyd, 1981; Bothelho de Sousa and Ross, 1990;]. These tests did not show any significant enhancement of flotation performance due to copper sulphate addition. Any cyanide originally present on this residual ore would have decomposed via UV. However no analysis of cyanide levels was done.

5.3. THE EFFECT OF COPPER SULPHATE ADDITION ON BUBBLE LOADING

The aim of these tests was to use the technique described in Ch. 3 to evaluate the effect of copper sulphate addition on the bubble loading obtained with different collector types, viz. pure PNBX, cyclohexyl DTC and the 90:10 mole ratio mixture of PNBX and cyclohexyl DTC. The conditions set for the bubble loading tests were the same as those set for the batch flotation tests. The size fraction of the pyrite was 53 x 75 μm and the tests were done at pH = 4. The collector dosage was constant for all collectors at 1.4×10^{-2} mmoles / 2 g pyrite. The results are shown in Table 5.5 together with the results obtained without copper sulphate (cf. Sec. 3.3.3, Table 3.5).

The significance of the difference in bubble loading due to the effect of copper sulphate addition was evaluated using the standard deviation obtained from the reproducibility tests (cf. Table 3.2) to obtain the 'T' values. The increase in bubble loading obtained with the addition of copper sulphate to PNBX was not significant whereas the decrease in bubble loading obtained with the addition of copper sulphate to cyclohexyl DTC or the 90:10 mixture was highly significant. Figure 5.12 shows the effect of copper sulphate addition on the mass per bubble obtained using PNBX, cyclohexyl DTC and the 90:10 mixture of PNBX and cyclohexyl DTC.

Table 5.5: The effect of collector type on bubble loading by pyrite with a dosage of 1.4×10^{-2} mmoles collector / 2 g pyrite

Collector Type	Test Number	CuSO ₄ Dosage (mmoles/t)	Overall Mass Recovery (%)	Average Mass per Bubble (mg)	Significance of Difference due to Addition
PNBX	15	nil	35.5	0.237	< 90%
PNBX	18	200	42.0	0.280	
oC6 DTC	16	nil	49.0	0.327	> 99.5%
oC6 DTC	19	200	12.4	0.082	
Mixture(1)	17	nil	61.8	0.412	> 99.5%
Mixture	20	200	37.8	0.252	

(1) Indicates 90:10 mole ratio mixture of PNBX:cyclohexyl DTC

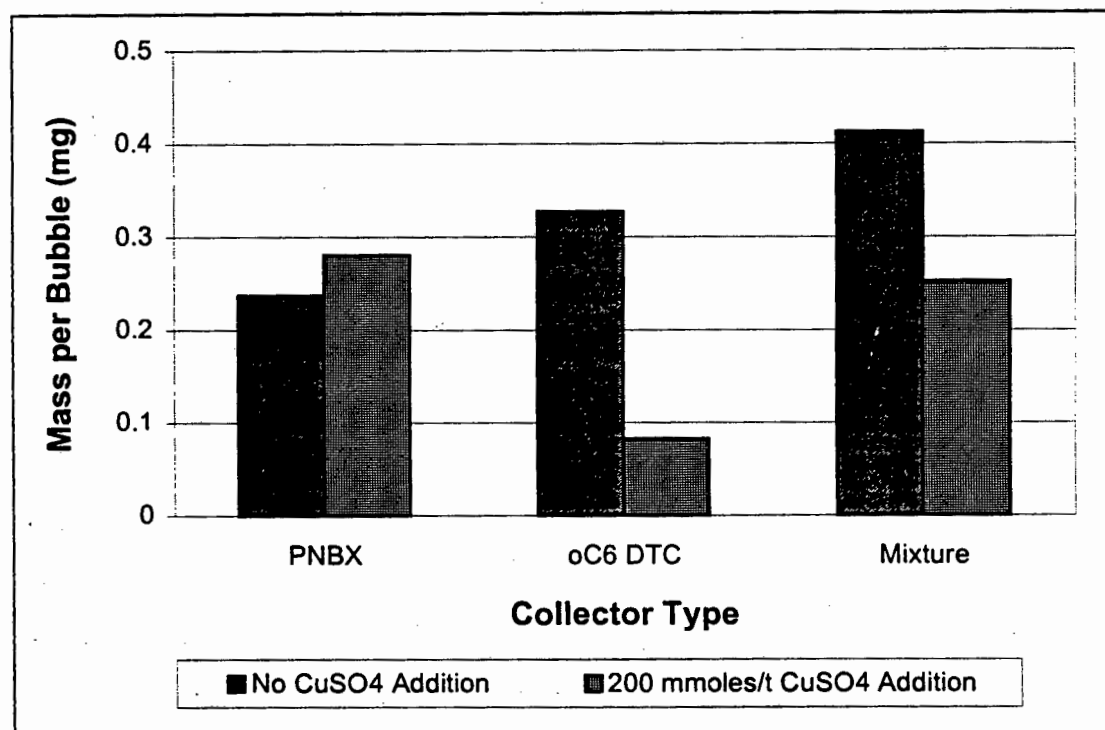


Figure 5.17: The effect of collector type on bubble loading by pyrite with a dosage of 1.4×10^{-2} mmoles collector / 2 g pyrite

The bubble loading tests showed that, at the conditions tested, viz. for pure pyrite at pH = 4, the addition of copper sulphate did not enhance the floatability of the thiol reagents tested. In the case of cyclohexyl DTC the decrease suggested the formation of a copper - dithiocarbamate complex that either formed on the mineral surface and was hydrophilic, or the complex was formed in solution and was not on the surface to create the necessary hydrophobicity. This is corroborated by Thorn [1962] who reported the use of the strong complexation properties of dithiocarbamates with heavy metals, particularly with copper in analytical chemistry. In the case of the PNBX:cyclohexyl DTC mixture, the decrease in bubble loading was greater than could be accounted for by the molar contribution of cyclohexyl DTC only and may indicate that in this case the PNBX was also complexed.

5.4 DISCUSSION

Although copper sulphate is added to the pulp in many South African pyrite flotation plants (cf. Sec. 1.4.4), the reason for its addition is ambiguous and the mechanisms of copper sulphate activation are still not clearly established. The aim of this chapter was to elucidate the role of copper sulphate in the flotation of pyrite at pH = 4 with and without mixtures of collectors.

As has been shown in Section 1.4.4, there are various mechanisms proposed for copper sulphate activation of pyrite. In some cases, copper sulphate is classified as a froth modifier [O' Connor et al 1988], in others it added to activate the mineral surface by the adsorption of copper ions on which the collector adsorption is enhanced. [Finkelstein and Allison, 1962; Leppinen, 1990; Leppinen et al, 1995; Nagaraj, 1995; Nagaraj and Brinen, 1995]. These were the two mechanisms considered as possibilities for these tests.

The third role, proposing the complexation of copper sulphate with any remaining cyanide on the residual ores [Lloyd, 1981; Bothelho de Sousa and Ross, 1990], was not investigated.

The fourth role proposed was that the increase the redox potential (ORP) of the pulp, caused by copper sulphate addition [Nicol, 1984], increased the oxidising environment favorable for the oxidation of the thiol collectors. The pulp potential was not measured for all the tests, although the tests with St Helena ore showed that the ORP of the pulp did increase with copper sulphate addition. The oxidation potential of the PNBX and cyclohexyl DTC to their respective dithiolates was also not measured so that direct evidence of this mechanism was not available. However, the evidence of the batch flotation tests, viz. sulphur grade vs sulphur recovery curves (cf. Figure 5.1) and the bubble loading tests (cf. Figure 5.17), showed that no improvement in floatability was obtained with copper sulphate addition.

For all the collectors tested with Buffelsfontein ore, the effect of copper sulphate addition on batch flotation was to increase mass and water recoveries. This was accompanied by significant decreases in grade. This effect did not enhance the overall metallurgical performance as the sulphur grade vs recovery relationship did not increase, but the froth characteristics were affected.

In the case of pure PNBX and the 90:10 mole ratio mixture of PNBX and cyclohexyl DTC the addition of copper sulphate increased the rate of flotation although in the case of the mixture the sulphur grade vs recovery curve decreased. In the case of pure PNBX, although the recovery was higher and the grade was lower there was no significant change to the sulphur grade vs sulphur recovery relationship with copper sulphate addition. No mineral surface analysis was done to identify whether any copper ions were adsorbed onto the pyrite surface or the gangue surfaces, but the results indicated that if there was adsorption of copper ions on the pyrite surface, this did not benefit the floatability of the pyrite.

In the case of cyclohexyl DTC, the addition of copper sulphate resulted in dramatically reduced sulphur grades and recoveries. Dithiocarbamates are well known for their strong copper complexing properties [Thorn, 1962]. This suggests the formation of an hydrophilic copper - dithiocarbamate complex on the surface in the case of cyclohexyl DTC. The use of surface spectrophotometric techniques such as TOF SIMS, [Nagaraj and Brinen, 1995] are recommended to confirm the distribution of the copper and collector ions.

Both batch flotation tests and bubble loading tests showed the same trends, in that copper sulphate addition did not increase the performance of the collectors tested. In the case of cyclohexyl DTC both bubble loading and grades vs recovery were considerably reduced. Within the limits of these tests the results indicate that for the flotation of pyrite at pH = 4, copper sulphate addition is not necessary to improve flotation performance.

The sulphur recovery by size showed that the initial recovery of sulphur in the coarse fraction with PNBX and the mixture was enhanced by the addition of copper sulphate. This was also observed by Allison et al [1982]. The final coarse sulphur recovery was not enhanced and the final grade was reduced.

The analysis of sulphur grade vs recovery by size showed that the sulphur grade of all size fractions was reduced with the addition of copper sulphate. In the fine fraction, this indicated that the additional gangue was collected by entrainment. However the activation of gangue by the copper sulphate cannot be dismissed as the grade was also decreased in the coarser fractions. copper sulphate has been reported to adsorb onto the gangue silicate minerals [Fuerstenau and Palmer, 1976; Chander, 1991; Nagaraj and Brinen, 1995;] and thereby activate both semi-liberated mixed mineral particles and gangue particles. TOF SIMS techniques, as used by Nagaraj and Brinen [1995] are recommended to confirm the presence of copper ions on gangue particles.

The presence of gangue in the froth zone has been reported to stabilise the froth [Harris, 1982] and increased recovery of gangue would also affect the froth characteristics resulting in the increased water recovery which would contribute to the earlier creation of a stable froth and increased rates of sulphur recovery. Thus copper sulphate would be added as a froth modifier which is the main reason given in the plant survey reported by O' Connor et al [1988].

These tests with and without copper sulphate addition suggest that for this system, viz. pyrite flotation at pH = 4, with xanthate and dithiocarbamate collectors, the role of copper sulphate addition was to modify froth characteristics. The effect of copper sulphate addition on the froth resulted in an increase in water recoveries, a lowering stability and bubble size, and increasing mobility of the surface froth. The change of surface froth due to copper sulphate addition may be exaggerated in laboratory batch flotation tests and further tests are required to confirm this effect in a continuous system and at plant conditions.

5.5 CONCLUSIONS

The batch flotation tests showed that no improvement to the overall sulphur grade vs recovery of pyrite at pH = 4 was obtained with the addition of copper sulphate. In the case of cyclohexyl DTC, the addition of copper sulphate caused a significant decrease in sulphur recovery and sulphur grade in the batch flotation tests. The bubble loading was similarly reduced. This suggests the formation of a hydrophilic copper - dithiocarbamate complex which should be further investigated. In the case of PNBX and the 90:10 mole ratio mixture of PNBX and cyclohexyl DTC, the rate of flotation increased with copper sulphate addition and an overall increase in sulphur recovery was obtained but with a decrease in grade.

The reduced bubble loading in the case of cyclohexyl DTC and the 90:10 mole ratio mixture of PNBX and cyclohexyl DTC, as well as the lack of significant improvement in the case of PNBX, also showed that copper sulphate addition did not improve the particle collection process of pyrite at pH = 4. For all tests, the addition of copper sulphate caused an increase in water and gangue recovery which was accompanied by improved froth characteristics. The surface froth characteristics were more mobile and less stable initially with addition of copper sulphate. These tests indicated that the predominant role of copper sulphate addition to pyrite flotation was as a froth modifier and although no metallurgical benefits were observed in laboratory scale tests, on the plant scale, operability may be improved.

Batch flotation tests with St Helena ore showed that the point of addition of copper sulphate made little difference to overall flotation performance.

CHAPTER 6: CONCLUDING REMARKS

This thesis has investigated the flotation performance obtained when mixtures of thiol collectors, viz. PNBX and cyclohexyl DTC, are used in the flotation of pyrite at pH = 4 with a view to investigating the synergistic effect which occurs when collectors are used. The effect of copper sulphate on the flotation performance obtained with pure PNBX and cyclohexyl DTC as well as with the mixture of PNBX and cyclohexyl DTC has also been investigated.

It has been clearly shown that synergism, defined as the combined effect that exceeds the sum of the parts, occurs between the collectors when they are added together in the flotation of pyrite. The results obtained showed that the change in performance was greater than the linearly additive contributions of the component collectors. The batch flotation tests confirmed the occurrence of synergism between the collectors. As these tests did not give any fundamental understanding of the cause of the enhanced flotation performance, further studies of the relevant flotation sub - processes were required to elucidate the mechanisms occurring, viz. bubble loading tests and collector - mineral adsorption studies. The adsorption step of the collector onto the mineral and the surface products formed creates the hydrophobicity necessary for mineral attachment to the bubble. The bubble loading step is responsible for the collection of the valuable mineral and its transport to the pulp phase. Although the froth phase is also a key controlling step in the flotation process, a thorough investigation of the froth phase was beyond the scope of this project. However, the surface froth characteristics of selected tests were analysed using digital image analysis.

The focus of the investigation was the 90:10 mole ratio of PNBX and cyclohexyl DTC. This mole ratio was selected in order to test the effect of a small amount of the one component as is typical of thermodynamic excess properties, and

also due to the high cost of dithiocarbamate collectors, although an economic assessment was not part of this thesis. Batch flotation tests with other mole ratios of PNBX and cyclohexyl DTC were tested and showed that this was not necessarily the optimum ratio for best metallurgical performance.

The batch flotation tests showed that sulphur grades, sulphur recoveries and rates of recovery, for all ratios of PNBX and cyclohexyl DTC tested, were enhanced above that which is predicted from the linear contribution of the constituent collectors. The water recovery was approximately proportional to the ratio of the component collectors and showed no synergistic enhancement. An increase in sulphur recovery indicated that the particle collection in the pulp was enhanced. An increase in the grade as well as the changes in water recovery and surface froth behaviour indicated that the froth zone was also affected by the nature of the collector. This illustrated the interactive nature of flotation parameters and that the benefit of the mixture was seen in both the pulp zone and the froth zone.

The flotation performance of the $< 25 \mu\text{m}$ fraction was not significantly improved with the use of mixtures, although the recovery increased this was at a grade penalty. The largest increase in performance resulting from the use of mixtures was in the $25 \times 75 \mu\text{m}$ fraction. Batch flotation tests with the 90:10 mole ratio mixture of PNBX and cyclohexyl DTC showed that increased dosage did not further improve flotation performance of any of the size fractions which indicated the possible economic benefits of using mixtures in place of higher dosages of the pure collectors.

The results of the bubble loading tests were entirely consistent with the batch flotation tests and showed an increased bubble loading with the mixture of collectors. The increased bubble loading is itself the outcome of a more fundamental process - the increased hydrophobicity of the mineral particle which is a result of the collector - mineral adsorption reactions.

In order to investigate the cause of the increased bubble loading, measurements of the collector mineral adsorption reactions were made, viz. thermochemical, kinetic and solubility measurements. The thermochemical tests showed a marked difference in the adsorption reactions between PNBX and cyclohexyl DTC and the pyrite surface. The enthalpy changes when PNBX was added to pyrite has corresponded to the established mechanisms showing the initial formation of the ferrous - thiolate followed by the formation of dixanthogen. In the case of the dithiocarbamate, only the formation of ferrous - thiolate was indicated. Dixanthogen was not formed with PNBX when ferrous sulphate was used in place of pyrite illustrating the requirement of the semiconducting nature of pyrite for the electron transfer to form dixanthogen.

The results from the kinetic adsorption tests were consistent with thermochemical test results. In the case of PNBX, the adsorption of PNBX continued until reagent depletion which corresponded to the formation of the dithiolate (dixanthogen). In the case of cyclohexyl DTC, the adsorption reached equilibrium after the adsorption of 2×10^{-6} moles / g pyrite, coinciding with the number of moles added before the termination of the reaction in the thermochemical tests, corresponding to the formation of the metal thiolate only.

The measurements of the solubility products showed that the metal thiolate salt formed in the case of cyclohexyl DTC was considerably less soluble than that formed with PNBX which also indicated the formation of the metal thiolate and not the dithiolate with pyrite. In order to confirm the nature of the surface products formed, the use of techniques such as TOF SIMS, XPS or FTIR would be required. The use of these techniques was beyond the scope of this project.

The thermochemical measurements with the mixture of PNBX and cyclohexyl DTC gave an increased enthalpy change which indicated the presence of a stronger mineral - surface reaction. This may result from the increased oxidation of xanthate to dixanthogen caused by the presence of the dithiocarbamate. It also may be caused by a stronger bond forming between

the mixed collector and the mineral surface due to the interactions of the pure collectors. The increased hydrophobicity of this product could be used to explain the synergistic behaviour observed in the bubble loading and batch flotation tests. Again direct methods of analysis would be required to confirm the nature of these surface products. The kinetic measurements showed no increase in rate of adsorption of xanthate with the 10% molar substitution of cyclohexyl dithiocarbamate, showing that there was no synergistic enhancement in the rate of adsorption onto pyrite.

It is thus proposed that the enhancement of flotation performance observed when a mixture of PNBX and cyclohexyl DTC is used is due to the fact that the cyclohexyl DTC adsorbs more rapidly than PNBX and forms the metal thiolate on the surface of the pyrite. The presence of the cyclohexyl DTC on the surface facilitates the formation of dixanthogen by the PNBX, as is indicated by the increased enthalpy change observed when mixture was used. Dixanthogen is a neutral molecule which is physisorbed and the presence of ferrous cyclohexyl DTC which is chemically bonded, increases the strength of collector attachment to the mineral surface, increasing the hydrophobicity of the pyrite surface. Alternatively, the increased enthalpy change may result from the formation of a thiol complex involving both the cyclohexyl DTC and the PNBX, but with the same result of increased hydrophobicity and strength of collector attachment to the pyrite surface. The effect of increased hydrophobicity is to decrease induction time, increasing the rate of flotation or to increase the tenacity of bubble - particle attachment, preventing elutriation and increasing the grade in the froth.

Although the findings of these tests are consistent with the literature they do not provide final definitive evidence of the surface products formed and thus confirmation of the mechanisms occurring.

As indicated at the outset of this thesis, this investigation was an attempt to explore a case study, in detail, of a system that demonstrates synergism, viz. the flotation of pyrite at pH = 4 using a 90:10 mixture of PNBX and cyclohexyl DTC. Although the mixture ratio was possibly not optimum a deliberate decision was made to use a low ratio of cyclohexyl DTC in order to understand the effect.

The addition of copper sulphate increased the rate of flotation with the PNBX and the 90:10 mole ratio mixture of PNBX and cyclohexyl DTC with an overall increase in sulphur recovery but with a decrease in grade. This showed that no improvement to the overall performance, as shown by the sulphur grade vs recovery relationship, was obtained. In the case of cyclohexyl DTC, the addition of copper sulphate caused a significant decrease in sulphur recovery and sulphur grade in the batch flotation tests. The bubble loading was similarly reduced. This suggests the formation of a hydrophilic copper - dithiocarbamate complex which should be further investigated. The effect of the addition of copper sulphate addition to PNBX was similar to that of the mixture.

For all tests, the addition of copper sulphate caused an increase in water and gangue recovery which was accompanied by improved froth characteristics. The surface froth characteristics were more mobile and less stable initially with addition of copper sulphate. These tests indicated that the predominant role of copper sulphate addition to pyrite flotation was as a froth modifier and although no metallurgical benefits were observed in laboratory scale tests, on the plant scale, operability may be improved, and this justifies its use.

Clearly this investigation represents the initial phases of an investigation into a complex but exciting research area. The positive findings indicate that considerable benefit could be obtained by carrying out more extensive detailed studies on other systems. Synergism in the use of mixtures of collectors presents exciting opportunities for improving performance especially in the case of differential flotation systems. As the momentum increases to greater

selectivity, it is likely that the possibilities presented by the synergistic effects in the case of collectors will ultimately have a major impact on the profitability of many plants. The results of this thesis represent a contribution towards a better understanding of these key phenomena.

LIST OF REFERENCES

Ackerman, P.K., Harris, G.H., Klimpel, R.R. and Aplan, F.F., 1987a. Evaluation of flotation collectors for copper sulphides and pyrite, I. Common sulphhydryl collectors. *Int. J. Miner. Process.* vol. 21, pp 105-127.

Adamek, G.B. and Hudson, E.G., 1969. Dithiocarbamate flotation collectors for metal sulphides. Canadian Patent No. 808,222 (CL. 361-16). 11 Mar., 1969, appl. 02, June 1966. 20, pp (CA 71-23866s).

Adkins, S.J. and Pearse, M.J., 1992. The influence of collector chemistry on the kinetics and selectivity in base metal sulphide flotation. *Miner. Engng.*, vol. 5, nos 3-5, pp 295-310.

Allison, S.A., Goold, L.A., Nicol, M.J. and Granville, A., 1972. A determination of the products of reaction between various sulphide minerals and aqueous xanthate solution, and a correlation of the products with electrode rest potentials. *Metall. Trans.*, vol. 3, pp 2613-2618.

Allison, S.A. and Finkelstein, N.P., 1971. Products of reaction between galena and aqueous xanthate solutions. *Inst. Mining Metall. Trans.*, vol. 80, pp C235-C239.

Allison, S.A., Dunne, R.C. and De Waal, S.A., 1982. The flotation of gold and pyrite from South African gold mine residues. *Proceedings of XIV Int. Miner. Process. Cong.*, Toronto, Canada, pp 11-9-18.

Anfruns, J.P. and Kitchener, J.A., 1976. The absolute rate of capture of single particles by single bubbles. in *Flotation A. M. Gaudin Memorial Volume*, ed M.C. Fuerstenau. AIME, New York.

Aupiais, J.E., 1992. Private communication.

Ball, B. and Rickard, R.S., 1976. The chemistry of pyrite flotation and depression. in *Flotation: A. M. Gaudin Memorial Volume*, ed M.C. Fuerstenau, AIME, New York, pp 458-484.

Bansal, V.K. and Biswas, A.K., 1975. Collector-frother interaction at the interfaces of a flotation system. *Trans. Instn. Min. Metall.*, pp C131-C135.

Barker, L.M., 1984. Effect of Electrolytes on the flotation of pyrite. MSc Thesis. University of Cape Town.

Bhaskar Raju, G. and Forsling, W., 1991. Adsorption mechanism of diethyl dithiocarbamate on covellite, cuprite and tenorite. *Colloids and Surf.*, vol. 60, pp 53-69.

Bothelho de Sousa, A.M.R., 1984. The effect of temperature on the flotation of pyrite. MSc thesis. University of Cape Town.

Bothelho de Sousa, A.M.R. and Ross, V.E., 1990. The flotation of pyrite from Buffelsfontein ore. Mintek Report No. M320D.

Bradshaw, D.J., Upton, A.E. and O' Connor, C.T., 1990. Annual Report UCT-KARBOCHEM Research Group.

Bradshaw, D.J. and O' Connor, C.T., 1992. A study of the pyrite flotation efficiency of dithiocarbamates using factorial design techniques. *Miner. Engng.*, vol. 5, nos 3-5, pp 317-329.

Brown, G.I., 1974. *Introduction to Physical Chemistry*, 2nd Edn. Longman, Hong Kong.

Buckenham, M.H. and Schulman, J.H., 1963. Molecular association in flotation. *Trans. Instn. Min. Metall.*, vol. 7, pp C1-C6.

Bushell, C.H.G. and Krauss, C.J., 1962. Copper activation of pyrite. *Bul. C.I.M.*, May, pp 314-318.

Bushell, L.A., 1970. The flotation plants of the Anglo-Transvaal Group. *J. S. Afr. Inst. Min. Metall.*, Jan, pp 213-228.

Cases J.M., Kongolo, M., de Donato, P., Michot, L.J. and Erre, R., 1993. Interaction between finely ground pyrite and potassium amyloxanthate in flotation: 1. Influence of alkaline grinding. *Int. J. Miner. Process.*, vol.38, pp 267-298.

Chander, S., 1988. Electrochemistry of sulphide mineral flotation. *Miner. and Metall. Process.*, pp 104-114.

Chander, S., 1991. Electrochemistry of sulphide flotation: Growth characteristics of surface coatings and their properties, with special reference to chalcopyrite and pyrite. *Int. J. Miner. Process.*, vol. 33, pp 121-134.

Chudacek, M.W. and Fichera, M.A., 1991. The relationship between the test-tube flotability test and batch cell flotation. *Min. Engng.*, vol. 4, no.1, pp 25-35.

Cilliers, J.J.C., Austin, R. and Henwood, D. 1991. An evaluation of formal experimental design procedures for flotation testwork. Undergraduate thesis University of Cape Town.

Crawford, R. and Ralston, J., 1988. The influence of particle size and contact angle in mineral flotation. *Int. J. Miner. Process.*, vol. 23, pp 1-24.

Crawford, R., Koolal, L.K. and Ralston, J., 1987. Contact angles on particles and plates. *Colloids and Surf.*, vol. 27, pp 57-64.

Critchley, J.K. and Riaz, M., 1991. Study of synergism between xanthate and dithiocarbamate collectors in flotation of heazlewoodite. *Trans. Instn. Min. Metall.*, vol. 100, pp C55-C57.

Crozier, R. D., 1980. Frother function in sulphide flotation. *Mining magazine*. pp 26-35

Crozier, R. D., 1991. Sulphide collector mineral bonding and the mechanism of flotation. *Miner. Engng.*, vol. 4, nos 7-11, pp 839-858.

Crozier, R. D., 1992. *Flotation: Theory, Reagents and Ore Testing*, Pergamon Press. New York.

Crozier, R.D. and Klimpel R., 1989. Frothers: Plant Practice. *Miner. Process. & Extr. Metall. Review*, vol. 5, pp 257-279.

Davidtz, J.C., 1994. Active functional group effects on the excess Gibbs free energies in flotation phenomena. Presented at 13th Annual Minerals Processing Symposium, Gordon's Bay.

de Donato, P., Cases J.M., Kongolo, M., 1979. Stability of the amyl xanthate ion as a function of pH: Modelling and comparison with the ethyl xanthate ion. *Int. J. Miner. Process.*, vol. 25, pp 1-28.

Dell, C.C. and Bunyard M.J., 1972. Development of an automatic flotation cell for the laboratory. *Trans. Inst. Min. Met.*, vol. 81, pp C246-C249.

Derjaguin, B.V. and Dukhin, S.S., 1960. Theory of flotation of small and medium-size particles. *Inst. Min. Metall.* pp221-245.

Diaz-Penafiel, P. and Dobby, G.S., 1994. Kinetic studies in flotation: Bubble size effects. *Min. Engng.*, vol. 7, nos 4, pp 465-478.

Dimou, A., 1986. The flotation of pyrite using xanthate collectors. Msc thesis, University of Cape Town.

Dippenaar, A. 1978. The effect of particles on the stability of flotation froths. Report Number 1988, National Institute for Metallurgy, Johannesburg.

Drysmala, J., Chmielewski, T., Wolters, K. L., Birlingmair, D. H. and Wheelock, T. D., 1992. Microflotation measurement based on modified Hallimond tube, *Trans. Instn. Min. Metall.* vol. 101, pp C17-C24.

Engelbrecht, J.A. and Woodburn, E.T., 1975. The effects of froth height, aeration rate and gas precipitation on flotation. *J. S. Afr. Inst. Min. Metall.*, Oct, pp 125-132.

Falvey, J.J., 1969. Dialkyl Dithiocarbamate as froth flotation collectors. U.S. Patent No. 3,464,551. (CL.209-166;BO36) 02 Sept. 1960, appl. 01 Nov. 1967, 4 pp. (CA 71-93755d).

Fichera, M.A. and Chudacek, M.W., 1992. Batch cell flotation models - A review. *Miner. Engng.*, vol. 5, nos 1, pp 41-55.

Fickling, R.S., 1986. An investigation into the froth flotation of four South African coals. Msc Thesis, University of Cape Town.

Finch, J.A. and Smith, G.W., 1979. Contact angle and wetting. *Minerals Sci. Engng.*, vol. 11, no 1, pp 36-63.

Finch, J. A., and Dobby, G.S. 1990. *Column Flotation*. Pergamon Press, Oxford.

Finkelstein, N.P. and Allison S.A., 1976. The chemistry of activation, deactivation and depression in the flotation of zinc sulphide: A review. in *Flotation: A. M. Gaudin Memorial Volume* ed M.C. Fuerstenau. AIME, New York, pp 414-457.

Finkelstein, N.P. and Goold, L.A., 1972. The reaction of sulphide minerals with thiol compounds. Mintek Report No 1439.

Finkelstein, N.P. and Poling G.W., 1977. The role of dithiolates in the flotation of sulphide minerals. *Miner. Sci. Engng.*, vol. 9, no. 4, pp 177-197.

Flint, L.R., 1974. A mechanistic approach to flotation kinetics. *Trans. Inst. Min. Metall.*, C90-C95.

Fornasiero, D. and Ralston, J., 1992. Iron hydroxide complexes and their influence on the interaction between ethyl xanthate and pyrite. *J. Colloid Interfacial Sci.*, vol. 151, pp 225-235.

Fuerstenau, D.W. and Palmer, B.R., 1976. Anionic flotation of oxides and silicates. in *Flotation: A. M. Gaudin Memorial Volume* ed M.C. Fuerstenau., AIME, New York, pp 148-196.

Fuerstenau D.W. and Mishra, R.K., 1980. On the mechanism of pyrite flotation with xanthate collectors. in *Complex Sulphide Ores*, ed M.J. Jones, Inst. Min. Metall., London, pp 271-278.

Fuerstenau D.W., 1982. Sulphide Mineral Flotation. in *Principles of Flotation*, ed R.P. King. S. Afr. Inst. Min. Metall. Johannesburg.

Gaudin, A. M., et al., 1934. Reactions of xanthate with sulphide minerals. AIME vol 112, p 319.

Gaudin, A. M., 1957. *Flotation*. 2nd ed. McGraw Hill Book Co., New York.

Gardner, J.R. and Woods, R., 1977. An electrochemical investigation of contact angle and of flotation in the presence of alkylxanthates. II. Galena and pyrite surfaces. *Aust. J. Chem.*, vol. 30, pp 981-991.

Glembotsky, A.V., Desiatov, A.M., Kondratieva, L.V., Riaboy, V.I., Petrova, L.N., Ustinov, I.D., Pomazov, V.D. and Krasnukhina, A.V. 1988. New reagents for sulphide and non-sulphide ores in the USSR. *Proceedings of XVI Int. Miner. Process. Cong. Stockholm*, pp 81-91.

Glembotsky, A.V., Glinkin, V.A., Seregin, V.P. and Greshnova, N.A., 1995. The replacement of cyanide by a new organic depressant in selective flotation of polymetallic lead - zinc - silver ores. *Proceedings of XIX Int. Miner. Process. Cong. San Francisco*, pp 205-207.

Gorain, B.K., Franzidis, J.P and Manlapig, E.V., 1995. Studies on impeller type, impeller speed and air flow rate in an industrial flotation cell. Part II: Effect on gas hold up. *Miner. Engng.*, vol. 8, no 12, pp 1557-1570.

Guy, P.J. and Trahar W.J., 1984. The influence of grinding and flotation environments on the laboratory batch flotation of galena. *Int. J. Miner. Process.*, vol. 12, pp 15-38.

Hanson, J.S. and Fuerstenau D.W., 1993. The mechanism of xanthate adsorption on pyrite. *Proceedings of XVIII Int. Miner. Process. Cong.*, Sydney, pp 657-661.

Hanson, J.S., Barbaro, M., Fuerstenau, D.W., Marabini, A. and Barbucci, R., 1988. Interaction of glycine and a glycine - based polymer with xanthate in relation to the flotation of sulphide minerals. *Int. J. Miner. Process.*, vol. 123, pp 123-135.

Harris, P.J. 1982. Frothing phenomena and froths. in *Principles of Flotation*, ed R.P. King. S. Afr. Inst. Min. Metall. Johannesburg.

Harris, P.J. 1984. Influence of substituent group on the decomposition of xanthates in aqueous solutions. *S. Afr. Tydskr. Chem.*, vol. 37, no 3, pp 91-94.

Harris, P.J. 1996. Private communication.

Harris, P.J. and Finkelstein, N.P., 1977. The interaction of pyrite, oxygen and xanthate. National Institute for Metallurgy, Report No 1854.

Harris, P.J. and Finkelstein, N.P., 1975. The interaction between sulphide minerals and xanthate. I: The formation of monothiocarbonate at galena and pyrite surfaces. *Int. J. Miner. Process.*, vol. 2, pp 77-100.

Haug, H.H. and Miller, J.D., 1978. Kinetics and thermochemistry of amyl xanthate adsorption by pyrite and marcasite. *Int. J. Miner. Process.*, vol. 5, pp 241-266.

Hewitt, D., Fornasiero, D. and Ralston, J., 1994. Bubble Particle Attachment Efficiency. *Miner. Engng.*, vol. 7, nos 5-6, pp 657-665.

Hodgson, M. and Agar, G.E., 1989. Electrochemical investigations into the flotation chemistry of pentlandite and pyrrhotite: process water and xanthate interactions. *Can. Metall. Q.*, vol. 28, no 3, pp 189-198.

Hornsby, D.T. and Leja, J., 1983. Critical surface tension of flotability. *Colloids and Surf.* vol. 7, pp 339-349.

Hu, Q., Wang, D. and li, B., 1992. An electrochemical investigation of the diethyldithiocarbamate - galena flotation system. *Int. J. Miner. Process.*, vol. 34, pp 289-305.

Huber-Panu, I., Ene-Danalache, E. and Cojocariu, D.G., 1976. Mathematical models of batch and continuous flotation. in *Flotation*, ed M.C. Fuerstenau. AIME New York.

Hudson, G.B. and Adamek, E.G., 1967. Dithiocarbamate collectors for flotation of sulphides from finely milled ores. Canadian Patent No. 771,182 (CL 260-445). Nov. 7, appl. Jun. 2, 1966. 17 pp. (CA 68-52204t).

Imaizumi and Inoue, 1965. Kinetic consideration of froth flotation. *Proceedings of VI Int. Miner. Process. Cong.*, Cannes, pp 581-589.

Israelachvili, J.N., 1992. Intermolecular and surface forces. 2nd ed. Academic Press. London. pp 122-141.

Jiwu, M. et al. 1984. Novel Frother collectors for flotation of sulphide minerals-CEED. in *Reagents in the Minerals Industry*. eds M.J. Jones and R. Oblatt. Inst. Min. Metall., London. pp 287-290.

Jowett, A., 1979. The formation and disruption of particle - bubble aggregates in flotation. In *Fine Particle Processing*, ed P. Somarsundaran, pp 720-753.

Kocabag, D., Shergold, H.L., and Kelsall, G.H., 1990. Natural oleophilicity / hydrophobicity of sulphide minerals, II. Pyrite. *Int. J. Miner. Process.*, vol. 29, pp 211-219.

Kakovsky, I.A., 1957. Physicochemical properties of some flotation reagents and their salts with ions of heavy iron-ferrous metals. *Proceedings of 2nd Int. Cong. Surface Activity*, London. vol. 4, pp 225-237.

Kelsall, D.F., 1961. Application of probability in the assessment of flotation systems. *Trans. Inst. Min. Metall.*, vol 70 pp 191-204.

Kelly, E.G. and Spottiswood, D.J., 1982. *Introduction to Minerals Processing*, John Wiley and Sons. USA.

Kim, J.Y., Chryssoulis, S.L. and Stowe, K.G. 1995. Effects of lead ions in sulphide flotation. Proceedings of SME Annual meeting, Denver, Colorado, pp 95-121.

King, R. P., 1982. *Principles of flotation*. S. Afr. Inst. Min. Metall. Johannesburg.

King, R. P., Hatton, T., A. and Hulbert, D., G. 1974. Bubble loading in flotation, Trans. I. M. M., Vol 83, pp C112-115.

Klimpel, R.D., 1988. The industrial practice of sulphide mineral collectors. in *Reagents in mineral Technology*, eds P. Somasundaran and B.M. Moudgil, Marcel Dekker Inc., New York. pp 663-713.

Klimpel, R.R. and Hansen, R.D., 1988. Frothers. in *Reagents in Mineral Technology*. eds P. Somasundaran and B.M. Moudgil, Marcel Dekker Inc., New York. pp 387-409.

Klimpel, R.R., 1984. Froth flotation: The kinetic approach. Proceedings of Mintek 50, Johannesburg, South Africa.

Labonté, G. and Finch, J.A., 1988. Measurement of electrochemical potentials in flotation systems, C. Inst. Min. Bull., vol. 81, no 920, pp 78-83.

Laskowski, J. S., 1974. Particle-bubble attachment in flotation, Min. Sci. Engng., vol. 6, no. 4, pp 223-235.

Laskowski, J. S., 1986. The relationship between flotability and hydrophobicity. in *Advances in Minerals Processing*, ed P. Somarsundaran, SME, Littleton, Colorado. pp 189-208.

Laskowski, J. S., 1996. Surfaces Processes in Flotation. Course notes.

Laskowski, J.S., 1989. Thermodynamic and kinetic flotation criteria. Miner. Process. & Extr. Metall. Review, vol 5. pp 25-41.

Laskowski, J.S., 1993. Frothers and Flotation Froth. Min. Process. & Extr. Metall. Review, vol. 12, pp 61-89.

Laskowski, J.S., Lui, Q. and Zhan, Y., 1996. Sphalerite activation: Flotation and electrokinetic studies. Proceedings of Minerals and Materials '96, Somerset West.

Lee, A.F., 1969. A new rapid bubble pick - up technique as a rapid flotation test method. J. S. Afr. Inst. Min. Metall., Dec., pp 94-99.

Leja, J. and He, B.Q., 1984. The role of flotation frothers in the particle - bubble attachment process. in *Principles of Mineral Flotation*. eds M.H. Jones and J.T. Woodcock, Aust. Inst. Min. Metall., pp 73-89.

- Leja, J. and Schulman, J.H., 1954. Flotation theory: Molecular interactions between frothers and collectors at solid - liquid interfaces. AIME, vol. 199, pp 221-228.
- Leja, J., 1973. Some electrochemical and chemical studies related to froth flotation with xanthates. Miner. Sci. Engng., vol. 5, no.4, pp 278-286.
- Leja, J., 1982. *Surface Chemistry of froth flotation*, Plenum Press, New York.
- Leja, J., 1989. Interactions of surfactants. Miner. Process. & Extr. Metall. Review, vol. 5, pp 1-22.
- Leja, J., Little, L.H. and Poling, G.W., 1963. Trans. Ins. Min. Metall., vol. 72, pp 414.
- Lekki, J. and Laskowski, J.S., 1971. On the dynamic effect of frother - collector joint action in flotation. Trans. Ins. Min. Metall., vol. 80, pp C174-C180.
- Lekki, J. and Laskowski, J.S., 1975. A new concept of of frothing in flotation systems and general classification of flotation frothers. Proceedings of XI Int. Miner. Process. Cong., Cagliari. pp 427-448.
- Leppinen, J.O., 1990. FTIR and flotation investigation of the adsorption of ethyl xanthate on activated and non activated sulphide minerals. Int. J. Miner. Process., vol. 30, nos 3-4, pp 245-263.
- Leppinen, J.O., Basilio, C.I. and Yoon, R.H. 1989. In situ FTIR study of ethyl xanthate adsorption on sulphide minerals under conditions of controlled potential. Int. J. Miner. Process., vol. 26, pp 259-274.
- Leppinen, J.O., Laajalehto, K., Kartio, I. and Suoninen, E., 1995. FTIR and XPS studies of surface chemistry of pyrite in flotation. Proceedings of XIX Int. Miner. Process. Cong. San Francisco, pp 35-38.
- Levay, G. 1996. Private Communication.
- Livshits, A.K. and Dudenkov S.V., 1965. Some factors in flotation froth stability. Proceedings of VII Int. Min. Process. Congress, New York, pp 367-371.
- Lloyd, P.J.D., 1981. The flotation of gold, uranium and pyrite from Witswatersrand ores. J. S. Afr. Ins. Min. Metall., vol. 81, pp 41-47.
- Luttrell, G.H. and Yoon, R.H., 1991. A flotation column simulator based on hydrodynamic principles. Int. J. Miner. Process., vol. 33, pp 355-368.
- Majima, H. and Peters, E., 1969. Electrochemistry of sulphide dissolution in hydrometallurgical systems. Proceedings of VIII Int. Min. Process. Congress, Leningrad, pp 5-17.

Malysa, K. and Pomianowski, A., 1976. Characterisation of co-operation between flotation frother and collector. *Physiochemical Problems of Mineral Processing*, Wroclaw Technical University, Wroclaw, no 10, pp 119-131.

Manev, E. and Pugh, R.J., 1993. Frother / collector interactions in thin froth films and flotation. *Colloids and Surf.*, vol. 70, pp 289-295.

Mangalam, V. and Khangaonkar, P.R., 1985. Zeta-Potential and adsorption studies of the chalcopyrite - sodium diethyl dithiocarbamate system. *Int. J. Miner. Process.*, vol. 15, pp 269-280.

Meilczarski, J. A., 1986. In situ ATR-IR spectroscopic study of xanthate adsorption on marcasite. *Colloids and Surf.*, vol. 17, pp 235-248.

Mellgren, O. and Ramachandra Rao, S., 1968. Heat of adsorption and surface reactions of potassium diethyl dithiocarbamate on galena. *Trans. Inst. Min. Met.*, C65-C71.

Mellgren, O., 1966. Heat of adsorption and surface reactions of potassium ethyl xanthate on galena. *Trans. Am. Inst. Min. Engrs.*, vol. 235, pp 46-60.

Mellgren, O., Gochin, R.J., Shergold H.L. and Kitchener J.A., 1973. Thermochemical measurements in flotation research. *Proceedings of X Int. Min. Process. Congr.*, London, pp 451-472.

Mingione, P.A., 1984. Use of dialkyl and diaryl dithiophosphate promoters as mineral flotation agents. in *Reagents in the Minerals Industry*, eds M.J. Jones and R. Oblatt. *Inst. Min. Metall.*, London. pp 19-24.

Mitrofanov, S.I., Kuz'kin, A.S. and Filimonov, V.N., 1985. Theoretical and practical aspects of using combinations of collectors and frothing agents for sulphide flotation, *Proceedings of 15th Congr. Int. Metall.*, St. Etienne, France, vol. 2, pp 65-73.

Montalti, M., Fornasiero, D. and Ralston, J., 1991. UV-Visible Spectroscopic Study of the kinetics of adsorption of ethyl xanthate on pyrite. *J. Colloid Interface Sci.*, vol. 143, pp 440-450.

Moolman, D.W., Aldrich, C., van Deventer, J.S.J. and Bradshaw, D.J., 1995. The interpretation of flotation froth surfaces using digital analysis and neural networks. *Chem. Eng. Sci.*, vol. 50, no 22, pp 3501 - 3513.

Nagaraj, D.R., 1988. The chemistry and application of chelating or complexing agents in minerals separations. in *Reagents in Mineral Technology*, eds P. Somasundaran and B.M. Moudgil, Marcel Dekker Inc., New York. pp 387-409.

Nagaraj, D.R., 1995. Recent developments in new sulphide and precious metals collectors and mineral surface analysis. *Proceedings of Interactions between Comminution and Downstream Processing*. S. Afr. Inst. Min. Metall., 5-6 June, Mintek, Johannesburg.

Nagaraj, D.R. and Brinen, 1995. Sims study of metal ion activation in gangue flotation. Proceedings of XIX Int. Miner. Process. Cong. San Francisco, pp 253-258.

Nedosekina, T.V., et al., 1985. The mechanism of combined thionocarbamate action in flotation of copper. Sov. J. Non-ferr. Met., vol. 26, no 10, pp 96-99.

Nicholson, R.S. and Shain, I., 1964. Theory of stationary electrode polarography, Anal. Chem., vol. 36, no 4, pp 706-723.

Nicol, M. J., 1984. An electrochemical study of the interaction of copper (II) ions with sulphide minerals. in *Electrochemistry in mineral and metal processing*. eds P.E. Richardson, S. Srinivasan and R. Woods. The Electrochemical Society. Pennington. New Jersey.

O' Connor, C.T. and Dunne, R. C., 1991. The practice of pyrite flotation in South Africa and Australia. Miner. Engng., vol. 4, nos 7-11, pp 1057-1069.

O' Connor, C.T. and Dunne, R.C., 1994. The flotation of gold bearing ores - a review. Min. Engng., vol. 7, no 7, pp 838-849.

O' Connor, C.T., Botha, C., Walls, M.J. and Dunne R.C., 1988. The role of copper sulphate in pyrite flotation. Min. Engng., vol.1, no 3, pp 203-212.

O' Connor, C.T., Randall, E.W. and Goodall, C.M., 1990. Measurement of the effects of physical and chemical variables in bubble size. Int. J. Miner. Process., vol. 28, pp 139-149.

O' Connor, C.T., Bradshaw, D.J. and Upton, A. E., 1990. The use of dithiophosphates and dithiocarbamates for the flotation of arsenopyrite. Min. Engng. vol. 3, nos 5, pp 447-459.

Orel, M.A., Chibisov, V.M. and Lapatukhin, I.V., 1986. Use of mixtures of butyl xanthate and hydrolyzed polyacrylamide when floating gold-containing ore. Sov. J. Non-ferr. Met., 27, no. 11, pp 97-98.

Oudenne, P.D. and de Cuyper J., 1987. Reagents and flotation flow sheet selection for the beneficiation of a complex sulphide ore containing copper and gold. Proceedings of 2nd Int. Symp. Benefic. Agglom., Bhubaneswar, India.

Persson, I., 1993. Adsorption of ions and molecules to solid surfaces in connection with flotation of sulphide minerals. J. Co-ordination Chem., vol. 32, no. 4. pp 261-341.

Plaskin, I.N. and Zaitseva, S.P., 1960. Effect of the combined action of certain collectors on their distribution between galena particles in a flotation pulp. (Mintek translation no. 1295, June 1988). Naachnye Soobshcheniya Institut Gonnogo dela Imeni AA Skochinskogo, Akademiya Nauk SSSR, Moskva, no. 6, pp 15-20.

Plaskin, I.N., Glembotskii, V.A. and Okolovich, A.M., 1954. Investigations of the possible intensification of the flotation process using combinations of collectors. (Mintek translation Feb. 1989). Naachnye Soobshcheniya Institut Gonnogo dela Imeni AA Skochinskogo, Akademiya Nauk SSSR, no. 1, pp 213-224.

Poling, G.W., 1976. Reactions between thiol reagents and sulphide minerals. in *Flotation: A. M. Gaudin Memorial Volume*. ed M.C. Fuerstenau. AIME, New York, pp 334-363.

Poling, G.W. and Leja J., 1963. Infrared study of xanthate adsorption on vacuum deposited films of lead sulphide and metallic copper under conditions of controlled oxidation. *J. Phys. Chem.*, vol. 67, pp 2121-2126.

Pomainowski, A. and Leja, J., 1963. Spectrophotometric study of xanthate and dixanthhogen solutions. *Can. J. Chem.*, vol. 41, pp 2219-2230.

Prestidge, C.A. and Ralston, J., 1996. Contact angle studies of particulate sulphide minerals. *Min. Engng.*, vol. 9, no 1, pp 85-102.

Pritzker, M.D., Yoon, R.H., Basilio, C. and Choi, W.Z., 1985. Solution and flotation chemistry of sulphide minerals. *Can. Metall. Q.*, vol. 1, pp 27-38.

Ralston J. and Healy T.W., 1980. Activation of zinc sulphide with Cu^{2+} , Cd^{2+} and Pb^{2+} . *Int. J. Miner. Process.*, vol. 7, pp 175-203.

Ralston J., 1994. A Unified Approach to Flotation. Proceedings of Fifth Mill Operator's Conference, Roxby Downs, Australia, pp15-27.

Rand D.A.J. and Woods, R., 1984. Eh measurements in sulphide mineral slurries. *Int. J. Miner. Process.*, vol. 13, pp 29-42.

Randall, E.W., Goodall, C.M., Fairlamb, P.M., Dold, P.L. and O'Connor, C.T., 1989. A method for measuring the sizes of bubbles in two - and three - phase systems. *J. Phys. E: Sci. Instrum.*, vol. 22, pp 827-833.

Rao, S.R., 1972. Thermochemistry of the adsorption of xanthate at pyrrhotite. *Trans. AIME*, no. 250, pp 199-203.

Ravindrath, K. and Patel, C.C., 1969. Adsorption of dithiocarbamates at sulphide mineral surfaces. *Ind. J. Tech.*, vol. 7 pp 324-328.

Richardson, P.E. and Walker, G.W., 1985. Proceedings of XV Int. Miner. Process. Cong. vol. 2, St Etienne, pp 198.

Rosen, M.J., 1989. *Surfactants and interfacial phenomena*, Second edition, Wiley, New York.

Schukarev, A.V., Kravets, I.M., Buckley, A.N. and Woods, R., 1994. Submonolayer adsorption of alkyl xanthates on galena. *Int. J. Miner. Process.*, vol. 41, pp 99-114.

Schulze, H.J., 1984. *Physico-chemical elementary processes in flotation*, Elsevier, New York.

Schulze, H.J., 1989. Hydrodynamics of bubble-mineral particle collisions. *Miner. Process. and Extr. Metall. Review*, vol. 5, pp 43-75.

Senmin Flotation Handbook, Senmin Ltd. P.O. Box 98881, Johannesburg, South Africa.

Smart, R. St.C., 1991. Surface layers in base metal sulphide flotation. *Miner. Engng.*, vol. 4, nos 7-11, pp 891-909.

Stonestreet, P., 1991. Reverse flotation: A novel process for the beneficiation of fine coal. PhD Thesis. University of Cape Town.

Stowe, K.G. Chryssoulis, S.L. and Kim, J.Y., 1994. Mapping of composition of mineral surfaces by TOF-SIMS. Presented at Minerals Engineering '94. Sept 26-28. Lake Tahoe.

Subrahmanyam, T.V. and Forssberg, K.S.E., 1993. Mineral solution - interface chemistry in minerals engineering. *Min. Engng.*, vol. 6, no 5, pp 439-454.

Sun, S.C. and Troxell, R.C., 1957. Try bubble pick up for rapid flotation testing. *Eng and Min. J.*, vol. 158, no 7, pp 79-80.

Sutherland, K.L. and Wark, I.W., 1955. *Principles of flotation*. Aust. Inst. Min. Metall., Melbourne.

Szatkowski, M. and Freyberger, W.L., 1985. Model describing mechanism of the flotation process. *Trans. Inst. Min. Metall.* vol. 94, pp C129-C135.

Taggart, A.F., del Guidice, G.R.M. and Ziehl, O.A., 1934. The case for the chemical theory of flotation. *Trans. AIME.*, vol. 112, pp 348-381.

Taggart, A.F., 1945. *Handbook of mineral dressing*. Wiley, New York.

Taggart, A.F. and Hassialis, M.D., 1946. Solubility product and bubble attachment in flotation. *Trans. AIME.*, vol. 169, pp 259-265.

Thorn, G.D. and Ludwig, R.A., 1962. *The dithiocarbamates and related compounds*. Elsevier Publishing Co. Amsterdam, New York.

Trahar, W.J. and Warren, L.J., 1976. The flotability of very fine particles - A review. *Int. J. Miner. Process.*, vol. 3, pp 103-131.

Trahar, W.J., 1981. A rational interpretation of the role of particle size in flotation. *Int. J. Miner. Process.*, vol. 8, pp 289-327.

Valdiviezo, E. and Oliveira, J.F., 1993. Synergism in aqueous solutions of surfactant mixtures and its effect on the hydrophobicity of mineral surfaces. *Miner. Engng.*, vol. 6, no 6, pp 655-661.

Van Lierde, A. and Lesoille, M., 1991. Compared effectiveness of xanthate and mercaptobenzothiazole as gold and arsenopyrite collectors. Proceedings of XVII Int. Miner. Process. Cong., Dresden. Sept. 1991, Vol. IV, pp 111-119.

Voigt, S., Szargan, R. and Suoninen E., 1994 Interaction of copper (II) ions with pyrite and its influence on ethyl xanthate adsorption. Sur. and Interface Anal., vol. 21, pp 526 - 536.

Vinogradova, O.I., 1993. Calculation of hydrodynamic interaction of a mineral particle with a bubble under conditions of mixed sorption coating of collector. Proceedings of XVIII Int. Miner. Process. Cong., Sydney, pp 745-749.

Wakamatsu, T. and Numata, Y., 1979. Fundamental study on the flotation of minerals using two kinds of collectors. in *Fine Particle Processing*. ed P. Somasundaran, pp 787-801.

Wang, X.H., 1995. Interfacial electrochemistry of pyrite oxidation and flotation II FTIR studies of xanthate adsorption on pyrite surfaces in neutral pH solutions. J. Coll. Interfac. Sci., vol. 171, pp 413-428.

Wang, X.H., Forssberg, K.S. and Bolin, N.J., 1989, The aqueous and surface chemistry of activation in the flotation of sulphide minerals - A review. Part II: A surface precipitation model. Miner. Process. and Extr. Metall. Rev., vol. 4, pp 167-199.

Wang, X.H. and Forssberg, K.S., 1991. Mechanisms of pyrite flotation with xanthates. Int. J. Miner. Process., vol. 33, pp 275-290.

Walker, G.W. Walters, C.P. and Richardson, P.E., 1986. Hydrophobic effects of sulphur and xanthate on metal and mineral surfaces. Int. J. Miner. Proc., vol.18, pp 119-137.

Wards Earth Science Catalogue, 1996-1997. P.O. Box 92912, Rochester, New York, 14692-9012.

Warren L.J., 1985. Determination of the contributions of true flotation and entrainment in batch flotation tests. Int. J. Miner. Process., vol. 14, pp 33-44.

Winter, G., 1975. Xanthates of sulphur: Their possible role in flotation. Inorganic and Nuclear Chemistry Letters, vol. 11, pp 113-118.

Woodburn, E.T. King, R.P. and Colborn, R.P., 1971. The effect of particle size distribution on the performance of a phosphate flotation process. Met. Trans. vol 2, pp 3163-3174.

Woods, R. 1984. Electrochemistry of sulphide flotation. in *Flotation: A. M. Gaudin Memorial Volume*. ed M.C. Fuerstenau. AIME., New York, pp 298-334.

Woods, R. 1984. Electrochemistry of sulphide flotation. in *Principles of the Minerals Industry*. eds M.H. Jones and J.T. Woodcock, Aust. Inst. Min. and Metall., Melbourne, pp 91-115.

Woods, R. 1994. Chemisorption of thiols and its role in flotation. Proceedings of IV Meeting of the Southern Hemisphere on Mineral Technology; and III Latin-American Congress on Froth Flotation. Concepcion, Chile. pp 1-14.

Wottgen, E. and Berg, I., 1968. Adsorption behaviour and collector effect of dithiocarbamates. Freiberg. Forschungsh., A, vol. 431, pp 31-38.

Wrobel, S.A., 1955. Power and stability of flotation frothers. Mine and Quarry. 19, pp 314-363.

Yarar, B., Haydon, B.C. and Kitchener, J.A., 1969. Electrochemistry of the galena-diethyldithiocarbamate-oxygen flotation. Trans. Inst. Min. and Metall., vol. 78, pp C181-C184.

Ye, Y., Khandrika, S.M. and Miller, J.D., 1988. Induction - time measurements at a particle bed. Presented at 117th AIME annual meeting, Phoenix, Arizona.

Yoon, R.H. and Basilio C.I., 1993. Adsorption of thiol collectors on sulphide minerals and precious metals - a new perspective. Proceedings of XVIII Int. Miner. Process. Cong., Sydney, pp 611-617.

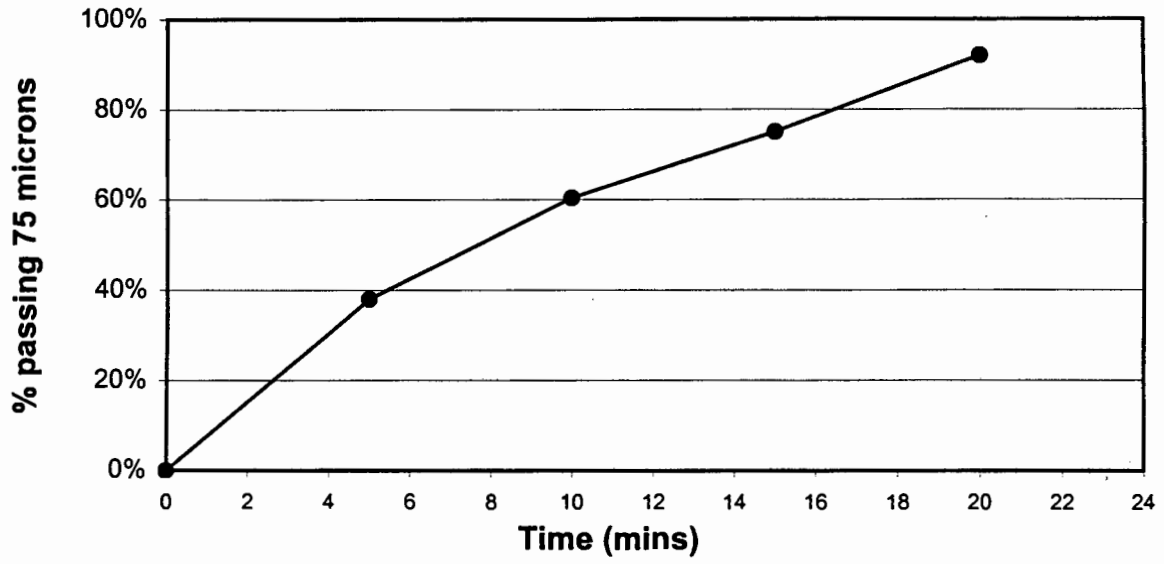
Yoon, R.H., Chen, Z., Finkelstein, N.P. and Richardson, P.E. 1995. An electrochemical study of sphalerite activation by copper in acid solution. Proceedings of XIX Int. Miner. Process. Cong., San Francisco, pp

Zaal, J.R., and Bryson, M.A.W., 1992. Private communication.

Zhou, Z.A., Egiebor, N.O. and Plitt, L.R., 1991. Effect of frothers in bubble rise velocity in a flotation column - I. Single Bubble system. Proceedings of Column '91, Sudbury, Canada. pp 249-261.

Zuninga, G.S. 1935. Flotation recovery is an exponential function of its rate. Boln. Soc. Nac. Min., Santiago, vol. 47, pp 83-86.

APPENDIX 2A
Milling Curve: Buffelsfontein Ore



APPENDIX 2B

SULPHUR ANALYSIS BY LECO SC32

The Leco sulphur analyser analyses a sample for sulphur content by burning a known mass of sample at 1350 C in the presence of excess oxygen. The sulphur dioxide gas given off is drawn through the combustion chamber by a vacuum pump. The gas passes through a pair of moisture traps filled with anhydrous magnesium perchlorate. The gas flow is controlled by a flow controller and then passes through the infra red detector cell. The principle of measurement is that the reduction in IR generated by a nichrome wire at 850 C, at specified wavelength, is due to absorption of SO₂ and is proportional to the concentration of SO₂ given off. The sulphur content of the sample is automatically calculated from the concentration of SO₂ and the mass of sample analysed

The Leco is calibrated before measurement using samples of known sulphur concentration. The system is calibrated for different standard according to the sulphur content of the samples to be measured.

APPENDIX 2C: STATISTICAL EVALUATION OF SIGNIFICANCE

The standard deviations and relative standard deviations were calculated using the following formulae:

$$\text{Standard deviation: } \sigma = \frac{\sqrt{\sum (x_i - x_m)^2}}{n}$$

$$\text{Relative Standard deviation: } = \frac{\sigma}{x_m} \times 100$$

where x_i = Result of test i,
 x_m = Mean result (n tests),
n = Number of tests.

'T' tests were used to compare the means and standard deviations of the reproducibility tests done in two different sets (B-R 1-3 vs B-R 4-8).

ANOVA was used to statistically ascertain the significance of the differences due to the changing parameters relative to the inherent experimental error of each experiment. The mean square (MS) of the difference was compared to the variance obtained from the reproducibility tests to obtain the 'F' value. The statistical significance of the 'F' value was then obtained from the appropriate tables, taking into account the degrees of freedom (Df). Thus the significance of the effect of each parameter on flotation performance was determined. The higher the percentage significance obtained, the higher the probability that the result observed and the conclusions drawn were valid. Generally, in the minerals processing context, effects above 95% are termed 'significant' and effects below 90% are termed 'not significant'. As shown in the results tables, (***) denotes a highly significant effect of greater than 99%, (**) denotes a significant effect between 95% and 99%, (*) denotes a slightly significant effect of between 90% and 95% and (~) denotes that the difference in effects was not significant.

APPENDIX 2D(i): REPRODUCIBILITY OF SULPHUR ASSAYS

Note: The concentrate, feed and tails were each sampled 9 times, and each sample analysed by Leco, 3 times so that results reported are for 27 assays

	Mean Total Sulphur (%)	Std Dev	Relative Std Dev (%)	MS Between Samples	MS Within Samples	F	Significance (DF = 8,18)
Concentrate	33.44	0.476	1.42	0.155	0.259	0.60	~
Feed	0.672	0.0293	4.35	1.50E-03	5.70E-04	2.62	95% - 97.5%
Tails	0.0415	0.0078	18.84	7.21E-05	5.62E-05	1.28	~

APPENDIX 2D(ii):

DETAILED REPRODUCIBILITY RESULTS: BUFFELSFONTEIN ORE

Reproducibility Tests : Buffelsfontein standard conditions:
Buffelsfontein Ore: SMBT (240 mmole/t), pH=4, 200 mmole/t CuSO₄

Test No.	Time (mins)	Cumul Mass(g)	Cum. mass Water(g)	%S Assay	Grade (%S)	%Pyrite Recovered	Klimpel Constants		Sulphur Balance	% Recovery by Size (µm)		
							k (min ⁻¹)	R (%)		+75	75x25	-25
B-R 1	1.0	23.2	102.2	27.2	27.2	81.7	7.83	97.5	111.9	91.8	85.1	52.7
	3.0	34.8	201.6	6.3	20.2	91.1				97.1	95.5	93.0
	7.0	44.0	276.5	2.9	16.6	94.5						
	13.0	48.8	301.6	1.4	15.1	95.4						
B-R 2	1.0	19.0	56.4	30.5	30.5	78.7	6.51	96.4	102.2	78.2	80.8	66.3
	3.0	30.0	138.2	7.7	22.1	90.1				93.6	93.5	98.7
	7.0	37.9	197.6	3.4	18.2	93.7						
	13.0	43.6	224.7	1.3	16.0	94.8						
B-R 3	1.0	21.7	85.1	30.4	30.4	85.1	5.48	96.1	112.5	89.6	83.8	63.6
	3.0	30.9	157.8	6.6	23.3	93.0				100.0	93.0	89.1
	7.0	39.3	218.7	2.7	18.9	95.9						
	13.0	43.4	232.3	1.3	17.2	96.6						
B-R 4	0.17	15.0	40.9	33.4	33.4	74.1	26.34	93.9	62.1			
	0.5	20.6	74.3	11.8	27.5	83.9						
	1.0	24.8	103.9	7.6	24.2	88.6						
	3.0	33.1	170.2	3.9	19.1	93.4						
	7.0	39.4	217.8	1.6	16.3	94.8						
	13.0	43.9	236.4	0.8	14.7	95.3						
B-R 5	0.17	13.0	24.1	37.2	37.2	68.2	20.10	93.4	109.8			
	0.5	18.6	52.4	15.7	30.7	80.7						
	1.0	22.6	73.5	10.3	27.1	86.5						
	3.0	31.3	131.5	5.0	21.0	92.6						
	7.0	39.0	192.4	1.6	17.2	94.4						
	13.0	43.0	212.2	1.0	15.7	95.0						
B-R 6	0.17	14.4	33.2	34.1	34.1	70.9	22.84	92.9	115.8			
	0.5	19.2	58.5	14.3	29.1	80.8						
	1.0	23.5	84.7	9.2	25.5	86.5						
	3.0	31.4	140.8	5.1	20.4	92.3						
	7.0	38.3	188.2	1.9	17.0	94.1						
	13.0	43.2	210.1	1.0	15.2	94.8						
B-R 7	0.17	13.6	26.1	37.0	37.0	70.0	20.21	95.1	111.4			
	0.5	18.3	47.2	16.5	31.6	81.1						
	1.0	23.1	74.8	10.6	27.3	88.1						
	3.0	31.2	128.1	5.4	21.6	94.2						
	7.0	39.3	185.3	2.1	17.6	96.5						
	13.0	43.0	200.5	1.0	16.2	97.0						
B-R 8	0.17	13.5	25.3	35.8	35.8	71.0	22.66	93.4	88.5			
	0.5	18.1	47.9	15.5	30.7	81.3						
	1.0	22.3	72.4	9.5	26.7	87.2						
	3.0	31.1	134.6	4.4	20.4	92.9						
	7.0	37.8	184.2	1.6	17.0	94.5						
	13.0	40.9	205.0	0.9	15.8	94.9						
Mean (1 min))		22.5	81.6	16.9	27.4	85.3						
Std Dev		1.70	15.94	10.40	2.18	3.41						
Relative Std Dev		7.5	19.5	61.5	8.0	4.0						
Mean (Final)		43.7	227.8	1.1	15.7	95.5	22.4	93.7		96.9	94.0	93.6
Std Dev		2.25	32.46	0.22	0.78	0.87	2.5	0.8		3.2	1.3	4.9
Relative Std Dev		5.1	14.2	19.8	4.9	0.9	11.3	0.9		3.3	1.4	5.2

APPENDIX 2D(iii):

SUMMARY OF BUFFELSFONTEIN RESULTS AND STANDARD DEVIATIONS

Calculation of Sulphur Balance

The sulphur balance was obtained using the calculated and measured feed grades, viz.

$$\text{Sulphur Balance} = \frac{f_m}{f_{\text{calc}}} \times 100$$

The calculated feed grade was determined using the concentrate and tails assays and concentrate and tails masses, viz.

$$f_{\text{calc}} = \frac{(C_m \times c_m + T_m \times t_m)}{F_m}$$

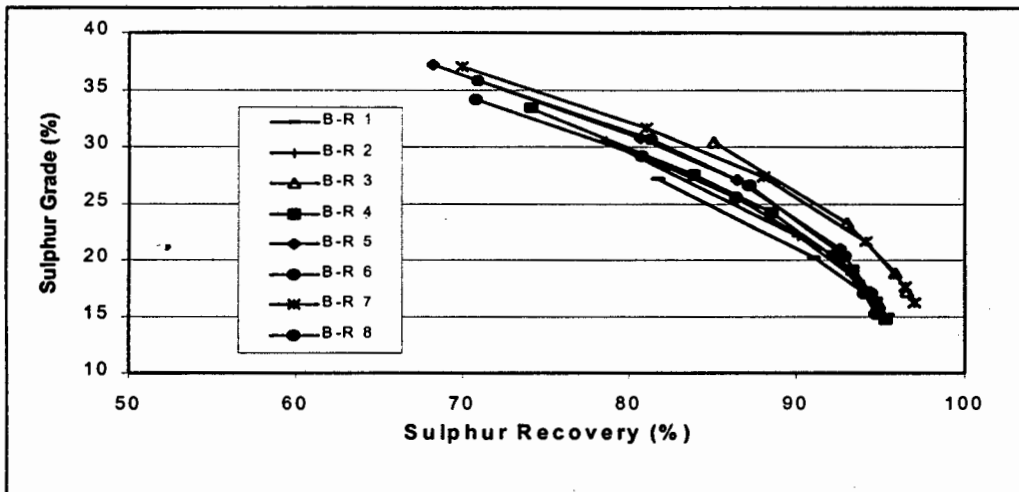
where	f_m	=	Measured feed assay
	F_m	=	Measured feed mass
	c_m	=	Measured overall concentrate grade
	C_m	=	Measured concentrate mass
	t_m	=	Measured tails assay
	T_m	=	Measured tails mass

If this balance was less than 85% or greater than 115%, the test was rejected as unreliable on the basis that this was the limit of the compounded intrinsic error in the experimental procedure.

Tests B-R 1-3 and tests B-R 4-8 were done approximately 1 year apart. The first reproducibility tests were done, in conjunction with tests B 9-24. For tests B-R 1-3, four concentrates were collected, viz after 1, 3, 7 and 13 mins respectively. For tests B-R 4-8, six concentrates were collected, the additional concentrates being collected after 0.167 min and 0.5 mins. Statistical analysis using standard 'T' tests, with the 95 % confidence level termed significant (cf. Sec. 2.2.4.2), showed that there was no significant difference between these two sets of tests with respect to the mass, water and final sulphur recoveries, grades or infinite time recoveries, R. The statistical probability of any differences between these two data sets was below the 90% confidence levels. There was, however, a significant difference (> 95%) in the rate of recovery. These data sets were compared using the recovery obtained after 1 min flotation time. This highlights the sensitivity of flotation tests to changing conditions, and consequently standard tests are done with each set of new tests in any batch flotation programme.

Summary of flotation reproducibility results (Buffelsfontein ore)

Test Number	Klimpel Model Constants		Mass Recovery (%)	Water Recovery (g)	Sulphur Recovery		Sulphur Grade		Sulphur Balance (%)
	(k) (min ⁻¹)	(R) (%)			1 min (%)	13 min (%)	1 min (%)	13 min (%)	
B-R 1	5.48	96.1	4.9	301.6	81.7	95.4	27.2	15.1	102.4
B-R 2	7.83	97.5	4.4	224.7	78.7	94.8	30.5	16.0	102.2
B-R 3	6.51	96.4	4.3	232.3	85.1	96.6	30.4	17.2	107.5
Mean (B-R 1-3)	6.61	96.7	4.5	252.9	81.8	95.6	29.4	16.1	-
Std Dev	1.18	0.73	0.31	42.38	3.20	0.93	1.86	1.06	-
Rel Std Dev (%)	17.84	0.75	6.87	16.76	3.91	0.97	6.39	6.57	-
B-R 4	13.10	95.9	4.4	236.4	83.9	95.3	24.2	14.7	102.5
B-R 5	10.44	95.6	4.3	212.2	86.5	95.0	27.1	15.7	104.7
B-R 6	10.66	95.4	4.3	210.1	86.5	94.8	25.5	15.2	103.5
B-R 7	10.03	97.7	4.3	200.5	88.1	97.0	27.3	16.2	101.4
B-R 8	11.34	95.7	4.1	205.1	87.2	94.9	26.7	15.8	90.9
Mean (B-R 4-8)	11.11	96.0	4.3	212.9	86.4	95.4	26.2	15.5	-
Std Dev	1.21	0.95	0.11	13.92	1.56	0.91	1.30	0.57	-
Rel Std Dev (%)	10.86	0.99	2.60	6.54	1.81	0.96	4.97	3.70	-
Mean (B-R 1-8)	9.42	96.3	4.4	227.9	84.7	95.5	27.4	15.7	-
Std Dev	2.58	0.88	0.22	32.44	3.16	0.86	2.17	0.78	-
Rel Std Dev (%)	27.40	0.92	5.14	14.24	3.74	0.90	7.94	4.93	-



Sulphur grade vs sulphur recovery for reproducibility tests (B-R 1-8) using SMBT as collector and 200 mmoles/t copper sulphate (Buffelsfontein ore)

APPENDIX 2D(iv):

DETAILED REPRODUCIBILITY RESULTS: BUFFELSFONTEIN ORE

Reproducibility results obtained with St Helena ore

St Helena Ore: Pure PNBX (400 mmol/t), pH=4, No CuSO₄

Test No.	Time (mins)	Cumul Mass (g)	Cum. mass Water (g)	%S Assay	Grade (%S)	%Pyrite Recovered	Klimpel Constants		Sulphur Balance
							k (min ⁻¹)	R _∞ (%)	
SH-R1	0.5	16.5	15.4	36.4	36.4	48.5	4.14	78.9	97.3
	1.0	20.4	21.5	26.9	34.6	57.1			
	3.0	27.5	36.8	21.1	31.1	69.1			
	7.0	33.5	53.1	16.3	28.4	77.1			
	13.0	35.7	58.9	14.9	27.6	79.7			
SH-R2	0.5	13.5	11.6	37.6	37.2	39.3	2.60	77.3	104.2
	1.0	17.1	16.4	28.7	35.2	47.4			
	3.0	23.2	28.0	25.3	31.9	59.2			
	7.0	31.6	47.4	20.0	28.7	72.2			
	13.0	38.3	68.7	17.4	25.9	81.3			
SH-R3	0.5	15.3	15.0	37.2	37.2	46.0	3.47	82.6	100.7
	1.0	20.3	22.7	28.9	35.2	57.6			
	3.0	27.4	43.3	22.5	31.9	70.4			
	7.0	34.1	66.9	15.7	28.7	78.9			
	13.0	40.2	92.7	10.4	25.9	84.0			
SH-R4	0.5	14.2	13.8	37.4	37.4	40.5	2.78	79.9	94.7
	1.0	18.9	20.5	29.6	35.5	50.9			
	3.0	26.6	36.7	24.2	32.2	65.1			
	7.0	32.5	52.7	18.9	29.8	73.5			
	13.0	41.4	82.6	14.0	26.4	83.0			
Mean (Final)		38.2	75.7	14.3	26.7	81.6	3.25	79.7	
Std Dev		2.5	14.9	2.9	0.8	1.9	0.70	2.2	
Relative Std Dev (%)		6.5	19.7	20.3	3.0	2.3	21.61	2.8	

STD DEV	0.5	1.3	1.7	0.5	0.4	4.4
	1.0	1.5	2.8	1.2	0.4	5.0
	3.0	2.0	6.3	1.9	0.5	5.0
	7.0	1.1	8.3	2.1	0.6	3.1
	13.0	2.5	14.9	2.9	0.8	1.9

APPENDIX 2D(v): Reproducibility tests obtained with St Helena ore

Summary of flotation reproducibility results (St Helena ore)

Test Number	Klimpel Model Constants		Mass Recovery (%)	Water Recovery (g)	Sulphur Recovery		Sulphur Grade		Sulphur Balance (%)
	(k) (min ⁻¹)	(R) (%)			1 min (%)	13 min (%)	1 min (%)	13 min (%)	
SH-R 1	4.14	79.0	3.57	58.9	57.1	79.7	34.6	27.6	97.3
SH-R 2	2.60	77.3	3.83	68.7	47.4	81.3	35.2	25.9	104.2
SH-R 3	3.47	82.6	4.02	92.7	57.6	84.0	35.2	27.4	100.7
SH-R 4	2.78	79.9	4.14	82.6	50.9	83.0	35.5	26.4	94.7
Mean	3.25	79.7	3.89	75.7	53.3	81.6	35.1	26.8	-
Std Dev	0.70	2.23	0.25	14.89	4.95	1.91	0.38	0.81	-
Rel Std Dev (%)	21.61	2.80	6.49	19.67	9.29	2.34	1.07	3.00	-

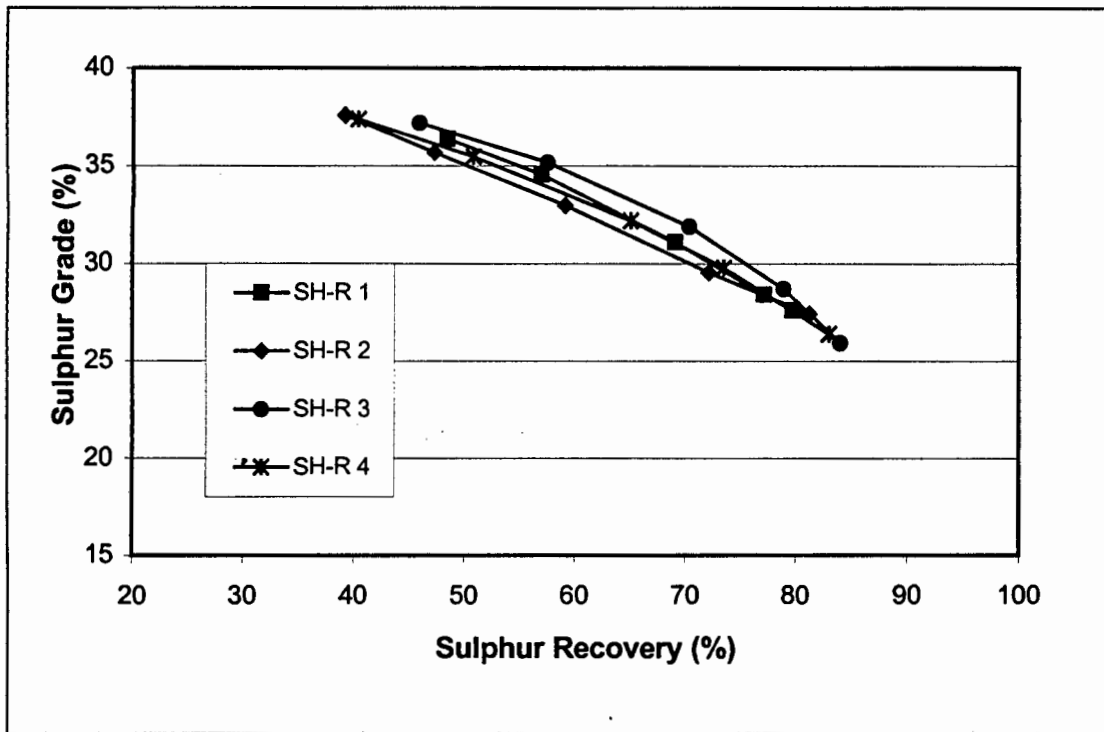


Figure 2.39: Sulphur grade vs sulphur recovery for reproducibility tests (SH-R 1-4) with 400 mmoles/t PNBX as collector (St Helena ore)

APPENDIX 2E(I):

Results obtained with Buffelsfontein Ore

Test No.		Time (mins)	Cum Mass Rec (g)	Water Rec (g)	%S Assay	Grade (%S)	%Pyrite Recovered	Sulphur Balance	Klimpel Constants		% Recovery by Size (μm)		
									k (min^{-1})	R_{∞} (%)	-25	75x25	+75
B-9	No Collector	0.2	10.9	87.4	0.9	0.9	1.57						
		0.5	16.5	142.5	1.0	0.9	2.4						
		1.0	20.7	188.1	1.2	1.0	3.3						
		3.0	25.8	244.0	2.2	1.2	5.0						
		7.0	30.9	298.7	4.3	1.7	8.6						
		13.0	33.9	322.4	6.4	2.1	11.8						
B-10	oC6 DTC 310 mmoles/t	1.0	24.9	125.7	25.6	25.6	77.1						
		3.0	35.1	209.0	10.7	21.3	90.3						
		7.0	42.2	271.9	5.6	18.6	95.1						
		13.0	46.2	302.0	2.7	17.3	96.4	123.96	4.63	97.80			
B-11	PNBX nil CuSO ₄ 310 mmoles/t	1.0	4.1	3.7	37.8	37.8	21.7				17.43	17.04	17.76
		3.0	13.7	33.3	25.5	29.2	55.6						
		7.0	24.5	68.8	13.3	22.2	75.5						
		13.0	30.8	114.2	11.9	20.1	85.9	91.12	0.60	98.60	79.34	69.25	79.08
B-12	95:5 nil CuSO ₄ 310 mmoles/t	1.0	10.7	8.2	35.6	35.6	49.8				33.3	67.8	42.1
		3.0	20.0	31.7	19.3	28.0	73.3						
		7.0	26.9	80.0	14.2	24.5	86.1						
		13.0	31.1	123.0	9.1	22.4	91.2	109.1	1.68	0.9	84.4	92.9	94.0
B-13	90:10 nil CuSO ₄ 310 mmoles/t	1.0	9.0	8.3	38.6	38.6	46.1				32.4	42.9	38.8
		3.0	16.4	32.2	20.0	30.2	65.8						
		7.0	27.5	94.4	14.0	23.6	86.5						
		13.0	32.8	131.5	9.3	21.4	93.0	108.5	1.27	1.0	91.2	95.0	92.2
B-14	85:15 nil CuSO ₄ 310 mmoles/t	1.0	12.6	14.9	37.5	37.5	62.8				51.8	65.5	65.0
		3.0	21.4	50.2	15.4	28.5	80.7						
		7.0	30.3	112.5	8.3	22.5	90.5						
		13.0	34.3	141.4	4.8	20.4	93.1	112.8	2.69	0.9	69.5	94.3	93.9
B-15	50:50 nil CuSO ₄ 310 mmoles/t	1.0	16.2	32.9	33.1	33.1	73.6				61.8	90.4	73.3
		3.0	23.9	76.5	12.7	26.5	87.2						
		7.0	31.2	136.2	6.7	21.9	93.8						
		13.0	35.5	171.4	3.4	19.6	95.8	110.0	4.00	1.0	99.4	100.0	87.1
B-16	PNBX nil CuSO ₄ 465 mmoles/t	1.0	4.5	2.4	39.0	39.0	24.3				20.93	36.04	22.16
		3.0	9.7	14.3	27.2	32.7	43.5						
		7.0	17.1	40.4	16.8	25.8	60.6						
		13.0	24.8	81.8	12.8	21.8	74.2	105.51	0.62	82.10	72.54	80.54	92.12
B-17	90:10 nil CuSO ₄ 465 mmoles/t	1.0	10.8	12.5	39.7	39.7	50.8				32.4	48.3	48.3
		3.0	16.2	28.1	22.1	33.9	64.8						
		7.0	31.7	75.0	12.8	23.5	88.4						
		13.0	38.9	134.8	4.5	20.0	92.2	113.4	1.50	0.9	81.1	96.3	95.6

APPENDIX 2 (II):

Results obtained with St Helena ore, no CuSO₄ addition

Test No.	Collector	Time (mins)	Mass Rec (g)	Water Rec (g)	%S Assay	Grade (%S)	%Pyrite Recovered	limpel Constant		Mass Balance	Eh (mV)
								k (min ⁻¹)	R (%)		
SH-5	PNBX	0.5	17.4	20.1	35.3	35.3	49.1				200.00
		1.0	22.3	40.3	25.5	33.1	59.1				-30.00
		3.0	39.5	50.4	15.4	25.4	80.3				
		6.0	49.3	109.3	6.9	21.7	85.7				
		10.0	57.0	164.8	4.0	19.3	88.2	3.26	90.0	99.0	140.0
SH-6	90:10 mix oC6 first	0.5	19.9	19.44	36.5	36.5	55.8				160.0
		1.0	24.7	38.8	25.95	34.5	65.3				-40.0
		3.0	39.7	46.5	15.5	27.3	83.2				
		7.0	47.7	78.0	6.9	23.9	87.5				
		13.0	54.7	115.7	3.9	21.3	89.6	3.38	91.7	98.7	100.0
SH-7	90:10 mix PNBX first	0.5	21.7	27.3	33.9	33.9	57.0				190.0
		1.0	27.2	54.5	24.1	31.9	67.4				-50.0
		3.0	42.6	65.0	13.5	25.2	83.5				
		7.0	50.8	120.5	6.2	22.2	87.5				
		13.0	57.5	171.4	3.8	20.0	89.5	3.74	91.3	97.4	120.0
SH-8	90:10 mix simult	0.5	19.2	22.7	34.9	34.9	51.1				190.0
		1.0	24.9	45.3	26.2	32.9	62.5				-70.0
		3.0	41.9	55.0	15.2	25.8	82.2				
		7.0	50.9	113.5	6.8	22.4	86.9				
		13.0	57.9	167.8	4.1	20.2	89.1	3.02	91.6	97.9	120.0
SH-9	90:10 mix premix	0.5	19.1	22.5	34.7	34.7	50.5				190.0
		1.0	25.0	45.0	27.0	32.9	62.5				-50.0
		3.0	40.9	54.4	15.8	26.2	81.6				
		7.0	49.8	105.9	7.2	22.8	86.5				
		13.0	56.7	155.6	4.2	20.5	88.7	3.05	91.0	98.8	110.0

APPENBIX 3A: Reproducibility data for bubble Sizes

Date	Number	Mean Diameter (mm)	Std Dev	Mean Surface Area(mm ²)	Total Surface Area(mm ²)	Total No. of Bubbles in 30 secs
4/2	1	0.939	0.28	3.01	6483.1	2154
	2	0.941	0.29	3.04	5856.5	1925
	3	0.946	0.28	3.07	6392.4	2082
	4	0.936	0.29	3.00	5962.3	1984
	5	0.938	0.29	3.03	5889.1	1942
	6	0.956	0.28	3.02	6483.1	1740
	7	0.971	0.32	3.30	5505.1	1667
	8	0.973	0.33	3.30	5529.6	1670
	9	0.980	0.35	3.40	6212.2	1827
	10	0.963	0.33	3.30	6281.7	1925
5/2	11	0.976	0.35	3.37	5816.0	1726
	12	0.955	0.34	3.23	5415.1	1675
	13	0.938	0.33	3.11	5214.4	1676
	14	0.943	0.31	3.10	5153.7	1660
	15	0.936	0.32	3.07	5138.1	1674
	16	0.949	0.33	3.18	5049.3	1588
	17	0.940	0.33	3.11	5123.8	1646
	18	0.969	0.35	3.30	3847.9	1158
	19	0.948	0.32	3.16	5044.5	1596
	20	0.948	0.32	3.15	5068.7	1608
8/2	21	0.961	0.32	3.22	5027.3	1557
	22	0.910	0.27	2.83	6447.4	2275
	23	0.917	0.26	2.85	6468.2	2272
	24	1.030	0.30	3.62	7877.8	2174
	25	0.957	0.28	3.12	6954.7	2231
	26	0.991	0.28	3.33	7247.2	2178
	27	0.990	0.28	3.34	7300.0	2186
	28	0.980	0.27	3.25	6823.6	2098
	29	0.944	0.26	3.02	6512.5	2158
	30	0.978	0.28	3.24	6796.7	2096
9/2	31	0.967	0.27	3.17	6403.6	2021
	32	0.939	0.26	2.98	5499.6	1846
	33	0.952	0.27	3.08	5687.1	1847
	34	0.932	0.26	2.94	5744.5	1957
	35	0.957	0.26	3.09	5876.3	1901
	36	0.955	0.27	3.09	5951.3	1924
	37	0.953	0.27	3.08	5593.0	1818
	38	0.943	0.26	3.00	5546.7	1849
	39	0.979	0.27	3.24	5633.0	1738
	40	0.967	0.27	3.17	5361.4	1579
	41	0.963	0.26	3.13	5417.6	1730
	42	0.969	0.25	3.15	6063.8	1926
43	0.982	0.25	3.23	5925.2	1836	
44	0.979	0.25	3.21	6401.5	1994	
45	0.961	0.25	3.10	6094.9	1963	
46	0.980	0.25	3.22	5928.0	1842	
47	0.975	0.25	3.19	6139.1	1926	
48	0.953	0.25	3.05	6049.3	1985	
49	0.953	0.25	3.05	5548.0	1820	
50	0.937	0.26	2.96	5626.1	1898	
51	0.941	0.26	2.99	5286.4	1769	
52	0.942	0.25	2.99	5525.4	1849	
	Mean	0.957	0.29	3.14	5888.9	1868.6
	Std. Dev	0.021	0.03	0.15	698.69	219.4
	Rel. Std Dev	2.170	11.14	4.63	11.86	11.7

APPENDIX 5A (i)

Results with copper sulphate obtained with Buffelsfontein Ore

Test No.	CuSO ₄ dos. 200 mmoles/t	Time (mins)	Cum Mass Rec (g)	Water Rec (g)	Froth Conc (%)	%S Assay	Grade (%S)	%Pyrite Recovered	Sulphur Balance	Klimpel Constants		% Recovery by Size (µm)			
										k (min ⁻¹)	R (%)	<25	75x25	>75	
B-18	oC6 DTC	0.2	14.2	98.7	12.6	11.3	11.3	21.9							
		0.5	21.2	151.4	12.3	11.4	11.3	32.8							
		1.0	28.5	208.1	12.0	14.4	12.1	47.0							
		3.0	40.5	297.9	12.0	18.4	14.0	77.1							
		7.0	48.4	364.7	11.7	9.8	13.3	87.7							
		13.0	51.7	385.1	11.8	5.4	12.8	90.1		1.69	94.7				
B-19	PNBX	1.0	17.6	56.9	3.2	25.3	25.3	61.3					51.80	65.50	65.00
		3.0	28.3	117.7	4.2	13.4	20.8	81.0							
		7.0	35.5	165.8	4.7	8.3	18.2	89.4							
		13.0	41.5	199.9	4.8	4.6	16.3	93.1	109.50	2.56	94.80	89.50	94.30	93.90	
B-20	90:10	1.0	21.4	96.5	4.5	23.0	23.0	62.8					39.8	39.2	76.8
		3.0	32.0	164.6	5.1	15.0	20.3	83.3							
		7.0	41.4	231.5	5.6	7.3	17.4	92.0							
		13.0	46.6	261.9	5.6	3.3	15.8	94.2	94.19	2.61349	0.96765	82.6	83.9	99.8	

APPENDIX 5A (ii)

Results with copper sulphate obtained with St Helena ore Ore

Test No.		Time (mins)	Cum Mass Rec (g)	Water Rec (g)	%S Assay	Grade (%S)	%Pyrite Recovered	Klimpel Constants		Mass Balance	Eh (mV)
								k (min ⁻¹)	R (%)		
SH-10	PNBX Cu before	0.5	20.5	30.3	35.0	35.0	51.2				190.0
		1.0	26.3	60.6	22.5	32.8	61.5				200.0
		3.0	42.8	74.0	15.6	26.2	79.8				
		6.0	52.6	137.6	8.0	22.8	85.4				
		10.0	61.9	197.2	4.6	20.0	88.4	3.64	89.1	100.1	130.0
SH-11	90:10 Mixture Simult Cu before	0.5	21.9	34.9	33.6	33.6	56.4				200.0
		1.0	28.3	69.8	21.6	30.9	67.0				220.0
		3.0	45.5	86.6	12.1	23.7	82.9				
		7.0	56.4	164.7	5.9	20.3	87.8				
		13.0	67.1	245.2	3.3	17.6	90.5	3.56	91.9	99.5	160.0
SH-12	90:10 Mixture Cu inbetween	0.5	23.2	39.0	32.5	32.5	58.1				200.0
		1.0	29.3	77.9	20.4	29.9	67.7				190.0
		3.0	46.1	95.7	11.6	23.2	82.8				
		7.0	58.2	176.2	5.6	19.6	88.0				
		13.0	69.3	269.7	3.0	16.9	90.6	3.68	91.8	98.8	150.0
SH-13	90:10 Mixture Cu after	0.5	22.2	26.5	33.0	33.0	54.7				190.0
		1.0	27.4	53.0	22.4	31.0	63.4				180.0
		3.0	49.5	64.1	13.5	23.2	85.6				
		7.0	60.0	115.7	4.9	20.0	89.5				
		13.0	68.8	183.3	3.0	17.8	91.5	2.92	94.6	100.8	150.0